Regulation of p53 by catalytically-inactive MDM2 mutants

Koji Nomura
BSc (Hons), MPhil

Submitted in fulfilment of the requirement for the degree of
Doctor of Philosophy (PhD)

Cancer Research UK - Beatson Institute

Institute of Cancer Sciences
College of Medical, Veterinary and Life Sciences
University of Glasgow

February 2019

Abstract

MDM2-MDMX complexes bind to p53, inhibiting the p53 transcriptional activity and targeting p53 for proteasomal degradation. Uncoupling p53 from MDM2 is therefore an attractive strategy to treat cancers that retain wild type p53. Small molecules that inhibit MDM2 binding to p53 release p53 from control by MDM2. While such inhibitors efficiently activate a p53 response, clinical trials have revealed that the therapeutic utility of these compounds is limited by on-target toxicities. I have therefore explored alternative mechanisms to therapeutically target MDM2, based on the hypothesis that inhibition of the MDM2 RING domain would lead to different outcomes than inhibition of the MDM2-p53 interaction. Using our crystal structure of E2 (UbcH5b)–ubiquitin-MDM2^{RING}-MDMX^{RING} complex as a starting point, MDM2 mutants that prevent E2–ubiquitin binding were designed.

MDM2 mutants that are unable to interact with E2–ubiquitin complex have lost their E3 ligase activity including the ability to ubiquitinate p53, despite retaining the ability to bind to p53, homo-dimerise and hetero-dimerise with MDMX. As a result, p53 protein accumulates in cells expressing these catalytically-inactive MDM2 mutants. However, the E2–ubiquitin non-binding MDM2 mutants retain the ability to limit p53 transcriptional activity under normal unstressed condition, despite the elevated p53 levels. As a result, cells can proliferate normally, but show a more robust induction of p53 activity in response to stress. These observations suggest that the direct inhibition of E3 activity of MDM2 may be less deleterious to normal cells than inhibition of the MDM2-p53 interaction. To test this, the development of novel *in vivo* models based on conditional knock-in of one of the MDM2 mutants identified in this study was initiated. Based on preliminary data, mice expressing these mutants are expected to be developmentally normal but less tumour prone due to an increased sensitivity to p53 activation.

This study provides mechanistic insight that will help in the development of novel inhibitors that targeting MDM2 while avoiding the on-target toxicities showed in the clinic by currently available MDM2 inhibitors.

Table of Contents

Abstract i

List of Tables v

List of Figures vi

List of Accompanying Material ix

Acknowledgement x

Author's Declaration xi

Abbreviations xii

Chapter 1 Introduction 1
1.1 The ubiquitin proteasome system 2
1.1.1 Regulation of ubiquitin proteasome system 2
1.1.2 Ubiquitin-like proteins 18
1.1.3 Ubiquitin proteasome system and cancer 21
1.2 p53 30
1.2.1 Structure of p53 32
1.2.2 p53 dysfunction 34
1.2.3 Cell survival and repair functions of p53 36
1.2.4 Cell elimination functions of p53 44
1.2.5 Transcription and post translational regulation of p53 47
1.3 MDM2 and MDMX 52
1.3.1 Structure of MDM2 and MDMX 52
1.3.2 Functions of MDM2 and MDMX 54
1.3.3 Transcription and Post translational regulation of MDM2 and MDMX 61
1.3.4 Additional mechanisms to inhibit MDM2 and MDMX 66
1.4 Other regulators of p53 67
1.5 Targeting ubiquitin proteasome system for cancer treatment 69
1.5.1 Targeting MDM2 and MDMX 70
1.5.2 Targeting other E3 ligases and DUBs 73
1.5.3 Proteasome inhibitors 75
1.5.4 Targeting the E1 activating enzymes 77
1.5.5 Targeting the E2 conjugating enzymes 78
1.5.6 Other approaches 78
1.6 Aims and Objectives 80

Chapter 2 Materials and methods 81
2.1 Animals 82
2.2 Cell culture and treatment 82

2.2.1 Materials 82
2.2.2 Methods 83
2.3 PCR and DNA preparation 84
2.3.1 Materials 84
2.3.2 Methods 86
2.4 Genomic DNA isolation and Genomic PCR / Genotyping 88
2.4.1 Materials 88
2.4.2 Methods 89
2.5 Transfection, infection and cell cloning 90
2.5.1 Materials 90
2.5.2 Methods 90
2.6 SDS-PAGE and Immunoblotting 92
2.6.1 Materials 92
2.6.2 Methods 93
2.7 Immunoprecipitation 94
2.7.1 Materials 94
2.7.2 Methods 95
2.8 Ubiquitination assay 95
2.8.1 Materials 95
2.8.2 Methods 96
2.9 Immunofluorescence 97
2.9.1 Materials 97
2.9.2 Methods 97
2.10 RNA Extraction and Quantitative Real-Time PCR (qPCR) 98
2.10.1 Materials 98
2.10.2 Methods 99
2.11 Chromatin Immunoprecipitation (ChIP) 99
2.11.1 Materials 99
2.11.2 Methods 101
2.12 Cell growth assay and cell staining 102
2.12.1 Materials 102
2.12.2 Methods 103
2.13 Cell cycle analysis 103
2.13.1 Materials 103
2.13.2 Methods 103
2.14 Structure analysis 104
2.15 Statistical analysis and reproducibility 104

Chapter 3 E3 ligase activity of MDM2 and MDMX 105
3.1 Structure of UbcH5B–ubiquitin-MDM2^{RING}-MDMX^{RING} 106

3.2 Attenuation of MDM2 E3 ligase activity 107
3.2.1 Targeting Separation of E2–ubiquitin complex and MDM2 109
3.2.2 Targeting MDM2-MDMX dimerisation 131
3.3 E3 ligase activity of MDMX 136
3.3.1 Differences between MDM2 and MDMX 136
3.4 Determination of the ubiquitination target of MDM2 by $p14^{ARF}$ 141
3.5 Summary and discussion 144

Chapter 4 Regulation of the p53 activity by MDM2 and MDMX 147
4.1 MDM2 I440 and R479 mutants limit p53 activity 148
4.1.1 Generation and validation of tetracycline inducible p53 knockdown-*MDM2* knockout cells 148
4.1.2 Effect of the MDM2 mutants on cell cycle 152
4.1.3 MDM2 I440 or R479 mutants localise on *p21* promoter 156
4.1.4 Effect of the MDM2 mutants on other p53 target genes 157
4.1.5 Effect of the MDM2 mutants on cell growth 160
4.2 MDM2 I440 and R479 mutants render cells stress sensitive 161
4.2.1 Dissociation of p53 and MDM2 162
4.2.2 Regulation of p53 target genes expression upon stress 163
4.2.3 Time course study of the stress response 164
4.2.4 Cell cycle and growth regulation upon stress 166
4.3 Regulation of p53 activity by MDM2 that do not dimerise 168
4.3.1 MDM2 Δ RING cannot limit p53 activity 169
4.3.2 Dimerisation-impaired MDM2 mutants cannot limit p53 activity .. 170
4.4 Importance of MDMX to regulate p53 activity 172
4.5 Summary and discussion 173

Chapter 5 Murine MDM2 176
5.1 Human MDM2 and Murine MDM2 177
5.2 Generating a murine *Mdm2* I438K conditional point mutant allele 179
5.2.1 Effect of *Mdm2* I438K mutant in BMK primary cells 181
5.2.2 Effect of inducible knock-in of *Mdm2* I438K mutant in MEFs 187
5.3 Discussion 190
5.3.1 Next steps for the *Mdm2* I438K mouse 191
5.3.2 Assessing post-developmental inducton of *Mdm2* I438K *in vivo* ... 193
5.3.3 Other options and future directions 193

Chapter 6 Overall summary and conclusions 195

Bibliography 203

Databases / Tools 240

List of Tables

Table 1-1: The hallmarks of cancer and the ubiquitin proteasome system 23
Table 1-2: Examples of p53-mediated cell death 46
Table 1-3: Examples of global knockout/knock-in mouse models 58
Table 1-4: Examples of tissue or cell type specific deletion of *Mdm2* or *Mdmx* in mice 59
Table 1-5: E3 ligases involved in p53 ubiquitination..... 68
Table 1-6: Example of deregulated ubiquitin E3 ligases in cancer 74
Table 2-1: Reagents for cell culture 82
Table 2-2: Solutions and buffers for cell culture..... 82
Table 2-3: Reagents for cell culture treatment 83
Table 2-4: Reagents for PCR and DNA preparation 84
Table 2-5: Solutions and buffers for PCR and DNA preparation..... 85
Table 2-6: Plasmids for over-expression..... 85
Table 2-7: Plasmids for knockout / knockdown 86
Table 2-8: Reagents for Genomic DNA isolation and Genomic PCR / Genotyping 89
Table 2-9: Solutions and buffers for Genomic DNA isolation and Genomic PCR / Genotyping 89
Table 2-10: Primers for genomic PCR (for sequencing) 89
Table 2-11: Primers for genotyping 89
Table 2-12: Reagents and kits for transfection, infection and cell cloning 90
Table 2-13: Reagents and kits for SDS-PAGE and immunoblotting 92
Table 2-14: Solutions and buffers for SDS-PAGE and immunoblotting 92
Table 2-15: Gels for SDS-PAGE 92
Table 2-16: Antibodies for immunoblotting..... 93
Table 2-17: Reagents and kits for immunoprecipitation 94
Table 2-18: Solutions and buffers for immunoprecipitation..... 95
Table 2-19: Antibodies for immunoprecipitation..... 95
Table 2-20: Reagents for ubiquitination assay..... 96
Table 2-21: Solutions and buffers for ubiquitination assay 96
Table 2-22: Reagents and Kits for immunofluorescence 97
Table 2-23: Solutions and buffers for immunofluorescence 97
Table 2-24: Antibodies for immunofluorescence 97
Table 2-25: Reagents and Kits for RNA extraction and qPCR..... 98
Table 2-26: Primers for qPCR 98
Table 2-27: Reagents for ChIP..... 99
Table 2-28: Solutions and buffers for ChIP 100
Table 2-29: Antibodies for ChIP..... 100
Table 2-30: Primers for ChIP 101
Table 2-31: Reagents for cell growth assay and cell staining 102
Table 2-32: Solutions and buffers for cell growth assay and cell staining 102
Table 2-33: Reagents for cell cycle analysis 103
Table 2-34: Solutions and buffers for cell cycle analysis 103
Table 3-1: Dissociation constants (K_d) for interactions between MDM2 I440 variants and UbcH5B–ubiquitin..... 116
Table 3-2: Dissociation constants (K_d) for interactions between MDM2 R479 variants and UbcH5B–ubiquitin..... 122
Table 6-1: Overall summary of selected MDM2 mutants in this study 202

List of Figures

Figure 1-1: Structure of Ubiquitin 3
Figure 1-2: Overview of some patterns of ubiquitin conjugation and their functional outcomes 4
Figure 1-3: Acyl adenylation of ubiquitin by E1 ubiquitin activating enzyme 5
Figure 1-4: Thioester formation between the E1 cysteine residue and the ubiquitin C-terminal 6
Figure 1-5: Trans-thioesterification of ubiquitin from E1 to E2..... 7
Figure 1-6: Isopeptide ligation of ubiquitin to the substrate by E3 ligase 8
Figure 1-7: Poly-ubiquitination catalysed by E3 ligase 9
Figure 1-8: Types of E3 ligases and their ubiquitin transfer..... 13
Figure 1-9: Structure and schematic model of 26S proteasome 16
Figure 1-10: Structure of ubiquitin, NEDD8 and SUMO-1 19
Figure 1-11: Cell cycle regulation by E3 ubiquitin ligases 25
Figure 1-12: Regulation of E2F1 and SKP2 in cell cycle 26
Figure 1-13: The canonical NF-κB activation pathway 28
Figure 1-14: Functions of the tumour suppressor p53 32
Figure 1-15: Functional domains of the p53 protein..... 33
Figure 1-16: *TP53* mutation rates in somatic cancers at the primary site 34
Figure 1-17: p53 mutation hotspots 35
Figure 1-18: Role of p53 in cell cycle regulation 37
Figure 1-19: Example of the regulation of cell growth and autophagy by p53 ... 39
Figure 1-20: Examples of the involvement of p53 in glycolysis and metabolism . 42
Figure 1-21: Role of p53 in apoptosis 45
Figure 1-22: Post-translational modifications by ubiquitin-like proteins..... 49
Figure 1-23: Phosphorylation, acetylation and methylation of p53 51
Figure 1-24: Functional domains of MDM2 and MDMX..... 53
Figure 1-25: Levels of wild type MDM2 protein and mice phenotypes 55
Figure 1-26: Transcriptional regulation of *MDM2* and *MDMX* 63
Figure 1-27: Phosphorylation sites of MDM2 and MDMX 64
Figure 1-28: Wild type p53 and *MDM2* amplification in human cancer patients . 69
Figure 1-29: Example of inhibitors of the p53-MDM2 interaction 71
Figure 1-30: Example of proteasome inhibitors 76
Figure 1-31: Mechanism of the E1 inhibitor TAK-243 77
Figure 1-32: Example of PROTAC 79
Figure 3-1: Structure of E2 (UbcH5B)–ubiquitin-MDM2^{RING}-MDMX^{RING} complex .. 106
Figure 3-2: Strategies to attenuate the intrinsic E3 ligase activity of MDM2 ... 108
Figure 3-3: Hydrophobic interaction between MDM2 RING domain and UbcH5B 110
Figure 3-4: Effect of MDM2 I440 mutants on p53 degradation and ubiquitination 112
Figure 3-5: Effect of MDM2 I440 mutants on p53 half-life 113
Figure 3-6: SPR analyses of MDM2 I440 mutants binding affinities for UbcH5B–ubiquitin 115
Figure 3-7: Hydrogen bonds between MDM2 RING domain and UbcH5B–ubiquitin 117
Figure 3-8: Effect of MDM2 R479 mutants on p53 degradation and ubiquitination 119
Figure 3-9: SPR analyses of MDM2 R479 mutants binding affinities for UbcH5B–ubiquitin 121
Figure 3-10: MDM2 I440 and R479 mutants can interact with MDMX 123
Figure 3-11: MDM2 I440 and R479 mutants can interact with p53..... 124

Figure 3-12: Model of the interaction between MDM2 C-terminal tail and E2-ubiquitin 125
Figure 3-13: MDM2 I440 and R479 mutants do not be reactivated by MDMX 126
Figure 3-14: Other hydrogen bonds between E2 and MDM2 RING domain 127
Figure 3-15: Effects of MDM2 V439, K473 and P476 mutants on p53 degradation 128
Figure 3-16: Other interaction sites between ubiquitin and MDM2 RING domain 129
Figure 3-17: Effects of MDM2 N433, H453 and V477 mutants on p53 degradation 130
Figure 3-18: Phosphorylation of MDM2 upstream RING domain disrupts MDM2-p53 interaction 131
Figure 3-19: Dimerisation interface of MDM2 and MDMX 132
Figure 3-20: Effect of MDM2 dimerisation impairment on p53 degradation and ubiquitination 134
Figure 3-21: Complementation between I440 and dimerisation impairment mutant 135
Figure 3-22: Differences between MDM2 and MDMX RING domains 137
Figure 3-23: Mutation of MDMX K478R is necessary to give MDMX an E3 ligase activity 139
Figure 3-24: SPR analysis of MDMX variants binding affinities for UbcH5B-ubiquitin 140
Figure 3-25: Complementation between MDM2 I440 mutants and MDMX K478R mutant 141
Figure 3-26: $p14^{ARF}$ switches substrate specificity of the MDM2-MDMX complex from p53 to MDMX 142
Figure 3-27: $p14^{ARF}$ promotes MDMX K478R "auto-ubiquitination" 143
Figure 4-1: Generation of inducible and reversible knockdown of p53 149
Figure 4-2: Attempt of the generation of CRISPR knock-in of *MDM2* I440K mutant 150
Figure 4-3: Generation and validation of *MDM2* knockout in the inducible p53 system 152
Figure 4-4: Effect of the expression of MDM2 mutants on p53 target genes involving in cell cycle regulation 154
Figure 4-5: Effect of the expression of MDM2 mutants on cell cycle 155
Figure 4-6: MDM2 I440 and R479 mutants localise on the *p21* promoter with p53 157
Figure 4-7: Effect of the expression of MDM2 mutants on other p53 target genes 159
Figure 4-8: Effect of the expression of MDM2 mutants on cell growth 161
Figure 4-9: Phosphorylation of p53 by chemical treatments 162
Figure 4-10: Cells expressing MDM2 I440 or R479 mutants can quickly induce p53 target genes upon stress 164
Figure 4-11: Time course study of ActD treatment in cells expressing MDM2 mutants 165
Figure 4-12: Time course study of nutlin-3 or doxorubicin treatment in cells expressing MDM2 mutants 166
Figure 4-13: Cells expressing I440 or R479 mutants can quickly arrest cell cycle at the G_1 upon stress 167
Figure 4-14: Effect of ActD treatment on cell growth in cells expressing MDM2 mutants 168
Figure 4-15: Generation and validation of *MDM2 Δ RING* mutant 169
Figure 4-16: MDM2 ΔRING can bind to p53 but cannot limit p53 activity 170

Figure 4-17: Dimerisation-impaired MDM2 mutants cannot limit p53 activity .. 171
Figure 4-18: Effect of MDMX knockdown in cells expressing MDM2 I440K or R479P mutants 172
Figure 5-1: Human MDM2 and Murine MDM2 177
Figure 5-2: Effect of human-corresponding MDM2 mutation in murine cells.... 178
Figure 5-3: Generating a murine *Mdm2* I438K conditional point mutant allele 180
Figure 5-4: Genotyping of BMK primary cells 182
Figure 5-5: Effect of Cre recombination and nutlin-3 treatment in BMK primary cells 184
Figure 5-6: Effect of Cre recombination and doxorubicin treatment in BMK primary cells 185
Figure 5-7: Cells expressing *Mdm2* I438K mutant can quickly arrest cell cycle at the G_1 upon stress 186
Figure 5-8: Genotyping of MEFs 187
Figure 5-9: Effect of 4-OHT on inducible Mdm2 I438K knock-in system in MEFs 188
Figure 5-10: Effect of Cre recombination and nutlin-3 or doxorubicin treatment on cell growth 190

List of Accompanying Material

Parts of this work have contributed to the publication that is enclosed at the back of the thesis:

NOMURA, K., KLEJNOT, M., KOWALCZYK, D., HOCK, A. K., SIBBET, G. J., VOUSDEN, K. H. & HUANG, D. T. 2017. Structural analysis of MDM2 RING separates degradation from regulation of p53 transcription activity. *Nature Structural & Molecular Biology*, 24, 578-587.

Acknowledgement

I would like to express my gratitude to my supervisor Professor Karen H. Vousden for giving me the opportunity to carry out my PhD project in her lab and for her great support and guidance throughout my entire research project.

I wish to thank my secondary supervisors Professor Danny T. Huang and Dr Karen Blyth for fruitful discussions, helpful experimental advice and input of new ideas. Also I acknowledge Dr Douglas Strathdee and his group for discussions and the generation of a novel mouse model.

I am grateful to Drs Andreas K. Hock, Timothy J. Humpton and all R15 lab members who have patiently taught me all the relevant techniques, corrected my early mistakes and had always been a pillar of support and assistance.

I thank Cancer Research UK for funding this research (C596/A17196), and the Cancer Research UK Beatson Institute - Molecular Technology Services Unit and Biological Services Unit for all their excellent support for the work carried out in this project.

I am particularly grateful to my family for their irreplaceable help, support and encouragement. I would like to give special thanks to my wife Aneela and my son Renn for their endless patience and support.

Author's Declaration

The work described in this thesis was carried out in the Cancer Research UK Beatson Institute between October 2014 and September 2018. The work was carried out under the supervision of Professor Karen H. Vousden and funded by Cancer Research UK (C596/A17196).

This thesis is the result of my own work and includes nothing which is the outcome of work done in collaboration, except where specifically indicated in the text. It is submitted for the degree of Doctor of Philosophy (PhD) at the University of Glasgow and has not been submitted for a degree or other qualification at any other Universities.

Abbreviations

4-OHT	4-hydroxytamoxifen
ABL	Abelson murine leukaemia viral oncogene homologue
ActD	Actinomycin D
AKT	Protein kinase B (Ak-mouse thymoma)
AMP	Adenosine monophosphate
AMPK	AMP kinase
ANOVA	Analysis of variance
APC	Adenomatous polyposis coli
APC/C	Anaphase promoting complex/cyclosome
APF1	ATP dependent proteolytic factor 1
APPBP1	Amyloid precursor protein-binding protein 1
APS	Ammonium persulphate
ARF	Alternative open reading frame
ATCC	American Type Culture Collection
ATG	Autophagy-related protein (gene)
ATM	Ataxia telangiectasia mutated
ATP	Adenosine triphosphate
ATR	Ataxia telangiectasia and Rad3 related
B2M	ß-2 microglobulin
BAK	Bcl-2 homologous antagonist killer
BAX	Bcl-2-associated X protein
BCA	Bicinchoninic acid
BCL	B cell lymphoma
BCR	Breakpoint cluster region protein
BH3	Bcl-2 homology domain
BMK	Baby mouse kidney primary cells
bp	Base pairs
BRCA1	Breast cancer 1
BSA	Bovine serum albumin
Cas9	CRISPR associated protein 9
Caspase	Cysteine-aspartic proteases
CBL	Casitas B-lineage lymphoma
CBP	CREB-binding protein
CCR4	Carbon catabolite repressor 4
CD	Cluster of differentiation
CDC	Cell-division cycle protein
CDH	CDC20-like protein
CDK	Cyclin dependant kinase
CDKN	CDK inhibitor (gene)
cDNA	DNA complementary to mRNA (complementary DNA)
CHD	Chromodomain helicase DNA-binding
CHIP	Carboxyl terminus of Hsc70-interacting protein
ChIP	Chromatin immunoprecipitation
CHK	Checkpoint kinase
cIAP	Cellular inhibitor of apoptosis 1/2
CK1	Casein kinase 1
CML	Chronic myeloid leukaemia
CMV	Cytomegalovirus
CNOT4	CCR4-NOT transcription complex, subunit 4

CNS	Central nervous system
CO_2	Carbon dioxide
COP1	Constitutively photomorphogenic 1
CP	Catalytic particle
CPT1C	Carnitine palmitoyltransferase 1C
Cre	Causes recombination
CREB	cAMP-response element-binding protein
CRISPR	Clustered regularly interspaced short palindromic repeat
DAPI	4', 6-diamidino-2-phenylindole
DBD	DNA-binding domain
DFd	Degrees of freedom denominator
DFn	Degrees of freedom numerator
DMEM	Dulbecco's modified Eagle medium
DMSO	Dimethyl sulphoxide
DNA	Deoxyribonucleic acid
DNA-PK	DNA dependent protein kinase
Doxy	Doxycycline
DP1	Dimerisation partner 1
DR5	Death receptor 5
DRAM	Damage regulate autophagy modulator
DUB	Deubiquitinase
E1A	Adenovirus early region 1A
ECM	Extracellular matrix
EDTA	Ethylenediaminetetraacetic Acid
EGFR	Epidermal growth factor receptor
ELF4	E74 like ETS transcription factor 4
EMT	Epithelial-mesenchymal transition
ER	Endoplasmic reticulum
ER^{T2}	Oestrogen receptor T2
ETS	E26 transformation-specific
EV	Empty vector
FADD	Fas-associated protein with death domain
FAO	Fatty acid oxidation
FAS	First apoptosis signal receptor
FAT	HLA-F adjacent transcript 10
FANCL	Fanconi anaemia complementation group L
FBP	F-box protein
FBS	Foetal bovine serum
FBXW	F-box/WD repeat-containing protein
FDA	US Food and Drug Administration
FLI1	Friend leukemia integration 1 transcription factor
FLP	Flippase
FLT3	FMS like tyrosine kinase 3
FMS	Feline McDonough sarcoma
FOXO	Forkhead box O
FRT	Flippase recognition target site
GADD45	Growth arrest and DNA-damage inducible gene 45
GEMM	Genetically engineered mouse model
GFP	Green fluorescent protein
GLUT	Glucose transporter
GST	Glutathione S-transferase
HAUSP	Herpes-virus associated ubiquitin-specific protease

HECT	Homologous to E6-AP carboxyl terminus
HER2	Human epidermal growth factor receptor 2
HGFR	Hepatocyte growth factor receptor
HIF1α	Hypoxia inducible factor 1α
HLI	HDM2 ligase inhibitor
hMOF	Human males absent on the first
HPV	Human papilloma virus
HSP	Heat shock protein
HUB1	Homologous to ubiquitin-1
IARC	International Agency for Research on Cancer
IF	Immunofluorescence
IFN	Interferon
IKK	IκB kinase
IL-R	Interleukin receptors
IP	Immunoprecipitation
IRAK	Interleukin-1 receptor-associated kinase
IRF	Interferon regulatory factor
ISG	Interferon-stimulated gene
ITS	Insulin-transferrin-selenium
IκB	Inhibitor of NF-κB
JUN	v-jun avian sarcoma virus 17 oncogene homologue
KAT5	Lysine acetyltransferase 5
K_d	Dissociation constants
kDa	Kilo Daltons
KRAS	Kirsten-rat sarcoma protein
LAP	Leukaemia associated protein
LB	Lysogeny broth
LOH	Loss of heterozygosity
LoxP	Locus of X-over P1 site
LPIN1	Lipin 1
LSL	Lox-stop-lox
LUBAC	Linear ubiquitin chain assembly complex
MAPK	Mitogen-activated protein kinase
MAX	Myc-associated factor X
MCD	Malonyl-coenzyme A decarboxylase
MCL	Myeloid cell leukaemia sequence
MDM2	Murine/mouse double minute 2, also known as HDM2 (*Human* double minute 2)
MEF	Mouse embryonic fibroblast primary cells
MHC	Major histocompatibility complex
MHD	Malate dehydrogenase
Min	Multiple intestinal neoplasia mutation
miR	Micro-RNA
MKRN1	Makorin ring finger protein 1
MOPS	3-(N-morpholino) propanesulfonic acid
MSL2	Male specific lethal 2
MRN	Double strand break repair proteins MRE11, RAD50 and NBS1
mRNA	Messenger RNA
mTOR	Mammalian target of rapamycin
mTORC	mTOR Complex
MYC	v-myc avian myelocytomatosis viral oncogene homologue
MYCBP	Myc-binding protein

NAE	NEDD8 activating enzyme
NCBI	National Center for Biotechnology Information
NEDD	Neural precursor cell expressed developmentally down-regulated protein
NEM	N-Ethylmaleimide
NEMO	NF-κB essential modulator
NER	Nucleotide excision repair
NES	Nuclear export signal
NFAT1	Nuclear factor of activated T-cells 1
NF-κB	Nuclear factor kappa light chain enhancer of activated B cells
NHEJ	Non-homologous end joining
NLS	Nuclear localisation signal
N-MYC	MYC neuroblastoma homologue
NoLS	Nucleolar localisation signal
NOT	Negative on TATA
OD	Oligomerisation domain
P (value)	Probability value
PA	Poly-adenylation signal
PAGE	Polyacrylamide gel electrophoresis
PAI-1	Plasminogen activator inhibitor 1
PAM	Protospacer adjacent motif
PANK1	Pantothenate kinase 1
PARP	Poly [ADP-ribose] polymerase
PAX	Paired box
PBS	Phosphate buffered saline
PCAF	p300/CBP-Associated Factor
PCI	Phenol-chloroform-isoamylalcohol
PCR	Polymerase chain reaction
PD	Proline rich domain
PDAC	Pancreatic ductal adenocarcinoma
PDB	Protein Data Bank
PDGFR	Platelet-derived growth factor receptors
PDH	Pyruvate dehydrogenase
PDHK	PDH kinase
PDPK1	3-phosphoinositide-dependent protein kinase 1
PDX1	Pancreatic and duodenal homeobox 1
PFA	Paraformaldehyde
PFK	Phosphofructokinase
PHD	Plant Homeo Domain
PHLDA3	Pleckstrin homology-like domain family A member 3
PI3K	Phosphatidylinositol-4,5-bisphosphate 3-kinase
PIAS	Protein inhibitor of activated signal transducer and activator of transcription
PIG3	p53-inducible gene 3
PIRH2	p53-Induced RING H2 protein
PMAIP1	Phorbol-12-myristate-13-acetate-induced protein 1, also known as NOXA (Latin for *damage*)
PNS	Peripheral nervous system
PPi	Pyrophosphate
PPP	Pentose phosphate pathway
PRIMT	Protein arginine N-methyltransferase
PROTAC	Proteolysis targeting chimera

PSA	Prostate specific antigen
PTEN	Phosphate and tensin homologue
PTP	Permeability transition pore
PUMA	p53 upregulated modulator of apoptosis
qPCR	Quantitative real-time polymerase chain reaction
RAD	Radiation sensitive
RAF	Rapidly accelerated fibrosarcoma
RAS	Rat sarcoma
RanBP2	RAS-related nuclear protein binding protein 2
RB	Retinoblastoma protein
RBCK1	RanBP-type and C_3HC_4-type zinc finger-containing protein 1
RBP	RING-box protein
rcf	Relative centrifugal force
RCR	RING-cysteine-relay
RD	Regulatory domain
RING	Really interesting new gene
RIP	Receptor-interacting serine/threonine-protein
RITA	Reactivation of p53 and induction of tumour cell apoptosis
RNA	Ribonucleic acid
RNF	RING finger protein
ROS	Reactive oxygen species
RP	Regulatory particles
RPL	60S ribosomal protein
rpm	Rotations per minute
RPN	Regulatory particle non-ATPase
RPS	40S ribosomal protein
RPT	Regulatory particle triple-A ATPase
RRC	Regulator of chromosome condensation
RRM2B	Ribonucleoside-diphosphate reductase subunit M2 B
RTK	Receptor tyrosine kinase
S (unit)	Svedberg sedimentation coefficient
SAE	SUMO-activating enzyme
SASP	Senescence-associated secretory phenotypes
SCF	SKP1, Cullin-1, FBP containing complex
SD	Standard deviation
SDS	Sodium dodecyl sulphate
SEM	Standard error of the mean
SHARPIN	SH3/Ankyrin domain gene-associated RH domain-interacting protein
shRNA	Small hairpin RNA
siRNA	Small interfering RNA
SIZ	SAP (scaffold attachment factor, acinus, protein inhibitor of activated signal transducer and activator of transcription) and MIZ1 (Msx2-interacting zinc finger)
SKP	S-phase kinase-associated protein
SLC	Solute carrier
SMAD	Small mothers against decapentaplegic
SMURF	SMAD ubiquitination regulatory factor
SMYD	SET and MYND domain
SNP	Single nucleotide polymorphism
SP1	Specificity protein 1 transcriptional factor
SPR	Surface plasmon resonance

STR	Short tandem repeats
SUMO	Small ubiquitin-related modifier
SUV39H1	Suppressor of variegation 3-9 homologue 1
SV40	Simian virus 40
TAD	Transactivation domain
TAE	Transporter associated with antigen processing proteins
TAF9	Transcription initiation factor TFIID subunit 9
TBS	Tris-buffered saline
TC	Tandem cysteine
TCA	Tricarboxylic acid
TERT	Telomerase reverse transcriptase
TEMED	Tetramethylethylenediamine
TGFß	Transforming growth factor ß
TIGAR	*TP53* Induced glycolysis and apoptosis regulator
T_m	Melting temperature
TNFR	Tumour necrosis factor receptor
TOPORS	DNA topoisomerase 1 binding arginine/serine rich protein
Tp53	Tumour protein 53 (human p53 gene)
TPP	Tripeptidyl peptidase
TRAF	TNF receptor associated factor
TRET	Telomerase reverse transcriptase
TRIM	Tripartite interaction motif
Trp53	Transformation related protein 53 (mouse p53 gene)
Ub	Ubiquitin
UBA	Ubiquitin-like modifier activating enzyme
UBA52	Ubiquitin A-52 residue ribosomal protein fusion product 1
UBB	Ubiquitin B
UBC	Ubiquitin-Conjugating enzyme
UBC (gene)	Polyubiquitin-C
U-box	Ubiquitin fusion degradation 2 homology
UEV	Ubiquitin-conjugating enzyme E2 variant
UFD	Ubiquitin fusion degradation
UFM	Ubiquitin-fold modifier
URM	Ubiquitin-related modifier
USP	Ubiquitin-specific-processing protease
UTR	Untranslated region
UV	Ultraviolet
VEGF	Vascular endothelial growth factor
VHL	Von Hippel-Lindau
WB	Western blot
WHO	World Health Organisation
WT	Wild type
WWP1	WW domain containing E3 ubiquitin protein ligase 1
XPC	Xeroderma pigmentosum group C
YY1	Yin Yang 1
ZF	Zinc finger domain
ß-TRCP	ß-transducin repeat containing E3 ubiquitin protein ligase

Chapter 1 Introduction

1.1 The ubiquitin proteasome system

Removal of unneeded proteins from the cells is an important facet of the systems that regulate gene expression (and thereby gene function) and a critical mechanism for protein quality control. Indeed, elimination of damaged or misfolded proteins is essential as they are toxic to the cell in many cases. As a result, accumulation of these proteins contributes to the pathogenesis of many types of diseases including neurodegenerative diseases, inflammatory and autoimmune diseases, and cardiovascular diseases (reviewed in (Hartl, 2017)). On the other hand, excessive removal of proteins may also lead to the progression of disorders including muscle wasting diseases (reviewed in (Sandri, 2013)). Before the ubiquitin proteasome system was identified, protein removal was initially thought to rely mainly on lysosomal degradation. This involves hydrolytic degradation of all types of biological polymers including proteins, nucleic acids, carbohydrates, and lipids (reviewed in (Varshavsky, 2006)). In 1977, an adenosine triphosphate (ATP) dependent protein degradation mechanism in reticulocytes (immature red blood cells which lack lysosomes) was described (Etlinger and Goldberg, 1977). The following year, Aaron Ciechanover, a graduate student in Avram Hershko's Lab, found that a small protein called APF1 (ATP dependent proteolytic factor 1), which was subsequently identified as the ubiquitin polypeptide that had been discovered in 1975, is covalently conjugated to proteins before their degradation (Ciehanover et al., 1978). In the early 1980s, the basic mechanisms of the sequential enzymatic conjugation of ubiquitin to proteins (ubiquitination) were mostly revealed (Hershko et al., 1980, Ciechanover et al., 1982, Hershko et al., 1983). The importance of this discovery was quickly recognised and in 2004, Drs Aaron Ciechanover, Avram Hershko and Irwin Rose were awarded the Nobel Prize in Chemistry for the discovery of ubiquitin-mediated protein degradation.

1.1.1 Regulation of ubiquitin proteasome system

The ubiquitin proteasome system is responsible for at least 80 % of cellular protein degradation (Collins and Goldberg, 2017) and processed through a substrate specific, ATP-dependent and enzymatic reactions, which is tightly regulated (Komander and Rape, 2012). Ubiquitination, the post-translational modification of target proteins by ubiquitin conjugation, controls the activity of

nearly every cellular process, including regulations of the cell cycle and the cell signalling. While it was initially described as a mechanism for protein turnover, it is now clear that ubiquitin can be linked to substrates in several different ways, resulting in a complex code of substrate modification.

1.1.1.1 Ubiquitin

Ubiquitin is a highly conserved small regulatory protein consisting of 76 amino acids with a molecular weight of 8.5 kDa (Komander and Rape, 2012). It is encoded by 4 different genes: *UBA52* (Ubiquitin A-52 residue ribosomal protein fusion product 1), *RPS27A* (ribosomal protein S27a), *UBB* (Ubiquitin B) and *UBC* (Polyubiquitin-C) (Wiborg et al., 1985, Finley et al., 1989, Baker and Board, 1991). The gene product of ubiquitin is initially fused either to ribosomal proteins (*UBA52* and *RPS27A*) or to each other forming linear poly-ubiquitin chain (*UBB* and *UBC*) (Wiborg et al., 1985, Finley et al., 1989, Baker and Board, 1991). Subsequently, deubiquitinases (DUBs) cleave and produce a single unit of ubiquitin ending with di-glycine (GG) motif at the C-terminal (Komander et al., 2009). Ubiquitin contains 7 lysine residues (K6, K11, K27, K29, K33, K48 and K63) that allow the formation of ubiquitin chains (Figure 1-1). Linkages via K48 and K63 are most abundant (Kulathu and Komander, 2012). Ubiquitin can also be linked through the ubiquitin amino terminal (N-terminal) methionine residue (M1) (Kirisako et al., 2006).

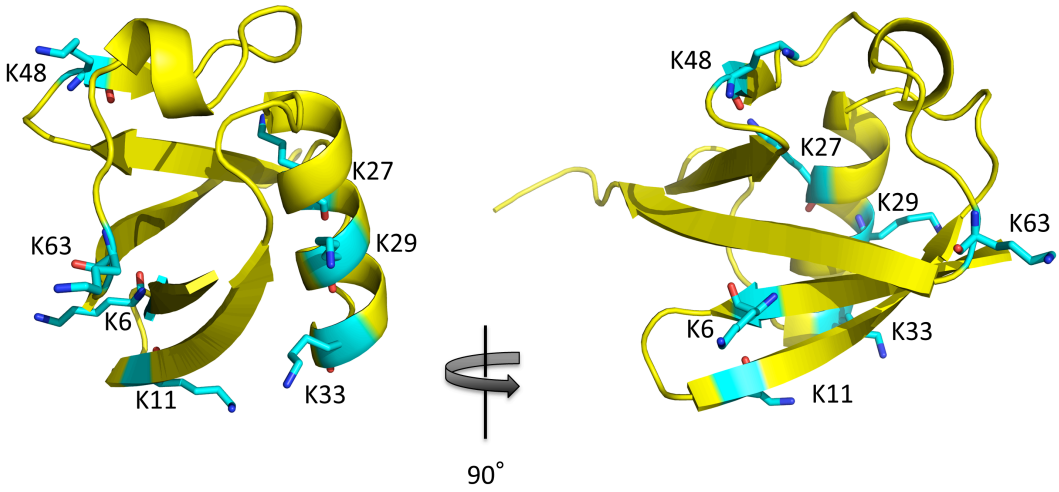

Figure 1-1: Structure of Ubiquitin

Ubiquitin contains 7 lysine residues (annotated in black). Ubiquitin chain can be formed through any of these residue and amino terminal methionine residue. Structure data is obtained from the Protein Data Bank (1UBQ) (Vijay-Kumar et al., 1987).

Ubiquitin conjugation can regulate a wide variety of processes, such as protein degradation, cell cycle progression and cell signal transduction; the outcome depending on the type of ubiquitination. Mono-ubiquitination and multiple mono-ubiquitination can regulate enzymatic activity, interaction and localisation of target proteins (reviewed in (Komander and Rape, 2012)) (Figure 1-2). K48-linked poly-ubiquitination marks target proteins for degradation by the 26S proteasome (Hershko and Ciechanover, 1992, Pickart, 2000) (Figure 1-2, also discussed in Section 1.1.1.3). K63-linked poly-ubiquitination chains are thought to alter activities during cell signalling and could lead to activation of NF-κB (Nuclear factor kappa-light-chain-enhancer of activated B cells), as well as to promote DNA repair or targeting to the lysosomal degradation (Thrower et al., 2000, Komander and Rape, 2012) (Figure 1-2). The first methionine residue (M1) of ubiquitin also allows the formation of a linear ubiquitin chain that is thought to be involved in regulating such as NF-κB activation and Wnt signalling transduction (Kirisako et al., 2006, Iwai and Tokunaga, 2009) (Figure 1-2, also discussed in Section 1.1.3.2). These different ubiquitin conjugations can be detected by ubiquitin receptors to mediate specific cellular processes, for example, shuttling ubiquitinated proteins to the 26S proteasome (reviewed in (Komander and Rape, 2012)). In addition, less well-understood poly-ubiquitination modes including mixed chains, branched chains and linear chains have been described (reviewed in (Komander and Rape, 2012)). The abundance of ubiquitin chains can be analysed with antibodies that specifically detect these linkages, mutagenesis analysis of ubiquitin by mutating lysine residue of it to arginine, or by quantitative proteomics.

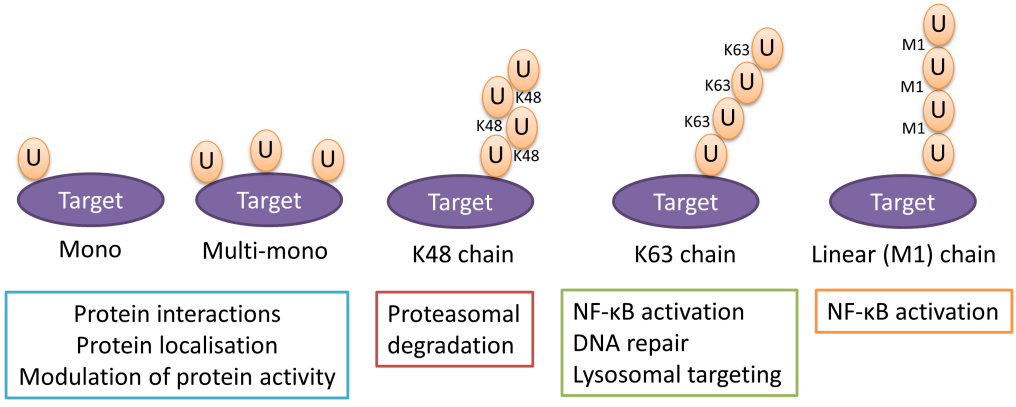

Figure 1-2: Overview of some patterns of ubiquitin conjugation and their functional outcomes

Types of ubiquitin conjugation are indicated. U = ubiquitin.

1.1.1.2 Enzymes involving in ubiquitination

Ubiquitin is attached to a protein by the sequential action of at least three enzymes: (1) E1 ubiquitin-activating enzyme, (2) E2 ubiquitin-conjugating enzyme, and (3) E3 ubiquitin ligase that is responsible for substrate specificity (Hershko and Ciechanover, 1998).

The process of ubiquitination begins with an E1 enzyme, which activates ubiquitin in an ATP-dependent manner. E1 recruits ATP-Mg^{2+} into the ATP binding site and through an acyl adenylation reaction, the C-terminal glycine of ubiquitin is non-covalently conjugated to E1 (via AMP with the support of the ubiquitin binding site on E1) (Tokgoz et al., 2006) (Figure 1-3).

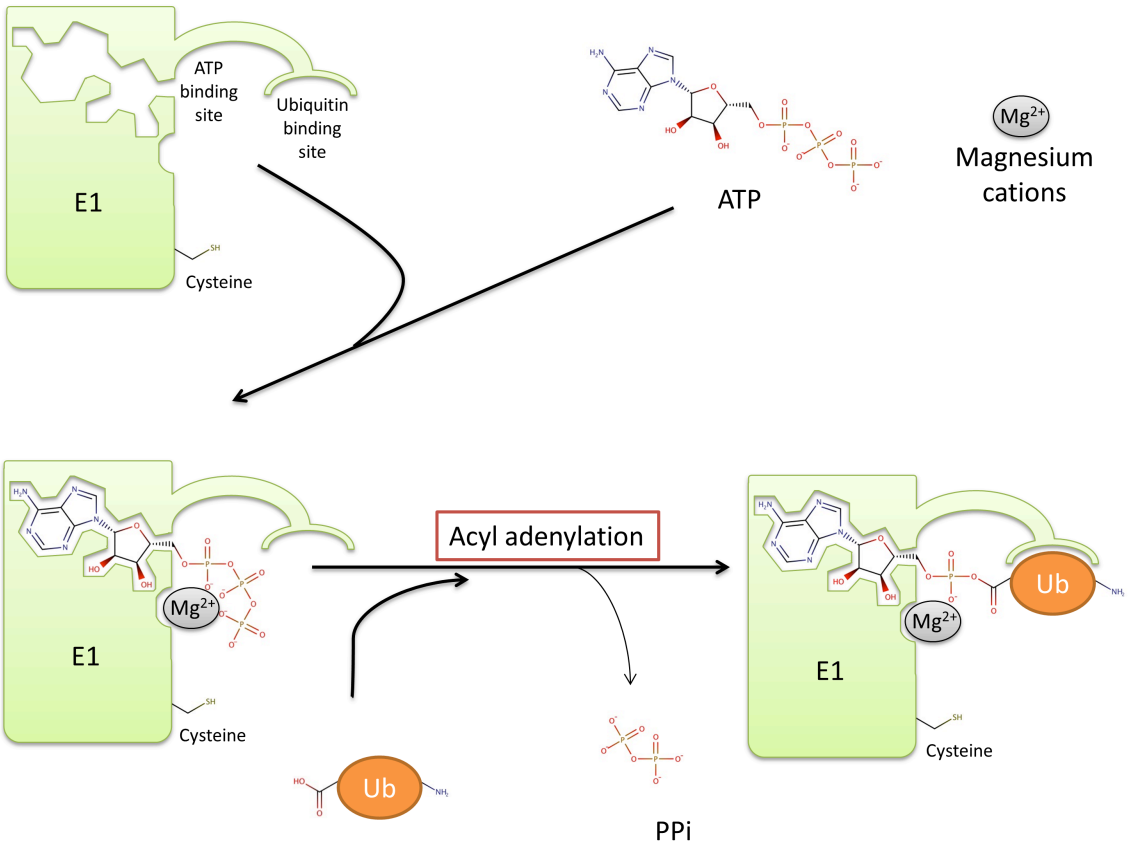

Figure 1-3: Acyl adenylation of ubiquitin by E1 ubiquitin activating enzyme

E1 = ubiquitin activating enzyme, ATP = adenosine triphosphate, Ub = ubiquitin and PPi = pyrophosphate.

Ubiquitin is then transferred to a cysteine residue on the E1 active site (acyl substitution) forming a high-energy thioester bond with the C-terminal glycine residue of ubiquitin (Tokgoz et al., 2006) (Figure 1-4). AMP is then released from the E1 (Figure 1-4). The E1 can also recruit another ATP for ubiquitin recruitment; so 2 ubiquitin molecules can be bound to the E1 at the same time. Although the function of the secondary-bound ubiquitin (through a non-covalent bond) is largely unknown, it has been reported that this may facilitate ubiquitin transfer to the E2 ubiquitin conjugating enzyme (Schulman and Harper, 2009).

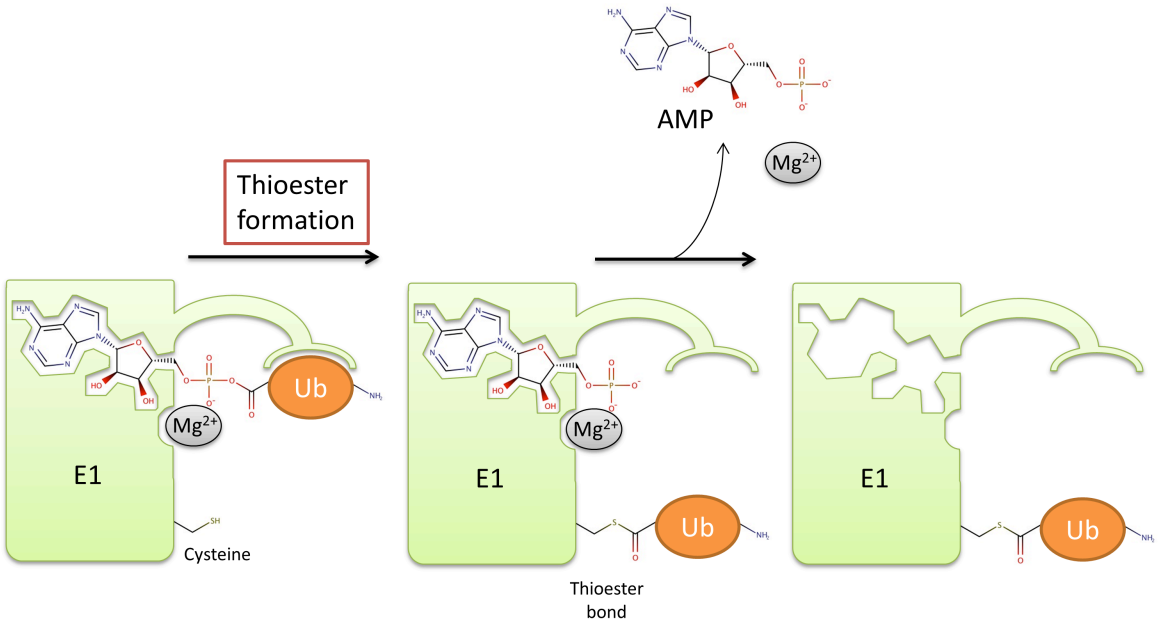

Figure 1-4: Thioester formation between the E1 cysteine residue and the ubiquitin C-terminal

E1= ubiquitin activating enzyme, AMP = adenosine monophosphate and Ub = ubiquitin.

The E1 then attaches the activated ubiquitin to a cysteine residue on an E2 enzyme through a trans-thioesterification reaction (Olsen and Lima, 2013) (Figure 1-5).

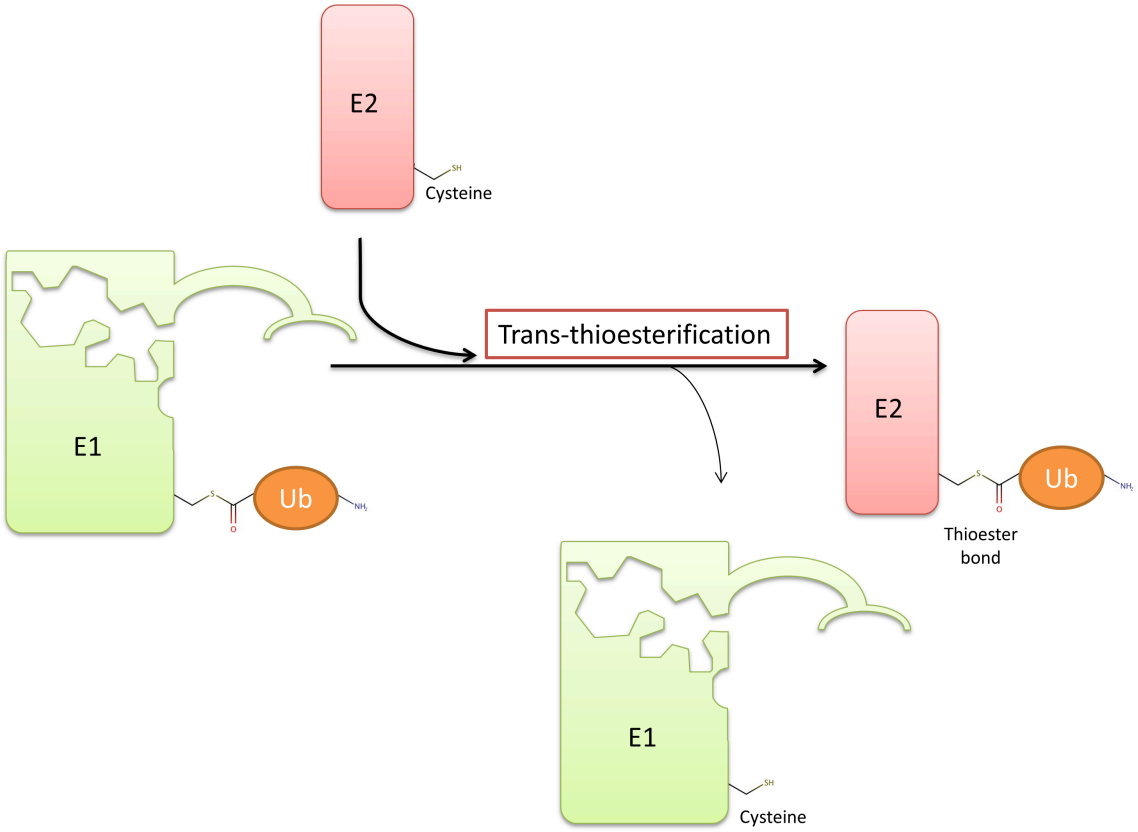

Figure 1-5: Trans-thioesterification of ubiquitin from E1 to E2
E1 = ubiquitin activating enzyme, E2 = ubiquitin conjugating enzyme and Ub = ubiquitin.

The E2-ubiquitin complex can then interact with the E3 ligase that is already bound to a protein substrate and, through isopeptide ligation reactions in the catalytic domain of the ligase, the E3 can transfer the ubiquitin from the E2 to an amino-group (mostly lysine residues) in the substrate via an isopeptide bond (Hershko and Ciechanover, 1998) (Figure 1-6). It is important to note that E3 ligases can also interact with E2-ubiquitin to form a "closed" conformation, which enhances the activity of ubiquitin transfer (Budhidarmo et al., 2012).

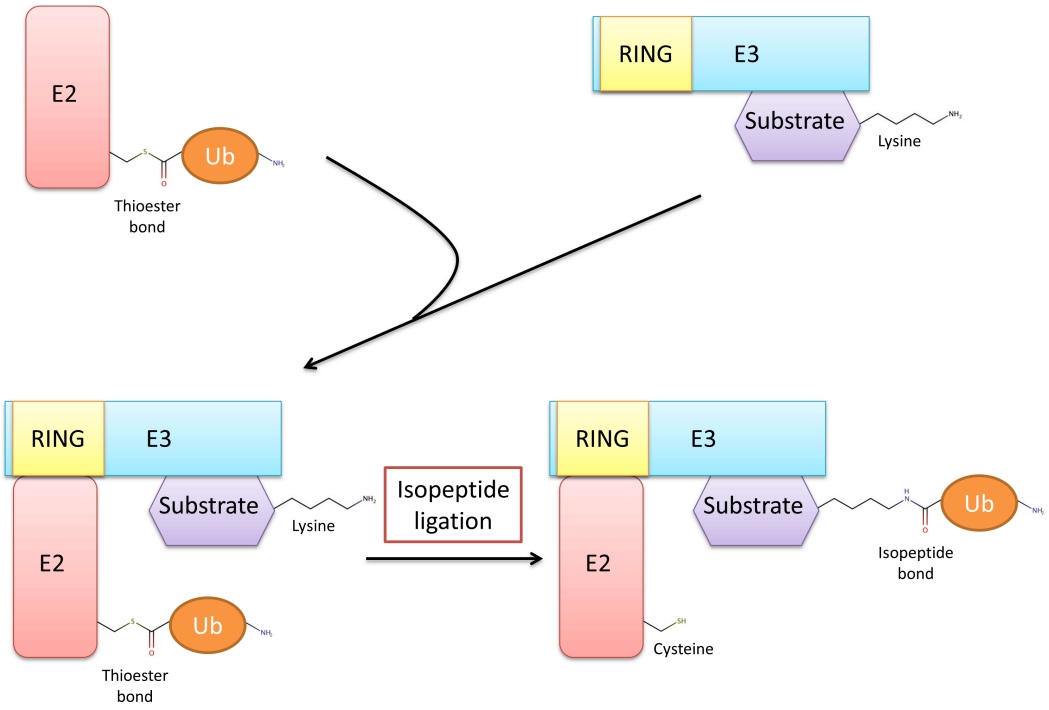

Figure 1-6: Isopeptide ligation of ubiquitin to the substrate by E3 ligase

E2 = ubiquitin conjugating enzyme, E3 = ubiquitin ligase (RING-type) and Ub = ubiquitin. Note that ubiquitin can also interact with E3 ligases.

This initially results in the mono-ubiquitination of proteins but these can re-enter the ubiquitination cycle resulting in poly-ubiquitination; ubiquitin is transferred to the lysine residue of ubiquitin that has already bound to the substrate, and further ubiquitins added to form chains (Hershko and Ciechanover, 1998, Pickart, 2000) (Figure 1-7).

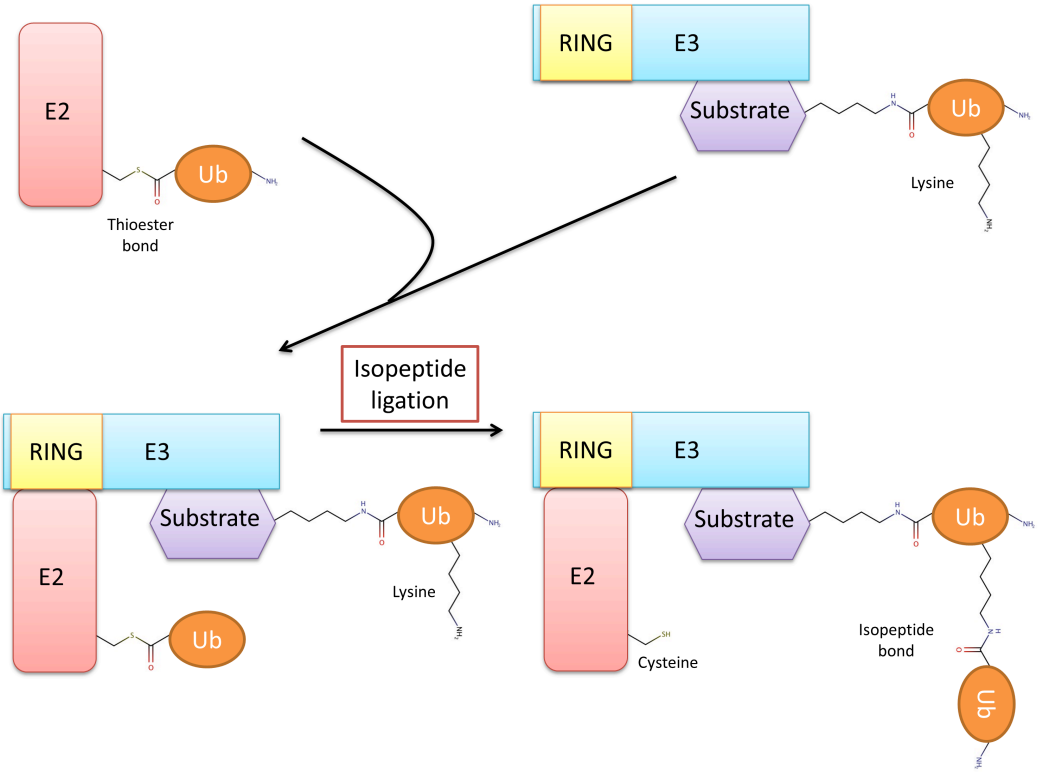

Figure 1-7: Poly-ubiquitination catalysed by E3 ligase
E2 = ubiquitin conjugating enzyme, E3 = ubiquitin ligase (RING-type) and Ub = ubiquitin.

The human genome encodes two E1 ubiquitin-activating enzymes, approximately 40 E2 ubiquitin-conjugating enzymes and more than 600 E3 ubiquitin ligases. E3 ligases are therefore believed to be primarily responsible for substrate specificity (Sun, 2006, Li et al., 2008), although some E3s can ubiquitinate multiple proteins targets.

Initially, UBA1 (Ubiquitin-like modifier activating enzyme 1) was thought to be the only E1 ubiquitin-activating enzyme in mammals but UBA6 was identified as an additional E1 for ubiquitin with different preferences for E2 ubiquitin conjugating enzymes (Pelzer et al., 2007, Jin et al., 2007).

Although E2 enzymes were thought to be promiscuous middle men in the ubiquitination process, it is now suggested that E2 enzymes play an important role in dictating the type and length of ubiquitin chain formed, and could also modulate target protein selection (Stewart et al., 2016). For example, it has

been reported that Ubc13 (Ubiquitin-conjugating enzyme 13)-UEV1A (Ubiquitin-conjugating enzyme E2 variant 1) complex mediates K63-linked, but not K48-linked, ubiquitination, whereas Ubc1, UbcH3 and Ubc7 from yeast mediate K48-linked ubiquitination (Hofmann and Pickart, 1999, Petroski et al., 2007, Petroski and Deshaies, 2005, Ryu et al., 2008). The activity of the E2 ubiquitin-conjugating enzymes is regulated through several mechanisms. One example is the conformational change of the E2–ubiquitin complex from an "open" state (little or no contact between E2 and ubiquitin) to "closed" state (contacts the crossover helix of E2 and the hydrophobic patch of ubiquitin) mediated by contact with an E3 ligase (Budhidarmo et al., 2012). Another example is the "backside" non-covalent binding of ubiquitin that enhances intrinsic lysine reactivity of the E2 (Brzovic et al., 2006, Buetow et al., 2015).

E3 ubiquitin ligases are classified into 3 major groups: (1) E3 ligases containing a RING (Really interesting new gene) domain and this group also includes the U-box (Ubiquitin fusion degradation 2 homology), (2) E3 ligases containing a HECT (Homologous to E6-AP carboxyl terminus) domain, and (3) E3 ligases containing RING-between-RING domain (Li et al., 2008).

RING E3 ligases are the largest and most abundant family (approximately 600 members in the human genome) of E3 ligases that contain a RING finger domain that is co-ordinated by 2 zinc atoms (Zn^{2+}) via eight conserved cysteines and histidines. The RING related E3 ligases including PHD (Plant homeo domain) finger protein and LAP (Leukaemia associated protein) finger protein are also belong to this group (Schindler et al., 1993, Saha et al., 1995, Deshaies and Joazeiro, 2009). These E3s interact with E2–ubiquitin complexes to catalyse the ubiquitin transfer from E2 to the lysine residue of the target protein directly (Joazeiro and Weissman, 2000) (Figure 1-8). Some RING E3 ligases, including MDM2 (Murine/mouse double minute 2 homologue) and BRCA1 (Breast cancer 1), are required to form homo- or hetero-dimers to display E3 ligase activity, whereas other E3 ligases including c-CBL (Casitas B-lineage lymphoma), CNOT4 (CCR4 (carbon catabolite repressor 4)-NOT (Negative on TATA) transcription complex, subunit 4) and RNF38 (RING finger protein 38) function as monomers (Zheng et al., 2000, Dominguez et al., 2004, Buetow et al., 2015, Buetow and Huang, 2016). The U-box E3 ligases are very similar to RING E3 ligases except

they lack the zinc-coordinating cysteine and histidine residues. Some of these also function by forming homo-dimers (Vander Kooi et al., 2006). In addition to these single subunit E3 ubiquitin ligases, there are also multi subunit E3 ubiquitin ligases, including the Cullin-RING E3 ligases and the anaphase promoting complex/cyclosome (APC/C) (Li et al., 2008). Cullin-RING E3 ligases comprise a Cullin protein, a RING-box protein (RBX1 or RBX2), an adaptor protein and a substrate recognition receptor (Lydeard et al., 2013, Petroski and Deshaies, 2005). The archetypical Cullin-RING E3 ligases contain SKP1 (S-phase kinase-associated protein 1), Cullin-1, FBP (F-box protein) and RBX1 (termed SCF-type E3 ligases). APC/C consists of 14 different subunits including APC2 (Cullin-like subunit), APC11 (RING domain-containing subunit) and a co-activator (Chang and Barford, 2014). In these complexes, the catalytic subunit that contacts to the E2–ubiquitin complex (RBX1 for SCF and APC11 for APC/C, for example) contain a RING domain, and as with other RING E3 ligases, directly transfers ubiquitin to the lysine residue of the target protein forming an isopeptide bond (Hershko and Ciechanover, 1998, Deshaies and Joazeiro, 2009) (Figure 1-8). The adapter and substrate recognition receptor (co-activator) subunits of these complexes can vary depending on the intracellular needs in order to target different protein for ubiquitination (Deshaies and Joazeiro, 2009).

A HECT domain is typically 40 kDa (350 amino acids) in size, forming a region homologous to that of E6-AP (a protein which was identified through association with p53 in the presence of the human papilloma virus E6 protein (Scheffner et al., 1990)). The human genome encodes 28 HECT E3 ligases (Scheffner and Kumar, 2014). These can also be further classified into 3 sub-families: (1) NEDD4 (Neural precursor cell expressed developmentally down-regulated protein 4) family HECT E3 ligases that contain WW domains (W for tryptophan), (2) HECT E3 ligases that contain an RCC1 (regulator of chromosome condensation 1)-like domain (termed HERC E3 ligases), and (3) HECT E3 ligases that contain neither WW domain nor RCC1-like domain (Scheffner and Kumar, 2014). Unlike RING E3 ligases, HECT E3 ligases accept the activated ubiquitin directly via a cysteine residue by forming a thioester bond and subsequently transfer it to the lysine residue of the substrate (Metzger et al., 2012) (Figure 1-8).

RING-between-RING-type E3 ligases contain 2 RING domains. There are 14 RING-between-RING E3 ligases identified so far (Marin et al., 2004). RING-between-RING ligases can function as hybrids of RING and HECT E3 ligases: the N-terminal RING domain (RING1) co-ordinates two Zn^{2+} atoms and interacts with an E2–ubiquitin complex, whereas the C-terminal RING (RING2) co-ordinates only one Zn^{2+} atom and first accepts ubiquitin via a thioester bond on its cysteine residue before transferring it to the lysine residue of the substrate (Wenzel et al., 2011) (Figure 1-8).

In addition, another type of E3 ligase: the RING-cysteine-relay (RCR) was recently described (Pao et al., 2018). RCR-type E3 ligases include MYCBP2 (Myc-binding protein 2) and unlike other E3 ligases, they catalyse non-lysine ubiquitination. First, they interact with E2–ubiquitin complex via their RING domain and accept ubiquitin via a thioester bond on their cysteine residue on the mediator loop in the tandem cysteine (TC) domain. Another cysteine residue within the TC domain then accepts ubiquitin via a thioester bond and ubiquitin is transferred to the threonine or serine residue (preference for threonine) of the substrate by forming an ester, instead of isopeptide bond (Pao et al., 2018) (Figure 1-8).

Single subunit E3 ligases:

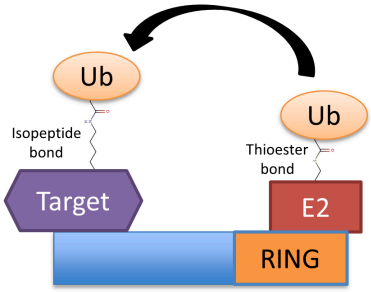

RING type E3 ligases

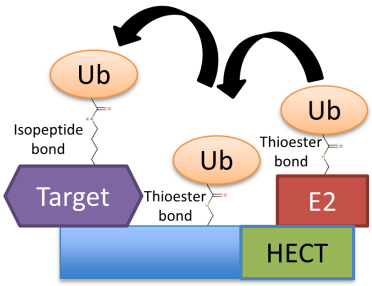

HECT type E3 ligases

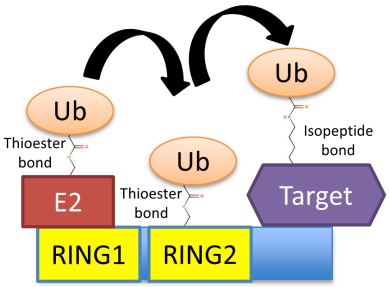

RING-between-RING E3 ligases

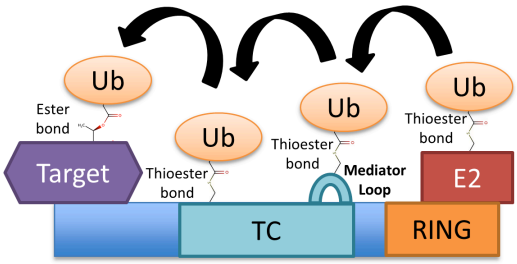

RING-cysteine-relay E3 ligases
(Non-lysine ubiquitination)

Multi subunit E3 ligases:

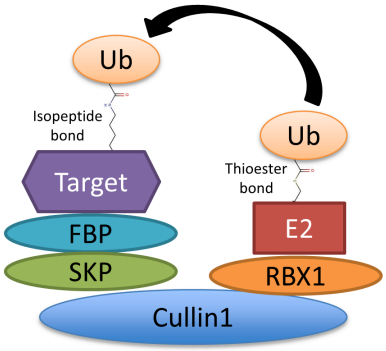

SCF type E3 ligase complexes

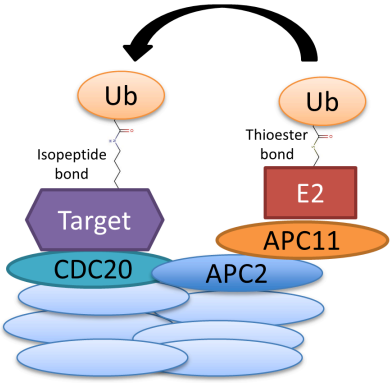

APC/C type E3 ligase complexes

Figure 1-8: Types of E3 ligases and their ubiquitin transfer

RING, SCF and APC/C directly transfer ubiquitin from E2 to the substrate. On the other hand, HECT-type and RING between-RING-type E3 ligases accept ubiquitin first through thioester bond on their cysteine residue and then transfer it to the substrate. The RING-cysteine-relay-type E3 ligases catalyse non-lysine ubiquitination. E2 = ubiquitin conjugating enzyme, Ub = ubiquitin, TC = tandem cysteine domain, RBX1 = RING-box protein 1, SKP = S-phase kinase-associated protein 1, FBO = F-box protein, APC = Anaphase promoting complex and CDC20 = Cell-division cycle protein 20. Types of ubiquitin conjugation are indicated.

Additional proteins, such as E4 ubiquitin chain elongating factors, have been shown to regulate poly-ubiquitination, but the details of their activity are not yet fully understood (Koegl et al., 1999). For example, UFD2 (Ubiquitin fusion degradation 2), which was originally classified as U-box-type E3 ligase, lacks its own substrate but promotes the poly-ubiquitination of another substrate of E3 ligases (Koegl et al., 1999). Furthermore, U-box E3 ligase CHIP (C-terminus of HSC70 interacting protein) and RING E3 ligase RAD5 (Radiation sensitive 5) also display E4-like activity, although they have their own E3 substrate (Pickart and Eddins, 2004). However, they may not be required for poly-ubiquitination as it occurs in cell free systems using a single E3 ligase (*in vitro* ubiquitination assay), suggesting that the E3 ligase itself is sufficient to poly-ubiquitinate its substrate.

1.1.1.3 The 26S proteasome

The 26S proteasome is a large (2,587,352 Da) multi-catalytic protease complex and plays a critical part in ubiquitin dependent proteolysis (Tanaka, 2009, Huang et al., 2016) (Figure 1-9a). It is located in both the nucleus and cytoplasm and recognises ubiquitinated proteins to degrade them into small peptides (Peters et al., 1994). The 26S proteasome is composed of a central 20S catalytic particle (CP) and one or two 19S regulatory particles (RP) (Tanaka, 2009, Huang et al., 2016) (Figure 1-9). Proteasomes containing one RP and a CP (RP1-CP) are "26S" (S for Svedberg sedimentation coefficient) and those containing two RPs and a CP (RP2-CP) are "30S", but both are generally referred to as the 26S proteasome.

The RP contains 6 ATPase subunits RPTs (Regulatory particle triple-A ATPase) and 13 non-ATPase subunits RPNs (Regulatory particle non-ATPase), and caps either or both sides of the CP (Tanaka, 2009). RPN10 and RPN13 are involved in the recognition of ubiquitinated substrates and RPTs are thought to regulate the entry of the ubiquitinated substrates into the CP by unfolding substrates via ATP hydrolysis (Schreiner et al., 2008). In addition, RPN11 regulates deubiquitination in an ATP-dependent manner (Verma et al., 2002). The removed ubiquitin molecules can be re-used (Tanaka, 2009).

The CP subunit forms a cylindrical stack of 4 layers (Tanaka, 2009, Huang et al., 2016) (Figure 1-9b). The 2 outer layers are composed of 7α subunits and the 2 inner layers 7ß subunits: each of these has distinct protease activities. For

example, β1 subunit functions as the caspase-like cysteine protease, β2 functions as the trypsin-like serine protease and β5 functions as the chymotrypsin-like serine protease (Tanaka, 2009, Huang et al., 2016) (Figure 1-9c). As a result, ubiquitinated substrates are hydrolysed into oligo-peptides (2-8 amino acids). Antigenic peptides processed by the proteasome (mainly by the immuno-proteasome) can be presented to the immune system on the major histocompatibility complex (MHC) class I molecules (Rock et al., 2002). These peptides are eventually degraded into a single amino acid by TPPII (Tripeptidyl peptidase II) or other amino-peptidases (Glas et al., 1998, Geier et al., 1999).

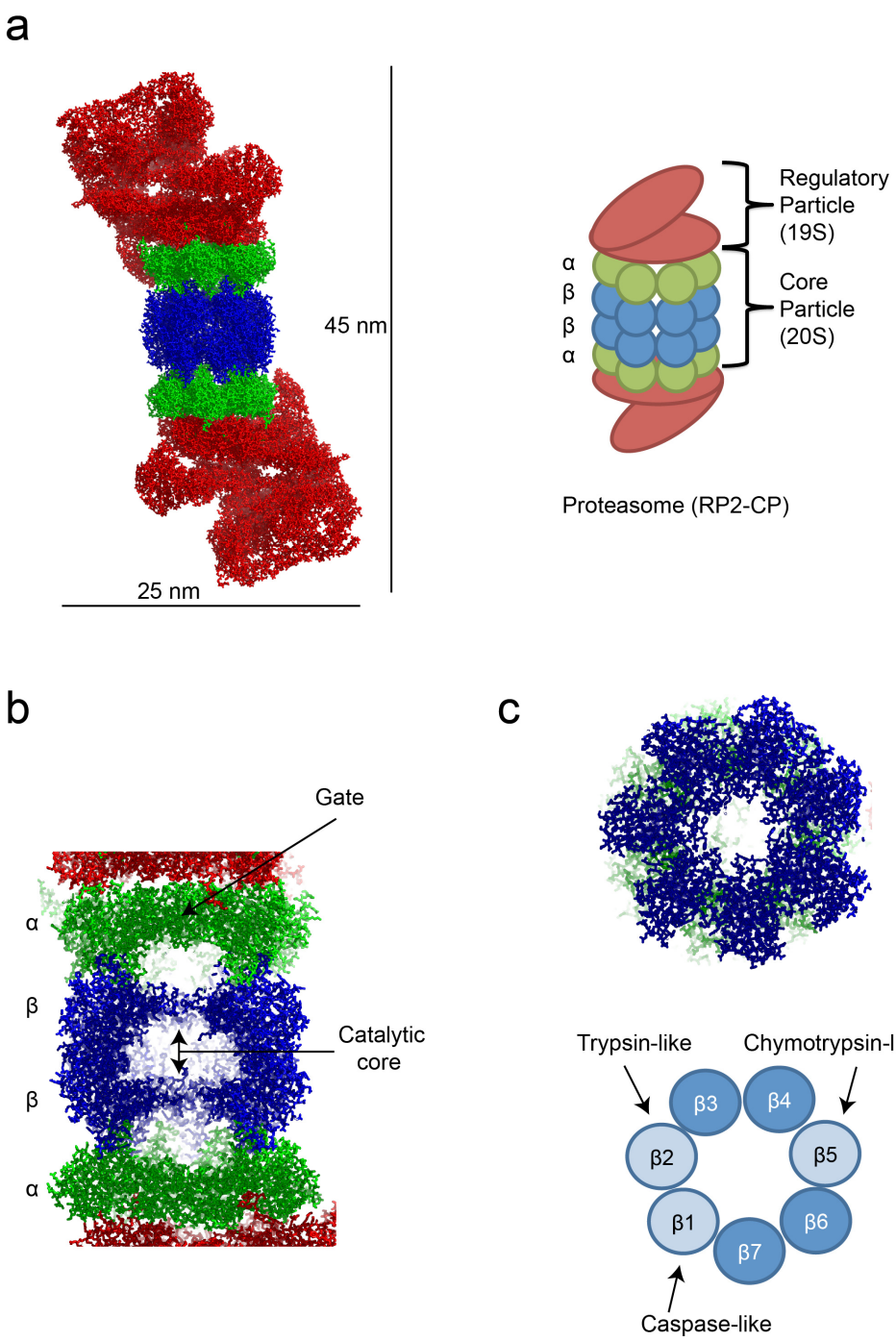

Figure 1-9: Structure and schematic model of 26S proteasome

(a) The regulatory particle (red), α subunits (green) and β subunits (blue). (b) Longitudinal section of the core particle. Gate and catalytic core are indicated. (c) Transverse section of β subunits and schematic model of β subunits. β1 subunit functions as caspase-like cysteine protease, β2 functions as trypsin-like serine protease and β5 functions as chymotrypsin-like serine protease. Structure data is obtained from Protein Data Bank (5GJR) (Huang et al., 2016).

It is generally thought that a ubiquitin chain of at least 4 ubiquitin subunits is required to function as a "tag" for 26S proteasomal degradation (Thrower et al., 2000). However, there are some exceptions, with evidence that mono-ubiquitination can be sufficient for proteasome recognition (Lam et al., 1997, Guterman and Glickman, 2004, Boutet et al., 2007). In fact, it has been demonstrated that small proteins (composed of less than 150 amino acids) with mono- or multiple-mono-ubiquitination can be degraded by 26S proteasome (Shabek et al., 2012). Recent works suggest that at least 4 molecules of ubiquitin, regardless of ubiquitination topology, are required for proteasomal degradation (Kirkpatrick et al., 2006, Lu et al., 2015a, Lu et al., 2015b). These studies demonstrated that cyclin B with a K48-linked tetra-ubiquitin chain, two K48-linked di-ubiquitin chains, or one K48-linked di-ubiquitin chain plus two mono-ubiquitinations showed no major differences in proteasome recognition and degradation kinetics. Interestingly, cyclin B with four mono-ubiquitinations can be recognised by 26S proteasome but not degraded. Thus, the results indicate that the number of ubiquitin subunits (at least 4 molecules) is important 26S proteasome recognition and the ubiquitin chain (at least one K48-linked di-ubiquitin chain) is required for degradation. Furthermore, substrate with K11-linked and, surprisingly, K63-linked ubiquitination can also be recognised and degraded by 26S proteasome in some situation (Saeki et al., 2009, Meyer and Rape, 2014, Kim et al., 2017). The structural stability of the substrate protein may also influence proteasomal degradation. It has been suggested that an unstructured region (20-30 amino acids) within the substrate is required to initiate efficient proteasomal degradation (Prakash et al., 2004, Inobe and Matouschek, 2014).

The proteasomes also play a critical role in the immune system. Pro-inflammatory cytokines such as IFN-γ (Interferon γ) induce alternative ß subunits ß1i, ß2i and ß5i, which substitute ß1, ß2 and ß5 respectively, and an alternative RP called PA28 (Proteasome activator 28) that does not contain RPTs, to form an immuno-proteasome (Brown et al., 1991, Glynne et al., 1991, Kelly et al., 1991, Ortiz-Navarrete et al., 1991). Antigenic peptides processed by this can be transported into the endoplasmic reticulum (ER) by the transporter associated with antigen processing proteins (TAEs) and then bound to MHC class I molecules (Rock et al., 2002). In addition, there is a thymus-specific proteasome, which

substitutes ß5 with an alternative ß subunit ß5t (which preferentially incorporates subunits ß1i and ß2i). This proteasome seems to be required to develop mature CD8-positive T-cells (cytotoxic T lymphocyte) (Murata et al., 2007, Kincaid and Murata, 2016).

1.1.1.4 Deubiquitination

It is also important to state that ubiquitination is a reversible process, and deubiquitinases (DUBs) remove (cleave) ubiquitin from proteins to further regulate their stability and function (Wilkinson, 1997, Reyes-Turcu et al., 2009, Komander et al., 2009). The human genome encodes approximately 100 DUBs that are classified as cysteine proteases or metalloproteases, which hydrolyse the isopeptide bonds of substrate-ubiquitin or ubiquitin-ubiquitin substrates and display both substrate and chain linkage specificities (Reyes-Turcu et al., 2009). DUBs have 3 main roles. One is to process ubiquitin precursors as discussed in Section 1.1.1.1. Second, DUBs can remove poly-ubiquitin chains from substrates and rescue proteins from degradation or reverse ubiquitin signaling (reviewed in (Komander et al., 2009)). Free poly-ubiquitin chains can also be deubiquitinated by DUBs into a single ubiquitin molecule so that it can be re-used (reviewed in (Komander et al., 2009)). And third, DUBs can edit the types of ubiquitin linkage (reviewed in (Komander et al., 2009)). For example, A DUB Ataxin-3 has been suggested to cleave K63 linkages in K48-K63 mixed linkage ubiquitin chains to ensure efficient proteasomal degradation (Winborn et al., 2008). Interestingly, DUBs can often be found in complexes with E3 ligases, which may contribute to limiting auto-ubiquitination of E3 ligase itself for degradation (de Bie et al., 2010, Xie et al., 2013, Sheng et al., 2006, Zou et al., 2014).

1.1.2 Ubiquitin-like proteins

In addition to ubiquitin itself, there are several ubiquitin-like proteins including NEDD8 and SUMO (Small ubiquitin-like modifier, including 4 confirmed isoforms SUMO-1, SUMO-2, SUMO-3 and SUMO-4) (reviewed in (Hochstrasser, 2009)) (Figure 1-10). These are structurally similar to ubiquitin, and like ubiquitin, they are attached to target proteins via an isopeptide bond catalysed by a series of enzymes in a reversible manner. Unlike ubiquitination, only one E2 and a limited number of E3s have been identified to be specifically involved in NEDD8

conjugation (NEDDylation) and SUMO conjugation (SUMOylation) to the target protein (reviewed in (Hochstrasser, 2009)). These modifications are thought to function mainly as a monomeric conjugation (mono-NEDDylation and mono-SUMOylation). However, *in vitro* results suggest that NEDD8 and SUMO proteins can be conjugated polymerically (Ohki et al., 2009, Yang et al., 2006b, Tatham et al., 2001).

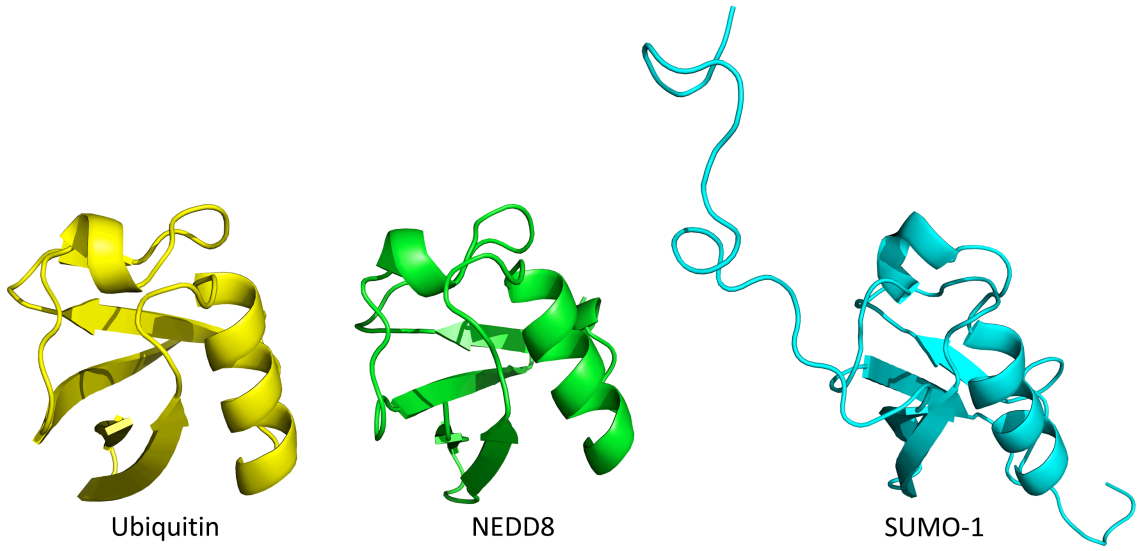

Figure 1-10: Structure of ubiquitin, NEDD8 and SUMO-1

Structure data is obtained from Protein Data Bank (Ubiquitin: 1UBQ (Vijay-Kumar et al., 1987), NEDD8: 1NDD (Whitby et al., 1998) and SUMO-1: 1A5R (Bayer et al., 1998)).

Modification with a UBLs begins with the action of a specific E1 activating enzyme complex; NEDD8 activating enzyme (NAE, a heterodimer composed of APPBP1 (Amyloid precursor protein-binding protein 1) and UBA3 (Ubiquitin like modifier activating enzyme 3) subunits) and SUMO activating enzyme (SAE, a heterodimer composed of SAE1 (SUMO-activating enzyme subunit 1) and UBA2 subunits), followed by an E2 conjugating enzyme (UBE2M (Ubc12) and UBE2F for NEDD8 or UBE2I (Ubc9) for SUMO) and then an E3 ligase (Liakopoulos et al., 1998, Huang et al., 2009, Johnson and Blobel, 1997). Several studies have demonstrated that NEDDylation can be catalysed by Cullin-RING E3 ligases containing RBX1 or RBX2 (Enchev et al., 2015) and SUMOylation can be catalysed by several proteins including RanBP1 (RAS-related nuclear protein binding

protein 1), SIZ1 (SAP (scaffold attachment factor, acinus, protein inhibitor of activated signal transducer and activator of transcription) and MIZ1 (Msx2-interacting zinc finger) 1), PIAS (Protein inhibitor of activated signal transducer and activator of transcription) family and ZNF451 (Gareau and Lima, 2010, Cappadocia et al., 2015).

Unlike ubiquitination, NEDDylation and SUMOylation do not directly target proteins for degradation. They are believed to be involved in modulating the interactions, localisation and activity of the target proteins, including the activity of some ubiquitin ligases. For example, NEDDylation of the Cullin subunit in the Cullin-RING E3 ligase complex stimulates binding of the E2 ubiquitin conjugating enzyme and augments its ubiquitination activity (Amir et al., 2002, Kawakami et al., 2001, Morimoto et al., 2000, Duda et al., 2008).

In general, the structure of the E2s (Ubc12 and Ubc9) is not compatible with interaction with E3 ubiquitin ligases; therefore, although a number of papers suggest that E3 ubiquitin ligases including MDM2 can catalyse SUMOylation and NEDDylation, it is unlikely that E3 ubiquitin ligases can catalyse transfer of UBLs under normal (physiological) condition (Professor Danny Huang *pers. comm.*, March 2018). Importantly, it has been reported when NEDD8 is overexpressed in cells it can be activated by the E1 ubiquitin activating enzyme UBA1, transferred to E2 ubiquitin conjugating enzymes and subsequently to a substrate via E3 ubiquitin ligases (Kim et al., 2011b, Hjerpe et al., 2012). For example, it has been reported that MDM2 catalyses NEDDylation of p53 under NEDD8 overexpressing condition (Xirodimas et al., 2004).

There are also numerous other ubiquitin-like proteins such ATG8 (Autophagy-related protein 8), ATG12, UFM1 (Ubiquitin-fold modifier 1), ISG15 (Interferon-stimulated gene 15), URM1 (Ubiquitin-related modifier-1), HUB1 (Homologous to ubiquitin-1) and FAT10 (HLA-F adjacent transcript 10). However, their E2s and/or E3s are yet to be fully identified (reviewed in (Hochstrasser, 2009)). Notably, ATG8 and ATG12 are activated by ATG7, which is an E1 activating enzyme that appears to regulate p53 response (discussed in Section 1.2.3.5).

1.1.3 Ubiquitin proteasome system and cancer

Each year, approximately 14.1 million people worldwide are diagnosed with cancer and 8.8 million die of their disease. Predictions made by WHO International Agency for Research on Cancer (IARC) suggest that the prevalence is expected to increase to 24 million in 2035.

Cancer is the result of the abnormal proliferation of "damaged" cells that have the ability to invade or spread throughout the body (Hanahan and Weinberg, 2011). In addition to general errors during DNA replication, accumulation of DNA damage by multiple stresses can cause genetic alternations of the cell. These may inactivate tumour suppressor genes or inappropriately activate proto-oncogenes (to become oncogenes) and contribute to tumourigenesis (Hanahan and Weinberg, 2011). Oncogenic mutations can be inherited or occur sporadically in somatic tissues. Large scale sequencing studies have shown that cancers are highly heterogeneous and subject to evolution over time, driving the emergence of increasingly malignant sub-clones or therapy resistance (reviewed in (Dagogo-Jack and Shaw, 2018)).

Tumour suppressor genes, such as *TP53* (which encodes p53), are negative regulators of cell proliferation (discussed in Section 1.2). They can be classified as either "caretaker genes" or "gatekeeper genes", or both (Pearson and Van der Luijt, 1998). Caretaker genes, such as *MSH2* (DNA mismatch repair mutator S homologue 2), indirectly suppress growth by allowing for effective repair of DNA damage or prevention of genomic instability (Mellon et al., 1996). On the other hand, gatekeeper genes, such as *RB* (Retinoblastoma susceptibility gene, which encodes pRB) and *APC* (Adenomatous polyposis coli), directly suppress tumour growth by regulating cell cycle progression and cell division (Murphree and Benedict, 1984, Nishisho et al., 1991). p53 has both caretaker and gatekeeper functions (discussed in Section 1.2.3 and Section 1.2.4). In general, loss-of function mutations within these genes are recessive, and therefore, alteration of both alleles is required for complete loss of the tumour suppressor function. Indeed, loss of heterozygosity (LOH), when one allele is mutated and the other is lost through a bigger deletion of the whole locus or through gene conversion, is frequently associated with the loss of tumour suppressor function (Cavenee et al., 1983).

Proto-oncogenes, such as *MYC* (v-myc avian myelocytomatosis viral oncogene homologue, which encodes c-MYC) or *JUN* (v-jun avian sarcoma virus 17 oncogene homologue, which encodes c-JUN), are positive regulators of normal cell growth (reviewed in (Croce, 2008)). They can become oncogenes by specific mutations that often lead to a change in their protein structure to be over-activated or by gene amplification, which increases protein levels (reviewed in (Croce, 2008)). In addition, chromosomal translocation can contribute to activate proto-oncogenes by hyper-expression of the gene or by producing hybrid proteins. For example, the Philadelphia chromosome produces an ABL1 (Abelson murine leukaemia viral oncogene homologue 1)-BCR (breakpoint cluster region protein) hybrid protein (known as BCR-ABL) as a result of chromosomal translocation between chromosomes 9 (where the *ABL1* gene is located) and 22 (where the *BCR* gene is located). This hybrid protein functions as a constitutively-active tyrosine kinase and therefore causes uncontrollable cell division leading to the chronic myeloid leukaemia (CML) (reviewed in (Cilloni and Saglio, 2012)).

In addition to genetic alternations, epigenetic modifications can also alter expression of the genes and contribute to tumour development (reviewed in (Iacobuzio-Donahue, 2009)). Gene expression can also be regulated post-transcriptionally by microRNAs, which are endogenous small non-coding RNA (approximately 22 nucleotide-long), and amplification and deletion and abnormal transcriptional control of microRNA genes are frequently found in cancers (reviewed in (Peng and Croce, 2016)). Although these altered cells are subject to elimination by body systems including the immune system, some cancer cells can evade elimination and form tumours, invade surrounding tissues and metastasise.

No cancers are identical between patients, but they share some common features, called "The hallmarks of cancer" (Hanahan and Weinberg, 2011) (Table 1-1). Although some of these are common in benign tumours, presence of all of them is thought to be required to form malignant tumours (Lazebnik, 2010).

Table 1-1: The hallmarks of cancer and the ubiquitin proteasome system

Capability	Examples of the involvement of ubiquitin proteasome system
Sustaining proliferative signalling	Degradation of Epidermal growth factor receptors (EGFRs).
Evading growth suppressors	Degradation of cyclin dependent kinase (CDK) inhibitors.
Resisting cell death	Regulation of apoptosis including degradation of pro-apoptotic Bcl-2 family members and death receptors. Regulation of anoikis including degradation of Caveolin-1.
Enabling replicative immortality	Degradation of the components of telomerase.
Inducing angiogenesis	Regulation of Vascular endothelial growth factor signalling. Degradation of hypoxia induced factors
Activating invasion and metastasis	Regulation of endothelial mesenchymal transition (EMT) including degradation of E-cadherin. Regulation of hepatocyte growth factor receptor (HGFR, also known as c-MET) signalling.
Deregulating cellular energetics	Regulation of glycolysis pathway. Regulation of AMP kinase (AMPK) activity.
Avoiding immune destruction	Regulation of NF-κB signalling. Activity of immunoproteasome.

The malfunction of the ubiquitin proteasome system is directly involved in the progression of many types of cancer by de-stabilising tumour suppressors such as p53, or by stabilising onco-proteins such as c-MYC (Ciechanover and Schwartz, 2004). For example, the overexpression of the RING E3 ligase *MDM2*, that degrades and represses the tumour suppressor p53, is associated with many tumours (discussed in Section 1.5). As the ubiquitin system controls the activity of nearly every cellular process, including cell cycle regulation, NF-κB activation and stress adaptation in hypoxia, it can also play a profound role in the control of tumourigenesis.

1.1.3.1 Cell cycle regulation

The cell cycle consists a series of stages including gap 1 (G_1) phase, DNA synthesis (S) phase, gap 2 (G_2) phase and mitosis (M) phase. This progress is tightly regulated by several cyclins and cyclin dependent kinases (CDKs) (Nigg, 1995). The ubiquitin-proteasome system is involved in the degradation of cyclins and CDK regulatory proteins. APC/C-type and SCF-type E3 ligase complexes are the key players in this process (Figure 1-11).

One important role of the ubiquitin-proteasome system in cell cycle regulation is to ubiquitinate cyclin B1 at the end of M phase, responding to the resolution of the spindle assembly checkpoint which ensures mitosis is completed before the degradation of cyclin B allows progress into G_1 (Sartor et al., 1992). The APC/C-CDC20 (cell-division cycle protein 20) complex is activated by CDK1 during this checkpoint and promotes ubiquitination of cyclin B1 (Kramer et al., 2000). It had been reported that increased expression of the SCF-SKP2 complex is associated with prostate and breast cancers (Mao et al., 2016, Karra et al., 2014). Deregulation of SCF-type E3 ligases is often found in cancers. The SCF-SKP2 complex degrades CDK inhibitor proteins including $p27^{Kip1}$ and p21 ($p21^{Cip1/Waf1}$) (Carrano et al., 1999, Carrano and Pagano, 2001, Bornstein et al., 2003). Aberrant degradation of CDK inhibitors lead to deregulation of cell cycle progression, resulting in uncontrolled proliferation. Amplification or overexpression of this complex is associated with many types of cancer including malignant melanoma, lymphoma, prostate and breast cancers (Rose et al., 2011, Latres et al., 2001, Yang et al., 2002, Zhang et al., 2016). On the other hand, some SCF-type E3 ligases appear to have tumour-suppressing function. In some cancers, cyclin E is overexpressed and SCF-FBXW7 (F-box/WD repeat-containing protein 7) complex ubiquitinates it for proteasomal degradation (Siu et al., 2012). Deletion or loss-of-function mutation of SCF-FBXW7 complex results in over-activation of cyclin E and shortening of G_1 phase, leading to premature S-phase entry, and is associated with cervical and gastric cancers (Ojesina et al., 2014, Milne et al., 2010). Interestingly, the RING-between-RING E3 ligase Parkin is also involved in cell cycle regulation by associating with CDC20 or CDH1 (DCD20-like protein 1) and deletion or loss-of-function mutation is associated with glioblastoma (Lee et al., 2015, Veeriah et al., 2010).

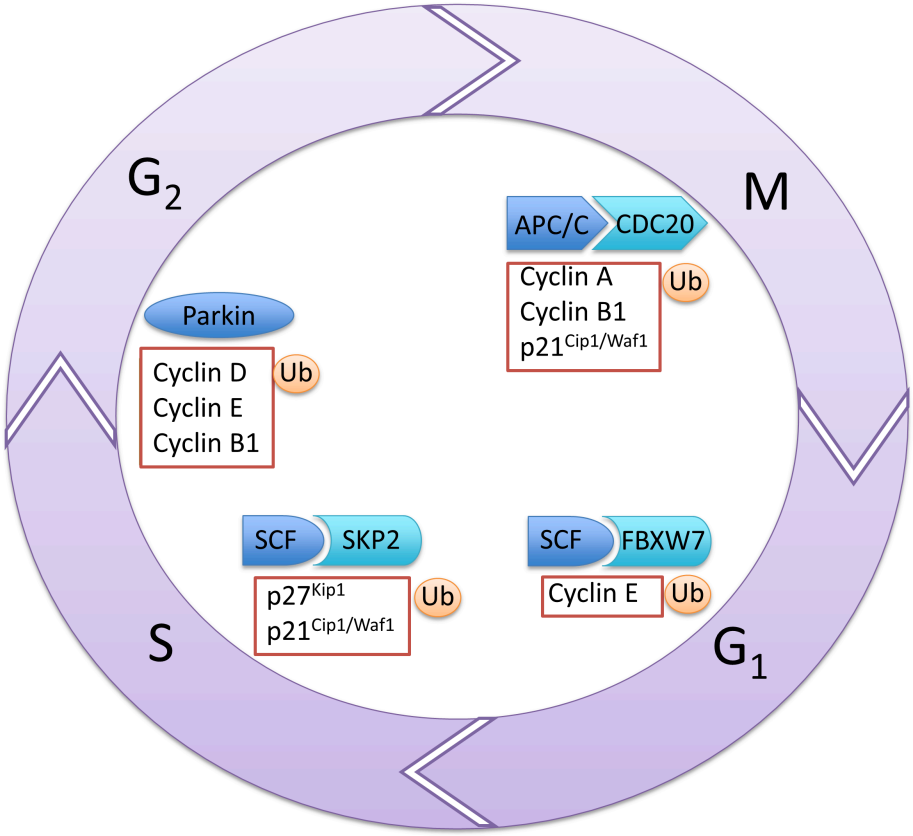

Figure 1-11: Cell cycle regulation by E3 ubiquitin ligases

The cell cycle is tightly regulated by ubiquitin proteasome system by regulating cyclins and CDK inhibitors level. G_1 = gap 1 phase, S = DNA synthesis phase, G_2 = gap 2 phase, M = mitosis phase, Ub = ubiquitin, SCF = SKP1, Cullin-1, FBP containing complex, SKP2 = S-phase kinase-associated protein 2, FBXW7 = F-box/WD repeat-containing protein 7, APC/C = Anaphase promoting complex/cyclosome and CDC20 = Cell-division cycle protein 20.

The transcription factor E2F1 is one of the most important regulators of the cell cycle program, which is restricted by the tumour suppressor pRB (Johnson and Schneider-Broussard, 1998) (Figure 1-12). Hypo-phosphorylated pRB binds to E2F1 to inhibit its transcriptional activity and the G_1-to-S promoting complexes cyclin D-CDK4/6 partially phosphorylate pRB and dissociate it from E2F1 (Resnitzky and Reed, 1995). E2F1 then binds to the transcriptional co-factor DP1 (Dimerisation partner 1), allowing the initiation of transcription to induce various genes including cyclin E, cyclin A, DNA polymerases and thymidine kinases (Ohtani et al., 1995). The cyclin E-CDK2 complex then hyper-phosphorylates and fully inactivates pRB, which contributes to the progress of cells into S phase (Resnitzky and Reed, 1995). In S phase, E2F1 is phosphorylated

by the S-to G_2 promoting cyclin A-CDK2 complex and dissociated from DP1. Phosphorylated E2F1 is then ubiquitinated by SCF-SKP2 (Marti et al., 1999, Meng and Ghosh, 2014). Interestingly, *SKP2* is one of the target genes for E2F1 (Zhang and Wang, 2006). In addition, pRB associates with APC/C-CDH1 and promotes SKP2 degradation (Binne et al., 2007). It has been reported that the decreased expression of CDH1 is found in breast cancer with SKP2 over-activation (Fujita et al., 2008).

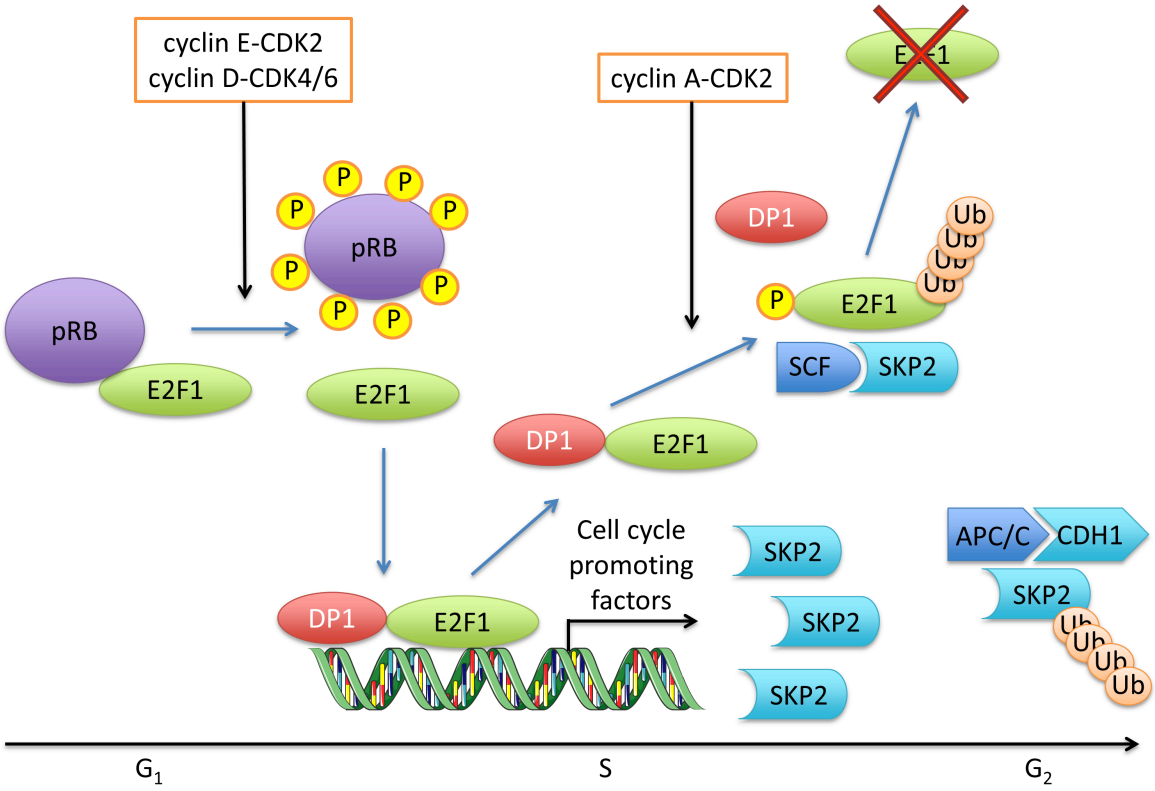

Figure 1-12: Regulation of E2F1 and SKP2 in cell cycle

pRB inhibits activity of E2F1 transcriptional factor. At the G_1 phase, pRB is hyper-phosphorylated by the cyclin D-CDK4/6 complexes, followed by the cyclin E-CDK complex. This allows E2F1/DP1 complex to transactivate cell cycle promoting factors and SKP2. At the S-phase, E2F1 is phosphorylated by cyclin A-CDK2 and DP1 is dissociated. Phosphorylated E2F1 is then ubiquitinated by SCF-SKP2 for degradation. SKP2 is also ubiquitinated by APC/C-CDH1 for degradation. G_1 = gap 1 phase, S = DNA synthesis phase, G_2 = gap 2 phase, P = phosphorylation and Ub = ubiquitin. Figure is adapted from Meng and Ghosh (2014).

1.1.3.2 NF-κB activation

NF-κB contributes to cell survival as well as to modulate the immune response. NF-κB is a transcription factor and there are two classes of NF-κB subunits: class I NF-κB (NF-κB1 and NF-κB2) and class II NF-κB (RelA, RelB and c-Rel) (reviewed in (Hayden and Ghosh, 2004)). NF-κB1 and NF-κB2 proteins are synthesised as large precursors, p105, and p100, which undergo selective degradation by the ubiquitin proteasome system to generate the mature NF-κB subunits, p50 and p52, respectively (reviewed in (Hayden and Ghosh, 2004)). NF-κB functions by forming homo- or hetero-dimers of class I NF-κB and class II NF-κB subunits - so far, dimeric complexes p50/RelA (the most abundant), RelA/RelA, RelA/c-Rel, RelA/p52, RelB/50, RelB/p52 c-Rel/c-Rel, p50/c-Rel, p52/c-Rel and p50/p50 have been described (reviewed in (Hayden and Ghosh, 2004)). NF-κB dimers are retained in the cytoplasm through interactions with IκB (Inhibitor of NF-κB). Upon stimulation, IκB dissociates from NF-κB dimers and NF-κB dimers enter the nucleus and subsequently transactivate target genes (reviewed in (Hayden and Ghosh, 2004)). This activation is tightly regulated by the ubiquitin proteasome system and many forms of ubiquitin chains are involved (reviewed in (Chen, 2005)) (Figure 1-13). NF-κB activation is mainly regulated by cytokine receptors including tumour necrosis factor receptors (TNFRs) and interleukin receptors (IL-Rs). The precursors of both cytokines TNFα and IL-1β are produced by macrophage and proteolytically activated by TNFα converting enzyme and caspase 1 respectively (Black et al., 1997, Raupach et al., 2006). These are then secreted in response to inflammatory stimuli. Upon IL-1β binding to the IL-Rs, IRAK1 (Interleukin-1 receptor-associated kinase 1) is ubiquitinated (K63-linked) by RING E3 ligase TRAF6 (TNF receptor associated factor 6) (Janssens and Beyaert, 2003). Similarly, upon TNFα binding to the TNFRs, RIP (Receptor-interacting serine/threonine-protein) kinases are ubiquitinated (K63-linked and K11-linked) by RING ubiquitin ligase TRAF2 and cIAP1/2 (Cellular inhibitor of apoptosis 1/2) (Devin et al., 2000). These ubiquitin chains may play an important role in activating the IKK (IκB kinase) complex composed of IKK1, IKK2 and NEMO (NF-κB essential modulator). The linear ubiquitin chain assembly complex (LUBAC), which is an E3 ubiquitin ligase complex composed of SHARPIN (SH3/Ankyrin domain gene-associated RH domain-interacting protein), RBCK1 (RanBP-type and C_3H-C_4-type zinc finger-containing protein 1, also known as HOIL-1) and the catalytic component RING-between-RING E3 ligase RNF31 (also

known as HOIP) ubiquitinates NEMO (M1-linked), which leads IKK2 phosphorylation (Iwai and Tokunaga, 2009). The IKK complex then phosphorylates IκB and it is ubiquitinated (K48-linked) by SCF-β-TRCP for proteasomal degradation (Winston et al., 1999). This allows NF-κB to enter the nucleus and transactivates target genes.

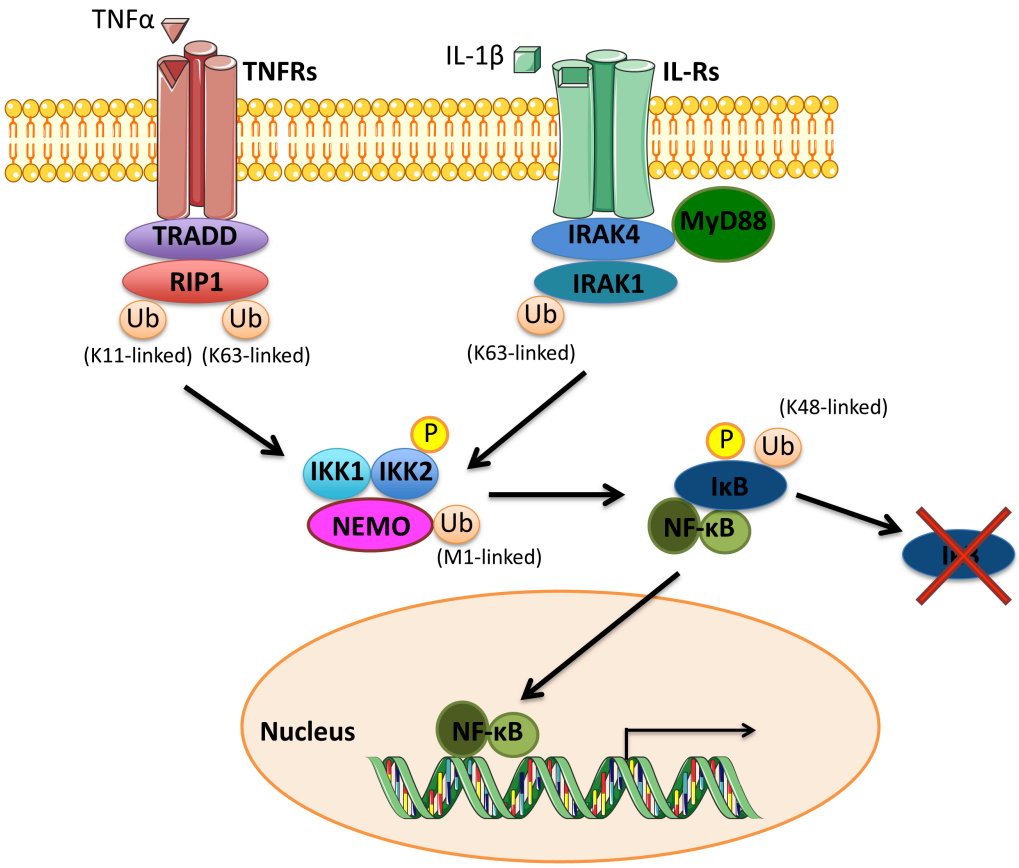

Figure 1-13: The canonical NF-κB activation pathway

K63-linked (and K11-linked) ubiquitination of IRAK1 and RIP1 leads to activate IKK complex. M1-linked ubiquitination of NEMO leads to IKK2 phosphorylation and phosphorylation of IκB. Phosphorylated IκB is then ubiquitinated (K48-linked) for proteasomal degradation, allowing NF-κB to enter nucleus. P = phosphorylation and Ub = ubiquitination (types of ubiquitination chains are indicated). Figure is adapted from Chen (2005).

Over-activation of NF-κB is frequently found in many types of cancers, with a clear contribution of the ubiquitin proteasome system. For example, increased expression of RNF31, a component of LUBAC, is observed in prostate cancer promoting abnormal cell proliferation, migration and invasion (Guo et al., 2015). Furthermore, several studies demonstrated that overexpression of cIAP1/2 is

involved in initiation of prostate, pancreatic and colorectal cancers (Krajewska et al., 2003, Esposito et al., 2007, Miura et al., 2009).

1.1.3.3 Stress adaptive regulation under hypoxia

The ubiquitin proteasome system plays fundamental role in stress adaptation. HIF1α (Hypoxia-inducible factor 1-alpha) is a subunit of the transcriptional factor HIF1 that plays an important role in response to systemic oxygen levels in cells. HIF1 transactivates more than 60 genes, including VEGF (Vascular endothelial growth factor) that is involved in angiogenesis, in order to promote oxygen delivery to hypoxic regions (reviewed in (Lee et al., 2004)). In addition, HIF1 regulates glucose metabolism by inducing most of the enzymes and receptors involve in the glycolytic pathway (reviewed in (Lee et al., 2004) also refer Section 1.2.3.4). Although *HIF1A* gene (which encodes HIF1α) is continuously expressed, HIF1α protein level is regulated by the tumour suppressor pVHL (von Hippel-Lindau tumour suppressor) that functions as an ubiquitin E3 ligase (as a part of Cullin-RING E3 ligase containing Elongin B, Elongin C, Cullin-2 and RBX1) under normoxic conditions (Tanimoto et al., 2000). Interaction of HIF1α with pVHL is regulated by prolyl-hydroxylation (the formation of hydroxyproline) of HIF1α catalysed by an oxygen sensor Procollagen-proline dioxygenase in an oxygen level dependent manner (Jewell et al., 2001). In response to hypoxia, the interaction with pVHL is disrupted, allowing the stabilisation of HIF1α, which hetero-dimerise with the other HIF1 subunit HIF1β and activates a transcriptional programme that regulates angiogenesis and glucose metabolism. This regulation is vital under hypoxic conditions, but may help tumour cells to survive. In fact, germline mutation of *VHL* (which encodes pVHL) causes von Hippel-Lindau syndrome, which is associated with tumours arising in multiple organs particularly in kidney (73 % of cases were renal angiomatosis (Ong et al., 2007)). In addition to VHL, SCF-FBXW7 also ubiquitinates HIF1α promoting proteasomal degradation, involving in a tumour suppression (Cassavaugh et al., 2011).

1.2 p53

p53, commonly referred to as "the guardian of the genome" (Lane, 1992), is one of the best studied tumour suppressing gene. It was first identified in 1979 as a cellular protein binding to the SV40 (simian virus 40) large tumour antigen (T-antigen) and was initially believed to be an "oncogene" as it was observed to be overexpressed and accumulated in the nuclei of tumour cells (Lane and Crawford, 1979, Linzer and Levine, 1979, Dippold et al., 1981). It has also been reported that p53 can form complexes with various proteins including the adenovirus E1B (Early region 1B), HSP70 (70 kDa heat shock protein) and the human papillomavirus types 16 and 18 E6 proteins (Sarnow et al., 1982, Pinhasi-Kimhi et al., 1986, Werness et al., 1990). However, in 1988, it has been confirmed that originally cloned mouse p53 was a tumour associated mutant version of p53 (Eliyahu et al., 1988, Finlay et al., 1988). 10 years after first discovery, p53 was finally recognised as a tumour suppressor that could suppress adenovirus E1A and RAS mediated transformation (Finlay et al., 1989). In addition, a series of studies in early 1990s has been demonstrated that p53 is required to induce cell cycle arrest or apoptosis in response to DNA damage (Kastan et al., 1991, Kastan and Kuerbitz, 1993, Lowe et al., 1993). Since then, p53 has been shown to be the most commonly mutated gene in cancers across a wide variety of tissues, with estimates of *TP53* alterations in up to 70 % of all cancers (Surget et al., 2013). Li-Fraumeni Syndrome, which is a cancer predisposition syndrome, was found to be due to germline mutations of *TP53* (Li and Fraumeni, 1969, Malkin et al., 1990, Malkin, 1993). *Trp53* (which encodes mouse p53) knockout mice are viable and appearing normal at birth but develop spontaneous neoplasms (mainly T-cell lymphoma) as early as 10 weeks of age (Donehower et al., 1992, Jacks et al., 1994). However, later studies revealed that *Trp53* knockout mice show some development abnormalities including neural tube-closure defects in female mice, depending on the strain (Armstrong et al., 1995, Sah et al., 1995, Choi and Donehower, 1999). It has been demonstrated that p53 can protect from radiation-induced birth defects and teratogenesis *in utero* (Baatout et al., 2002, Norimura et al., 1996). "Super p53" mice, carrying a p53 transgenic allele in addition to the endogenous alleles, display an increased DNA damage response and enhanced tumour resistance with normal ageing (Garcia-Cao et al., 2002). Similarly, "Super Arf/p53" mice, carrying an additional copy of $p19^{ARF}$ (discussed

in Section 1.3.4) and p53 alleles, showed delayed onset of ageing in addition to enhanced tumour resistance (Matheu et al., 2007). On the other hand, augmentation of wild type p53 by deleting exons 1-6 from 1 allele (*Trp53*$^{+/\Delta exons1-6}$), which cannot be negatively regulated by MDM2, enhances tumour resistance but accelerates ageing and shortens longevity (Tyner et al., 2002). In addition, it has been reported that inappropriate activation of p53 results in developmental disorders (Van Nostrand et al., 2014). Therefore, p53 is also referred to as a "double edged sword".

Under normal conditions, p53 is a short-lived protein that is continuously repressed and degraded by the action of MDM2. MDM2 can hetero-dimerise with MDMX, which is a related protein that does not have intrinsic E3 activity (discussed in Section 1.3.1). Although MDM2 homo-dimer can ubiquitinate p53, it is believed that MDM2 functions as a heterodimer with MDMX *in vivo* (Hock and Vousden, 2014). A wide variety of stresses, including oncogene activation, genotoxic damage, nutrient deficiencies and telomere erosion result in the stabilisation and activation of p53. Importantly, p53 can promote both cell death and cell survival. Depending on the stress, active p53 then induces target genes and microRNAs that can mediate a multitude of responses including cell cycle arrest, DNA repair, cell growth inhibition, metabolism and ROS regulation, senescence, ferroptosis, autophagy or apoptosis (Sullivan et al., 2012, Riley et al., 2008, Vousden and Lane, 2007, Hermeking, 2012, Bieging et al., 2014) (Figure 1-14).

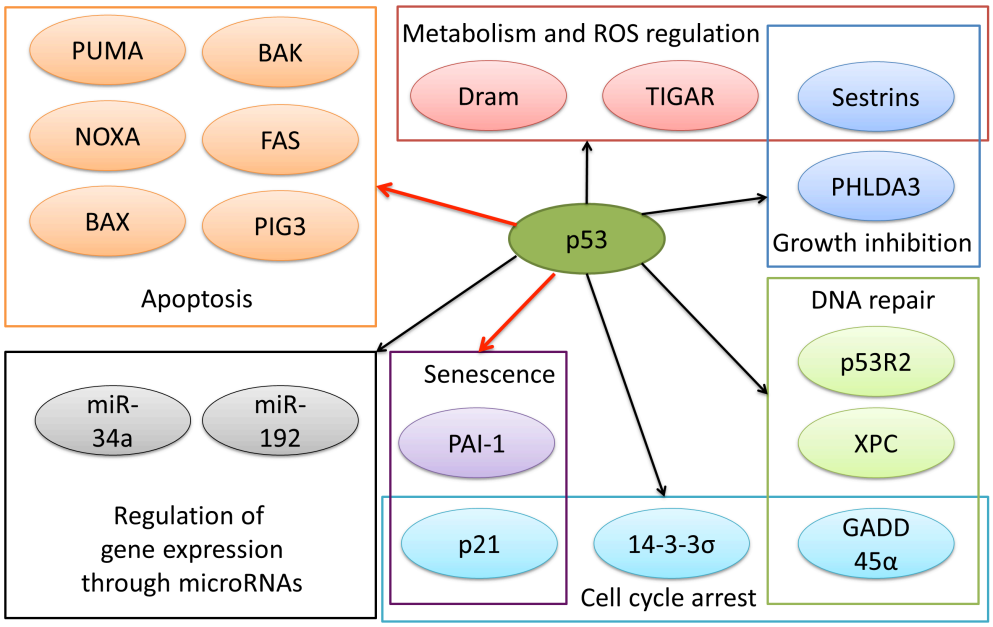

Figure 1-14: Functions of the tumour suppressor p53

Examples of p53 target genes are shown in boxes. Black arrows indicate the outcomes of p53 activation upon repairable stress and red arrows indicate the outcome of p53 activation upon non-repairable or oncogenic stimuli. Figure is adapted from Bieging *et al.* (2014).

In addition to its tumour suppression function, p53 has also been implicated in the development of various disorders including obesity, diabetes, ischaemia, and many forms of neurodegenerative diseases as it can induce cell death and regulate redox stress (Vousden and Lane, 2007, Vousden and Ryan, 2009).

1.2.1 Structure of p53

The human gene encoding p53 (*TP53*) is located on the short arm of chromosome 17 (locus 17p13.1) and contains 11 exons (of which 10 encode protein). Human p53 comprises 393 amino acid residues and functions as a transcriptional factor by forming a homo-tetramer. At the N-terminal, there are two distinct transactivation domains (TADI and TADII), followed by a proline rich domain (PD) and the core DNA-binding domain (DBD). At the C-terminal, there is a bipartite nuclear localisation signal (NLS), a nuclear export signal (NES) an oligomerisation (tetramerisation) domain (OD), and a lysine rich regulatory domain (RD) (Figure 1-15).

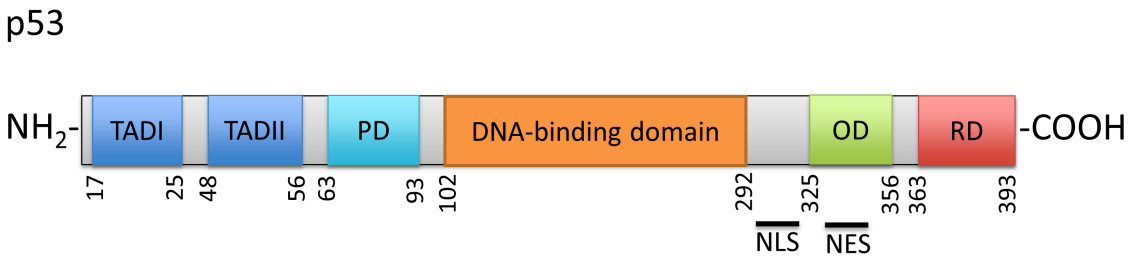

Figure 1-15: Functional domains of the p53 protein

TAD = transactivation domain, PD = proline rich domain, OD = oligomerisation domain, RD = Regulatory domain, NLS = nuclear localisation signal and NES = nuclear export signal. Generated from UniProt database (https://www.uniprot.org).

TADI and TAD II are responsible for the recruitment of proteins that are required for p53-mediated transcriptional activation, such as TAF9 (Transcription initiation factor TFIID subunit 9, also known as TAFII-31 (TATA-binding polypeptide associated factor)) (Lu and Levine, 1995). Although TADI is sufficient to induce some p53 target genes, both TADI and TADII are required to respond upon oncogenic stimuli such as acute DNA damage (Brady et al., 2011). The PD seems to be required for apoptotic signalling but not growth arrest (Sakamuro et al., 1997). Although the central core DNA-binding domain is required for sequence specific DNA binding, it is also strongly influenced by DNA topology (Kern et al., 1991, Jagelska et al., 2010, Jagelska et al., 2008). This region is highly conserved, containing 4 of the 5 conserved boxes that have been identified in p53 (the other, box I, is located in TADI). Numerous structural studies have shown that the integrity of these conserved boxes are crucial for DNA interaction (Pavletich et al., 1993, Cho et al., 1994, Kitayner et al., 2006, Gorina and Pavletich, 1996, Derbyshire et al., 2002, Joo et al., 2002). The oligomerisation domain is required to form a p53 homo-tetramer – the fully functional form of p53 (Jeffrey et al., 1995).

In addition to p53 motifs, the overall structural conformation and the DNA binding cooperativity of p53 may influence the selection of its target genes (Goh and Lane, 2012, Schlereth et al., 2010). These are regulated by several post-translational modifications of p53 (discussed in Section 1.2.5). Indeed, lysine residues in the DNA-binding domain seem to be important for the induction of

cell cycle arrest, senescence and apoptosis but not metabolic adaptation or ferroptosis (Li et al., 2012, Bieging et al., 2014).

1.2.2 p53 dysfunction

Loss of p53 function contributes to development of many types of cancer. There are mutations in the *TP53* gene in approximately 50 % of cancers which lead to the expression of mutant p53 or loss of p53 expression (Bullock and Fersht, 2001). Mutation rates of *TP53* in somatic cancers vary depending on the primary site of tumour (Figure 1-16) but in some cancers, such as high grade ovarian or triple negative breast, virtually all the tumours contain p53 mutations.

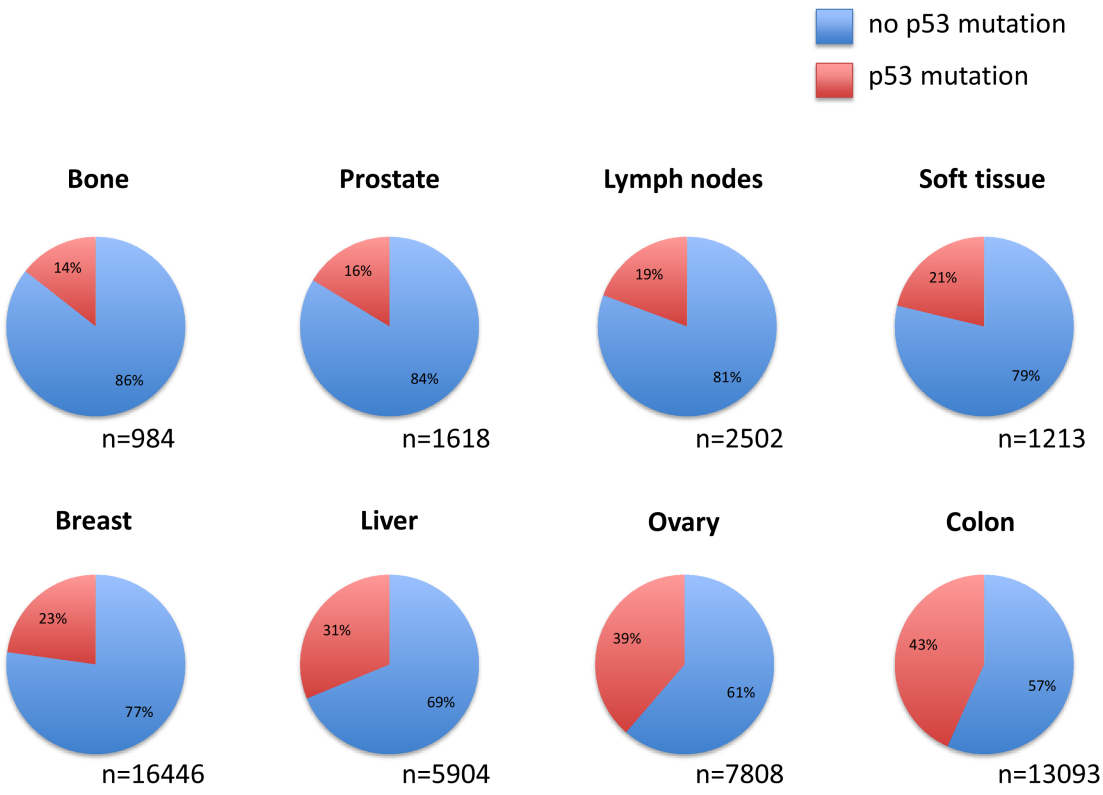

Figure 1-16: *TP53* mutation rates in somatic cancers at the primary site

n = number of cancers. Generated from the IARC TP53 database. Version R18, April 2016 (http://p53.iarc.fr).

According to the IARC TP53 database (version R18, April 2016), 73.2 % of somatic mutations in *TP53* are missense mutations. There are 6 most common "hotspot" missense point mutations of p53 in cancer; R175H, G245S, R248W/Q, R249S, R273C/H and R282W, all of which are located within the most conserved region of the DNA-binding domain (Figure 1-17).

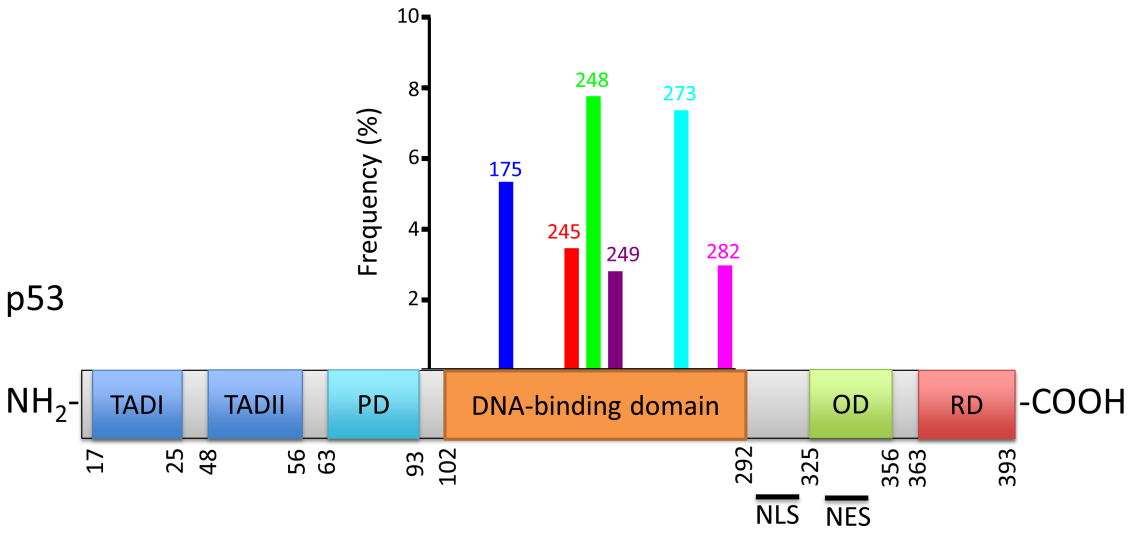

Figure 1-17: p53 mutation hotspots

The codon number of the 6 most common mutations (more than 2 % frequency) is given and their location in the p53 DNA-binding domain shown. TAD = transactivation domain, PD = proline rich domain, OD = oligomerisation domain, RD = Regulatory domain, NLS = nuclear localisation signal, NES = nuclear export signal. Generated from IARC TP53 database. Version R18, April 2016 (http://p53.iarc.fr).

R175H, G245S, R249S and R282W are classified as conformational mutants, which alter the structure of p53. R248W/Q and R273C/H are classified as contact site mutants, which involve a substitution of an amino acid that is critical for DNA contact. As a result, these mutants inhibit the tumour suppressive function of wild type p53 (loss-of-function) and/or potentiate oncogenic properties such as increased metastatic potential through an array of mutant specific activities including aberrant protein interactions or altered gene regulation (gain-of-function) (Lang et al., 2004, Olive et al., 2004). Interestingly, some of these mutants (R175H, R248W and R273H) exhibit a dominant negative effect over wild

type p53; suggesting that a mutation in one allele of *TP53* could be a trigger to initiate cancer (Willis et al., 2004).

1.2.3 Cell survival and repair functions of p53

In response to low levels of stress or damage, cells may primarily undergo cell cycle arrest to allow time for repair of damaged DNA prior to re-entry into the cell cycle. Once that has happened, p53 is deactivated and cells can resume proliferation. If the damage is too severe or the cell cannot adapt, p53 can trigger responses that eliminate the irreparably damaged cell. Examples of the functions of p53 upon repairable stress include cell cycle arrest, cell growth inhibition, DNA repair, metabolism and antioxidant and induction of autophagy.

1.2.3.1 Cell cycle arrest

p53 can inhibit cell cycle progression in multiple ways by transactivating cyclin dependent kinase inhibitors such as p21, GADD45α (Growth arrest and DNA damage 45α) and 14-3-3σ (Espinosa and Emerson, 2001) (Figure 1-18). This allows the affected cells to resolve the stress (Agarwal et al., 1995).

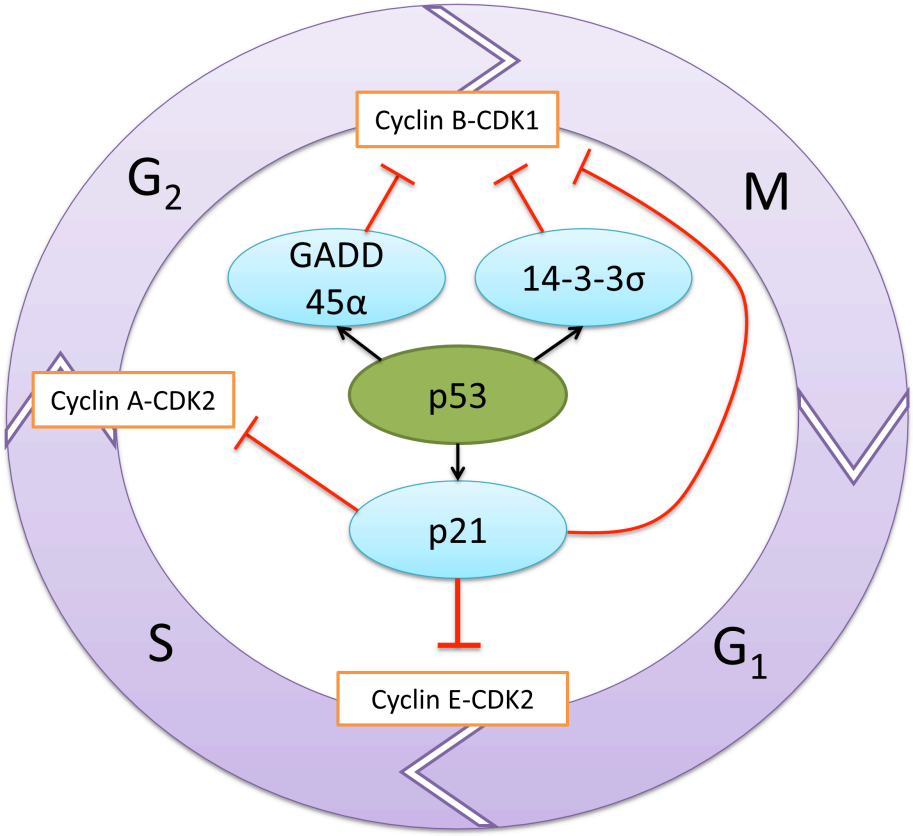

Figure 1-18: Role of p53 in cell cycle regulation

p53 transactivates target genes that inhibit activity of several cyclin-CDK complexes. G_1 = gap 1 phase, S = DNA synthesis phase, G_2 = gap 2 phase, M = mitosis phase and CDK = cyclin dependent kinase.

CDKN1A (cyclin-dependent kinase inhibitor 1A, which encodes $p21^{Cip1/Waf1}$) was one of the first discovered and best-studied p53 target genes. p21 directly inhibits the activity of the G_1-to-S promoting complex cyclin E-CDK2 so that cells cannot progress to S phase, because pRB remains hypo-phosphorylated and inhibits E2F1. Interestingly, however, p21 could promote tumourigenesis by promoting the assembly of the cyclin D-CDK4/6 complexes without inhibiting their kinase activity (LaBaer et al., 1997). In addition to G_1 arrest, p21 can also inhibit the S-to-G_2 promoting complex cyclin A-CDK2 and the G_2-to-M promoting complexes cyclin B-CDK1 and cyclin A-CDK1. Other p53 target gene products GADD45α and 14-3-3σ can also contribute to cell cycle arrest at the G_2 checkpoint by interfering with cyclin B-CDK1 complex formation and

sequestering cyclin B-CDK1 complex outside the nucleus, respectively (Zhan et al., 1999, Maeda et al., 2002, Laronga et al., 2000, Chan et al., 1999).

1.2.3.2 Cell growth inhibition

Cell growth is regulated through a number of cell signalling pathways such as the MAP (mitogen-activated protein) kinase signalling the PI3K (Phosphatidylinositol-4,5-bisphosphate 3-kinase), AKT (Protein kinase B) and mTOR (mammalian target of rapamycin) signalling pathways (Figure 1-19). These signalling pathways also regulate the activity of transcriptional factors FOXO (Forkhead box O) that are important regulators of cell death (Roy et al., 2010) (Figure 1-19). Deregulations leading to hyper-activation of these pathways are frequently involved in tumour development. Two mTOR complexes, mTORC1 and mTORC2, play distinct roles; mTORC1 acts as nutrient, energy and redox sensor and promotes protein synthesis while mTORC2 phosphorylates and activates AKT (Sabatini, 2017) (Figure 1-19). The activity of mTORC1 is monitored by AMPK (5' adenosine monophosphate-activated protein kinase) and is responsible for the autophagy regulation (Kim et al., 2011a) (Figure 1-19, also discussed in Section 1.2.3.5). p53 regulates cell growth by inducing the expression of proteins such as PHLDA3 (Pleckstrin homology-like domain family A member 3) and Sestrins. Sestrins are involved in lowering ROS levels to limit DNA damage and resulting genomic instability (Budanov et al., 2004, Sablina et al., 2005). AKT can be activated by PDPK1 (3-phosphoinositide-dependent protein kinase 1), a downstream effector of PI3K, and promotes cell growth in numerous ways. PHLDA3 attenuates this AKT activity and halts cell growth (Kawase et al., 2009) (Figure 1-19). Sestrins can attenuate mTORC1 activity through AMPK activation (p53 also directly activates expression of AMPK) and subsequently inhibit cell growth (Budanov and Karin, 2008) (Figure 1-19). In addition, it has been reported that p53 directly transactivates the tumour suppressor PTEN (Phosphatase and tensin homologue) that negatively regulates AKT pathway and the FOXO transcriptional factors to attenuate cell growth pathways (Figure 1-19).

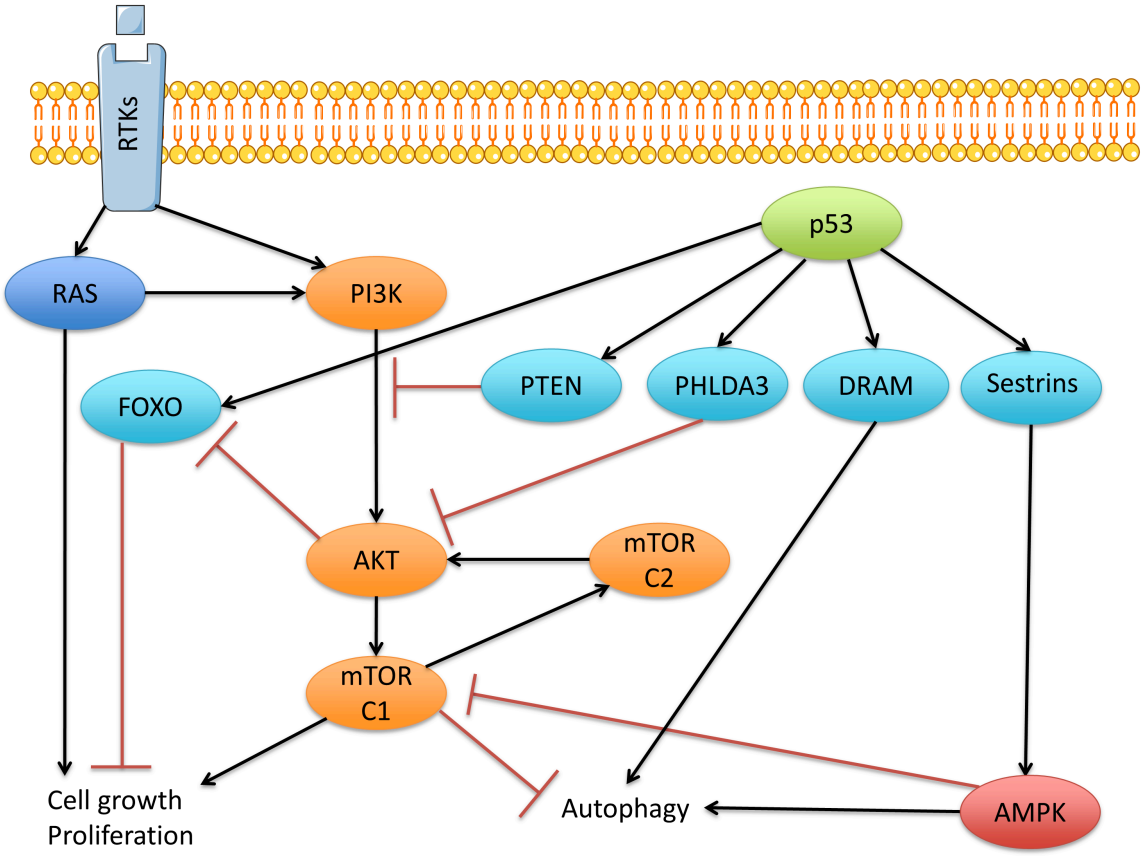

Figure 1-19: Example of the regulation of cell growth and autophagy by p53

Cyan: p53 target genes. RTKs = receptor tyrosine kinases, RAS = rat sarcoma protein, PI3K = phosphatidylinositol-4,5-bisphosphate 3-kinase, AKT = protein kinase B, mTORC = mammalian target of rapamycin complex, FOXO = forkhead box O, AMPK = 5' adenosine monophosphate-activated protein kinase, PTEN = phosphatase and tensin homologue, PHLDA3 = pleckstrin homology-like domain family A member 3 and DRAM = damage-regulated autophagy modulator.

1.2.3.3 DNA repair

The p53 target gene products p53R2 (also known as RRM2B, Ribonucleoside-diphosphate reductase subunit M2 B) and XPC (Xeroderma pigmentosum group C) are induced after DNA damage to promote DNA repair and maintain genomic stability. p53R2 encodes a subunit of ribonucleotide reductase and XPC encodes a component of the nucleotide excision repair (NER). In addition, p53 can activates PARP1 (Poly [ADP-ribose] polymerase 1), which detects and promotes the repair of single-strand DNA breaks, in response to ROS-induced DNA damage. GADD45α is also involved in DNA repair by acting as an adaptor between chromatin and repair factors (Niehrs and Schafer, 2012).

1.2.3.4 Metabolism and antioxidant

Nutritional stresses trigger p53 activation through activation of AMPK, MDH1 (malate dehydrogenase 1) and ribosomal proteins, for example. As a result, p53 plays a critical role in regulating energy metabolism to conserve energy by lowering rates of glycolysis and supporting mitochondrial respiration (reviewed in (Kruiswijk et al., 2015)) (Figure 1-20).

p53 suppresses transcription of SLC2A1 (Solute carrier family 2 member 1, also known as GLUT1, glucose transporter type 1) to downregulate cellular glucose uptake (Zhang et al., 2013). In addition, p53 indirectly suppresses another glucose transporter SLC2A3 (also known as GLUT3) by attenuating NF-κB (Kawauchi et al., 2008) (Figure 1-20).

p53 induces the expression of TIGAR (TP53-inducible glycolysis and apoptosis regulator), an enzyme involved in reducing fructose-2,6-bisphosphate levels so limiting glycolysis and rechanneling glucose derived carbons into the oxidative pentose phosphate pathway (oxPPP) (Bensaad et al., 2006) (Figure 1-20). The oxPPP is a major source of nicotinamide adenine dinucleotide phosphate (NADPH) that contributes to the limitation of cellular reactive oxygen species (ROS) by recycling reduced glutathione (GSH). In addition, p53 can directly inhibit expression of another enzyme called PGM (phosphoglycerate mutase) to limit glycolysis (Kondoh et al., 2005) (Figure 1-20). Furthermore, p53 indirectly downregulates enzymes involving in glycolysis through induction of a number of microRNAs such as miR-34a that represses the hexokinase1, the hexokinase 2 and the glucose-6-phosphate isomerase (Kim et al., 2013). Therefore, activation of p53 results in lowering both glucose flux to pyruvate (as a result of limiting glycolysis) and ROS.

Acetyl-coenzyme A (Acetyl CoA), which is generated from pyruvate by PDH (Pyruvate dehydrogenase), can enter the tricarboxylic acid (TCA) cycle and promote mitochondrial respiration. p53 indirectly promotes Acetyl CoA production by inhibiting expression of PDK2 (PDH kinase 2) which negatively regulates PDH (Contractor and Harris, 2012) (Figure 1-20). In addition, p53 can induce Parkin, which augments the expression of an important PDH subunit

PDHA1 (Pyruvate Dehydrogenase E1 Alpha 1 Subunit) and promotes the formation of PDH (Zhang et al., 2011) (Figure 1-20).

Furthermore, p53 promotes catabolic reactions such as fatty acid oxidation (FAO) while blocking anabolic reactions such as fatty acid synthesis. p53 transactivates CPT1C (Carnitine palmitoyltransferase 1C), an important transporter of fatty acids into mitochondria upon nutrient deprivation (Sanchez-Macedo et al., 2013) (Figure 1-20). Enzymes involving FAO including MCD (Malonyl-CoA decarboxylase), LPIN1 (Lipin 1) and PANK1 (Pantothenate kinase 1) are also transactivated by p53 upon nutrient deprivation (Liu et al., 2014, Assaily et al., 2011, Wang et al., 2013) (Figure 1-20). Elevated FAO results in increased oxidative phosphorylation, which sustains ATP levels and promotes cell survival during nutrient deprivation (Sanchez-Macedo et al., 2013).

Overall, in response to nutrient stress, p53 helps conserve energy while mobilising alternative fuel sources in addition to promoting autophagy (discussed in Section 1.2.3.5).

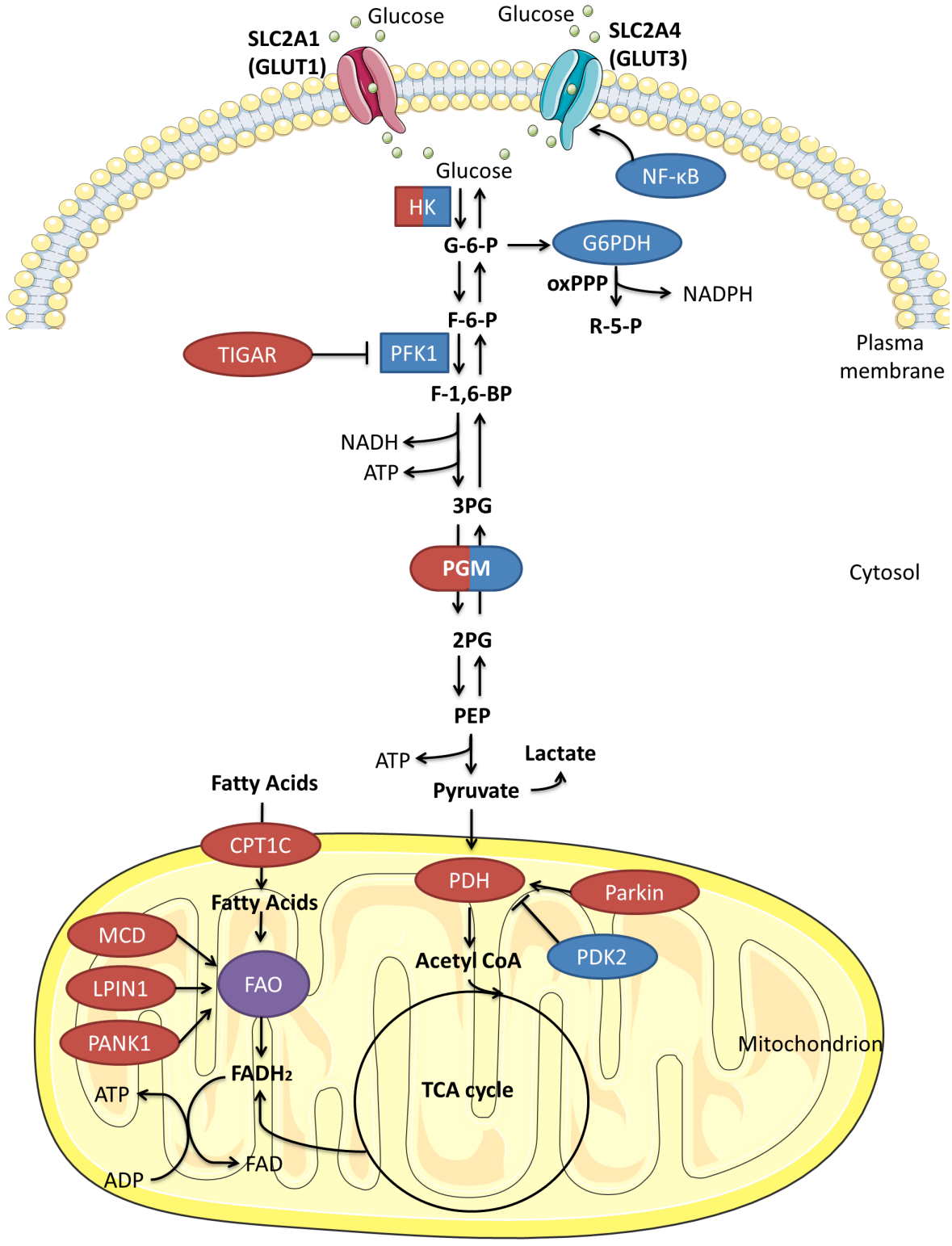

Figure 1-20: Examples of the involvement of p53 in glycolysis and metabolism

Blue: proteins that are downregulated by p53. Red: proteins that are upregulated by p53. NF-κB = nuclear factor-κB, HK = hexokinases, G6PDH = glucose-6-phosphate (G-6-P) dehydrogenase, PFK1 = phosphofructokinase 1, TIGAR = TP53-inducible glycolysis and apoptosis regulator, PGM = phosphoglycerate mutase, PDH = pyruvate dehydrogenase, PDHK2 = PDH kinase 2, CPT1C = carnitine palmitoyltransferase 1C, MCD = malonyl-coenzyme A decarboxylase, LPIN1 = lipin1, PANK1 = pantothenate kinase 1, oxPPP = oxidative pentose phosphate pathway and FAO = fatty acid oxidation. Figure is adapted from Kruiswijk *et al.* (2015).

1.2.3.5 Autophagy

Autophagy is a regulated cellular process that involves degradation of cytoplasmic components (reviewed in (Parzych and Klionsky, 2014)). Autophagy contributes to the recycling of cellular components through a formation of double-layer structure called autophagosome followed by lysosomal degradation to provide cells with nutrients such as essential amino acid, nucleotides and fatty acids. Autophagy also functions as a quality control mechanism, allowing for the removal of damaged organelles such as mitochondria (through a specific form of autophagy called mitophagy) (reviewed in (Parzych and Klionsky, 2014)). Autophagy is negatively regulated by mTOR (Jung et al., 2010) (Figure 1-19). DRAM (Damage-regulated autophagy modulator), which is transactivated by p53 and promotes autophagy, can replenish nutrients to the cells, which may contribute to cell survival (Amaravadi et al., 2007) (Figure 1-19). On the other hand, it has also been reported that DRAM-induced autophagy promotes Type II programmed cell death (Crighton et al., 2006). Another autophagy protein ATG7, which is an E1 ubiquitin-like modifier-activating enzyme, appears to regulate p53 response. In the presence of ATG7, it binds to p53 and induces p21 to induce cell cycle arrest, whereas p53 induces apoptosis in the absence of ATG7 (Lee et al., 2012b).

However, autophagy can help cancer cells to survive. For example, tumours with activated RAS require autophagy for tumour progression (Yang and Klionsky, 2010). In fact, antioxidant function of p53 attenuates autophagy (Bensaad et al., 2009). Furthermore, cytoplasmic p53 inhibits autophagy; knockout, knockdown and pharmacological inhibition of p53 enhances autophagy, which could result in promoting survival of p53-deficient cancer cells, and inhibition of p53 degradation (by inhibiting its E3 ligases including MDM2) prevents autophagy and inhibits cancer cell survival (Tasdemir et al., 2008).

1.2.3.6 Other functions

p53 may be involved in numerous other functions including the regulation of tumour microenvironment signalling (reviewed in (Bieging et al., 2014)). Notably, p53 can attenuate angiogenesis by promoting degradation of HIF1α indirectly (Ravi et al., 2000). p53 can also activate secretion of growth inhibitors and

exosomes (Komarova et al., 1998, Yu et al., 2006). Furthermore, p53 transactivates several microRNAs that regulate gene expression of several targets in order to attenuate tumour development. For example, miR-34a is one of the many p53 target genes and attenuates gene expression of several oncogenes post-transcriptionally including c-MYC, HGFR (c-MET) and BCL-2 (Zhao et al., 2013, Zhang et al., 2014a, Yang et al., 2014).

Based on the meta-analysis data aimed at identifying p53 target genes many p53 target genes are identified only in a small number of studies and have a higher likelihood of being false positives, although well-known p53 target genes were identified in majority of datasets, only *CDKN1A* and *RRM2B* were identified in all 16 data sets (Fischer, 2017). This implies that primary function of p53 is to arrest cell cycle and repair DNA. Notably, *FBXW7* is also p53 target gene and supports the tumour suppressing effects of p53 (Mao et al., 2004, Fischer, 2017).

1.2.4 Cell elimination functions of p53

If the stress persists or the damage is too severe, p53 can help to eliminate cells from the proliferative compartment.

One of the best-understood mechanisms of cell elimination by p53 is apoptosis (Type I programmed cell death) (Nakano and Vousden, 2001, Oda et al., 2000). p53 promotes both intrinsic and extrinsic apoptosis pathway by inducing proteins such as PUMA (p53 upregulated modulator of apoptosis), NOXA (also known as PMAIP1, Phorbol-12-myristate-13-acetate-induced protein 1), BAX (BCL-2-associated X protein), BAK (BCL-2 homologous antagonist killer), PIG3 (p53-inducible gene 3) and FAS (First apoptosis signal receptor, also known as CD95) (Figure 1-21).

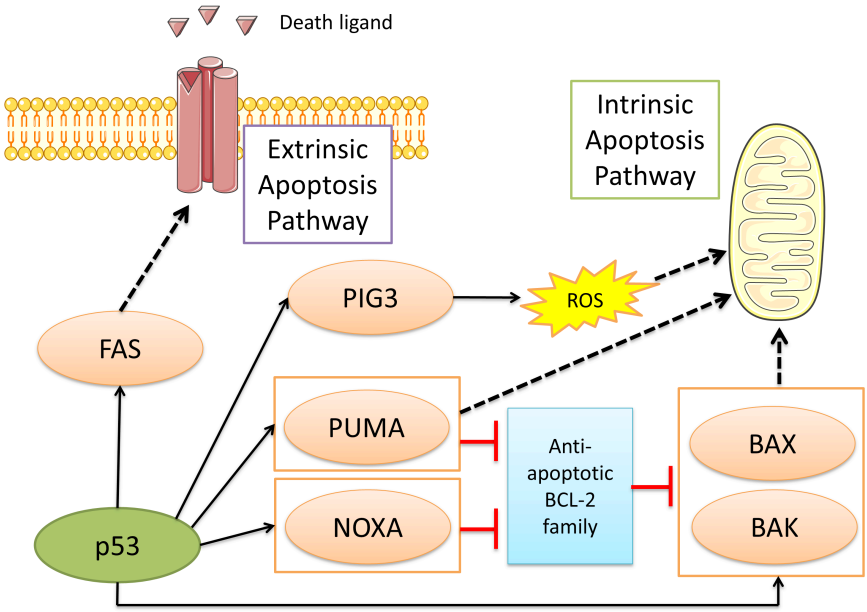

Figure 1-21: Role of p53 in apoptosis

p53 transactivates target genes to promote both intrinsic and extrinsic apoptosis pathways. ROS = reactive oxygen species.

PUMA, NOXA, BAX and BAK belong to pro-apoptotic BCL-2 (B-cell lymphoma 2) family and are transactivated by p53 upon non-repairable or oncogenic stimuli. PUMA and NOXA bind to and inhibit the anti-apoptotic BCL-2 family proteins that prevent BAX- and BAK-promoted apoptotic activity (Yu et al., 2001, Oda et al., 2000). BAX, BAK and also PUMA localise to and open the outer membrane of mitochondria in order to release cytochrome c and initiate the caspase-9 dependent intrinsic apoptosis cascade (Chipuk et al., 2004). PIG3 is also induced by p53 and increases intracellular ROS, and subsequent initiation of intrinsic apoptosis cascade. Interestingly, p53 has transcriptionally independent apoptotic functions; cytoplasmic p53 is sequestered by anti-apoptotic BCL-2 family proteins such as BCL-XL, and after genotoxic stress, PUMA (transcribed by nuclear p53) displaces p53 from them to allow p53 to induce mitochondrial permeabilisation and intrinsic apoptosis cascade (Chipuk et al., 2005). In addition, it has also reported that p53 is accumulated in the mitochondrial matrix upon oxidative stress and interact with cyclophilin D that regulates mitochondrial permeability transition pore (PTP) opening to induce cell death (Vaseva et al., 2012).

p53 potentiates the expression of several trans-membrane death receptors including FAS (Munsch et al., 2000). Following ligand binding, caspase-8 dependent extrinsic apoptosis pathway is initiated.

In addition to apoptosis and autophagy-induced cell death, p53 has been implicated in mediating other forms of cell death including anoikis, necroptosis, paraptosis, pyroptosis and ferroptosis (Ravid et al., 2005, Tu et al., 2009, Ohlsson et al., 1998, Gupta et al., 2001, Jiang et al., 2015a) (Table 1-2).

Table 1-2: Examples of p53-mediated cell death

Mode of cell death	Definition	Role of p53
Anoikis	Cell death induced when cells detach from the surrounding extracellular matrix (ECM)	p53-dependent cell death
Necroptosis	Programmed necrotic cell death	p53 transactivates the lysosomal protease cathepsin Q
Paraptosis	Programmed cell death induced by IGF-IR (swelling of mitochondria or endoplasmic reticulum (ER) and cytoplasmic vacuolisation)	p53 isoform (Δ40p53 (p44) that lacks N-terminal region) upregulates IGF-IR (insulin-like growth factor 1 receptor)
Pyroptosis	Inflammatory form of regulated cell death	p53 transactivates caspase-1
Ferroptosis	Iron-dependent regulated cell death	p53 represses transcription of the cysteine/ glutamate transporter SLC7A11

p53 may also promote irreversible cell cycle arrest or senescence by inducing PAI-1 (Plasminogen activator inhibitor 1) (Kortlever et al., 2006). In addition, prolonged p21-mediated cell cycle arrest leads to senescence by up-regulating another CDK inhibitor $p16^{INK4a}$ (encoded by *CDKN2A*) (Stein et al., 1999). Activation of senescence, however, can trigger the release of the senescence-associated secretory phenotypes (SASP) that may promote cancer and other age-related diseases (Coppe et al., 2008).

Interestingly, p53 retains tumour suppressing functions even in the absence of p21, PUMA and NOXA (Jiang et al., 2011a, Valente et al., 2013). Although cells from deficient mice ($Trp53^{+/+}$, $Cdkn1a^{-/-}$, $Puma^{-/-}$ and $Noxa^{-/-}$) were completely deficient in p53-dependent apoptosis, these mice did not develop spontaneous tumour in contrast to *Trp53* knockout mice (Valente et al., 2013).

1.2.5 Transcription and post translational regulation of p53

p53 can be a potent inhibitor of cell viability and p53 function must be kept tightly controlled to allow cell and organismal survival. The activity and stability of p53 is regulated through a variety of transcriptional and post-translational events including phosphorylation, acetylation, methylation, NEDDylation, SUMOylation and ubiquitination (reviewed in (Gu and Zhu, 2012)). In addition, p53 expression can also be negatively regulated by several microRNAs such as miR-125b and miR-504 (Le et al., 2009, Hu et al., 2010).

1.2.5.1 Transcription regulation

Although p53 is constitutively expressed, transcription of p53 is influenced by several transcriptional factors and co-transcriptional factors. Transcriptional factors, such as c-MYC/MAX (MYC-associated factor X) heterodimer and C/EBPβ (CCAAT-enhancer-binding proteins), bind to the *TP53* promoter and regulate its transcription (Roy et al., 1994, Reisman et al., 2012). Co-transcriptional factors either enhance (such as E1A) or repress (such as PAX (paired box) gene family) transcription of p53 (Stuart et al., 1995). In addition, translation of p53 is also regulated, by such as ribosomal protein RPL26 and nucleolin (Takagi et al., 2005). CHD8 (Chromodomain helicase DNA-binding 8) appears to be negatively regulating p53 transcriptional activity through histone H1 recruitment (Nishiyama et al., 2009).

1.2.5.2 Ubiquitination

p53 levels are predominantly regulated through its rapid turnover via the proteasome (Lopes et al., 1997). Therefore, the ubiquitination of p53 is a critical in keeping p53 in check under normal conditions. Target residues for ubiquitination are shown in Figure 1-22. While several proteins are involved in controlling p53 localisation and activity, many studies have highlighted the importance of MDM2 as a core component of p53 regulation (discussed in Section 1.3). It has also been suggested that other E3 ligases, such as PIRH2 (p53-induced RING-H2 domain protein), COP1 (Constitutively photomorphogenic 1), TRIM24 (Tripartite motif-containing 24), MKRN1, ARF-BP1 (also known as HUWE1, HECT, UBA and WWE domain containing 1 or MULE, MCL-1 ubiquitin ligase E3), E4F1 (E4F transcription factor 1) and MSL2 (Male specific lethal 2) are also

involved in p53 ubiquitination. Details of these mechanisms of regulation will be discussed in Section 1.4. Stabilisation of p53 is achieved by inactivating these E3 ligases in response to various stimuli including hypoxia, nutrient depletion, telomere erosion, oncogene activation and ribosomal stress. A number of E4 ubiquitin elongation factors are also suggested to contribute to the poly-ubiquitination of p53, including CBP (CREB-Binding protein)-p300, UBE4B and Gankyrin (Shi et al., 2009, Wu et al., 2011, Higashitsuji et al., 2005).

In addition to poly-ubiquitination of p53, mono-ubiquitination of p53 may be involved in mediating its nuclear export and translocation to the mitochondria upon stress, resulting in the induction of apoptosis by interacting with BCL2 family members in mitochondria (Marchenko et al., 2000, Marchenko et al., 2007, Carter et al., 2007).

There are numbers of DUBs involve in the deubiquitination of p53, resulting in further levels of regulation of p53 stability. These include HAUSP (Herpesvirus-associated ubiquitin-specific protease, also known as USP7, Ubiquitin-specific-processing protease 7), USP10, USP29 and USP42 (Cummins et al., 2004, Yuan et al., 2010, Liu et al., 2011, Hock et al., 2011).

1.2.5.3 NEDDylation

It has been reported that SCF-FBXO11 is involved in the NEDDylation of p53, resulting in attenuation of p53 activity without affecting its stability (Abida et al., 2007). Target residues for NEDDylation are shown in Figure 1-22. Although a number of papers have suggested that MDM2 is involved in NEDDylation of p53, structurally, the NEDD8 E2 enzyme (Ubc12) is not compatible with MDM2 RING domain. Therefore, under normal condition, it is unlikely that MDM2 catalyses NEDDylation of p53. However, there is a possibility that MDM2 may be able to conjugate NEDD8 to p53 if NEDD8 is activated by E1 ubiquitin activating enzyme under NEDD8 overexpressing condition as reported (Xirodimas et al., 2004).

1.2.5.4 SUMOylation

SUMOylation can modify p53 function (Figure 1-22). Some studies have reported that SUMOylation regulates relocation of p53 from nucleus to the cytoplasm, resulting in attenuation of its transcriptional activity (Pichler and Melchior,

2002). On the other hand, other studies have suggested that SUMOylation of p53 enhances its transcriptional activity (Melchior and Hengst, 2002). SUMOylation of p53 could be regulated by SUMO E3 ligases including TOPORS (DNA topoisomerase 1 binding arginine/serine rich protein) and PIAS family members (Weger et al., 2005, Schmidt and Muller, 2002). It is also suggested that MDM2 can catalyse p53 SUMOylation, but again, SUMO E2 enzyme (Ubc9) is not structurally compatible with MDM2 RING domain.

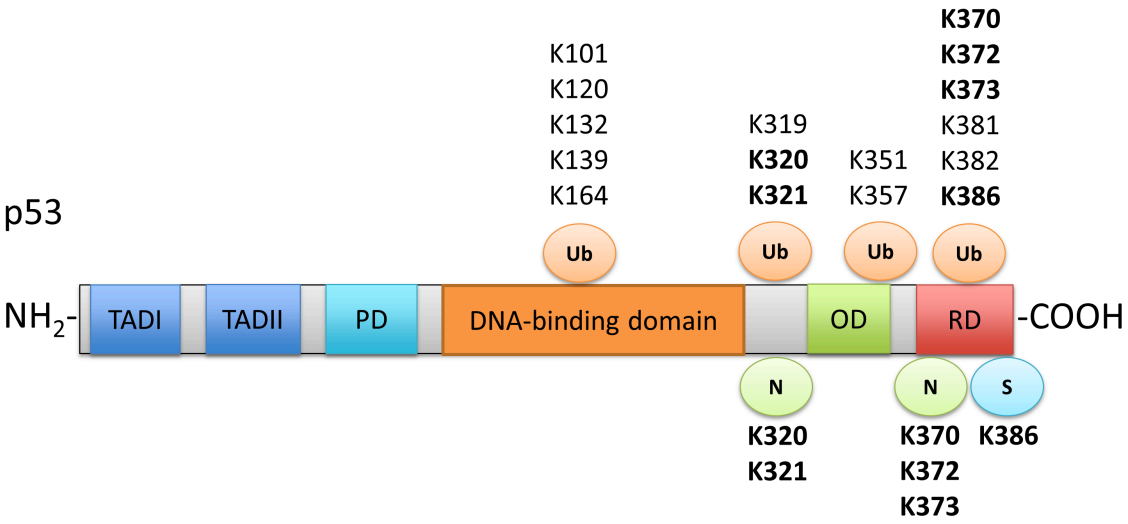

Figure 1-22: Post-translational modifications by ubiquitin-like proteins

TAD = transactivation domain, PD = proline rich domain, OD = oligomerisation domain, RD = Regulatory domain, NLS = nuclear localisation signal, NES = nuclear export signal, Ub = ubiquitination, N = NEDDylation and S = SUMOylation. Target residues are indicated. Bold: Both ubiquitination and NEDDylation (or SUMOylation) target.

1.2.5.5 Phosphorylation

Phosphorylation of p53 is mediated by various protein kinases at multiple phosphorylation sites (Figure 1-23). ATM (ataxia-telangiectasia mutated), a serine/threonine kinase, directly phosphorylates serine 15 (S15) and S46 of p53 upon DNA damage (Canman et al., 1998, Saito et al., 2002). In addition, ATM can indirectly promote phosphorylation of p53 through CHK2 (Checkpoint kinase 2), which phosphorylates S20 of p53 (Hirao et al., 2000, Matsuoka et al., 2000). Patients with inactive CHK2 mutants show Li-Fraumeni like syndromes (Vahteristo et al., 2001, Lee et al., 2001). Other kinases that target p53 include

ATR (Ataxia telangiectasia and Rad3 related) and DNA-PK (DNA-dependent protein kinase), which phosphorylate S15 and S37, and casein kinases (CK1δ, CK1ε), which phosphorylates S6 and S9 and threonine 18 (T18) (Tibbetts et al., 1999, Shieh et al., 1997, Knippschild et al., 1997). In addition, AMPK is involved in S15 phosphorylation (Jones et al., 2005), although this may not be direct. Phosphorylation of the N-terminal of p53 is believed to be involved in MDM2-p53 dissociation, allowing p53 stabilisation and activation. Interestingly, some of these kinases also phosphorylate MDM2, which may also modulate p53 stabilisation and activation (discussed in Section 1.3.3.2).

1.2.5.6 Acetylation

Acetylation is also a powerful mechanism for activating p53 function by enhancing its DNA binding and transcriptional activity. This can also occurs as a result of cellular stress. Multiple sites in p53 including in the DBD and C-terminal can be acetylated (Figure 1-23). This is regulated by several acetyltransferases such as, PCAF (P300/CBP-associated factor), KAT5 (lysine acetyltransferase 5) and hMOF (human males absent on the first) (Sykes et al., 2006, Allis et al., 2007). In addition, CBP-p300 is also known to promote acetylation of p53 (Ito et al., 2001). As acetylation occurs on the lysine residues (Figure 1-23), acetylation can prevent ubiquitination and *vice versa*, depending on the stress. As well as promoting p53 stabilisation by preventing ubiquitination, the acetylation can inhibit the formation of MDM2/MDMX complexes on target gene promoters and recruit co-factors for the promoter specific activation of p53 transcriptional activity (Barlev et al., 2001).

1.2.5.7 Methylation

Methylation of p53 is regulated by methyltransferases SMYD2 (SET and MYND domain containing 2), SET7/9, SET8, G9A/GLP and PRIMT5 (Protein arginine N-methyltransferase 5) (reviewed in (West and Gozani, 2011)). Interestingly, mono-methylation of p53 at K370 and K382 represses p53 transcriptional activity, while di-methylation of these sites can activate p53 (Huang et al., 2006, Shi et al., 2007, Huang et al., 2007).

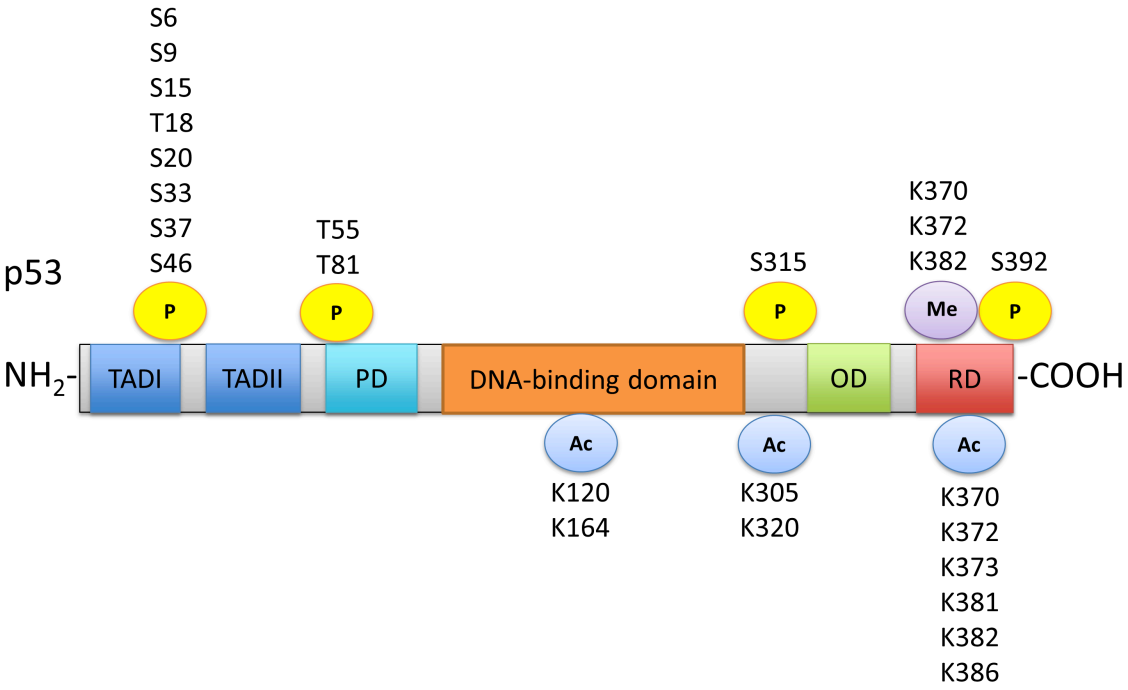

Figure 1-23: Phosphorylation, acetylation and methylation of p53

TAD = transactivation domain, PD = proline rich domain, OD = oligomerisation domain, RD = Regulatory domain, NLS = nuclear localisation signal, NES = nuclear export signal, P = phosphorylation, Ac = acetylation and Me = methylation. Target residues are indicated.

1.3 MDM2 and MDMX

1.3.1 Structure of MDM2 and MDMX

MDM2 was first discovered on the "double minutes" which are products of gene amplification (small fragments of extrachromosomal DNA) found in mouse cell line 3T3DM, with other co-amplified proteins MDM1 and MDM3 (Fakharzadeh et al., 1991). Therefore, human MDM proteins are also referred as HDM (*Human* double minutes) proteins. Functions of MDM1 and MDM3 are yet to be elucidated, although it has been suggested that MDM1 binds to microtubules and could contributes to cell cycle regulation by regulating centrosome duplication (Van de Mark et al., 2015). On the other hand, MDM2 is one of the best studied proteins as is a main negative regulator of p53.

The human *MDM2* gene is located on the long arm of chromosome 12 (locus 12q15) and contains 12 exons (of which the first 2 are untranslated regions (5' UTR)). The full-length human MDM2 protein has 491 amino acids and consists of several conserved functional domains, including the N-terminal p53-binding domain, a nuclear export signal (NES), nuclear localisation signal (NLS), the central acidic domain, RanBP2 (RAS-related nuclear protein binding protein 2)-type zinc finger domain, nucleolar localisation domain (NoLS) and the C-terminal RING domain (Figure 1-24).

MDMX (also known as MDM4) is a close homologue to MDM2 (90 % homologous) that can bind and inhibit p53 transcriptional activity (Shvarts et al., 1996, Parant et al., 2001b, Migliorini et al., 2002a). The human *MDMX* gene is located on the long arm of chromosome 1 (locus 1q32) and contains 11 exons and an additional exon 1ß (exon 1 is a 5' UTR). Human MDMX comprises 490 amino acid residues and contains same domains as MDM2, except it lacks NLS, NES and NoLS (Figure 1-24). Interestingly, although MDMX contains RING domain, it is catalytically inactive.

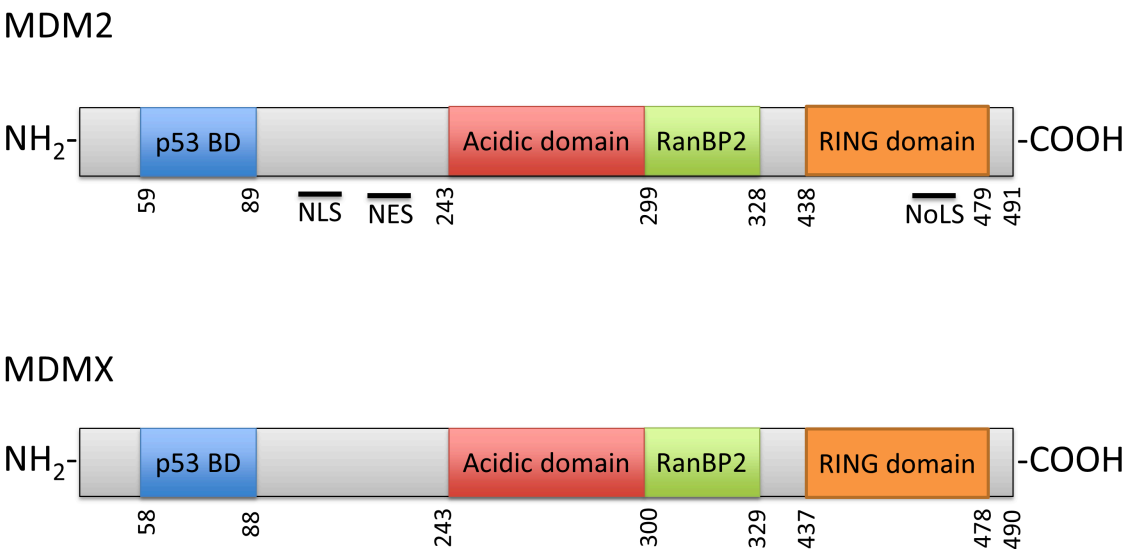

Figure 1-24: Functional domains of MDM2 and MDMX

p53 BD = p53-binding domain, RanBP2 = RAS-related nuclear protein binding protein 2-type zinc finger domain, NLS = nuclear localisation signal, NES = nuclear export signal and NoLS = nucleolar localisation signal. Generated from UniProt database (https://www.uniprot.org).

1.3.1.1 N-terminal p53-binding domain

The p53-binding domain of MDM2 forms a hydrophobic cleft into which the p53 N-terminal α-helix (phenylalanine 19 (F19), tryptophan 23 (W23) and leucine 26 (L26)) binds (Kussie et al., 1996). Mutation within this region, for example in residues glycine 58 (G58), glutamine 68 (Q68), valine 75 (V75) or cysteine 77 (C77) of MDM2, result in the loss of p53 binding (Freedman et al., 1997). MDM2 contains NLS and NES, which are not found in MDMX. MDM2 is primary localised in the nucleus while MDMX is primary localised in cytoplasm. The NLS and NES allow MDM2 to shuttle between cytoplasm (where it binds to MDMX and can relocate MDMX to the nucleus) and nucleus (where it binds to p53) (Roth et al., 1998, Freedman and Levine, 1998).

1.3.1.2 The central domain

The central part of both MDM2 and MDMX includes aspartic acid- and glutamic acid- rich region, often referred as the acidic domain, and RanBP2-type zinc finger domain. Although the acidic domain seems to have some critical role for MDM2/MDMX activity towards p53, the details of this are not yet fully understood

(Argentini et al., 2001). Some studies have suggested that this region serves as an additional binding site for p53 to regulate its transcriptional activity, and others have suggested that it regulates p53 ubiquitination (Wallace et al., 2006, Ma et al., 2006, Argentini et al., 2001). The RanBP2-type zinc finger domain seems to have a role in mediating interaction of MDM2 with ribosomal proteins (Lindstrom et al., 2007). The RanBP2-type zinc finger domain of MDMX interacts with CK1α, which phosphorylates MDMX at S289 to enhance its ability to inhibit p53 activity (Chen et al., 2005b).

1.3.1.3 C-terminal RING domain

The RING domains of MDM2 and MDMX are classified as C_2H_2-C_4 type (first zinc is co-ordinated by 2 cysteines and 2 histidines and second zinc is co-ordinated by 4 cysteines), which is a slightly unusual form, as many other RING domains are co-ordinated by C_4-C_4 or C_3H-C_4 motifs (Tan et al., 2017). The RING domain of MDM2 has intrinsic ubiquitin E3 ligase activity, which is lacking in the MDMX RING domain.

The MDM2 RING domain interacts with the E2–ubiquitin complex and transfers ubiquitin to its target proteins, which include p53, MDMX and MDM2 itself (Fuchs et al., 1998, Pan and Chen, 2003, Fang et al., 2000). The MDM2 RING domain interacts with another MDM2- or MDMX- RING domain in order to form homo- and hetero- dimer, respectively. This dimerisation is critical for its E3 ligase activity and its ability to attenuate p53 transcriptional activity (discussed in Section 1.3.2). The MDMX RING domain cannot form homo-dimer and only functions as an E3 when dimerising with MDM2. The MDM2 RING domain (but not the MDMX RING domain) also contains a nucleolar localisation signal (NoLS), which may be required for its (and $p14^{ARF}$) re-localisation to nucleolus (Lohrum et al., 2000b).

1.3.2 Functions of MDM2 and MDMX

MDM2 and MDMX are the major negative regulators of p53. Mouse models have shown that MDM2 has a fundamental role in keeping p53 in check: deletion of *Mdm2* in mice result in early embryonic lethality due to uncontrolled p53 activation (Montes de Oca Luna et al., 1995, Jones et al., 1995) (Figure 1-25, Table 1-3). Similarly, loss of *Mdm2* in adult mice results in 100 % lethality; they

became moribund within a few days after induction (Zhang et al., 2014b). Haploinsufficiency of *Mdm2* (*Mdm2*$^{+/-}$) seems to be sufficient to control p53 under normal condition and is viable (Montes de Oca Luna et al., 1995) (Figure 1-25). Although *Mdm2*$^{+/-}$ mice live normal life spans and have no visible phenotypes, they are radiosensitive and show delayed tumour formation (Terzian et al., 2007). Mice with a hypomorphic allele of *Mdm2* (*Mdm2*$^{Hypomorphic/-}$), which expresses approximately 30 % of wild type MDM2 protein, were viable but very small, lymphopenic and radiosensitive due to uncontrolled p53 (Mendrysa et al., 2003) (Figure 1-25).

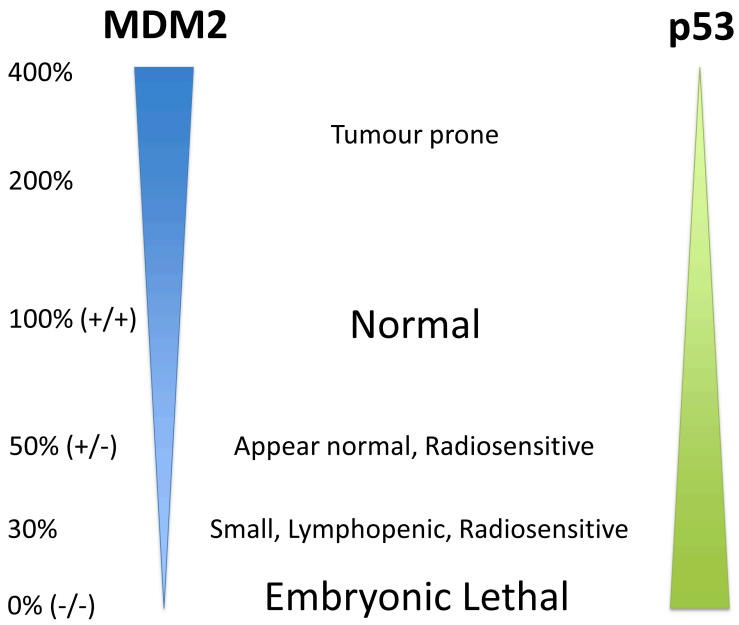

Figure 1-25: Levels of wild type MDM2 protein and mice phenotypes

Approximate MDM2 protein expression levels (%) are indicated. Figure is adapted from Wu and Prives (2018).

Similar to *Mdm2*, loss of *Mdmx* expression in mice results in p53-mediated early embryonic lethality (Parant et al., 2001a, Finch et al., 2002, Migliorini et al., 2002b). In both cases, the embryonic lethality can be rescued by deletion of *Trp53* (Table 1-3).

1.3.2.1 The p53-dependent functions

In healthy viable cells, MDM2 is primary localised in the nucleus where it binds and inhibits p53 activation. It has been reported that AKT promotes nuclear localisation of MDM2 (Mayo and Donner, 2001). On the other hand, MDMX is primarily localised in the cytoplasm, but is shuttled to nucleus by binding to MDM2 to promote the nuclear accumulation of MDMX (Stad et al., 2001, Li et al., 2002, Migliorini et al., 2002a), although MDM2-independent nuclear localisation of MDMX is also seen in response to DNA damage (Li et al., 2002, LeBron et al., 2006). MDM2 and MDMX interact with p53 through their N-terminal p53-binding domains in the nucleus and directly inhibit the ability of p53 to function as a transcription factor, by altering the interaction with other components of the transcriptional machinery (Shi and Gu, 2012, Momand et al., 1992, Oliner et al., 1993). This was the first functional role of MDM2 reported against p53, and is independent of the ubiquitin E3 ligase activity. The RING domain at the C-terminal of MDM2 functions to bind the E2 ubiquitin-conjugating enzyme including UbcH5B and UbcH5C, and facilitate ubiquitination of p53 and targeting it to the proteasome via K48 interlinked poly-ubiquitination (Moll and Petrenko, 2003, Saville et al., 2004). MDM2 ubiquitinates the C-terminal of p53 at any of the 6 lysines (K370, K372, K373, K381, K382, and K386) and mutation of these lysines decrease p53 ubiquitination (Gu and Zhu, 2012). However, MDM2 can also ubiquitinates other regions of p53, including the DNA-binding domain, in certain conditions. Mutation of MDM2 C464 residue (which is involved Zn^{2+} co-ordination of the RING domain) to alanine (C464A) results in the loss of E3 ligase activity and the enhanced p53 stability (Honda et al., 1997, Geyer et al., 2000). Corresponding mutation in mice (*Mdm2*^{C462A}) results in the early embryonic lethality similar to that seen in complete *Mdm2* knockout (Itahana et al., 2007) (Table 1-3). This mutant cannot dimerise due to destruction of RING domain and has also lost ability to limit the p53 transcriptional activity (Itahana et al., 2007). Other domains of MDM2, such as central acidic domain and C-terminal tail, are also important for the ubiquitination of p53 (Argentini et al., 2001, Kawai et al., 2003b, Meulmeester et al., 2003, Uldrijan et al., 2007). Furthermore, it has been reported that MDM2 shuttles p53 to the 26S proteasome and acts as a bridging molecule between p53 and 26S proteasome as MDM2 can directly interact with several components of the 26S proteasome and enhances association of p53 (Kulikov et al., 2010). Low levels of MDM2 appear to

promote mono-ubiquitination of p53, which is sufficient to prevent its transcriptional activity and mediate its nuclear export, although this may contribute to the activation of cytoplasmic activities of p53 (Li et al., 2003).

Although MDMX has a putative RING domain that is important for the interaction with MDM2, it cannot homo-dimerise and possesses no intrinsic E3 activity in cells (Jackson and Berberich, 2000, Stad et al., 2001). In cell free systems, however, MDMX has been shown to homo-dimerise at a high (micro-molar) concentration. A recent study has suggested that a single gain-of-function mutation from asparagine 448 to alanine in the MDMX protein (MDMX N448C) allows for homo-dimerisation, which is sufficient to re-activate its E3 activity (Iyappan et al., 2010). The ability of MDMX to interact with MDM2 through the RING domains has been described to both inhibit or enhance MDM2 E3 ligase activity, depending on MDMX abundance (Linares et al., 2003, Jackson and Berberich, 2000, Stad et al., 2000). However, it now seems clear that MDMX is an important binding partner of MDM2, contributing to the E3 ligase activity of the hetero-dimeric complex. For example, an important function of the C-terminal tail of MDM2 could be contributed by the corresponding region of MDMX (Uldrijan et al., 2007, Poyurovsky et al., 2007). Similar to *Mdm2*^{C462A} mice, deletion or destruction of MDMX RING domain in mice (*Mdmx*$^{\Delta RING}$ and *Mdmx*^{C462A}, respectively) results in a p53-dependent embryonic lethal phenotype (Huang et al., 2011b, Pant et al., 2011) (Table 1-3). *Mdm2* C-terminal tail mutant mice retain the ability to control p53 activity, despite accumulation of p53 (Tollini et al., 2014). Unlike *Mdm2*^{C462A} mice, these mice are viable and can respond oncogenic stimuli quickly. These results suggest that hetero-dimerisation is crucial to regulate p53 transcriptional activity, especially during embryonic development (Table 1-3). In addition, although *Mdm2*$^{+/-}$ or *Mdmx*$^{+/-}$ mice are viable, double-haploinsufficiency mice are in general not viable – occasionally born but die within 20 days of birth (Grier et al., 2006, Terzian et al., 2007).

Table 1-3: Examples of global knockout/knock-in mouse models

Genotype	Model	Fate	With *Trp53*$^{-/-}$
Trp53$^{-/-}$	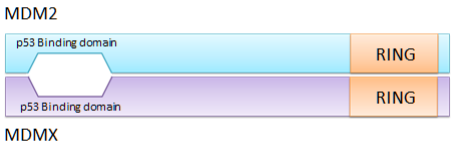	Develop normally Early tumour development	N/A
Mdm2$^{-/-}$		Embryonic lethal (E4.5~E7.5) Increased apoptosis	Viable
Mdmx$^{-/-}$	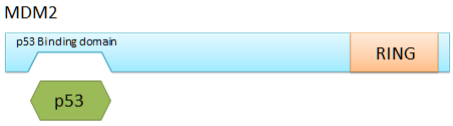	Embryonic lethal (E7.5~E8.5) Decreased cellular proliferation	Viable
Mdm2^{C462A}	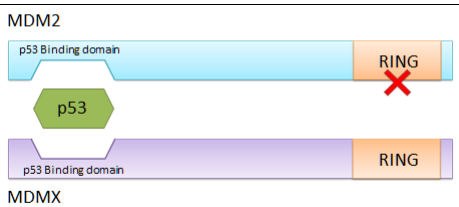	Embryonic lethal (~E8.5) Decreased cellular proliferation	Viable
Mdm2 C-terminal mutant	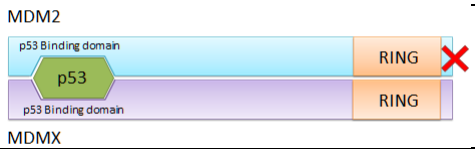	Viable Rapid induction of p53 target genes upon oncogenic stimulation	N/A
Mdmx^{C462A}	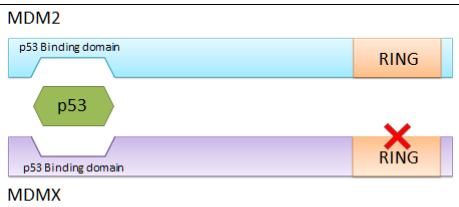	Embryonic lethal (~E9.5) Decreased cellular proliferation Increased apoptosis	Viable
MDMX$^{\Delta RING}$	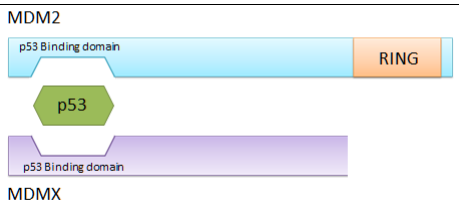	Embryonic lethal (~E9.5)	Viable

In addition to the global knockout/knock-in models, several tissue or cell type specific effects of MDM2 or MDMX have also been investigated in mice using tissue-type or cell-type specific Cre strains (Table 1-4). One strategy is to use floxed *Mdm2* or *Mdmx* and delete them in the specific tissues or cells, and the other strategy is to use the loxP-stop-loxP (LSL) p53 (*Trp53*$^{LSL/-}$) in the *Mdm2*$^{-/-}$ or *Mdmx*$^{-/-}$ background mice and express p53 in the specific tissues or cells. Interestingly, *Mdm2* and *Mdmx* display different phenotypic defects and, in general, loss of *Mdmx* is tolerated by many types of tissue or cell (Table 1-4). For example, both *Mdm2* and *Mdmx* seem to be required for the brain

development whereas *Mdm2* but not *Mdmx* is required for the heart development (Table 1-4). Smooth muscle specific deletion of *Mdm2* but not *Mdmx* in adult stage, using *Sm22* promoter driven Cre-ER^{T2} system (Kuhbandner et al., 2000), results in 100 % lethality; they quickly lost their weight and became moribund between 8 - 11 days after induction (Boesten et al., 2006). Although all of these phenotypes are linked to uncontrolled p53 activity, the degree of its effect seems to be highly tissue/cell type specific upon the loss of *Mdm2* or *Mdmx*.

Table 1-4: Examples of tissue or cell type specific deletion of *Mdm2* or *Mdmx* in mice

Targeted Tissue/Cell	Driver	Expression initiation	*Mdm2* floxed mice	*Mdmx* floxed mice	Reference
Brain (CNS and PNS)	*Nestin* (*Nes*-Cre)	E10.5 (Graus-Porta et al., 2001)	Embryonic lethal (occasionally viable but die within a few days)	Embryonic lethal	(Grier et al., 2006, Xiong et al., 2006)
			Embryonic lethal ($p53^{LSL/-}$ $Mdm2^{-/-}$)	Viable ($p53^{LSL/-}$ $Mdmx^{-/-}$)	(Francoz et al., 2006)
Heart (Cardiomyocyte)	*a-myosin heavy chain* (*aMyHC*-Cre)	E8.5 (Agah et al., 1997)	Embryonic lethal (~E13.5)	Viable (die within a year)	(Xiong et al., 2007)
Intestine (Epithelial cells)	*Villin 1* (*Villin*-Cre)	E9 (Madison et al., 2002)	Viable (lower body weights)	Viable	(Valentin-Vega et al., 2008, Valentin-Vega et al., 2009)
Eye (Retinal cells)	*Pax6* (*Le*-Cre)	E9 (Ashery-Padan et al., 2000)	Viable (eye-less phenotype, neonatal lethality)	Viable (eye-less phenotype)	(Zhang et al., 2014b)
Kidney (Ureteric bud)	*Homeobox B7* (*aHoxb*-Cre)	E9.5 (Zhao et al., 2004)	Viable (neonatal lethality)	Viable	(Hilliard et al., 2011, El-Dahr et al., 2017)
Liver (Hepatocyte)	*Albumin (Alb*-Cre*)*	E10.5 (Postic et al., 1999)	Viable	*Not tested*	(Kodama et al., 2011)
Endothelial cells	*Tek* RTK (*Tek*-Cre)	E9 (Kisanuki et al., 2001)	Embryonic lethal (~E10.5)	*Not tested*	(Zhang et al., 2012a)
Oocytes	*Zona Pellucida 3* (*Zp3*-Cre)	Before first meiotic division (de Vries et al., 2000)	Viable (decreased fertility)	Viable (no decreased fertility)	(Livera et al., 2016)

1.3.2.2 The p53-independent functions

Overexpression of *Mdm2* in mice accelerates spontaneous tumourigenesis and mortality in a p53-independent manner (Jones et al., 1998). Furthermore, overexpressed MDM2 also shows p53-independent oncogenic functions including elevation of VEGF, which contributes tumour growth and metastasis (Ganguli and Wasylyk, 2003). Overexpression of *Mdmx* also leads to spontaneous tumourigenesis in mice (Xiong et al., 2010). Therefore, it is clear that MDM2 and MDMX can function in a p53-independent manner.

The best known p53-independent function of MDM2 and MDMX is to inhibit DNA double strand break repair, which is normally recognised by the DNA repair complex called MRN (MRE11, RAD50 and NBS1). MRN initiates the DNA repair process by activating ATM serine/threonine kinase, and depending on the phosphorylation events, cells undergo DNA repair such as non-homologous end joining (NHEJ) and homologous recombination. MDM2 and MDMX directly inhibit the DNA repair complex MRN in an E3-ligase independent manner and promote genomic instability (Eischen, 2017). Similarly, MDM2 interacts with pRB (to inhibit pRB binding to E2F1) and E2F1/DP1 (to stimulate transcription) and disrupts regulation of restriction point in G_1 phase (Martin et al., 1995). On the other hand, MDM2 promotes degradation of E2F1/DP1 in S phase and inhibits E2F-mediated apoptosis (Lundgren et al., 1997).

MDM2 can ubiquitinate other proteins, including CHK2 and ribosomal proteins as well as the transcriptional factor FOXO3A, which is one of an important regulator of cell death (Fu et al., 2009, Kass et al., 2009, Xiong et al., 2011, Ofir-Rosenfeld et al., 2008).

MDM2 may also be involved in epithelial-mesenchymal transition (EMT) regulation; EMT is essential for cell differentiation during embryogenesis but this could help tumour cells to gain ability to metastasis. Loss of the adhesion molecule epithelial cadherin (E-cadherin) is considered to be a key process in EMT. SNAI1 (Snail family zinc finger 1, also known as Snail) and SNAI2 (also known as Slug) are the transcriptional repressor of E-cadherin and thus promote EMT (Batlle et al., 2000, Vesuna et al., 2008). MDM2 can ubiquitinate E-cadherin and upregulate SNAI1 expression, but paradoxically, MDM2 can also ubiquitinate

SNAI2 for proteasomal degradation (Yang et al., 2006a, Lu et al., 2016, Wang et al., 2009).

Moreover, MDM2 can modulate telomerase regulation; there is a hypothesis that the cell life is determined by the length of telomeres that are located at the end of each chromosomes and get shorter and shorter after each cell division. Once telomeres become depleted, called Hayflick limit, cells undergo senescence. Telomerase elongates telomeres and up-regulation of telomerase activity is frequently found in many types of cancer. One of the most important components of telomerase is TRET (Telomerase reverse transcriptase) and MDM2 has been reported to ubiquitinate TERT and attenuate telomere elongation (Oh et al., 2010).

MDMX can interact with and inhibit the E2F and SMADs (Small mothers against decapentaplegic) transcription factors to modulate their transcriptional activity (Kadakia et al., 2002, Wunderlich et al., 2004). MDM2 may also be involved in epigenetic reprogramming as well as genomic instability and tumourigenesis, through its interaction with the histone methyl-transferase SUV39H1 (Suppressor of variegation 3-9 homologue 1) (Chen et al., 2010, Onder et al., 2012, Peters et al., 2001).

1.3.3 Transcription and Post translational regulation of MDM2 and MDMX

As both MDM2 and MDMX are main regulators of p53, their expression and activity must be tightly regulated. Under cellular stress conditions such as DNA damage, MDM2 and MDMX are post-translationally modified and inhibited so that p53 becomes stabilised and active.

1.3.3.1 Transcriptional regulation

MDM2 has 2 promoters: P1 is located upstream of exon 1 and P2 is located between exon 1 and exon 2) (Figure 1-26). Interestingly, *MDM2* contains 2 start codons (ATG). Full length MDM2 (90 kDa) is translated from the first ATG in exon 3 and a short form of MDM2 (76 kDa), which lacks the first 49 amino acids, is translated from the second ATG in exon 4. The short form seems to lack ability to bind p53 and have a dominant negative effect towards full length MDM2

(Perry et al., 2000). *MDMX* also has 2 promoters; P1 is located upstream of exon 1 and P2 is located between exon 1 and exon 1ß) (Figure 1-26). Similar to *MDM2*, *MDMX* also contains 2 start codons. Full length MDMX is translated from the ATG in exon 2 and a long form of MDMX (MDMX-L, 18 amino acid longer) is translated from an alternative ATG in exon 1ß (Phillips et al., 2010). MDMX-L seems to have less ability to limit p53 activity. Interestingly, p53 induces the transcription of MDM2 (and MDMX-L in certain conditions) and establishes a negative feedback loop; thereby allowing for a quick recovery by degrading p53 following stress resolution (Barak et al., 1993, Picksley and Lane, 1993, Khoo et al., 2014) (Figure 1-26). Mice lack *Mdm2* P2 promoter ($Mdm2^{P2/P2}$), which abolishes negative feedback loop, show normal basal p53 levels but radiosensitive. *MDM2* transcription is also regulated by various other factors including oncogenic stimuli and immune responses (Figure 1-26). For example, the ETS (E26 transformation-specific) transcription factor family including FLI1 (Friend leukemia integration 1 transcription factor) and ELF4 (E74 like ETS transcription factor 4), which are associated with over-activation of RAS signalling pathway in response to mitogens, can upregulate both *MDM2* and *MDMX* expression (Gilkes et al., 2008, Ries et al., 2000). In fact, over-activation of RAS and over-expression of *MDM2* and *MDMX* are frequently found in melanoma and colorectal cancer. Overexpression of FLI1 and ELF4 indirectly inactivates p53 through increased *MDM2* expression and has been implicated in tumourigenesis (Truong et al., 2005, Sashida et al., 2009). TGFß signalling upregulates *MDM2* through SMAD3 and high levels of activated SMAD3 and MDM2 are found in late-stage of breast cancer (Araki et al., 2010). The NFAT1 (Nuclear factor of activated T-cells) transcription factor can also upregulate *MDM2* and both NFAT1 and MDM2 are highly expressed in hepatocellular cancer (Zhang et al., 2012b). N-MYC (MYC neuroblastoma homologue) is a member of the MYC family and stimulates *MDM2* expression to avoid p53-mediated apoptosis (Slack et al., 2005a, Slack et al., 2005b). NF-κB can also regulate *MDM2* transcription, which may be important for survival of activated T cells (Busuttil et al., 2010). IRF8 (Interferon regulatory factor 8) also induces transcription of *MDM2* to allow B cell proliferation in germinal centre (Zhou et al., 2009). E2F1 seems to attenuate p53-mediated transactivation of *MDM2* upon DNA damage (Tian et al., 2011). The tumour suppressor PTEN down-regulates *MDM2* but which transcription factor is involved is still unknown (Chang et al., 2004).

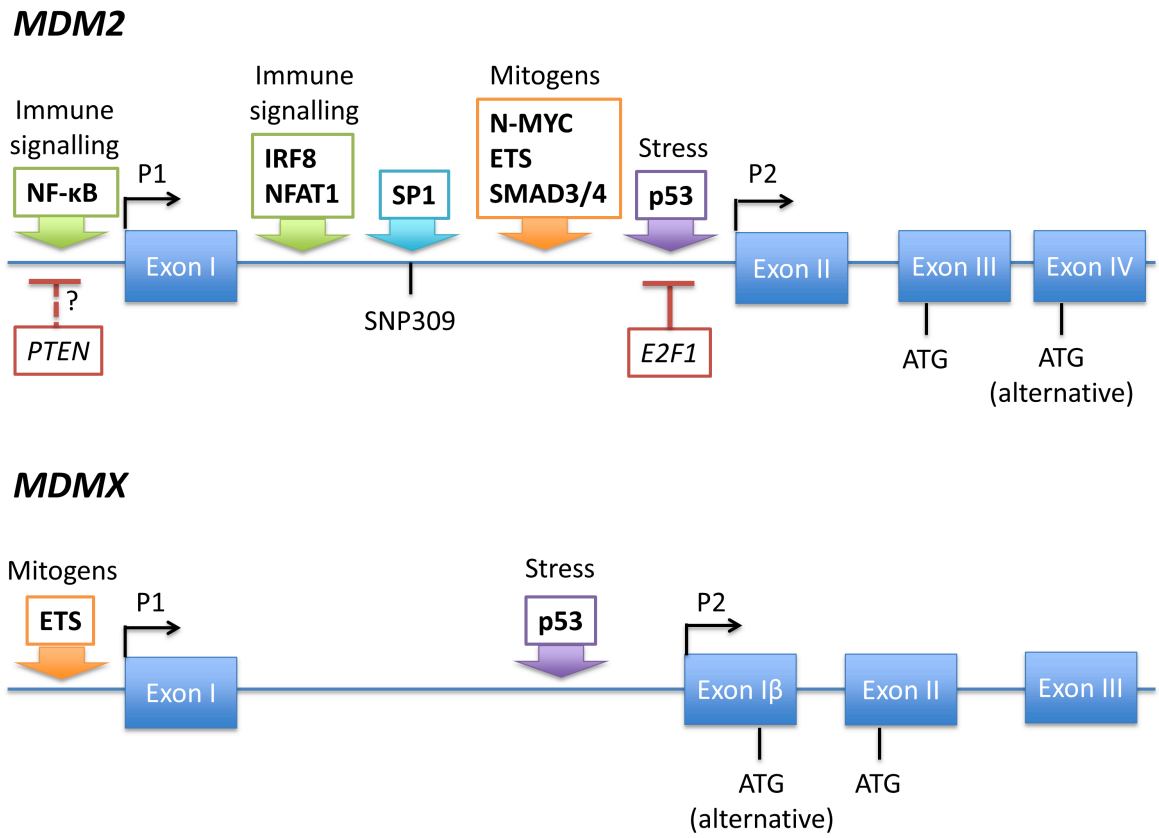

Figure 1-26: Transcriptional regulation of *MDM2* and *MDMX*

Positive modulators (bold) and negative regulators (italic) of the expression of *MDM2* and *MDMX*. P1 = first promoter, P2 = second promoter, ATG = start codon, PTEN = Phosphate and tensin homologue, IRF8 = Interferon regulatory factor 8, NFAT1 = Nuclear factor of activated T-cells 1, SP1 = specificity protein 1 transcriptional factor, N-MYC = MYC neuroblastoma homologue, ETS = E26 transformation-specific and SMAD = Small mothers against decapentaplegic.

1.3.3.2 Phosphorylation

Kinases that are activated in response to DNA damage include ATM and DNA-PK, which phosphorylate MDM2 at residues between RanBP2 zinc finger and RING domains (S386, S395, S407, T419, S425 and S429) and in N-terminal (S17), respectively, thereby inactivating MDM2 towards p53 (Maya et al., 2001) (Figure 1-27). Corresponding phosphorylation site mutant mice (*Mdm2*$^{S394A/S394A}$) are radiation resistant and show accelerated spontaneous tumour development (Gannon et al., 2012). ATM also phosphorylates MDMX at residue S403 while ABL1 (Abelson murine leukaemia viral oncogene homologue 1) phosphorylates MDMX Y99. Both of these phosphorylation events lead to the dissociation of p53-MDMX binding (Chen et al., 2005b, Zuckerman et al., 2009). MDM2 proteins carrying

serine to aspartic acid mutations to mimic phosphorylation (6D;S386, S395, S407, T419, S425 and S429 or the single substation S429D) show attenuated E3 ligase activity due to decreased dimerisation, while mutations of these serine residues to alanine, to prevent phosphorylation, enhance E3 activity due to increased dimerisation (Cheng et al., 2011). On the other hand, AKT phosphorylates MDM2 S166 and S186 and MDMX S367, and enhances their activity against p53 (Mayo and Donner, 2001, Lopez-Pajares et al., 2008).

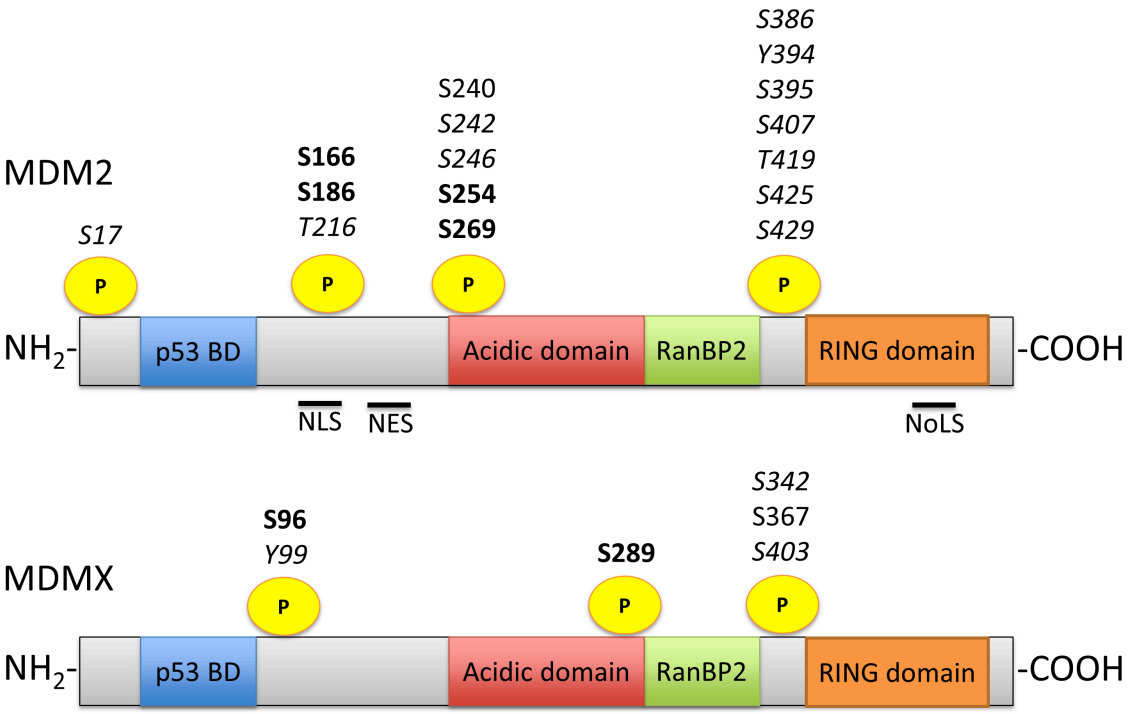

Figure 1-27: Phosphorylation sites of MDM2 and MDMX

p53 BD = p53-binding domain, RanBP2 = RAS-related nuclear protein binding protein 2-type zinc finger domain, NLS = nuclear localisation signal, NES = nuclear export signal, NoLS = nucleolar localisation signal and P = phosphorylation. Target residues are indicated. Bold: increased activity, Italic: decreased activity.

1.3.3.3 Ubiquitination

As discussed, MDM2 can function as an E3 ligase as a homo-dimer or hetero-dimer with MDMX, and through these interactions MDM2 can auto-ubiquitinate and target MDMX for proteasomal degradation. In normal unstressed cell, MDMX is fairly stable but it is degraded by MDM2 upon stress (Kawai et al., 2003a).

Some studies have suggested that the E3 activity of MDM2 can be toggled between the control of the MDM2/MDMX complex and the control of p53. For example, DNA damage induced phosphorylation of MDMX enhances the degradation of MDMX by MDM2, allowing for the stabilisation of p53 (Chen et al., 2005b). MDM2 can be ubiquitinated by SCF-β-TRCP and NEDD4 upon DNA damage (Wang et al., 2012, Xu et al., 2015). However, this degradation phenotype of MDM2 after phosphorylation can be due to the specificity of antibody. For example, MDM2 antibody SMP14, which recognises the epitope including AKT phosphorylation show reduced binding affinity to MDM2 compared to other MDM2 antibodies (Cheng and Chen, 2011)

HAUSP deubiquitinates MDM2 and MDMX as well as p53. It has been reported that knockdown or knockout of HAUSP stabilises of p53 due to de-stabilisation of MDM2 and MDMX (Meulmeester et al., 2005, Li et al., 2004). In fact, HAUSP binds to MDM2 with a higher affinity compared with p53 under normal condition (Hu et al., 2006). This interaction allows more efficient stabilisation of p53 upon stress. The activity of HAUSP towards MDM2 and MDMX is disrupted upon stress, when is can switch to targeting p53 to allow efficient activation of p53 (Meulmeester et al., 2005).

1.3.3.4 Other post-translational modifications

Acetylation of MDM2 within the RING domain is mediated by CBP-p300 and results in decreased E3 activity (Wang et al., 2004). TRIM27 and the onco-protein SKI (named after Sloan-Kettering Institute) promote SUMOylation of MDM2 to support its stabilisation (Chu and Yang, 2011, Ding et al., 2012). Similarly, MDMX can be SUMOylated, although the consequences of this modification are unknown (Pan and Chen, 2005). In addition, expression of *MDM2* and *MDMX* are also negatively regulated by several microRNAs. Interestingly, some of them are p53 target genes. For example, miR-192, miR-194 and miR-215 can attenuate *MDM2* expression and miR-199a-3p and miR-34a can attenuate *MDMX* expression, all of them are transactivated by p53 (Khella et al., 2013, Mandke et al., 2012).

1.3.4 Additional mechanisms to inhibit MDM2 and MDMX

In addition to the post-translational modifications, there are several additional mechanisms to inhibit MDM2 and MDMX.

The tumour suppressor $p14^{ARF}$ (Alternate open reading frame of *CDKN2A*, $p19^{ARF}$ in mice), which is induced by transcription factors E2F1 and c-MYC, interacts with and inhibits the ability of MDM2 to ubiquitinate and degrade p53 (Eischen et al., 1999, Abida and Gu, 2008). Importantly, $p14^{ARF}$ is not required to activate p53 in response to DNA damage (Kamijo et al., 1999). $p14^{ARF}$ mainly accumulates in the nucleolus where it binds to MDM2. This MDM2-$p14^{ARF}$ interaction prevents MDM2 from shuttling between the nucleus and cytoplasm (Lohrum et al., 2000a). In addition, $p14^{ARF}$ appears to be involved in blocking the interaction between MDM2 and 26S proteasome. Furthermore, overexpression of $p14^{ARF}$ potentiates SUMOylation of MDM2 and inhibits MDM2 functions (Xirodimas et al., 2002).

Similarly, several 60S ribosomal proteins including RPL5, RPL11 and RPL23 have been shown to bind to the central acidic domain of MDM2 to attenuate its activities in response to ribosomal stress (Dai et al., 2004). The 40S ribosomal proteins RPS14, RPS25, RPS27 and RPS27-Like also inhibit MDM2. Furthermore, 40S ribosomal proteins RPS3, RPS7 and RPS25, bind to both p53 and MDM2 to stabilise p53. Mice expressing an *Mdm2* mutant that cannot interact with the ribosomal proteins ($Mdm2^{C305F/C305F}$) show accelerated c-MYC-induced lymphoma development (Macias et al., 2010). It has also been reported that PML (Promyelocytic leukaemia protein) stabilises p53 by sequestering MDM2 to the nucleolus, which is potentiated by RPL11 (Bernardi et al., 2004).

It is important to note that $p14^{ARF}$ and the ribosomal proteins bind MDM2 independently of the p53-binding domain (there are also endogenous MDM2 inhibitors that directly inhibit p53-binding domain including DHCR24 (24-Dehydrocholesterol reductase, also known as Seladin-1) that is activated upon oxidative stress (Wu et al., 2004)), and that the details of how p53 is protected from MDM2 regulation can vary depending on the type of stress.

1.4 Other regulators of p53

Although MDM2 is widely recognised as a critical negative regulator of p53, other E3 ubiquitin ligases can regulate p53 stability (Table 1-5). For example, PIRH2, COP1 and TRIM24 are additional RING domain E3 ligases that have been reported to mediate p53 ubiquitination (Leng et al., 2003, Dornan et al., 2004b, Allton et al., 2009). Interestingly, they all are p53 target gene as well (Leng et al., 2003, Dornan et al., 2004b, Jain et al., 2014). Overexpression of PIRH2 and COP1 in cells decreases p53-mediated apoptosis and cell arrest and depletion of TRIM24 results in a corresponding increase in p53 level. Their importance in human disease has also been recognised, as PIRH2 was reported to be overexpressed in lung and prostate cancers, COP1 in ovarian and breast cancers and TRIM24 in breast cancer, whilst retaining wild type alleles of p53 (Duan et al., 2004, Logan et al., 2006, Dornan et al., 2004a, Tsai et al., 2010). Although *Pirh2* and *Trim24* knockout mice are viable, *Cop1* knockout mice are embryonic lethal phenotype (Jung et al., 2011, Jiang et al., 2015b, Migliorini et al., 2011). Importantly, this embryonic lethality was not rescued by the loss of *Trp53*, suggesting that COP1 plays a critical role in regulating other proteins in addition to p53 (Migliorini et al., 2011). Paradoxically, decreased expression of COP1 was also found in several cancers including gastric cancer (Sawada et al., 2013). In fact, Migliorini *et al.* (2011) suggested that COP1 functions as a tumour suppressor by regulating the stability of JUN onco-protein. Therefore, further investigation will be required to assess the specific contribution of COP1 in tumourigenesis. MKRN1 (Makorin RING finger protein 1) ubiquitinates a component of death receptor such as FADD (Fas-associated protein with death domain) and p21 as well as p53 but *Mkrn1* deficient mice are viable with no apparent developmental deficits (Gray et al., 2006, Lee et al., 2009, Lee et al., 2012a). Other E3 ligases include the HECT E3 ligase ARF-BP1, which has also been shown to directly bind to and ubiquitinate p53 for proteasomal degradation (Chen et al., 2005a). *Arf-bp1* knockout mice are embryonic lethal phenotype and pancreatic ß-cells specific deletion of *Arf-bp1* resulted in diabetes, which was partially rescued by the deletion of *Trp53* (Kon et al., 2012). Upregulation of ARF-BP1 was found in breast and lung cancers, whereas downregulation was found in glioblastoma and thyroid cancer (Adhikary et al., 2005, Zhao et al., 2009, Ma et al., 2016). The activity of ARF-BP1 and MDM2 is strongly attenuated by $p14^{ARF}$.

Ubiquitination of p53 by E4F1 and MSL2 seems to play a role independent of proteasomal degradation. E4F1 is an atypical E3 ligase as this is a transcriptional factor and contains neither RING domain nor HECT domain. E4F1 promotes mono- di- or tri- ubiquitination of p53 and regulates its localisation (Le Cam et al., 2006). MSL2 specifically mono-ubiquitinate K351 and K357 of p53 and targets it for nuclear export (Kruse and Gu, 2009).

Table 1-5: E3 ligases involved in p53 ubiquitination

E3 ligase	Other substrates	Knockout mice	Malfunction in cancer*
MDM2	E2F1/DP1 FOXO3A CHK2 Ribosomal proteins E-cadherin Snail TERT	Embryonic lethal Rescued by *Trp53*$^{-/-}$ (Montes de Oca Luna et al., 1995, Jones et al., 1995)	**Tumours of diverse tissue of origin** (discussed in Section 1.3)
PIRH2	p27^{Kip1} p73 c-Myc	Viable (Jung et al., 2011)	**Lung cancer** **Prostate cancer**
COP1	JUN p27^{Kip1}	Embryonic lethal Not rescued by *Trp53*$^{-/-}$ (Migliorini et al., 2011)	**Breast cancer** **Ovarian cancer** **Bladder cancer** *Gastric cancer*
TRIM24	*None identified*	Viable (Jiang et al., 2015b)	**Testis cancer**
MKRN1	FADD p21$^{Cip1/Waf1}$ TERT	Viable (Gray et al., 2006)	**Testis cancer**
ARF-BP1	N-MYC MCL1 B-catenin	Embryonic lethal (Kon et al., 2012)	**Breast cancer** **Lung cancer** *Glioblastoma*

*** Bold: upregulation, Italic: downregulation**

Interestingly, conformational mutants of p53 are highly poly-ubiquitinated through a mechanism that is not mediated by MDM2 or other known E3 ligases for p53 (Lukashchuk and Vousden, 2007). This poly-ubiquitination appears to be predominantly mediated by the U-box-type E3 (or E4) ligase CHIP and can be observed without proteasome inhibitors. Therefore, it is possible that ubiquitination of these p53 mutants may comprise K63-linked or other mixed chain forms. Consistently, CHIP mediates various form of ubiquitination including K63-linked depending on the E2 (Windheim et al., 2008). This suggests that gain-of-function of mutant p53 may be linked to the ubiquitin signalling.

1.5 Targeting ubiquitin proteasome system for cancer treatment

Although loss-of-function mutations in *TP53* have been frequently identified in many types of cancers, malignant tumours that retain wild type p53 genes are often compromised in signals upstream of p53 that prevent p53 accumulation and activation (Cho et al., 1994, Kastan, 2007). Therefore, stabilising and reactivating p53 in malignancies that retain an intact p53 locus could be a potential target for anti-cancer therapy.

Cancers that retain wild type p53 often have defects in the pathway that allow for stress-induced inhibition of MDM2. For example, gene amplification and protein overexpression of *MDM2* is frequently observed in at least 19 tumour types including soft tissue tumours, osteosarcomas, liposarcomas and oesophageal carcinomas (Momand et al., 1998) (Figure 1-28). Importantly, p53 mutation and *MDM2* amplification tend to be mutually exclusive within a tumour sample.

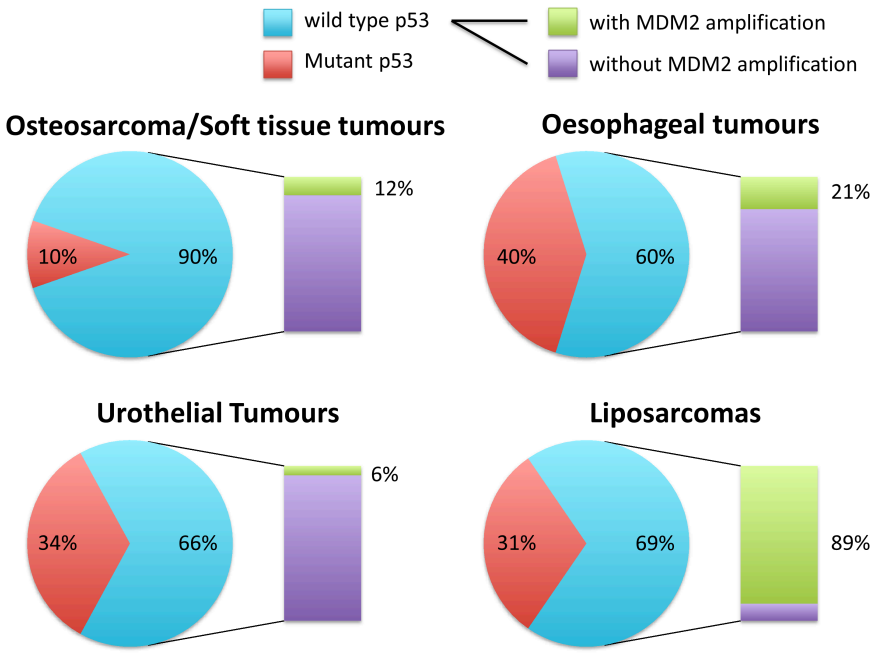

Figure 1-28: Wild type p53 and *MDM2* amplification in human cancer patients

n **= 94 (osteosarcomas, soft tissue tumours), *n* = 72 (oesophageal tumours), *n* = 50 (urothelial tumours) and *n* = 13 (liposarcomas). Generated from Momand *et al.* (1998).**

In addition, many tumours exhibit high MDM2 protein levels without *MDM2* gene amplification, including melanoma, breast cancer, retinoblastoma and Ewing's sarcoma (Gembarska et al., 2012, Lam et al., 2010, McEvoy et al., 2012, Pishas et al., 2011). This overexpression could be due to increased transcription and translation, or single nucleotide polymorphism (SNP) 309 T>G that increases MDM2 mRNA and protein about 2-4 fold by recruiting the transcriptional factor Sp1 (Bond et al., 2004). A mouse model has shown that mice with SNP309 (*Mdm2* SNP309G/G) increased *Mdm2* expression and accelerated spontaneous tumourigenesis (Post et al., 2010). Therefore, the contribution of *MDM2* overexpression in carcinogenesis could be much higher than that estimated by *MDM2* gene amplification.

Although *MDMX* is constitutively expressed in healthy tissues, *MDMX* is overexpressed in several types of cancers including retinoblastomas, breast cancers, melanomas and colon carcinomas. Again, these cancers retain wild type p53, suggesting an importance of MDMX in controlling cancer development (McEvoy et al., 2012, Lam et al., 2010, Gembarska et al., 2012, Gilkes et al., 2008).

In addition to *MDM2* or *MDMX* overexpression, the p53 pathway can also be inactivated by other mechanisms, including loss of MDM2/MDMX negative regulators such as $p14^{ARF}$ along with $p16^{INK4a}$.

1.5.1 Targeting MDM2 and MDMX

Inhibition of MDM2 or MDMX can be achieved by inhibiting the p53-MDMX or the p53-MDMX interactions, the MDM2 E3 ligase activity or the DUBs for MDM2 or MDMX. Importantly, this approach will only be applicable for patients with wild type p53 containing tumour. Therefore, analysis of p53 status of tumour will be required to apply these compounds.

1.5.1.1 Inhibitors of the interactions between p53 and MDM2/MDMX

Most activity has focused in targeting the N-terminal of MDM2 and MDMX, where p53 binds into a deep hydrophobic pocket (Chi et al., 2005). Nutlin-3 and its derivative RG7112 and Idasanutlin (RG7388) are cis-imidazoline compounds and they bind to MDM2 within this region (Poyurovsky et al., 2010, Ding et al., 2013)

(Figure 1-29). These compounds disrupt the interaction between MDM2 and p53 resulting in the stabilisation and activation of p53. Although on-target toxicities including thrombocytopaenia and neutropaenia appear to be limiting the efficacy and utility of these compounds, Idasanutlin is currently progressing through clinical trials (Phase III) in treatment for acute myeloid leukaemia (AML) (Clinical Trials Identifier: NCT02545283). Interestingly, these compounds appear not to disrupt the interaction between MDMX and p53, although MDM2 and MDMX share more than 50 % of amino acid sequence in their p53-binding domain.

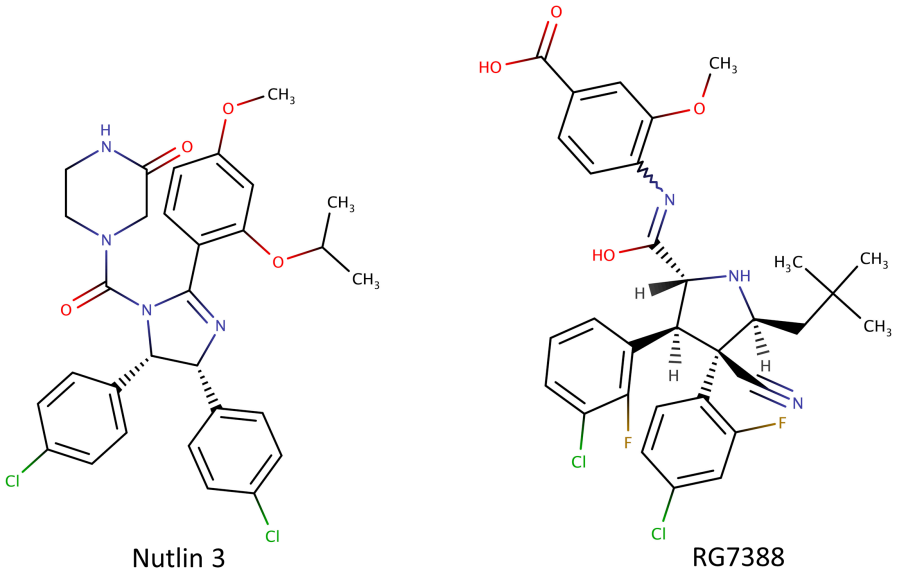

Figure 1-29: Example of inhibitors of the p53-MDM2 interaction
Chemical structure is obtained from PubChem database (https://pubchem.ncbi.nlm.nih.gov).

A number of additional compounds targeting the N-terminal of MDM2 are being developed. For example, MI-219 (Spiro-oxinadole compounds) was designed based on the crystal structure of p53 and mimics residues F19, W23 and L26 in the MDM2 binding site (Ding et al., 2005). Another example is the bound stapled peptides SAH-p53 (Stabilised alpha-helix of p53) series that covers the p53 binding pocket on MDM2 (Bernal et al., 2007, Baek et al., 2012). WK298 (Imidazo-indoles compound) seems to interact both MDM2 and MDMX and inhibit their activity (Popowicz et al., 2010).

While most of these compounds bind MDM2, RITA (Reactivation of p53 and induction of tumour cell apoptosis) is a thiophene compound that was thought to bind to transactivation domain of p53, where MDM2 binds (Issaeva et al., 2004). However, a later study failed to confirm that RITA binds to p53 to disrupt the p53-MDM2 interaction (Krajewski et al., 2005).

1.5.1.2 Inhibitors of the E3 ligase activity of MDM2

HLI98 (HDM2 ligase inhibitor 98 class) and HLI373 were identified in a screen for inhibitors of MDM2 auto-ubiquitination. HLI98 is relatively insoluble but HLI373 is water-soluble. These compounds also inhibit the ubiquitination of p53 and are believed to attenuate the E3 ligase activity of MDM2; although HLI98 can inhibit E2 ubiquitin conjugation enzyme UbcH5B and other unrelated RING and HECT E3 ligases (Yang et al., 2005). Similar results were obtained using further derivative compounds (Roxburgh et al., 2012). In addition, Sempervirine attenuates auto-ubiquitination of MDM2 and ubiquitination of p53 (Sasiela et al., 2008). Notably, although these compounds do not target the p53/MDM2 interaction, they appear to fully activate p53, suggesting they do not allow for the retention of binding. This hypothesises that these compounds alter the structure of MDM2 RING domain and so function analogously to the MDM2 C464A mutant.

1.5.1.3 Inhibitor of DUBs

HAUSP (USP7) efficiently de-ubiquitinates MDM2 and MDMX to stabilise them, making in an attractive therapeutic target as its knockdown causes severe MDM2 depletion and leads to G_1 cell cycle arrest in colon cancer cells. Several pre-clinical chemicals (such as P5091 and HBX19,818) have been developed to inhibit HAUSP in order to promote MDM2 degradation and stabilise p53 (Meulmeester et al., 2005). Recently, additional specific small molecule inhibitors of HAUSP (including FT671 and GNE-6640) are introduced (Turnbull et al., 2017, Kategaya et al., 2017). Indeed, FT671 elevated p53 level in the melanoma cell (MM.1S) xenograft model and attenuated tumour growth in a dose dependent manner with no obvious adverse effects (Turnbull et al., 2017).

1.5.2 Targeting other E3 ligases and DUBs

Alterations of the ubiquitin-proteasome system are involved in progression of many types of cancer, as discussed above. In addition to compounds targeting p53 reactivation, many compounds targeting other specific E3 ligases have been discovered, including inhibitors of SCF-SKP2, APC/C-CDC20 and SCF-β-TRCP and enhancers of SCF-FBXW7.

SCF-SKP2 is one of a main tumour-promoting complex affecting many pathways including cell cycle regulation and EMT. Notably, some natural compounds including vitamin D_3, curcumin (as in turmeric and some gingers), lycopene (as in tomatoes) and quercetin (as in many fruits and vegetables) have been reported to attenuate the expression of SKP2 and show some anti-tumour effects (Yang and Burnstein, 2003, Huang et al., 2011a).

APC/C-CDC20 mediates cell cycle regulation mainly at the end of M phase (spindle checkpoint) by degrading cyclin B1 and several CDK inhibitors. Therefore, unlike APC/C-CDH1, over-activation of APC/C-CDC20 promotes tumourigenesis. Compounds from some medicinal mushrooms seem to attenuate the expression of CDC20 but detailed mechanisms are largely unknown (Jiang and Sliva, 2010, Jiang et al., 2011b).

SCF-β-TRCP plays both tumour promoting and tumour suppressing roles. However, as overexpression of β-TRCP is often observed in many types of cancer, inhibition of SCF-β-TRCP would be beneficial. Erioflorin (from common woolly sunflower) has been shown to be an SCF-β-TRCP inhibitor, by inhibiting the binding of its substrate (Blees et al., 2012).

SCF-FBXW7 is a tumour supressing E3 ligase and *FBXW7* is a p53 target gene. Some plant extracts, including Oridonin (from medicinal herbs including *Rabdosia rubescens, Isodon japonicus and I trichocarpus*) and Genistein (from soybean) seem to upregulate FBXW7 expression and promote c-MYC degradation and apoptosis (Huang et al., 2012, Ma et al., 2013).

In addition, there are many other E3 ligases that are believed in involved in the pathogenesis of cancer (Table 1-6).

Table 1-6: Example of deregulated ubiquitin E3 ligases in cancer

E3 ligases	Tumour	Substrates	Affected pathways	Malfunction in cancer*
APC/C-CDC20	Promoting	Cyclin A Cyclin B1 $p21^{Cip1/Waf1}$ MCL1	Cell cycle Apoptosis	**Prostate cancer** **Breast cancer**
SCF-SKP2	Promoting	$p27^{Kip1}$ $p21^{Cip1/Waf1}$ AKT FOXO E-cadherin	Cell cycle PI3K signalling EMT	**Malignant melanoma** **Lymphoma** **Prostate cancer**
APC/C-CDH1	Suppressing	SKP2	Cell cycle	*Breast cancer*
SCF-FBXW7	Suppressing	Cyclin E XRCC4 mTOR c-Myc c-Jun MCL1 Notch HIF1α	Cell cycle DNA repair Apoptosis PI3K signalling Notch signalling Stress adaptation Angiogenesis	*Cervical carcinoma* *Gastric cancer* *Endometrial cancer* *Colorectal cancer*
Parkin	Suppressing	Cyclin E Cyclin D Cyclin B1 MCL1	Cell cycle Apoptosis	*Glioblastoma* *Non-small cell lung cancer*
BRCA1	Suppressing	Histones	DNA repair Gene expression	*Breast cancer* *Ovarian cancer*
FANCL	Suppressing	FANCD2	DNA repair	*Fanconi anaemia-associated cancers*
NEDD4	Promoting	RAS AKT PTEN Notch	RTK signalling Notch signalling	**Colorectal cancer** **Breast cancer** **Gastric cancer** **Glioma**
TRAF2	Promoting	GßL RIP kinases	PI3K signalling NF-κB activation	**Epithelial cancer**
TRAF6	Promoting	mTOR IRAK1 STAT3	PI3K signalling NF-κB activation JAK-STAT signalling	**Urothelial bladder cancer**
c-Cbl	Promoting or Suppressing	EGFR HGFR (c-MET) ß-catenin	RTK signalling Wnt signalling	**Lymphoma** **Colorectal cancer** *Myeloid neoplasms*
SCF-ß-TRCP	Promoting or Suppressing	ß-catenin VEGFR2 IκB TWIST1	Wnt signalling NF-κB activation Angiogenesis EMT	**Colorectal cancer** **Pancreatic cancer** **Ovarian cancer** **Breast cancer**
SMURF1	Promoting	SMAD1 SMAD5	TGFß signalling	**Colorectal cancer** **Pancreatic cancer**
SMURF2	Suppressing	SMAD2 SMAD3	TGFß signalling EMT	*Pancreatic cancer*
TRIM62	Suppressing	SMAD3	TGFß signalling EMT	*Breast cancer* *Non-small cell lung cancer*
cIAP1/2	Promoting	RIP kinases	NF-κB activation	**Breast cancer**
LUBAC	Promoting	NEMO	NF-κB activation	**Breast cancer**
pVHL	Suppressing	HIF1α	Stress adaptation Angiogenesis	*von Hippel-Lindau syndrome*
MKRN1	Suppressing or promoting	TRET FADD $p21^{Cip1/Waf1}$	Telomere elongation Apoptosis Cell cycle	**Testis cancer**
ZNRF1	Suppressing	Caveolin-1	Anoikis	*Leukaemia*
SCF-FBXO11	Suppressing	SNAI1	EMT	*Lymphoma*

*** Bold: upregulation, Italic: downregulation**

Since E3 ligases have relatively high substrate specificity, targeting E3 ligases could be a valuable approach to treat cancer.

1.5.3 Proteasome inhibitors

Pre-clinical studies indicate that proteasome inhibitors are cytotoxic to cancer-derived cells, and induce p53-dependent apoptosis in colon cancer, melanoma and multiple myeloma cells (Almond and Cohen, 2002, Ding et al., 2007, Qin et al., 2005). Proteasome inhibitors are currently the only compounds targeted ubiquitin proteasome system that approved by FDA. These include Bortezomib (Velcade, approved in 2008) and Carfilzomib (Kyprolis, approved in 2012) and currently used for treatment of multiple myeloma (Figure 1-30).

Bortezomib (a boronated MG132) is a reversible, potent and selective proteasome inhibitor that mainly inhibits the ß5 chymotrypsin-like serine protease subunit (Boccadoro et al., 2005, Dicato et al., 2006, Orlowski and Kuhn, 2008). Carfilzomib is an irreversible proteasome inhibitor derived from epoxomicin and showed enhanced anti-multiple myeloma activity compared with Bortezomib (Kuhn et al., 2007). Other proteasome inhibitors (such as CEP-18770, NPI-0052 and ONYX0912) are in clinical trials.

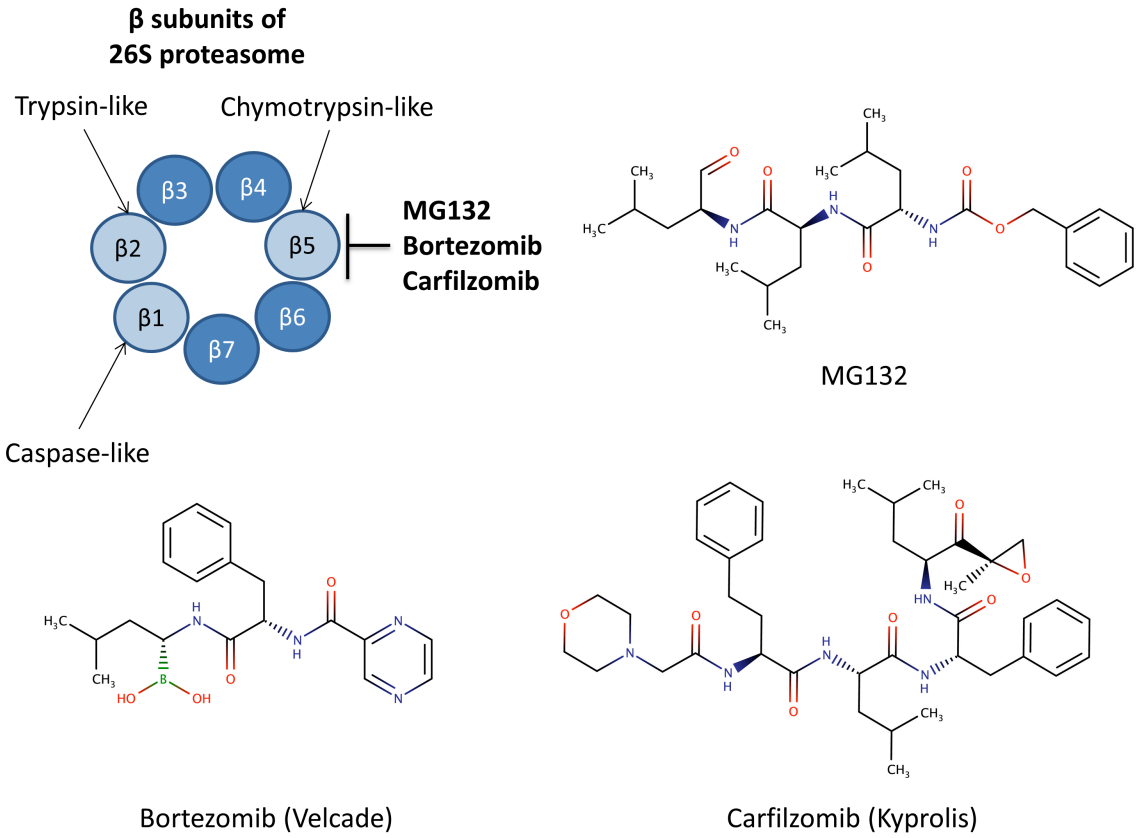

Figure 1-30: Example of proteasome inhibitors

MG132, Bortezomib and Carfilzomib inhibit activity of β5 chymotrypsin-like serine protease subunit of 26S proteasome. Chemical structure is obtained from PubChem database (https://pubchem.ncbi.nlm.nih.gov).

Although these inhibitors have been developed with the view of stabilising the pool of tumour suppressors, including p53, they are extremely non-selective and different mechanisms seem to be involved in different cell types (Almond and Cohen, 2002). For example, this class of inhibitors have been shown to cause endoplasmic reticulum stress, inhibition of NF-κB, and activation of stress-activated protein kinases such as JNK (c-Jun N-terminal kinase) (Fribley et al., 2006, Nemeth et al., 2004, Meriin et al., 1998). They may also be involved in attenuating cell cycle by potentiating CDK inhibitors. Importantly, some studies have suggested that, unlike inhibiting MDM2-p53 interaction, cells can still limit p53 activity in the presence of proteasome inhibitors in normal unstressed cells (Siliciano et al., 1997, Stommel and Wahl, 2004, Zhu et al., 2007).

1.5.4 Targeting the E1 activating enzymes

Several E1 inhibitors have been identified including PYR-41 (4[4-(5-nitro-furan-2-ylmethylene)-3,5-dioxo-pyrazolidin-1-yl]-benzoic acid ethyl ester) and another compound (5′-O-sulfamoyl-N6-[(1S)-2,3-dihydro-1H-inden-1-yl]-adenosine) (Yang et al., 2007, Chen et al., 2011). These compounds block ATP-PPi exchanging and stabilises proteins including p53 and IκB. Recently, a potent mechanism-based small-molecule E1 inhibitor TAK-243 (previously known as MLN7243) was identified (Hyer et al., 2018) (Figure 1-31). This compound forms a covalent bond with the C-terminal of ubiquitin and occupies ATP and ubiquitin binding sites on E1.

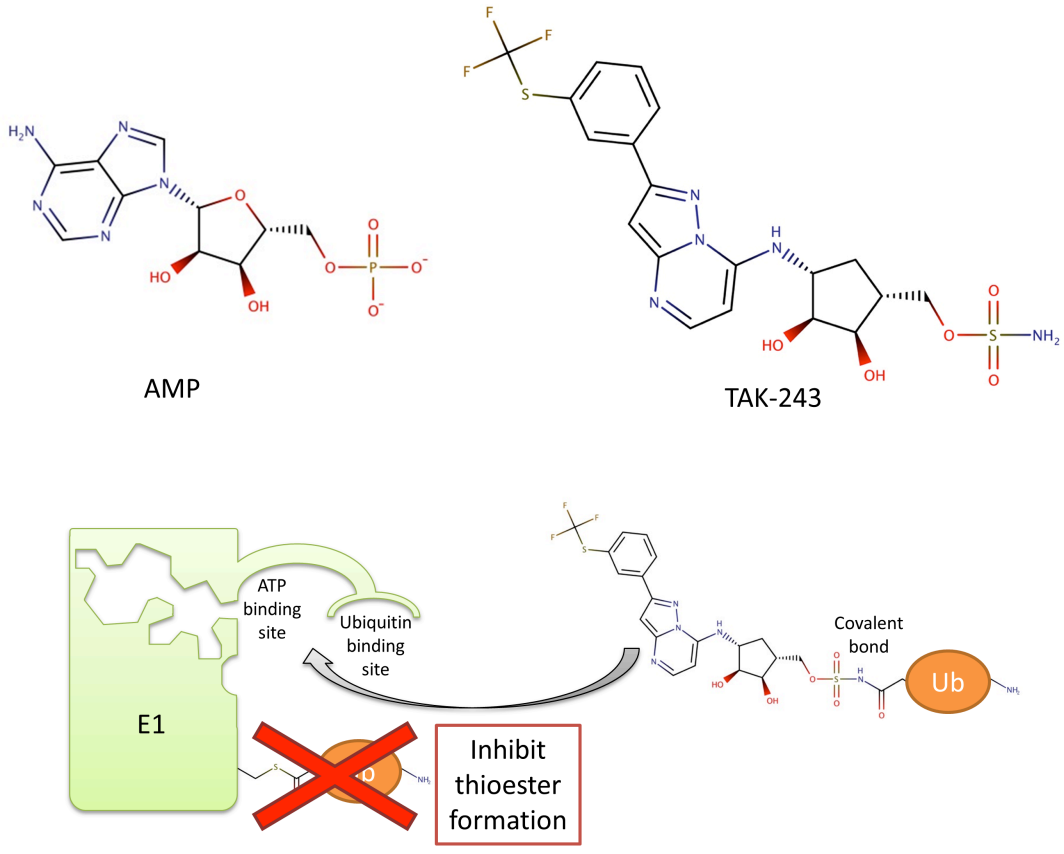

Figure 1-31: Mechanism of the E1 inhibitor TAK-243

TAK-243 forms covalent bond with the C-terminal of ubiquitin and occupies ATP and ubiquitin binding sites on E1. Ub = ubiquitin and E1 = ubiquitin activating enzyme. Chemical structure is obtained from PubChem database (https://pubchem.ncbi.nlm.nih.gov).

Interestingly, inhibition of the ubiquitin E1 appears to potentiate NEDDylation and SUMOylation in the cells. In addition to the attenuation of proteasomal degradation of ubiquitinated proteins, inhibition of E1 could also lead disruption of the degradation-independent functions of ubiquitination (discussed in Section 1.3.2.2 for example).

Another interesting approach is the inhibition of the NEDD8 activating enzyme (NAE) as activities of SCF-type ubiquitin E3 ligases are partly mediated by NEDDylation. MLN4924 is the NAE inhibitor and has been shown to attenuate various SCF-type E3 ligase activities.

1.5.5 Targeting the E2 conjugating enzymes

As E2s are involved in determining types of ubiquitin conjugation, it is possible to block specific ubiquitin chains formation by targeting specific E2. For example, CC0651 inhibits the E2 conjugate enzyme UbcH3, so inhibits K48-linked ubiquitination and degradation of SCF-SKP2 substrate $p27^{Kip1}$ and suppresses cell growth. On the other hand, Leucettamol A and Manadosterols A and B inhibit the formation of the E2 conjugating enzyme complex Ubc13-UEVA, thus blocking some K63-linked ubiquitination but no other forms, including K48-linked ubiquitination.

1.5.6 Other approaches

The ubiquitin proteasome system can be harnessed to facilitate the degradation of proteins using the proteolysis targeting chimera (PROTAC) technology. This strategy forces protein to be targeted by E3 ligases for ubiquitination. PROTAC consists 2 ligands (one for binding to the target protein and another for binding to an E3 ligase) and a bridging linker. Ligands can be either peptide or small molecule. Indeed, a hetero-bifunctional all-small-molecule PROTAC has advantages in terms of cell permeability and stability. One example is ubiquitination and degradation of the androgen receptor by MDM2 (Schneekloth et al., 2008). This PROTAC uses a small molecule non-steroid selective androgen receptor ligand modulator and nutlin-3 (as a ligand for MDM2) to allow degradation of the androgen receptor by MDM2 (Figure 1-32).

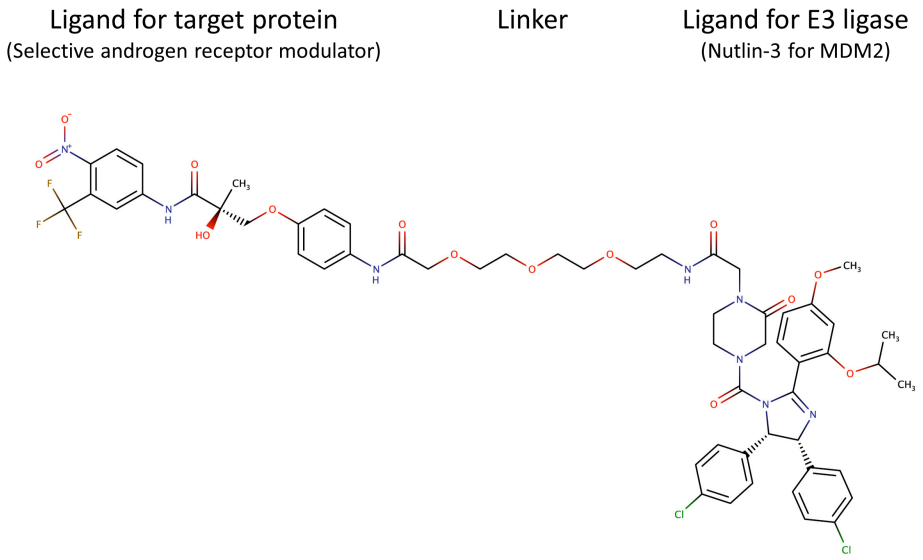

Figure 1-32: Example of PROTAC

PROTAC contains the ligand for target protein, linker and ligand for E3 ligase. Chemical structure is obtained from PubChem database.

Several PROTACs based on other E3s such as pVHL Cullin-RING E3 ligase and cIAP have been developed, based on small molecules that bind with affinity without affecting their E3 activity (Itoh et al., 2010, Bondeson et al., 2015). Although there are several technical difficulties, it may be possible to selectively degrade disease-causing proteins using PROTAC technology. For example, degradation of mutant p53 ubiquitinated by E3 ligases (other than MDM2) could be of potential interest.

1.6 Aims and Objectives

As discussed, it is clear that inhibition of the MDM2 RING domain (which need not prevent the interaction of MDM2 with p53) would lead to different outcomes than inhibition of the MDM2-p53 interaction (which does not impact E3 activity of MDM2). The aim of this study was to explore the potential of targeting the E3 ligase function of MDM2 as a novel therapeutic strategy. This has been addressed in 3 main sections:

1. Characterisation of MDM2 point mutations that do not dimerise or do not interact with the E2–ubiquitin complex without altering RING-domain conformation, guided by our novel structure (Chapter 3)

2. Cellular evaluation of these mutants in terms of regulation of p53 activity under normal and stress condition (Chapter 4)

3. Evaluation of these mutants in mouse primary cells and discussion of our novel mouse models (Chapter 5)

Chapter 2 Materials and methods

2.1 Animals

All animal work was carried out under the UK Home Office guidelines in line with Animal (Scientific Procedures) Act 1986 and the EU Directive 2010. Experimental cohorts and breeding stocks were maintained for defined periods of time and the health of animals was checked at least twice weekly. Maintenance and breeding strategies are discussed monthly with Dr Karen Blyth (Cancer Research UK Beatson Institute). Animals were euthanised by carbon dioxide (CO_2) asphyxiation or by cervical dislocation. Mouse ear notching, tail clipping and general husbandry (such as food, water and housing) were carried out by the Cancer Research UK Beatson Institute - Biological Services Unit. Genotyping was carried out by Transnetyx, Inc. (Cordova, TN, US).

2.2 Cell culture and treatment

2.2.1 Materials

Reagents used for cell culture are listed in Table 2-1, solutions and buffers used for cell culture are listed in Table 2-2 and other reagents used for treatment of cells are listed in Table 2-3.

Table 2-1: Reagents for cell culture

Reagent	Source
Dulbecco's modified Eagle medium (DMEM)	Life Technologies
Foetal bovine serum (FBS)	Life Technologies
L-glutamine	Life Technologies
Penicillin/ Streptomycin	Life Technologies
Gentamycin	Sigma-Aldrich
Insulin-Transferrin-Selenium (ITS)	Sigma-Aldrich Life Technologies
Collagenase/Dispase	Sigma-Aldrich

Table 2-2: Solutions and buffers for cell culture

Solution	Composition
Phosphate Buffered Saline (PBS) pH 7.4	170 mM NaCl (Fisher Scientific) 3.3 mM KCl (Fisher Scientific) 1.8 mM Na_2HPO_4 (Fisher Scientific) 10.6 mM KH_2PO_4 (Fisher Scientific)
Trypsin-EDTA	PBS 0.25 % Trypsin (Life Technologies) 1 mM EDTA (Sigma-Aldrich)

Table 2-3: Reagents for cell culture treatment

Reagent	Source
Doxycycline	Sigma-Aldrich
(Z)-4-hydroxytamoxifen (4-OHT)	Sigma-Aldrich
Dimethyl sulphoxide (DMSO)	Sigma-Aldrich
Nutlin-3	Sigma-Aldrich
Doxorubicin	Sigma-Aldrich
Actinomycin D	Beatson Cancer Centre

2.2.2 Methods

Human osteosarcoma U2OS or human embryonic kidney HEK293 (including 293T and 293T Phoenix Ecotropic) cells were obtained from the American Type Culture Collection (ATCC) and cultured in DMEM supplemented with 10 % FBS and 2 mM L-Glutamine. All cell lines were mycoplasma negative and were authenticated by the short tandem repeats (STR) multiplex assay. Baby mouse kidney (BMK) primary cells (below) were cultured in DMEM supplemented with 5 % FBS, 2 mM L-Glutamine, penicillin/streptomycin, gentamycin and ITS. Mouse embryonic fibroblast (MEF) primary cells (below) were cultured in DMEM supplemented with 10 % FBS, 2 mM L-Glutamine, penicillin/streptomycin and gentamycin. All cells were maintained in a controlled humidified atmosphere containing 5 % CO_2 at 37 ºC.

Where indicated, cells were treated with indicated reagents. Concentrations used and treatment periods are defined in each figure legend or in the main text.

2.2.2.1 Isolation of BMK primary cells

BMK primary cells are isolated from 4-5 days old baby mice. Baby mice were sacrificed by cervical dislocation and both kidneys are isolated. Both kidneys were placed on 100 mm dish with 1.5 ml of collagenase (0.1 U/ml)/dispase (0.8 U/ml) solution, minced by scalpel and incubated at 37 ºC for 40 minutes. After incubation, minced kidneys were titurated and single cells were isolated. Cells were then seeded in 150 mm dishes and cultured in DMEM supplemented with 5 % FBS, 2 mM L-glutamine, penicillin/streptomycin, gentamycin and ITS.

2.2.2.2 Isolation of MEF primary cells

Pregnant female mice 13-14 days after copulation confirmed by plug detection (E13.5-E14.5) were sacrificed for MEFs by cervical dislocation. Fur was sprayed with 70 % ethanol and the intact uterus containing embryos was extracted. The uterus was then sectioned between each embryo and the membranes and umbilical cord were removed. Embryos were decapitated and their abdominal wall was incised to remove haematopoietic tissue and tubular intestine. Each embryo body was then placed on 100 mm dish with 1.5 ml of trypsin-EDTA, minced by scalpel and incubated at 37 ºC for 40 minutes. After incubation, minced embryo was titurated and single cells were isolated. Cells were then seeded in 150 mm dishes and cultured in DMEM supplemented with 10 % FBS, 2 mM L-Glutamine, penicillin/streptomycin and gentamycin.

2.3 PCR and DNA preparation

2.3.1 Materials

Reagents used for PCR and DNA preparation are listed in Table 2-4, solutions and buffers used for PCR and DNA preparation are listed in Table 2-5, plasmids used for over-expression are listed in Table 2-6 and plasmids used for knockout / knockdown used for treatment are listed in Table 2-7.

Table 2-4: Reagents for PCR and DNA preparation

Reagent / Kit	Source
In-Fusion HD EcoDry cloning kit	Clontech
KOD Hot Start PCR master mix	Novagen
Agarose	Melford Laboratories
Ethidium Bromide	Sigma-Aldrich
Restriction enzymes	New England BioLabs
Ampicillin	Sigma-Aldrich
Kanamycin	Sigma-Aldrich
RNase A	Qiagen
QIAGEN-tip 50	Qiagen
Isopropanol	Fisher Scientific
Ethanol	Sigma-Aldrich

Table 2-5: Solutions and buffers for PCR and DNA preparation

Solution	Composition
TAE buffer	40 mM Tris-HCl (pH 8.0) (Sigma-Aldrich) 20 mM Acetic acid (Fisher Scientific) 1 mM EDTA (Sigma-Aldrich)
(6x) DNA sample buffer	30 % Glycerol (v/v) (Sigma-Aldrich) 0.5 % Orange G (w/v) (Sigma-Aldrich)
Lysogeny broth (LB)	1 % Bacto-tryptone (Fisher Scientific) 86 mM NaCl (Fisher Scientific) 0.5 % Yeast extract (Sigma-Aldrich) 1.5 % agar (Fluka)
Bacteria re-suspension buffer (Qiagen)	50 mM Tris-HCl (pH 8.0) 10 mM EDTA 100 µg/ml RNase A
Bacteria lysis buffer (Qiagen)	200 mM NaOH 1 % SDS (w/v)
Neutralisation buffer (Qiagen)	3.0 M Potassium acetate (pH 5.5)
Equilibration buffer (Qiagen)	750 mM NaCl 50 mM MOPS (pH 7.0) 15 % Isopropanol (v/v) 0.15 % Triton X-100 (v/v)
Washing buffer (Qiagen)	1.0 M NaCl 50 mM MOPS (pH 7.0) 15 % Isopropanol (v/v)
Elution buffer (Qiagen)	1.25 M NaCl 50 mM Tris-HCl (pH 8.5) 15 % Isopropanol (v/v)

Table 2-6: Plasmids for over-expression

Encode	Plasmid	Tag	Assays	Reference
p53	pCB6	N/A	Degradation assay Ubiquitination assay Co-IP	(Chen et al., 1995)
MDM2	pCMV	N/A	Degradation assay Ubiquitination assay Co-IP Immunofluorescence	(Kawai et al., 2003b)
MDMX	pcDNA3.1	Myc	Degradation assay Ubiquitination assay Co-IP	(Weber et al., 2005)
MDMX	pEGFP-C1	GFP	Immunofluorescence	(Uldrijan et al., 2007)
MDM2-MDMX chimera (1-421: MDM2, 422-490: MDMX)	pCMV	FLAG	Degradation assay Ubiquitination assay Co-IP	(Sharp et al., 1999)
$p14^{ARF}$	pcDNA3.1	FLAG	Degradation assay Ubiquitination assay	-
Ubiquitin	pDG268	His GFP	Ubiquitination assay	(Tsirigotis et al., 2001)
mCherry	pmCherry-C1	N/A	Degradation assay Ubiquitination assay Co-IP	(Werner et al., 1996)
MDM2 (murine)	pcDNA3.1	N/A	Degradation assay	-
p53 (murine)	pcDNA3.1	N/A	Degradation assay	-

Table 2-7: Plasmids for knockout / knockdown

Plasmid	Target	Purpose	Reference
Tet-pLKO-puro	p53	Inducible knockdown	(Wiederschain et al., 2009)
pX335-U6-Chimeric_BB-CBh-hSpCas9n(D10A)	*MDM2*	CRISPR knockout	(Cong et al., 2013)

Target sequences
p53 (shRNA): GAC TCC AGT GGT AAT CTA C
MDM2 knockout (CRISPR guide A): ATC GTT TAG TCA TAA TAT AC TGG (PAM*)
MDM2 knockout (CRISPR guide B): TAT TGT TCA AAT GAT CTT CT AGG (PAM*)
MDM2 ΔRING (CRISPR guide A): ACA AGG TTC AAT GGC ATT AA GGG (PAM*)
MDM2 ΔRING (CRISPR guide B): TGT CAA GGT CGA CCT AAA AA TGG (PAM*)
* PAM = Protospacer adjacent motif (*N*GG)

CRISPR guides were designed based on the Optimized CRISPR design tool (http://crispr.mit.edu).

2.3.2 Methods

2.3.2.1 Plasmid cloning and agarose gel electrophoresis

Plasmid DNA cloning was carried out using In-Fusion HD EcoDry cloning kit (Clontech). The linearised DNA vector was prepared by appropriate restriction enzyme digestion, or by PCR using KOD hot start PCR master mix as described above with an optimised PCR program (95 ºC for 2 minutes (polymerase activation), 40 cycles of 95 ºC for 20 seconds (denature), 55 °C for 10 seconds (annealing) and 70 ºC for 25 seconds/kbp (extension)). Digested DNA vector or PCR product was then separated by agarose gel electrophoresis. The gel is prepared by dissolving the 1 - 2 % agarose (w/v) in TAE buffer, depending on the size of the product. Ethidium bromide (250 nM final concentrations) was then added to the melted agarose before pouring it into a cast. A comb is placed in the cast to create wells for loading samples. DNA sample buffer was added to the digested DNA vector or PCR product. Samples were loaded into the gel slab in TAE buffer and ran electrophoresis at 80 V. Under UV light, a gel piece containing linearised plasmid DNA was removed and purified using spin column (Macherey-Nagel).

The gene of interest with 15 bp extensions complementary to both vector ends was prepaid by PCR using the same procedure described above (for more than 200 bp insert) or purchased as a double strand DNA (for less than 200 bp insert).

Approximately 200 ng of linearised and 200 ng of insert in 10 µl of dH_2O were then applied into In-Fusion HD EcoDry and cloning incubated the reaction at 37 ºC for 15 minutes and at 50 ºC for 15 minutes.

2.3.2.2 Mutagenesis PCR

All mutations in plasmid DNA were generated by site-directed mutagenesis PCR using KOD hot start PCR master mix and verified by DNA sequencing. Primers for site-directed mutagenesis PCR were deigned and mutagenesis codon was selected based on the Graphical Codon Usage Analyser (GCUA) tool (http://gcua.schoedl.de). Primers contain mutagenesis codon in the centre with melting temperature (T_m) of 58-60 ºC both arm containing approximately 25 bp each. 0.3 µM each of Sense (5') and anti-sense (3') primers and 0.2 ng/µl of template DNA were added to the PCR mix and ran PCR with an optimised PCR program (95 ºC for 2 minutes (polymerase activation), 20 cycles of 95 ºC for 20 seconds (denature), 55 ºC for 10 seconds (annealing) and 70 ºC for 25 seconds/kbp (extension)). After PCR reaction, 0.02 unit/µl of DpnI restriction enzyme was added and mixtures were incubated at 37 ºC for 3 hours in order to digest methylated template DNA.

2.3.2.3 Plasmid DNA preparation and sequencing

Products from DNA cloning or mutagenesis PCR were then expanded and purified by DNA preparation. The competent bacteria cells including the *Escherichia coli* DH5α competent cells (Cancer Research UK Beatson Institute - Molecular Technology Services), Stellar competent cells (Clontech) or Stbl3 competent cells (Thermo Fisher Scientific) were thawed on ice. 0.5 µg of DNA plasmid was added to 50 µl of bacteria, mixed and incubated on ice for 20 minutes. After a heat shock of 45 seconds at 42 ºC, the cells were incubated in 0.5 ml of LB for 1 hour at 37 ºC with shaking at 200 rpm. Cells were spread on agar plates with ampicillin or kanamycin and grown upside down at 37 °C overnight. The next day the colonies were inoculated in 5 ml of LB with ampicillin or kanamycin and grown overnight at 37 °C whilst shaking at 200 rpm. Bacteria culture was harvested by centrifugation at 4000 rpm for 10 minutes at room temperature. Small scale plasmid DNA preparations (Miniprep) using an alkaline lysis method of DNA isolation were performed by Cancer Research UK Beatson Institute -

Molecular Technology Services Unit with the QIAgen BioRobot 9600 according to the manufacturer's instructions, followed by DNA sequence.

Large scale DNA preparations (Maxiprep) were then performed using the same method as Minipreps until the colony formation step. Colonies were incubated in 300 ml of LB with ampicillin or kanamycin and grown overnight at 37 °C whilst shaking at 180 rpm. Bacteria culture was harvested by centrifugation at 4000 rpm for 10 minutes at room temperature. Bacteria pellet was re-suspended in 10 ml of the bacteria re-suspension buffer. 10 ml of bacteria lysis buffer was then added and mixed gently but thoroughly by inverting 4-6 times, and incubated at room temperature for 5 minutes. In this alkaline condition, proteins and chromosomal DNA are denatured but plasmid DNA remains stable. 10 ml of the neutralisation buffer was then mixed immediately but gently by inverting 4-6 times, and incubated on ice for 20 minutes. This allows proteins and chromosomal DNA precipitate but plasmid DNA remains in solution. Mixture was then centrifuged at 20,000 rcf for 30 minutes at 4 °C. Supernatant containing plasmid DNA promptly was then removed for gravity flow. QIAGEN-tip 50 was equilibrated by applying 10 ml of the equilibration. Supernatant was then applied to the QIAGEN-tip 50 and allow it to enter the resin by gravity flow. QIAGEN-tip 50 was washed twice with 30 ml of the washing buffer and plasmid DNA was then eluted by 15 ml of elution buffer followed by DNA precipitation by adding 10.5 ml of isopropanol. Mixture was immediately centrifuged at 15,000 rcf for 30 minutes at 4 °C, and DNA pellet was washed with 5ml of 70 % ethanol and centrifuged at at 15,000 rcf for 15 minutes at 4 °C. Pellet was dried and re-suspended in 400 µl of dH_2O. Maxi Preps were also performed by Cancer Research UK Beatson Institute - Molecular Technology Services Unit.

2.4 Genomic DNA isolation and Genomic PCR / Genotyping

2.4.1 Materials

Reagents used for Genomic DNA isolation and Genomic PCR / Genotyping are listed in Table 2-8, solutions and buffers used for Genomic DNA isolation and Genomic PCR / Genotyping are listed in Table 2-9, primers used for genomic PCR

(for sequencing) are listed in Table 2-10 and primers used for genotyping are listed in Table 2-11.

Table 2-8: Reagents for Genomic DNA isolation and Genomic PCR / Genotyping

Reagent	Source
KOD Hot Start PCR master mix	Novagen
Isopropanol	Fisher Scientific
Ethanol	Sigma-Aldrich
Agarose	Melford Laboratories
Ethidium Bromide	Sigma-Aldrich

Table 2-9: Solutions and buffers for Genomic DNA isolation and Genomic PCR / Genotyping

Solution	Composition
DNA isolation buffer	100 mM Tris-HCl (pH 8.8) (Sigma-Aldrich) 5 mM EDTA (Sigma-Aldrich) 0.2 % SDS (Fisher Scientific) 200 mM NaCl (Fisher Scientific) 100 µg/ml Proteinase K (Melford Laboratories)
DNA elution buffer	5 mM Tris-HCl (pH 8.5) (Sigma-Aldrich)
TAE buffer	40 mM Tris-HCl (pH 8.0) (Sigma-Aldrich) 20 mM Acetic acid (Fisher Scientific) 1 mM EDTA (Sigma-Aldrich)
(6x) DNA sample buffer	30 % Glycerol (v/v) (Sigma-Aldrich) 0.5 % Orange G (w/v) (Sigma-Aldrich)

Table 2-10: Primers for genomic PCR (for sequencing)

Target	Primers (5'-3')
MDM2 p53-binding domain	For: TCC TGG TTG TTT ACC CCT ATT CAG Rev: GCC AGA GCT CAG GTT CTC AAA TA
MDM2 RING domain	For: ACA CAA GCT TCA CAA TCA CAA GAA Rev: TTC AGG TTG TCT AAA TTC CTA GGG T

Table 2-11: Primers for genotyping

Target	Primers (5'-3')	Expected band size
Mdm2 I438K targeted allele	For: TTT CCT GCT TGC CTT GAA CTG Rev: ATG CAG CCA TTT TTA GGC CG	1034 bp (Wild type) 675 bp (Targeted allele)
Cre recombinase	For: AGC AAC ATT TGG GCC AGC TA Rev: GGT GCT AAC CAG CGT TTT CG	353 bp

2.4.2 Methods

Genomic DNA is isolated from cells or mouse tissues (tail, liver or kidney). Briefly, cells or tissues were incubated in 500 µl of DNA isolation buffer overnight at 50 °C. 500 µl of 100 % isopropanol was then added to it and mixed. Mixture was centrifuged at 16,100 rcf for 5 minutes. Supernatant was removed

and pellet was washed with 70 % ethanol. Pellet was dried at 55 °C for 10 minutes and re-suspended in DNA elution buffer.

PCR primers were designed using Primer Blast tool (NCBI). 0.3 µM each of sense (5') and anti-sense (3') primers and 0.2 ng/µl of template DNA were added to the KOD hot start PCR master mix and ran PCR with an optimised PCR program (95 °C for 2 minutes (polymerase activation), 40 cycles of 95 °C for 20 seconds (denature), 55 °C for 10 seconds (annealing) and 70 °C for 25 seconds/kbp (extension)).

For genotyping, agarose gel electrophoresis was performed with 2 % agarose in TAE buffer as described above. Images are captured by GelDoc-It imager (UVP).

2.5 Transfection, infection and cell cloning

2.5.1 Materials

Reagents and kits used for transfection, infection and cell cloning are listed in Table 2-12.

Table 2-12: Reagents and kits for transfection, infection and cell cloning

Reagent / Kit	Source
GeneJuice	Novagen
Lipofectamine 2000	Life Technologies
jetPRIME	Polyplus Transfection
Lullaby	OZ Biosciences
Nucleofection Kit V	Lonza
OptiMEM	Life Technologies
Polybrene	Sigma-Aldrich
Puromycin	Sigma-Aldrich
Blasticidine	Thermo Fisher Scientific
G418 Geneticin (Neomycin)	Invivogen
Hygromycin B	Thermo Fisher Scientific

2.5.2 Methods

2.5.2.1 Chemical-based transfection

Cells were transfected with GeneJuice, Lipofectamine 2000, jetPRIME or Lullaby (for siRNA) transfection reagent, according to the manufacturer's instructions.

Briefly, a mixture of DNA plasmid (or siRNA) and transfection reagent (in OptiMEM or manufacturer's provided solution) was added to plates drop-wise. Cells were incubated for 24 hours. Cell number, medium, transfection reagent volumes and amount of DNA were scaled depending on plate size.

Transfected cells were selected with the selective agent, where necessary.

2.5.2.2 Electroporation-based transfection

Cells were also transfected with Nucleofection Kit V according to the manufacturer's instructions. Briefly, Approximately 5 x 10^6 cells were mixed with 5 µg of plasmid DNA in the nucleofector solution and were transfer to the nucleofector cuvette. Cells were then electroporated with the cell-type specific program and were then transferred into cell culture plate. Cells were incubated for 24 hours.

2.5.2.3 Virus infection

HEK293T (for lentivirus infection) or HEK293T Phoenix Ecotropic (for retrovirus infection) cells were transfected with retroviral plasmid or lentiviral plasmid (with psPAX2 (packaging plasmid) and pCMV-VSV-G (enveloping plasmid)) with GeneJuice transfection reagent overnight. Media were replaced and incubated for further 48 hours. This virus-containing media were filtered with 0.45 µm filter unit and added to the target cells with polybrene (10 µg/ml). After 24-48 hours, media were replaced and selected with the selective agent.

Purified adenovirus particles (Ad5CMV-Cre or Ad5CMV-EV) were gifted from University of Iowa - GTVC and directly added to the cell culture according to the manufacturer's instructions.

2.5.2.4 Cell cloning

Approximately 500 cells were seeded in 150 mm dishes and allowed colony formation. Colonies were then isolated using cell cloning cylinders (VWR) according to the manufacturer's instructions.

2.6 SDS-PAGE and Immunoblotting

2.6.1 Materials

Reagents and kits used for SDS-PAGE and immunoblotting are listed in Table 2-13, Solutions and buffers used for SDS-PAGE and immunoblotting are listed in Table 2-14, Gels used for SDS-PAGE are listed in Table 2-15 and antibodies used for immunoblotting are listed in Table 2-16.

Table 2-13: Reagents and kits for SDS-PAGE and immunoblotting

Reagent / Kit	Source
NuPAGE Bis-Tris (10 % or 4-12 %) gels	Life Technologies
NuPAGE MOPS running buffer	Life Technologies
Nitrocellulose membrane (0.2 µm)	GE Healthcare
Odyssey Blocking buffer	LI-COR
Pierce BCA Protein Assay Kit	Thermo Fisher Scientific
Odyssey stripping buffer	LI-COR

Table 2-14: Solutions and buffers for SDS-PAGE and immunoblotting

Solution	Composition
Cell lysis buffer (1 % Triton X-100)	1 % Triton X-100 (Sigma-Aldrich) 150 mM NaCl (Fisher Scientific) 50 mM Tris-HCl (pH 8.0) (Sigma Aldrich)
3x SDS Sample Buffer	188 mM Tris-HCl (pH 6.8) (Sigma Aldrich) 9 % SDS (Fisher Scientific) 15 % β-mercaptoethanol (Sigma-Aldrich) 30 % Glycerol (Sigma-Aldrich) 0.1 % Orange G (Sigma-Aldrich)
SDS-PAGE running buffer	0.1 % SDS (Fisher Scientific) 192 mM Glycine (Sigma-Aldrich) 25 mM Tris-HCl (pH 8.3) (Sigma-Aldrich)
Electroblotting buffer	192 mM Glycine (Sigma-Aldrich) 25 mM Tris-HCl (pH 8.3) (Sigma-Aldrich) 20 % Methanol (VWR)
Tris-Buffered Saline (TBS)	25 mM Tris-HCl (pH 7.4) (Sigma-Aldrich) 137 mM NaCl (Fisher Scientific) 5 mM KCl (Fisher Scientific)
TBS-T (TBS-Tween)	TBS 0.1 % Tween-20 (Sigma-Aldrich)
Blocking buffer	TBS-T 5 % Skimmed milk powder (Marvel)

Table 2-15: Gels for SDS-PAGE

Gel	Composition
Resolving gel	8-12 % Acrylamide (National diagnostics) 375 mM Tris-HCl (pH 8.8) (Sigma-Aldrich) 0.1 % SDS (Fisher Scientific) 0.1 % APS (Sigma-Aldrich) 50 mM TEMED (Sigma-Aldrich)
Stacking gel	5 % Acrylamide (National diagnostics) 500 mM Tris-HCl (pH 6.8) (Sigma-Aldrich) 0.4 % SDS (Fisher Scientific)

Table 2-16: Antibodies for immunoblotting

Primary Antibody	Description	Supplier	Dilution used	Species used
p53	mouse monoclonal (DO-1)	Santa Cruz Biotechnology	1:1000	Human
p53	rabbit polyclonal (FL-393)	Santa Cruz Biotechnology	1:1000	Human
p53	mouse monoclonal (1C12)	Cell Signaling Technology	1:1000	Mouse
MDM2	mouse monoclonal (Ab-1)	Calbiochem	1:1000	Human
MDM2	mouse monoclonal (Ab-2)	Calbiochem	1:1000	Human Mouse
MDMX	rabbit polyclonal (A300-287A)	Bethyl Laboratories	1:1000	Human
MDMX	mouse monoclonal (8C6)	EMD Millipore	1:1000	Human
p21	rabbit or goat polyclonal (C-19)	Santa Cruz Biotechnology	1:1000	Human Mouse
PIG3	rabbit polyclonal (PC268)	Calbiochem	1:1000	Human
TIGAR	mouse monoclonal (F-5)	Santa Cruz Biotechnology	1:1000	Human
BAX	mouse monoclonal (D2D)	Santa Cruz Biotechnology	1:1000	Human
phospho-p53 (S15)	rabbit polyclonal (9284)	Cell Signaling Technology	1:1000	Human
phospho-p53 (S20)	rabbit polyclonal (9287)	Cell Signaling Technology	1:1000	Human
Actin	rabbit or goat polyclonal (I-19)	Santa Cruz Biotechnology	1:1000	Human Mouse
α-Tubulin	mouse monoclonal (DM1A)	Santa Cruz Biotechnology	1:1000	Human
mCherry	goat polyclonal (AB0040)	Acris Antibodies	1:2500	Human Mouse
Secondary antibody				
IRDye 680LT-conjugated secondary antibody		LI-COR	1:10000	
IRDye 800CW- conjugated secondary antibody		LI-COR	1:10000	

2.6.2 Methods

Cells were washed with PBS and proteins were extracted with cell lysis buffer supplemented with or without the protease inhibitor cocktail (cOmplete Tablets Mini EDTA-free, Roche Diagnostics) and/or the phosphatase inhibitor cocktail (PhosSTOP, Roche Diagnostics), which were then centrifuged at 16,100 rcf at 4 ºC for 10 minutes. Where appropriate, protein concentration in cellular lysate was determined using the BCA protein assay, with concentrations normalised to the lowest-concentration sample. Samples were heated to 99 ºC for 10 minutes with sample buffer whilst shaking at 1,000 rpm before separation by SDS-PAGE. Samples were loaded on appropriate SDS-polyacrylamide gels (8 %, 10 % or 12 % acrylamide content) or precast NuPAGE Bis-Tris (10 % or 4-12 %) gels.

Electrophoresis was performed in SDS-PAGE running buffer or NuPAGE MOPS running buffer at 140 V on Hoefer Mighty Small vertical units SE250 (Amersham) or NuPAGE Mini Gel Tank (Life Technologies). Protein was then transferred to nitrocellulose membrane using the Hoefer TE22 Mini transfer tank (Amersham) at 200 mA for 2 hours. After the transfer, the membrane was blocked with 5 % skimmed milk blocking buffer or Odyssey blocking buffer for 1 hour, and was then incubated with primary antibodies overnight at 4 ºC.

After this incubation time, the membrane was washed with TBS-T and incubated with appropriate IRDye 680LT-conjugated or IRDye 800CW-conjugated secondary antibodies for 1 hour, then washed with TBS-T and TBS, and membrane-bound secondary antibodies were detected using Odyssey scanner (LI-COR). Images were analysed by Image Studio (LI-COR) and data were normalised to actin or α-tubulin expression, as appropriate.

Where necessary, membrane-bound antibodies were removed with stripping buffer according to the manufacturer's instructions and re-probed.

2.7 Immunoprecipitation

2.7.1 Materials

Reagents and kits used for immunoprecipitation are listed in Table 2-17, solutions and buffers used for immunoprecipitation are listed in Table 2-18 and antibodies used for immunoprecipitation are listed in Table 2-19.

Table 2-17: Reagents and kits for immunoprecipitation

Reagent / Kit	Source
Dynabeads Protein G magnetic beads	Life Technologies
Pierce BCA Protein Assay Kit	Thermo Fisher Scientific

Table 2-18: Solutions and buffers for immunoprecipitation

Solution	Composition
Cell lysis buffer (1 % Triton X-100)	1 % Triton X-100 (Sigma-Aldrich) 150 mM NaCl (Fisher Scientific) 50 mM Tris-HCl (pH 8.0) (Sigma-Aldrich)
Phosphate Buffered Saline (PBS) pH 7.4	170 mM NaCl (Fisher Scientific) 3.3 mM KCl (Fisher Scientific) 1.8 mM Na_2HPO_4 (Fisher Scientific) 10.6 mM KH_2PO_4 (Fisher Scientific)
3x SDS Sample Buffer	188 mM Tris-HCl (pH 6.8) (Sigma-Aldrich) 9 % SDS (Fisher Scientific) 15 % β-mercaptoethanol (Sigma-Aldrich) 30 % Glycerol (Sigma-Aldrich) 0.1 % Orange G (Sigma-Aldrich)

Table 2-19: Antibodies for immunoprecipitation

Primary Antibody	Description	Supplier
p53	mouse monoclonal (DO-1)	Santa Cruz Biotechnology
p53	rabbit polyclonal (FL-393)	Santa Cruz Biotechnology
MDM2	mouse monoclonal (Ab-1)	Calbiochem
MDMX	rabbit polyclonal (A300-287A)	Bethyl Laboratories

2.7.2 Methods

Proteins were extracted from the cells with the cell lysis buffer supplemented with the protease inhibitor cocktail (cOmplete Tablets Mini EDTA-free, Roche Diagnostics) and normalised as described in immunoblotting section. Cellular lysates containing 250 µg proteins were incubated with 2 µg of anti-p53 DO-1 or FL-393, anti-MDM2 Ab-1, anti-MDMX A300-287A or mouse or rabbit control IgG for 1 hour at 4 ºC, and then incubated with Dynabeads protein G magnetic beads overnight at 4 ºC on the rotator. The immunoprecipitates were washed 3 times with PBS and heated to 99 ºC for 10 minutes with sample buffer whilst shaking at 1,000 rpm. After removing magnetic beads, SDS-PAGE and immunoblotting were performed as described in immunoblotting section.

2.8 Ubiquitination assay

2.8.1 Materials

Reagents used for ubiquitination assay are listed in table 2-20 and solutions and buffers used for ubiquitination assay are listed in Table 2-21.

Table 2-20: Reagents for ubiquitination assay

Reagent	Source
Dynabeads His-Tag Isolation & Pull down magnetic beads	Life Technologies
N-Ethylmaleimide (NEM)	Sigma-Aldrich
MG132 (Z-Leu-Leu-Leu-al)	Sigma-Aldrich

Table 2-21: Solutions and buffers for ubiquitination assay

Solution	Composition
Phosphate Buffered Saline (PBS) pH 7.4	170 mM NaCl (Fisher Scientific) 3.3 mM KCl (Fisher Scientific) 1.8 mM Na_2HPO_4 (Fisher Scientific) 10.6 mM KH_2PO_4 (Fisher Scientific)
Ubiquitination assay buffer A (UBA)	6 M Guanidine hydrochloride (Sigma-Aldrich) 300 mM NaCl (Fisher Scientific) 50 mM Phosphate (pH 8.0) (Sigma-Aldrich) 100 µg/ml N-Ethylmaleimide (Sigma-Aldrich)
Ubiquitination assay buffer C (UBC)	300 mM NaCl (Fisher Scientific) 50 mM Phosphate (pH 8.0) (Sigma-Aldrich)
Ubiquitination assay buffer B (UBB)	UBA:UBC = 1:1
3x SDS Sample Buffer	188 mM Tris-HCl (pH 6.8) (Sigma-Aldrich) 9 % SDS (Fisher Scientific) 15 % β-mercaptoethanol (Sigma-Aldrich) 30 % Glycerol (Sigma-Aldrich) 0.1 % Orange G (Sigma-Aldrich)

2.8.2 Methods

U2OS cells grown in 100 mm dishes were transiently transfected with 2 µg of pCB6 p53, 3.9 µg of pCMV MDM2, FLAG-tagged MDM2/X chimera, pcDNA3.1 myc-tagged MDMX or derived mutants, 3.9 µg of pDG268, 6x His-tagged Ubiquitin GFP and 0.2 µg of pmCherry-C1 using GeneJuice transfection reagent and cultivated for further 24 hours. Cells were treated for 5 hours with proteasome inhibitor MG132 (10 mM) and 10 minutes with NEM (100 µg/ml). After treatment, cells were harvested in PBS, preserved some as an input sample, and then lysed in UBA buffer supplemented with the protease inhibitor cocktail (cOmplete Tablets Mini EDTA-free, Roche Diagnostics). Lysates were boiled at 99 ºC for 20 minutes with 1,000 rpm shake. His-tag pull-down was performed using 50 µl of Dynabeads His-Tag Isolation & Pull down Beads overnight and beads were washed with UBA, UBB, UBC then PBS and heated to 99 ºC for 10 minutes with sample buffer whilst shaking at 1,000 rpm. After removing magnetic beads, SDS-PAGE and immunoblotting were performed as described in immunoblotting section. Ubiquitinated p53 was detected using anti-p53 FL-393 or DO-1 antibodies; p53, MDM2 (and MDM2/MDMX chimera), MDMX, actin and mCherry levels in the input were detected using antibodies describes in immunoblotting section.

2.9 Immunofluorescence

2.9.1 Materials

Reagents and kits used for immunofluorescence are listed in Table 2-22, solutions and buffers used for immunofluorescence are listed in Table 2-23 and antibodies used for immunofluorescence are listed in Table 2-24.

Table 2-22: Reagents and Kits for immunofluorescence

Reagent / Kit	Source
Paraformaldehyde (PFA)	Sigma-Aldrich
VECTASHIELD Mounting Medium with DAPI	Vector laboratories
Glycine	Sigma-Aldrich

Table 2-23: Solutions and buffers for immunofluorescence

Solution	Composition
Phosphate Buffered Saline (PBS) pH 7.4	170 mM NaCl (Fisher Scientific) 3.3 mM KCl (Fisher Scientific) 1.8 mM Na_2HPO_4 (Fisher Scientific) 10.6 mM KH_2PO_4 (Fisher Scientific)
PBS-T (PBS-Tween)	PBS 0.1 % Tween-20 (Sigma-Aldrich)
Cell permeabilisation buffer	PBS 0.2 % Triton X-100 (Sigma-Aldrich)
Blocking buffer	PBS 0.5 % Bovine serum albumin (BSA) (Sigma-Aldrich)

Table 2-24: Antibodies for immunofluorescence

Primary Antibody	Description	Supplier
MDM2	mouse monoclonal (Ab-1)	Calbiochem
Secondary Antibody		
Alexa568-conjugated donkey anti mouse		Life Technologies

2.9.2 Methods

Cells were grown on 13 mm glass-coverslips (VWR) placed into 6 well plates. Cells were transfected with MDM2 wild type or mutants and GFP-tagged MDMX overnight then washed and fixed with 4 % PFA in PBS for 20 minutes at room temperature and PFA was quenched with 30 mM glycine in PBS. Cells were washed and permeabilised with the cell permeabilisation buffer for 10 minutes at room temperature. Cells were then washed with PBS and blocked with the blocking buffer for 3 hours at room temperature and were then incubated with anti-MDM2 Ab-1 antibody (1:100) overnight at 4 ºC. After this incubation time,

cells were washed with PBS-T and incubated with secondary antibody (1:200) for 2 hours, then washed with PBS-T and then PBS. Coverslips were washed with double-distilled water to remove any salt residues and then mounted with VECTASHIELD Mounting Medium with DAPI. Images were taken using confocal microscope Fluoview FV1000 (Olympus).

2.10 RNA Extraction and Quantitative Real-Time PCR (qPCR)

2.10.1 Materials

Reagents and kits used for RNA extraction and qPCR are listed in Table 2-25 and primers used for qPCR are listed in Table 2-26.

Table 2-25: Reagents and Kits for RNA extraction and qPCR

Reagent / Kit	Source
RNeasy Mini Kit	Qiagen
RNase-Free DNase Set	Qiagen
High-Capacity RNA-to-cDNA Kit	Life Technologies
Fast SYBR green master mix	Life Technologies

Table 2-26: Primers for qPCR

Human		(5'-3')
β-2 microglobulin (B2M)	For: Rev:	GTG CTC GCG CTA CTC TCT C GTC AAC TTC AAT GTC GGA T
CDKN1A (p21)	For: Rev:	TGG GAG CGG ATA GAC ACA TC GGC TCT CTG CTT GTC ATC CTT
TIGAR	For: Rev:	CGC GTG GAG AAA CAA GAT TT CCG TAT TTC CTT TCC CGA AG
FAS	For: Rev:	GTA CGG AGT TGG GGA AGC TC AGG GCT TAT GGC AGA ATT GG
PUMA	For: Rev:	GAA TCC ACG GCT TTG GAA AA TGG CCA CAC TCA CCA CAA AT
PHLDA3	For: Rev:	GAC CCT CGT GTC CTA AAC CA CTC GTC CAT TCC TTC AGC TC
PIG3	For: Rev:	TCT CTG AAG CAA CGC TGA AAT TC ACG TTC TTC TCC CAG TAG GAT CC
SESTRIN1	For: Rev:	TTG AAG CCC TCA TGG AAA AG AGT CCT GGA CAC GAA ATG TTG
SESTRIN2	For: Rev:	ACT CTG GGG GCT TTG AGT CT GTC TTC CAC AAA GCA CAG CA
GADD45a	For: Rev:	CAG AAG ACC GAA AGG ATG GA ATC TCT GTC GTC GTC CTC GT
GADD45B	For: Rev:	CGC TGG AAG AGC TCG TGG CG ACC ACG CTG TCT GGG TCC ACA T
DRAM	For: Rev:	GGG AAC AAC ACC TCC AGA GA TGA ACC ACT GGC ACA GCT AA
XPC	For: Rev:	ACC CGG CTG GTA TTG TCT CT GTT CCT CTT CCC TTT GGC AC
14.3.3σ	For: Rev:	AGC CGG GTC TTC TAC CTG AA GTT GGC GAT CTC GTA GTG GA

BAX	For: Rev:	ATG GAC GGG TCC GGG GAG ATC CAG CCC AAC AGC CGC
Mouse		**(5'-3')**
β-2 microglobulin (B2m)	For: Rev:	CGG CCT GTA TGC TAT CCA GA GGG TGA ATT CAG TGT GAG CC
Cdkn1a (p21)	For: Rev:	CCT GGT GAT GTC CGA CCT G CCA TGA GCG CAT CGC AAT C
Mdm2	For: Rev:	CCA ACC ATC GAC TTC CAG CAG CAT T GAT TGG CTG TCT GCA CAC TGG G
Bax	For: Rev:	GGA CAG CAA TAT GGA GCT GCA GAG G GGA GGA AGT CCA GTG TCC AGC C

2.10.2 Methods

RNA was extracted using RNeasy Mini Kit and RNase-Free DNase Set according to the manufacturer's instructions. RNA concentration was determined using a Nanodrop 2000c (Thermo Scientific). The complementary DNA (cDNA) was synthesised through reverse transcription from 1 µg RNA using High-capacity RNA-to-cDNA Kit. The quantitative real-time PCR (qPCR) reaction was performed with 10 ng of cDNA using Fast SYBR green master mix. The amount of fluorescent PCR product accumulating during the PCR programme (20 seconds at 95 ºC hot start, 40 cycles of 3 seconds denaturing at 95 ºC, 30 seconds annealing/elongation at 60 ºC) was detected by the ABI 7500 Fast System (Thermo Scientific). Gene expression was quantified relative to the housekeeping gene B2M according to the comparative ΔΔCt method.

2.11 Chromatin Immunoprecipitation (ChIP)

2.11.1 Materials

Reagents used for ChIP are listed in Table 2-27, solutions and buffers used for ChIP are listed in Table 2-28, antibodies used for ChIP are listed in Table 2-29 and primers used for ChIP are listed in Table 2-30.

Table 2-27: Reagents for ChIP

Reagent	Source
Glycine	Sigma-Aldrich
Dynabeads Protein G	Life Technologies
phenol-chloroform-isoamylalcohol (PCI)	Sigma-Aldrich
Glycogen	Life Technologies

Table 2-28: Solutions and buffers for ChIP

Solution	Composition
Phosphate Buffered Saline (PBS) pH 7.4	170 mM NaCl (Fisher Scientific) 3.3 mM KCl (Fisher Scientific) 1.8 mM Na_2HPO_4 (Fisher Scientific) 10.6 mM KH_2PO_4 (Fisher Scientific)
X-linking solution	1 % Formaldehyde (Sigma-Aldrich) 100 mM HEPES-KOH (Fisher Scientific) 50 mM NaCl (Fisher Scientific) 1 mM EDTA (Sigma-Aldrich) 0.5 mM EGTA (Sigma-Aldrich)
ChIP cell lysis buffer (CLB)	10 mM Tris-HCl (pH 8.0) (Sigma-Aldrich) 10 mM NaCl (Fisher Scientific) 0.2 % IGEPAL CA-630 (Sigma-Aldrich) 10 mM NaBu (Sigma-Aldrich) 50 µg/ml PMSF (Sigma-Aldrich) 1 µg/ml Leopeptin (Sigma-Aldrich)
Nuclei lysis buffer (NLB)	50 mM Tris-HCl (pH 8.0) (Sigma-Aldrich) 10 mM EDTA (Sigma-Aldrich) 1 % SDS (Fisher Scientific) 10 mM NaBu (Sigma-Aldrich) 50 µg/ml PMSF (Sigma-Aldrich) 1 µg/ml Leopeptin (Sigma-Aldrich)
IP dilution buffer (IPDB)	20 mM Tris-HCl (pH 8.0) (Sigma-Aldrich) 150 mM NaCl (Fisher Scientific) 2 mM EDTA (Sigma-Aldrich) 1 % Triton X-100 (Sigma-Aldrich) 0.01 % SDS (Fisher Scientific) 10 mM NaBu (Sigma-Aldrich) 50 µg/ml PMSF (Sigma-Aldrich) 1 µg/ml Leopeptin (Sigma-Aldrich)
Modified IPDB (IPDBmod)	NLB:IPDB = 1:4
IP wash buffer 1 (IPWB1)	20 mM Tris-HCl (pH 8.0) (Sigma-Aldrich) 50 mM NaCl (Fisher Scientific) 2 mM EDTA (Sigma-Aldrich) 1 % Triton X-100 (Sigma-Aldrich) 0.01 % SDS (Fisher Scientific)
IP wash buffer 2 (IPWB2)	10 mM Tris-HCl (pH 8.0) (Sigma-Aldrich) 250 mM LiCl (Sigma-Aldrich) 1 mM EDTA (Sigma-Aldrich) 1 % IGEPAL CA-630 (Sigma-Aldrich) 1 % Sodium deoxycholate (Sigma-Aldrich)
IP elution buffer (IPEB)	100 mM $NaHCO_3$ (Sigma-Aldrich) 1 % SDS (Fisher Scientific)
Tris-EDTA (TE)	10 mM Tris-HCl (pH 8.0) (Sigma-Aldrich) 1 mM EDTA (Sigma-Aldrich)

Table 2-29: Antibodies for ChIP

Primary Antibody	Description	Supplier
p53	mouse monoclonal (DO-1)	Santa Cruz Biotechnology
MDM2	mouse monoclonal (SMP14)	Santa Cruz Biotechnology

Table 2-30: Primers for ChIP

Target		(5'-3')
p21 -2350 bp (promoter)	For: Rev:	CTG GAC TGG GCA CTC TTG TC CCC CTT CCT CAC CTG AAA AC
p21 +50 bp (non-specific)	For: Rev:	GGC ACT CAG AGG AGG TGA GA ACC CGC GCA CTT AGA GAC AC

2.11.2 Methods

Approximately 5 x 10^7 cells were seeded on 150 mm dish. After 2 days, cells were washed and fixed in 1 % formaldehyde in serum-free DMEM for 10 min. Cross-linking reaction was stopped by adding glycine (final concentration 125 mM) for 5 minutes. Media was completely aspirated and cells were washed 4 times with ice cold PBS. Cells were then harvested in 5 ml of ChIP cell lysis buffer and incubated for 10 minutes on ice. Cells were then centrifuged at 2,500 rpm for 5 minutes at 4 ºC and nuclei was re-suspended and incubated in 1.2 ml of NEB for 10 minutes on ice. 0.72 ml of IPDB and samples were sonicated using the Bioruptor sonicator (high setting, 30 seconds on/30 seconds off) for 30 minutes (replaced ice every 10 minutes). 4.1 ml of IPDB was added and chromatin was precleared by 20 µl of normal mouse IgG and 50 µl of Dynabeads protein G for 4 hours on a rotating wheel at 4 ºC. IPDBmod was made by combining 1:4 NLB:IPDM. Supernatant was transferred to new Eppendorf tubes and set up in necessary conditions for ChIP with p53 and MDM2. Samples were incubated on a rotating wheel overnight at 4 ºC.

ChIP Target conditions
p53: 0.675 ml chromatin + 0.675 ml IPDBmod + 7.5 µg p53 antibody (DO1)
MDM2: 0.675 ml chromatin + 0.675 ml IPDBmod + 7.5 µg MDM2 antibody (SMP14)
Negative control: 0.675 ml chromatin + 0.675 ml IPDBmod + 7.5 µg IgG

50 µl of Dynabeads protein G was added to the samples and they were incubated for 3 hours on a rotating wheel overnight at 4 ºC. Beads were washed twice with IP wash buffer 1, once with IP wash buffer 2, then twice with TE buffer. ChIP materials were eluted in 300 µl of ChIP elution buffer on a Thermomixer heat block (Eppendorf) at 900 rpm overnight for 65 ºC. Input samples were similarly processed.

Following this, 200 µl of samples were transferred to fresh Eppendorf tubes and 200 µl of TE buffer. 400 µl of PCI was added to the samples and they were

transferred to the phase-lock tubes (5 Prime) for DNA isolation. Samples were spun at 14,000 rcf for 5 minutes at room temperature and upper phase was transferred to Eppendorf tubes. 16 µl of 5 M NaCl and 8 µl of glycogen (5 mg/ml) was added and vortexed. 1 ml of ice cold 100 % ethanol was then added to the samples, vortexed and stored at -80 ºC for 30 minutes. Following this, samples were spun at 16,100 rcf for 15 minutes at 4 ºC, and the supernatant was discarded. Pellets were washed with 1 ml ice cold 80 % ethanol and spun at 16,100 rcf for 10 min at 4 ºC. The supernatant was discarded and pellets were dried at room temperature then DNA was eluted in 50 µl of 10 mM Tris-HCl and heated on a Thermomixer heat block for 10 minutes at 50 ºC in order to dissolve the pellet. Samples were then analysed via qPCR as described above with a modified PCR programme (20 seconds at 95 ºC hot start, 45 cycles of 3 seconds denaturing at 95 ºC, 30 seconds annealing/elongation at 60 ºC). Values were calculated as % input.

2.12 Cell growth assay and cell staining

2.12.1 Materials

Reagents used for cell growth assay and cell staining are listed in Table 2-31 and solutions and buffers used for cell growth assay and cell staining are listed in Table 2-32.

Table 2-31: Reagents for cell growth assay and cell staining

Reagent	Source
Foetal bovine serum (FBS)	Life technologies
CASYton	OMNI Life Science

Table 2-32: Solutions and buffers for cell growth assay and cell staining

Solution	Composition
Phosphate Buffered Saline (PBS) pH 7.4	170 mM NaCl (Fisher Scientific) 3.3 mM KCl (Fisher Scientific) 1.8 mM Na_2HPO_4 (Fisher Scientific) 10.6 mM KH_2PO_4 (Fisher Scientific)
Trypsin-EDTA	PBS 0.25 % Trypsin (Life Technologies) 1 mM EDTA (Sigma-Aldrich)
Cell staining buffer	PBS 0.04 % Sulphorhodamine B (SRB) (Sigma-Aldrich) 1 % Acetic acid (Fisher Scientific)

2.12.2 Methods

Cells were harvested with trypsin-EDTA and stopped trypsinisation by ice cold 2 % FBS in PBS. 200 µl of them were mixed with 19.8 ml of CASYton and the number of viable cells was counted using CASY cell counter.

For cell staining, cells were fixed with ice-cold 100 % methanol and stained with cell staining buffer.

2.13 Cell cycle analysis

2.13.1 Materials

Reagents used for cell cycle analysis are listed in Table 2-33 and solutions and buffers used for cell cycle analysis are listed in Table 2-34.

Table 2-33: Reagents for cell cycle analysis

Reagent	Source
Propidium iodide (PI)	Sigma-Aldrich
Foetal bovine serum (FBS)	Life technologies
RNase A	Qiagen

Table 2-34: Solutions and buffers for cell cycle analysis

Solution	Composition
Phosphate Buffered Saline (PBS) pH 7.4	170 mM NaCl (Fisher Scientific) 3.3 mM KCl (Fisher Scientific) 1.8 mM Na_2HPO_4 (Fisher Scientific) 10.6 mM KH_2PO_4 (Fisher Scientific)
Trypsin-EDTA	PBS 0.25 % Trypsin (Life Technologies) 1 mM EDTA (Sigma-Aldrich)

2.13.2 Methods

For analysis of cell cycle profile, cells were harvested with trypsin-EDTA, stopped trypsinisation by ice cold 2 % FBS in PBS and then cells were washed in PBS and fixed in ice cold 70 % ethanol for at least 30 minutes at 4 ºC. Cells were rehydrated with PBS and treated with 50 µg/ml RNase A in PBS for at least 15 minutes. DNA was stained with PI before flow cytometric analysis (Attune NxT, Thermo Fisher Scientific). DNA content was analysed in channel FL2 and the percentage of cells in each phase was determined by DNA content analysed by

FlowJo 10 software (FlowJo) based on the Watson Pragmatic algorithm (Watson et al., 1987).

2.14 Structure analysis

Crystal structure of E2 (UbcH5B)–ubiquitin-MDM2^{RING}-MDMX^{RING} complex was generated by Professor Danny Huang's group (Cancer Research UK Beatson Institute) and structural analyses were performed with PyMol software (Schrödinger).

2.15 Statistical analysis and reproducibility

Experimental data are expressed as mean ± standard deviation (SD) unless otherwise indicated. Statistical differences were analysed by one- or two-way analysis of variance (ANOVA) followed by Tukey's *post hoc* test (two-tailed), as appropriate. All statistical analyses were performed with Prism 6 (GraphPad Software). Statistical significance was defined as $P < 0.05$. *F* statistics and degrees of freedom for ANOVAs (*F* (DFn, DFd)) were also reported. Each experiment was repeated independently at least three times and sample sizes and numbers of repeats are defined in each figure legend.

Chapter 3 E3 ligase activity of MDM2 and MDMX

3.1 Structure of UbcH5B–ubiquitin-MDM2^{RING}-MDMX^{RING}

The crystal structure of E2 (UbcH5B)-ubiquitin-MDM2^{RING}-MDMX^{RING} was developed by Professor Danny Huang group at the Cancer Research UK Beatson Institute and its co-ordinates and structure factors have been deposited in Protein Data Bank (PDB) under accession code of 5MNJ (Nomura et al., 2017).

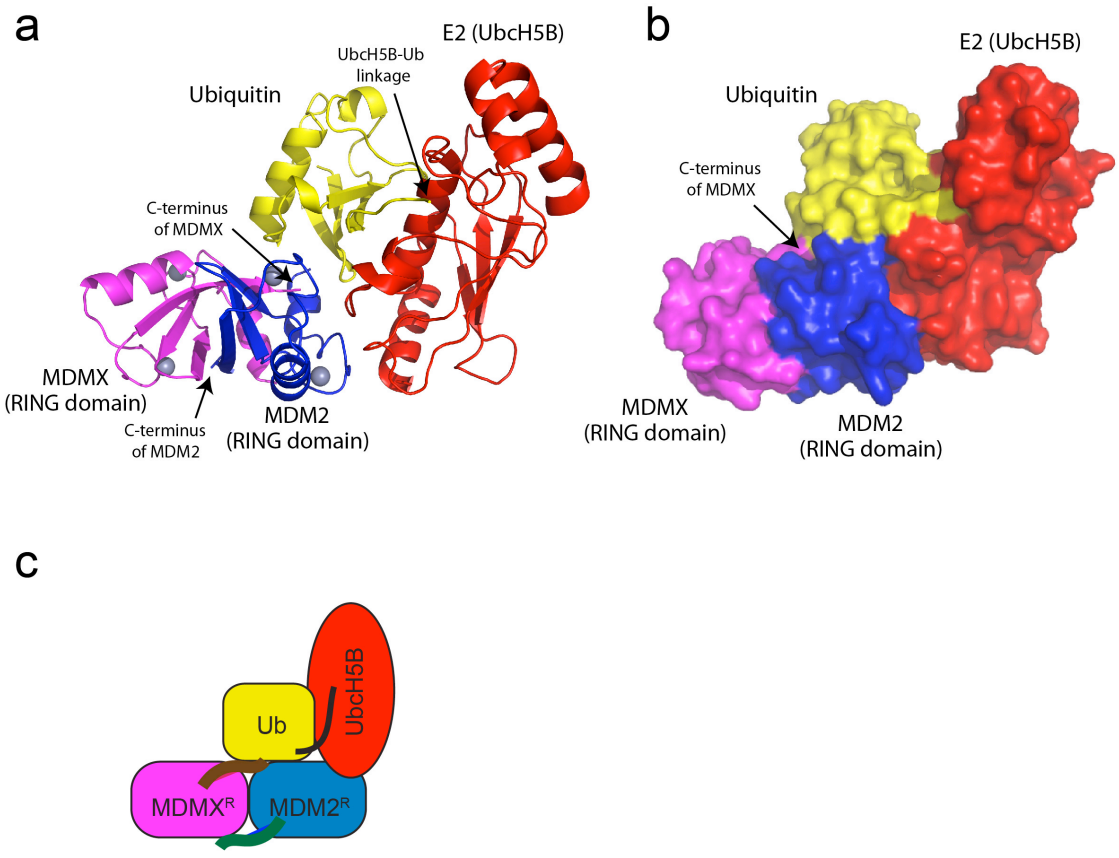

Figure 3-1: Structure of E2 (UbcH5B)–ubiquitin-MDM2^{RING}-MDMX^{RING} complex

(a) Ribbon representation of the E2 (UbcH5B)–ubiquitin-MDM2^{RING}-MDMX^{RING} complex: UbcH5B (red), ubiquitin (yellow), MDM2^{RING} (blue) and MDMX^{RING} (pink). Zn^{2+} are depicted as grey spheres. UbcH5B–ubiquitin linkage, MDM2 C-terminal tail and MDMX C-terminal tail are indicated with arrows. (b) Surface representation of the E2 (UbcH5B)–ubiquitin-MDM2^{RING}-MDMX^{RING} complex, coloured and oriented as in cartoon representation. MDMX C-terminal tail is indicated is indicated with an arrow. Co-ordinates and structure factors for this complex are available at PDB with accession code of 5MNJ. (c) Schematic drawing of the structure complex coloured as in cartoon representation. Black line indicates the C-terminal tail of the ubiquitin. Green and brown lines indicate the C-terminal tail of MDM2 and MDMX, respectively.

This structure contains the human MDM2 RING domain (from amino acid 428 to 491), the MDMX RING domain (from amino acid 427 to 490) and the UbcH5B-ubiquitin complex (en dash (–) indicates covalent bond) (Figure 3-1). Two point mutations were introduced within UbcH5B: C85K was introduced to form an isopeptide bond with the ubiquitin glycine 76 (G76) residue at the C-terminal. This irreversible bond stabilises UbcH5B–ubiquitin to allow crystallisation. S22R was introduced to prevent non-covalent ubiquitin binding via the "backside" of UbcH5B. The structure shows the active form of UbcH5B–ubiquitin configuration that is referred to as the folded-back configuration (Dou et al., 2013, Plechanovova et al., 2012, Dou et al., 2012, Branigan et al., 2015, Buetow et al., 2015, Koliopoulos et al., 2016, Sanchez et al., 2016, Scott et al., 2014). This configuration is stabilised by MDM2 and MDMX RING domains. The MDM2 RING domain contacts both UbcH5B and ubiquitin in a similar manner as observed in other structures of RING E3s bound to E2–ubiquitin complex (Figure 3-1). In contrast, the MDMX RING domain only contacts ubiquitin via C-terminal tail and core RING domain did not bind an E2–ubiquitin complex (Figure 3-1).

3.2 Attenuation of MDM2 E3 ligase activity

To date, studies on the MDM2 ligase-independent regulation of p53 are based on MDM2 C464A (or C462A in mouse), a mutant that disrupts Zn^{2+} co-ordination and abolishes the RING domain fold (Itahana et al., 2007, Honda et al., 1997, Kubbutat et al., 1997, Geyer et al., 2000). It remains unclear whether the RING domain fold is important for MDM2 ligase-independent functions, since the RING domain may regulate a variety of other biological functions including interactions with DNA, RNA and lipid substrates, dimerisation and other protein binding (Klug, 1999, Hall, 2005, Brown, 2005, Gamsjaeger et al., 2007, Matthews and Sunde, 2002). Therefore, it is important to explore in more detail the functional requirements for MDM2 E3 activity and to understand how important transcriptional repression of p53 by MDM2/X independently of E3 ligase activity is to regulate p53.

There are several potential strategies to attenuate MDM2 E3 ligase activity other than destructing its RING co-ordination, including separation of E2–ubiquitin complex and MDM2 RING domain, disruption of closed folded back configuration

of E2-ubiquitin complex by altering ubiquitin alignment, and disruption of homo- and hetero-dimerisation of MDM2 (Figure 3-2).

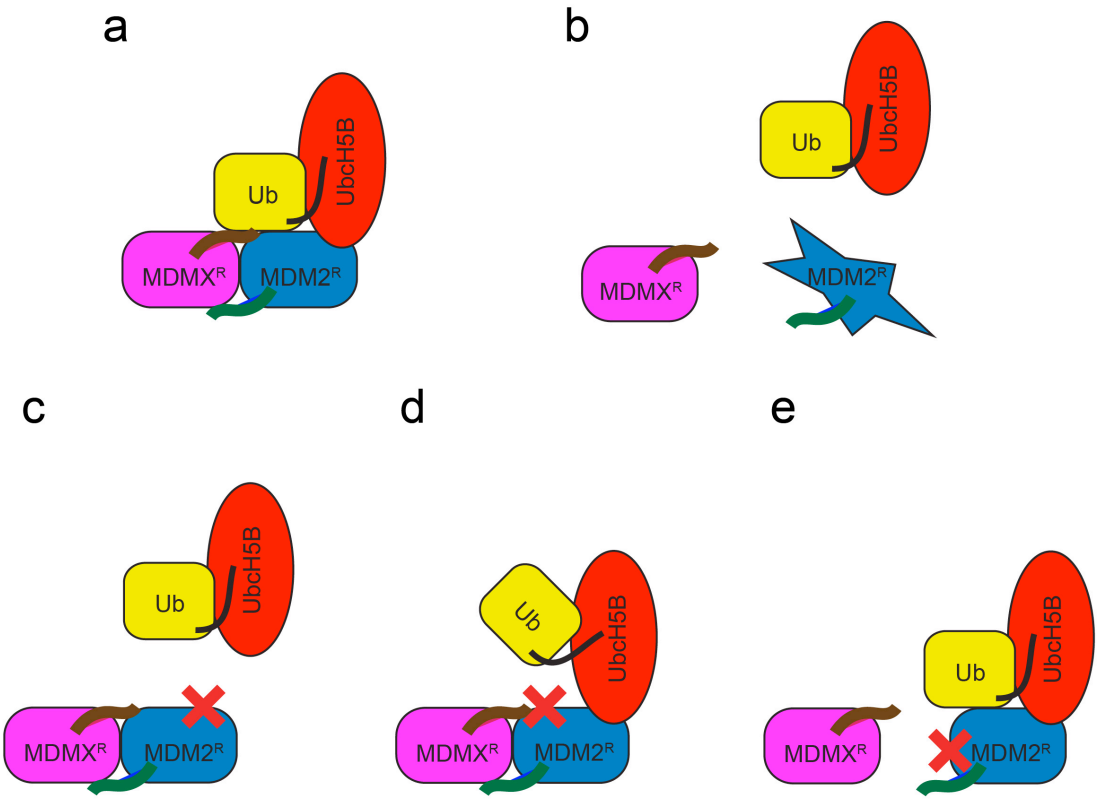

Figure 3-2: Strategies to attenuate the intrinsic E3 ligase activity of MDM2

(a) Schematic drawing of the structure complex. (b) MDM2 C464A model. (c) Targeting interaction between MDM2 RING domain and E2–ubiquitin complex. (d) Targeting ubiquitin alignment by MDM2 RING domain. (e) Targeting homo- and hetero- dimerisation. Black line indicates the C-terminal tail of the ubiquitin. Green and brown lines indicate the C-terminal tail of MDM2 and MDMX, respectively.

Guided by the structure, several specific point mutations within the MDM2 RING domain were generated to test whether these mutants has lost their intrinsic E3 ligase activity without affecting their RING domain structure and their ability to bind to p53.

3.2.1 Targeting Separation of E2–ubiquitin complex and MDM2

3.2.1.1 Targeting E2-MDM2 interaction

Isoleucine 440 (I440) is the hydrophobic core of MDM2 and is important for the hydrophobic interaction with N-terminal α1 helix and L1 and L2 loops of UbcH5B, particularly with F62 in the L1 loop and P95 and A96 in the L2 loop (Figure 3-3). This interaction resembles other RING-E2 interactions described previously for other E3 ligase complexes. For example, mutation of the corresponding isoleucine residue in BRCA1 (I26) into alanine abrogates its E3 ligase activity *in vitro* (Brzovic et al., 2003, Christensen et al., 2007).

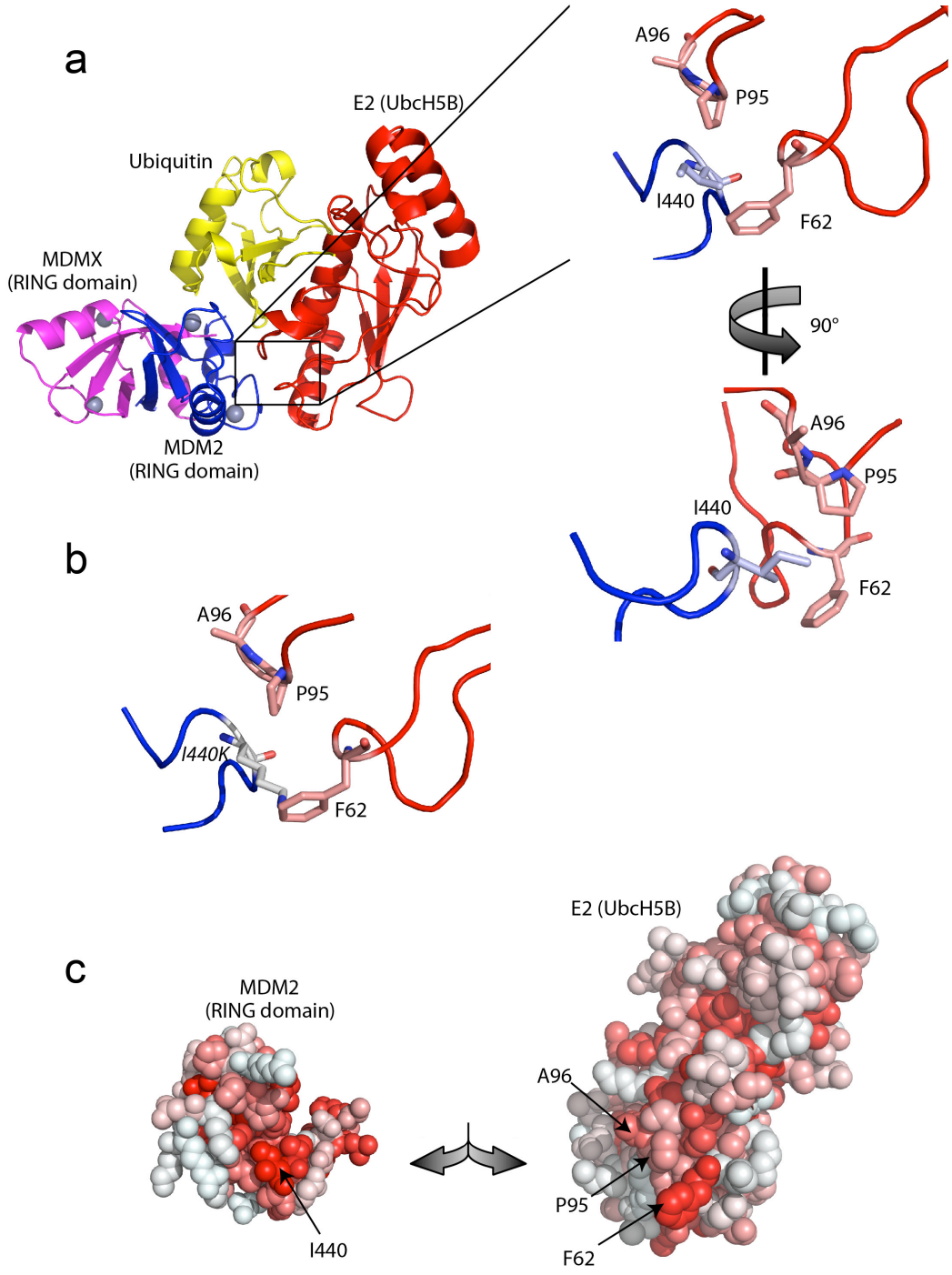

Figure 3-3: Hydrophobic interaction between MDM2 RING domain and UbcH5B

(a) Close-up view of MDM2 RING domain and UbcH5B interaction. MDM2 I440 interacts with N-terminal α1 helix and L1 and L2 loops of UbcH5B through hydrophobic interaction. UbcH5B (red), ubiquitin (yellow), MDM2^{RING} (blue) and MDMX^{RING} (pink). (b) MDM2 I440K model. To obtain this model, MDM2 residue was mutated *in silico*. (c) Space filling representation of the E2 (UbcH5B)-MDM2 RING domain binding interface. Red colour indicates high hydrophobicity and white colour indicates low hydrophobicity.

Therefore, I generated point mutants of I440 converting a hydrophilic amino acid including lysine (K), arginine (R) aspartic acid (D) and glutamic acid (E), an amphipathic amino acid tyrosine (Y), and an alanine (A).

Over-expression of wild type MDM2 significantly promoted degradation of p53 in U2OS cells (to 7.2 ± 2.1 % of the level compared with no MDM2 over-expression (empty vector (EV) control)) (Figure 3-4a, b). On the other hand, expression of MDM2 C464A mutant did not reduce p53 level compared with no MDM2 over-expression, which is significantly different from over-expression of wild type MDM2 (Figure 3-4a, b). Expression of MDM2 mutants with alanine or hydrophilic amino acid substitutions of I440 completely attenuated the ability of MDM2 to reduce p53 levels similar to a negative control C464A (Figure 3-4a, b). However, MDM2 I440Y mutant retained the ability to degrade p53 (31.1 ± 18.8 %) and no significant difference to wild type MDM2 was observed (Figure 3-4a, b). This may be because tyrosine can still interact with E2 through its hydrophobic benzene ring. In order to confirm that the inability to lower p53 levels of the I440 mutants is due to the difference of their ability to ubiquitinate p53, ubiquitination assays were performed. These show that wild type MDM2 and MDM2 I440Y can ubiquitinate p53 whereas the other I440 mutants lost its ability to ubiquitinate p53 (Figure 3-4c).

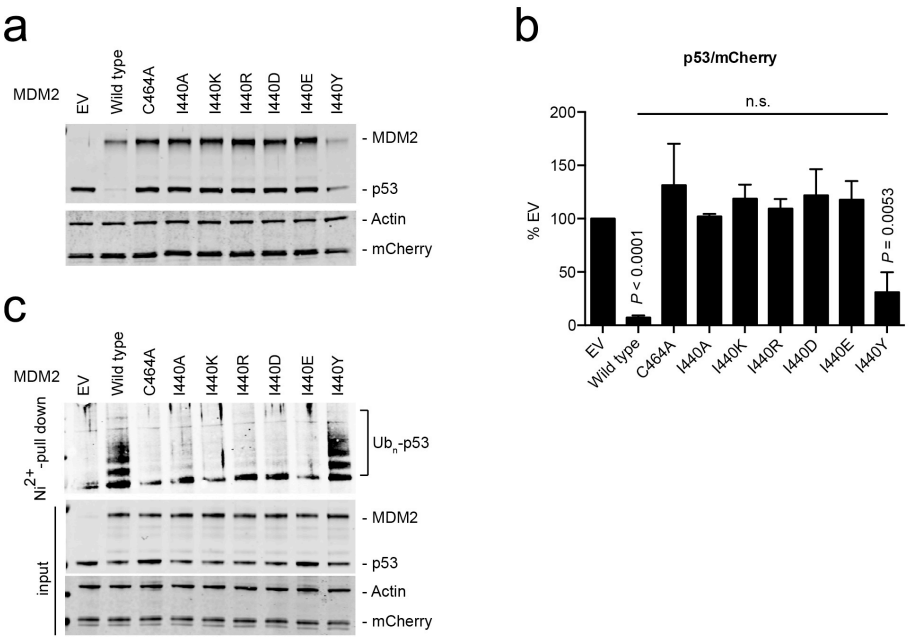

Figure 3-4: Effect of MDM2 I440 mutants on p53 degradation and ubiquitination

U2OS cells were transiently transfected with combinations of plasmid vectors coding for p53, mCherry, His-Ubiquitin-GFP (ubiquitination assay) and wild type MDM2 or the MDM2 I440 mutants for 24 hours. (a,b) p53 degradation assay showing that MDM2 I440 mutants (not I440Y) do not promote degradation of p53. *P* values (one-way ANOVA with Tukey's *post hoc* test): vs. empty vector (EV) control. "n.s." indicates not significant vs. wild type. *F* (8, 18) = 16.96. Error bars indicate mean ± SD. *n* = 3 independent experiments. (c) Ubiquitination assay showing that MDM2 I440 mutants (not I440Y) abolish p53 ubiquitination. Cells were treated with proteasome inhibitor MG132 for 5 hours then lysates were pull-downed with the nickel beads (His-tag pull-down). Ubiquitin-conjugated p53 was detected by western blot.

As MDM2 I440K and I440E mutants strongly attenuated p53 ubiquitination and degradation, these two mutants were selected for further investigation. To test whether MDM2 I440 mutants can affect p53 stability, p53 half-life assays were carried out. Co-expression of wild type MDM2 quickly led to the significant reduction of p53 signal within 30 minutes after treatment of the protein biosynthesis inhibitor cycloheximide (to 68.7 ± 19.0 %). Further reductions were observed in 60 minutes (38.4 ± 12.7 %) and in 90 minutes (16.0 ± 10.0 %) (Figure 3-5). This indicates that wild type MDM2 leads to rapid degradation of p53. In contrast to that, MDM2 I440K and I440E mutants did not reduce the p53 signal over time, supporting the conclusion that they cannot facilitate the degradation of p53 (Figure 3-5). Interestingly, MDM2 I440Y mutant was still able to reduce p53 protein levels; a significant reduction within 60 minutes (to 52.0 ± 14.5 %)

after cycloheximide treatment and a further reduction in 90 minutes (29.5 ± 13.5 %), consistent with the observation that I440Y substitution still can ubiquitinate p53 (Figure 3-5).

Taken together, these results suggest that single mutation of MDM2 I440 into a hydrophilic amino acid is sufficient to attenuate E3 activity of MDM2 towards p53, leading to a stabilisation of p53 levels.

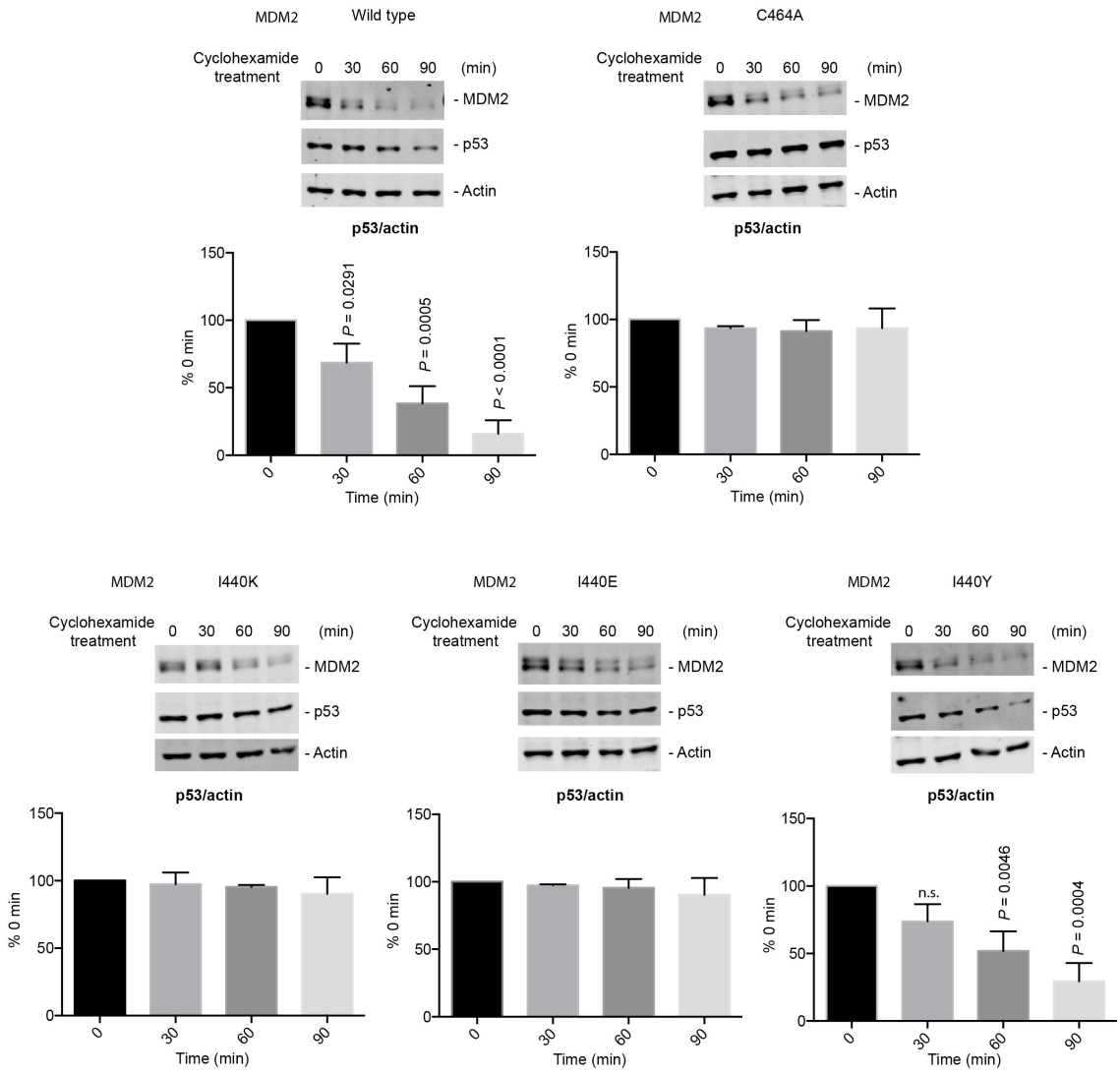

Figure 3-5: Effect of MDM2 I440 mutants on p53 half-life

p53 half-life assay showing that p53 was quickly degraded by expressing wild type MDM2 and MDM2 I440Y mutant but not by expressing MDM2 I440K and I440E mutants. U2OS cells were transiently transfected with combinations of plasmid vectors coding for p53, mCherry and wild type MDM2 or the MDM2 I440 mutants for 24 hours. Cells were treated with protein synthesis inhibitor cycloheximide for 0, 30 60 or 90 minutes then changes in p53 level were analysed by western blot. *P* values (one-way ANOVA with Tukey's *post hoc* test): vs. each 0 min. "n.s." indicates not significant. *F* (3, 8) = 35.10 (wild type) and *F* (3, 8) = 19.68 (I440Y). Error bars indicate mean ± SD. *n* = 3 independent experiments each.

The results generated so far support a model where I440 mutations of MDM2 are inactive due to an inability to recruit E2–ubiquitin. To confirm that these MDM2 mutants do not interact with E2–ubiquitin complex, surface plasmon resonance (SPR) analyses were performed by Dr Gary Sibbet with Biacore T200 (GE Healthcare). Briefly, GST-tagged MDM2 (from amino acid 398 to 491, termed MDM2 398-C) variants were immobilised to a CM-5 sensor chip coupled with anti-GST antibody and serially diluted UbcH5B–ubiquitin complex was injected to measure their interaction by SPR. To enhance their interaction, ubiquitin lacking the C-terminal di-glycine motif (UbΔGG) was added to saturate backside of UbcH5B (non-covalent ubiquitin binding) as previously described (Buetow et al., 2015). The value of the equilibrium dissociation constants (K_d) was obtained by fitting a plot of response at the equilibrium against the concentration and the steady-state affinity analyses were performed with BIAevaluation software (GE Healthcare). K_d corresponds to the analyte (UbcH5B–ubiquitin) concentration at which half of immobilised proteins (MDM2 398-C) are occupied at equilibrium.

The results suggest that wild type MDM2 readily interacts with E2–ubiquitin complex with K_d of 1.2 ± 0.2 μM (Figure 3-6, Table 3-1). On the other hand, mutations of I440 into hydrophilic residues completely abrogate interaction with E2–ubiquitin complex (Figure 3-6, Table 3-1). Interestingly, the MDM2 I440Y mutant was still able to interact with E2–ubiquitin complex but its K_d indicates that their interaction had 60-fold weaker affinity than that of wild type MDM2 (K_d = 71 ± 2 μM) (Figure 3-6, Table 3-1). The low binding affinity explains how MDM2 I440Y mutant can still ubiquitinate and degrade p53 in cells.

Taken together, MDM2 I440E and I440K mutants abrogate E3 ligase activity by disrupting interaction between MDM2 RING domain and E2–ubiquitin complex.

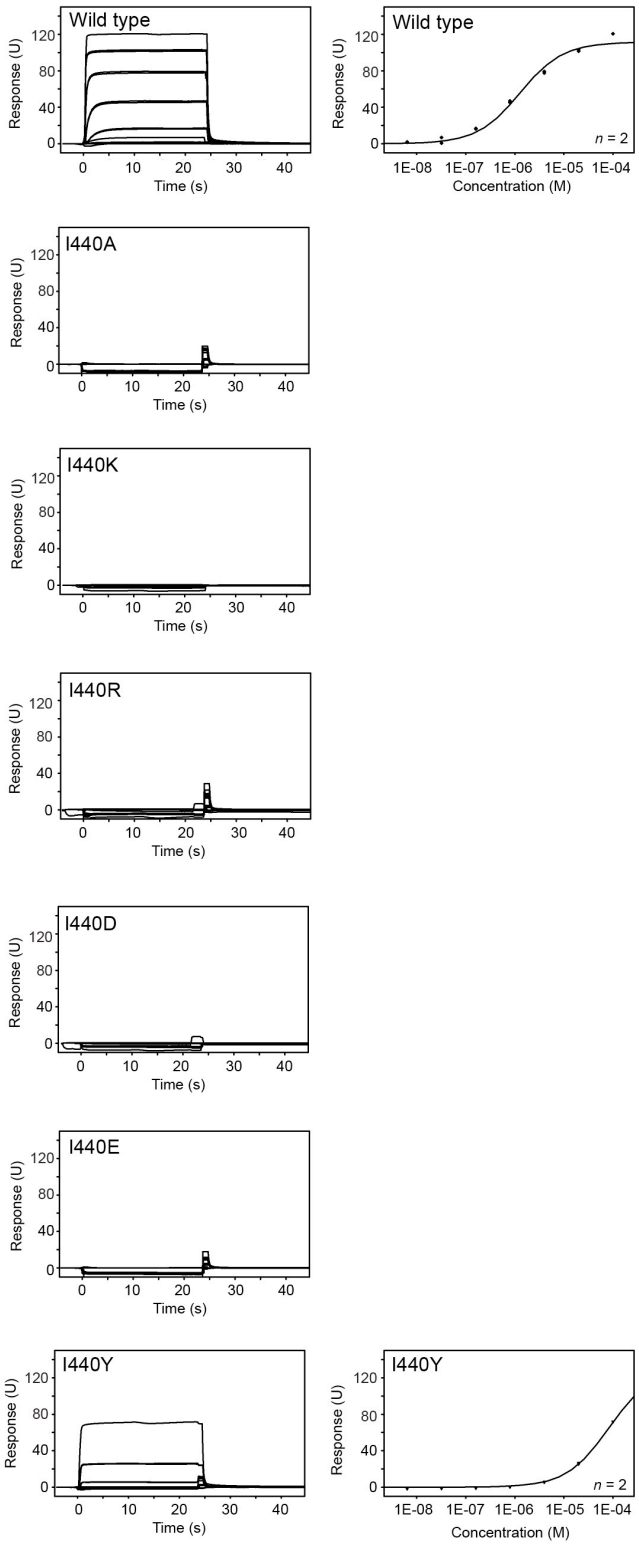

Figure 3-6: SPR analyses of MDM2 I440 mutants binding affinities for UbcH5B–ubiquitin

Representative sensorgrams (left) and binding curves (right) for GST-MDM2 398-C variants with UbcH5B–ubiquitin in the presence of UbΔGG are shown. Only sensorgram is shown for GST-MDM2 398-C variants that displayed no measurable UbcH5B–ubiquitin binding in the presence of UbΔGG. All experiments were performed in duplicates by Dr Gary Sibbet.

Table 3-1: Dissociation constants (K_d) for interactions between MDM2 I440 variants and UbcH5B–ubiquitin

Immobilised Protein	Analyte	K_d (μM)
MDM2 398-C	UbcH5B-Ub + UbΔGG	1.2 ± 0.2
MDM2 398-C I440A	UbcH5B-Ub + UbΔGG	N.M.
MDM2 398-C I440K	UbcH5B-Ub + UbΔGG	N.M.
MDM2 398-C I440R	UbcH5B-Ub + UbΔGG	N.M.
MDM2 398-C I440D	UbcH5B-Ub + UbΔGG	N.M.
MDM2 398-C I440E	UbcH5B-Ub + UbΔGG	N.M.
MDM2 398-C I440Y	UbcH5B-Ub + UbΔGG	71 ± 2

SEM are indicated. N.M. indicates no measurable binding. Representative sensorgrams and binding curves are shown in Figure 3-6.

3.2.1.2 Targeting ubiquitin alignment

Based on the structure shown in Figure 3-7, arginine 479 (R479) seems to be critical for both binding and aligning C-terminal tail of the ubiquitin to the active site of UbcH5B. R479 forms hydrogen bonds with the carbonyl oxygens of Q92 of UbcH5B and Q40 and R72 of ubiquitin (Figure 3-7). This corresponding arginine residue is commonly known as the "linchpin" arginine residue and is conserved in approximately 40 to 50 % of RING E3s (Pruneda et al., 2012). In cancer patients with c-CBL mutant, this corresponding arginine residue (c-CBL R420) has been mutated to glycine (G), glutamine (Q), leucine (L) or proline (P) (Kales et al., 2010). It has been demonstrated that the c-CBL R420Q mutation inhibits ubiquitination and endocytosis of its target RTKs including EGFR, PDGFR (Platelet-derived growth factor receptors) and FLT3 (FMS (Feline McDonough Sarcoma) like tyrosine kinase 3) that is frequently linked in leukaemic transformation (El-Gamal et al., 2013).

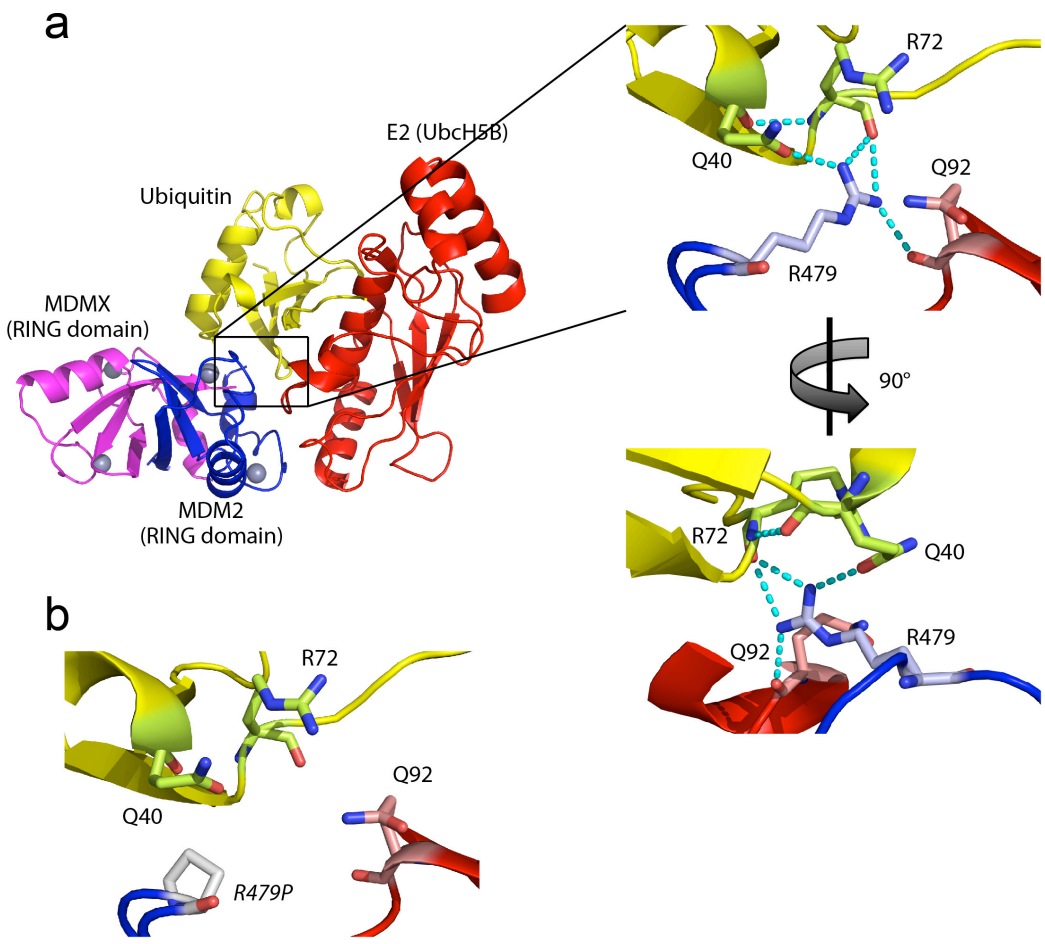

Figure 3-7: Hydrogen bonds between MDM2 RING domain and UbcH5B–ubiquitin

(a) Close-up view of MDM2 RING domain and UbcH5B–ubiquitin interaction. MDM2 R479, the "linchpin" arginine residue, interacts with Q92 of UbcH5B and Q40 and R72 of ubiquitin through hydrogen bonds. UbcH5B (red), ubiquitin (yellow), $MDM2^{RING}$ (blue) and $MDMX^{RING}$ (pink). Cyan dots indicate hydrogen bonds. (b) MDM2 R479P model. To obtain this model, MDM2 residue was mutated *in silico*.

Therefore, the MDM2 R479 residue was mutated into hydrophobic amino acids including alanine (A), isoleucine (I), glycine (G), proline (P), phenylalanine (F) and into lysine (K) as in MDMX, to investigate how they affect MDM2 E3 ligase activity.

MDM2 R479A, R479I and R479K mutants did not affect the ability of MDM2 to ubiquitinate p53 displaying significant ability to degrade p53 to 29.0 ± 14.8 %, 14.8 ± 3.9 % and 3.7 ± 1.8 % respectively compared with no MDM2 over-expression (Figure 3-8 a-c). Although MDM2 R479G and R479F mutants still possess ability to ubiquitinate p53 and significantly promote degradation of p53

to 51.0 ± 16.4 % and 51.4 ± 15.5 % respectively, they significantly attenuate degradation of p53 compared to wild type MDM2 (Figure 3-8 a-c). Notably, MDM2 R479P mutant has lost its ability to ubiquitinate p53 and did not promote degradation of p53 (Figure 3-8 a-c). Furthermore, this mutant completely attenuated its auto-ubiquitination (Figure 3-8d).

Interestingly, although the MDM2 R479K mutant (corresponding to K478 in MDMX) ubiquitinates p53, double mutation of MDM2 R479K-Q480K (corresponding to K478-K479 in MDMX) significantly attenuated E3 ligase activity compared to the MDM2 wild type (Figure 3-8e, f). This could suggest that the double mutation of MDM2 R479K-Q480K (MDMX K478-K479) may cause a steric hindrance between MDM2 and the E2–ubiquitin complex resulting in a loss of the E3 ligase activity.

Taken together, MDM2 R479 modulates E3 ligase activity by interacting with E2 as well as with ubiquitin. Indeed, the MDM2 R479P mutant completely abrogates its E3 ligase activity by disrupting interaction with E2–ubiquitin complex (like the MDM2 I440 mutants).

Further effects in terms of p53 degradation and ubiquitination were not observed in double mutations I440K-R479P and I440E-R479P, suggesting that I440K, I440E or R479P single mutations are enough to completely inactivate E3 activity (Data not shown).

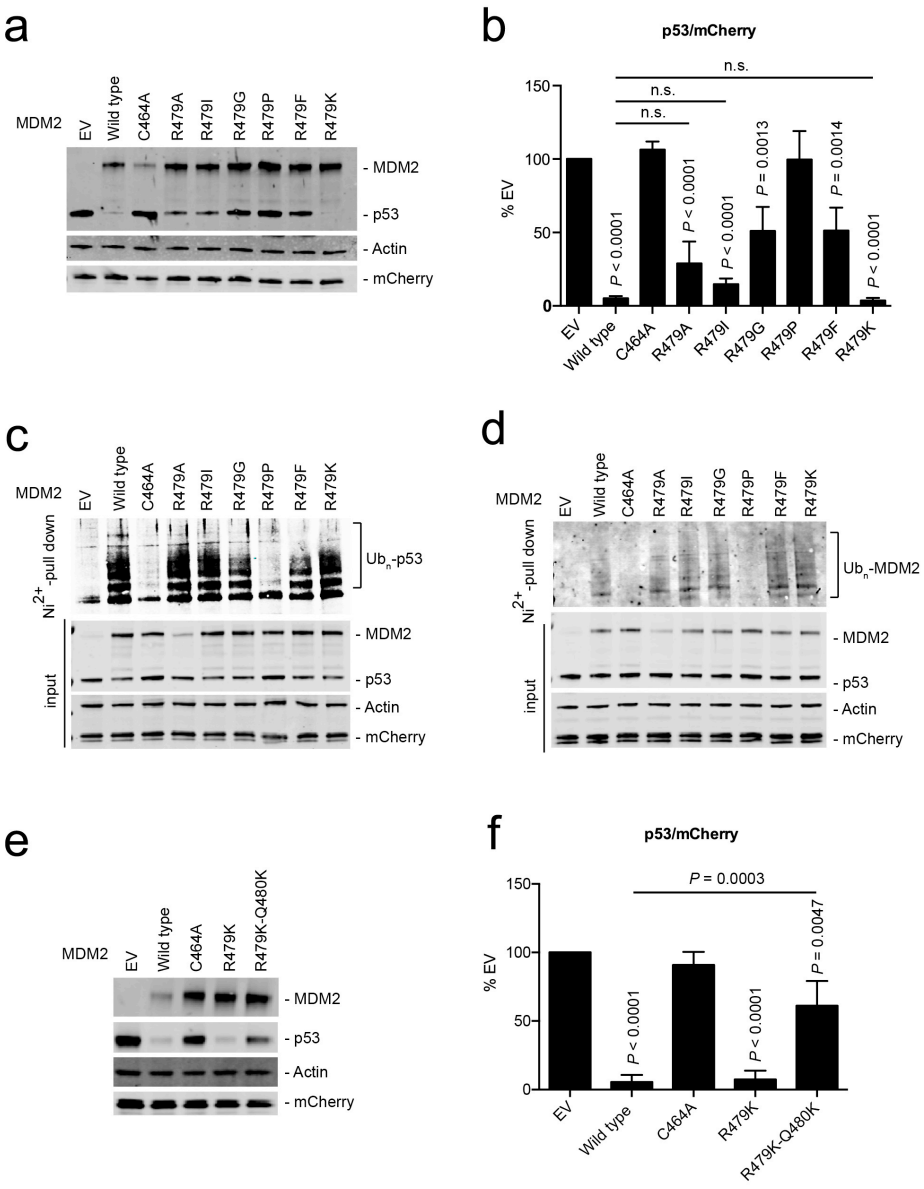

Figure 3-8: Effect of MDM2 R479 mutants on p53 degradation and ubiquitination

U2OS cells were transiently transfected with combinations of plasmid vectors coding for p53, mCherry, His-Ubiquitin-GFP (ubiquitination assay) and wild type MDM2 or the MDM2 R479 mutants for 24 hours. (a,b) p53 degradation assay showing that MDM2 R479 mutants have no or reduced ability to promote degradation of p53. *P* values (one-way ANOVA with Tukey's *post hoc* test): vs. EV. "n.s." indicates not significant vs. wild type. *F* (8, 18) = 40.90. Error bars indicate mean ± SD. *n* = 3 independent experiments. (c,d) Ubiquitination assay showing that MDM2 R479 mutants abolish or reduce p53 ubiquitination and MDM2 auto-ubiquitination. Cells were treated with proteasome inhibitor MG132 for 5 hours then lysates were pull-downed with the nickel beads (His-tag pull-down). Ubiquitin-conjugated p53 and MDM2 were detected by western blotting. (e,f) p53 degradation assay showing that although MDM2 R479K promotes degradation of p53, double mutation of MDM2 R479K-Q480K (as in MDMX) attenuated its E3 ligase activity. *P* values (one-way ANOVA with Tukey's *post hoc* test): vs. EV (vertical), vs. wild type (horizontal). *F* (4, 10) = 62.54. *n* = 3 independent experiments.

In accordance with these results, SPR analysis performed by Dr Gary Sibbet, demonstrated that MDM2 R479P mutant does not interact with E2–ubiquitin complex (Figure 3-9, Table 3-2), thereby explaining why it cannot ubiquitinate or degrade p53. Other MDM2 R479 mutants were still able to interact with E2–ubiquitin complex but their K_d value indicates that their interaction had 6 to 43-fold weaker affinity than that of wild type MDM2 (Figure 3-9, Table 3-2).

Taken together, these results explain why R479P mutant did not ubiquitinate p53 but other R479 mutants did.

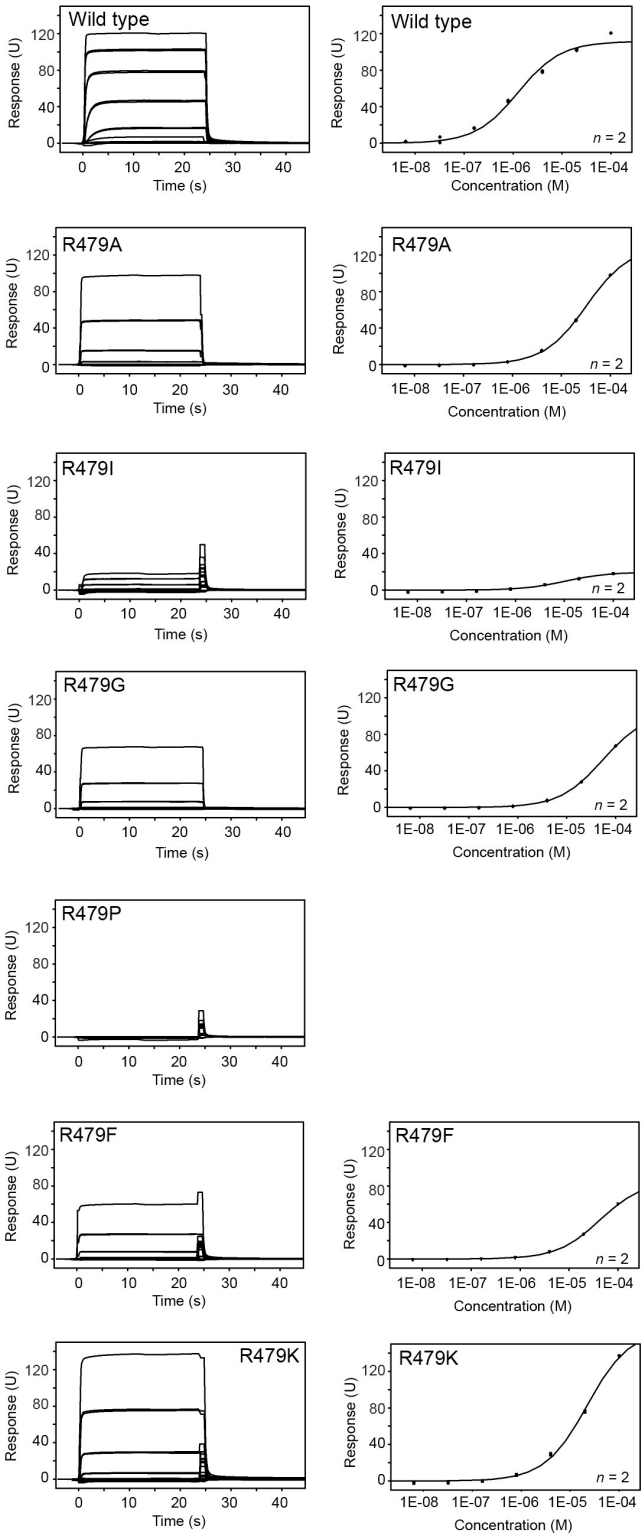

Figure 3-9: SPR analyses of MDM2 R479 mutants binding affinities for UbcH5B–ubiquitin

Representative sensorgrams (left) and binding curves (right) for GST-MDM2 398-C variants with UbcH5B–ubiquitin in the presence of UbΔGG are shown. Only sensorgram is shown for GST-MDM2 398-C variants that displayed no measurable UbcH5B–ubiquitin binding in the presence of UbΔGG. All experiments were performed in duplicates by Dr Gary Sibbet.

Table 3-2: Dissociation constants (K_d) for interactions between MDM2 R479 variants and UbcH5B–ubiquitin

Immobilised Protein	Analyte	K_d (μM)
MDM2 398-C	UbcH5B-Ub + UbΔGG	1.2 ± 0.2
MDM2 398-C R479A	UbcH5B-Ub + UbΔGG	32 ± 1
MDM2 398-C R479I	UbcH5B-Ub + UbΔGG	7 ± 1
MDM2 398-C R479G	UbcH5B-Ub + UbΔGG	52 ± 2
MDM2 398-C R479P	UbcH5B-Ub + UbΔGG	N.M.
MDM2 398-C R479F	UbcH5B-Ub + UbΔGG	41 ± 2
MDM2 398-C R479K	UbcH5B-Ub + UbΔGG	22 ± 2

SEM are indicated. N.M. indicates no measurable binding. Representative sensorgrams and binding curves are shown in Figure 3-9.

3.2.1.3 I440 or R479 mutants can hetero-dimerise and interact with p53

MDM2 C464A mutant is not able to dimerise with MDM2 or MDMX due to the disruption of a zinc co-ordination residue within the RING domain. This inability to form a correctly folded RING dimer is the cause of loss of E3 ligase activity. Based on the structure described above, the prediction is that MDM2 I440 and R479 mutants possess ability to interact with MDMX and these mutants do not alter any RING domain structure. To test this, co-immunoprecipitation and immunofluorescence were carried out.

Co-immunoprecipitation results suggest that unlike the MDM2 C464A mutant, all I440 and R479 mutants retain some ability to interact with MDMX in solution (Figure 3-10a). To confirm this, the ability of the various MDM2 mutants to re-localise MDMX to the nucleus (an activity that depends on MDM2-MDMX interaction) was tested by immunofluorescence. As published before by Uldrijan *et al*. (2007), MDMX alone was localised in the cytoplasm. Co-expression of wild type MDM2 re-localised MDMX into the nucleus whereas C464A mutants did not (Figure 3-10b). Unlike C464A mutant, I440 mutants retained the ability to relocalise MDMX into the nucleus in a similar manner as wild type MDM2 (Figure 3-10b). Therefore, these results confirm that MDM2 I440K and I440E, like wild type MDM2 can efficiently interact with MDMX in cells.

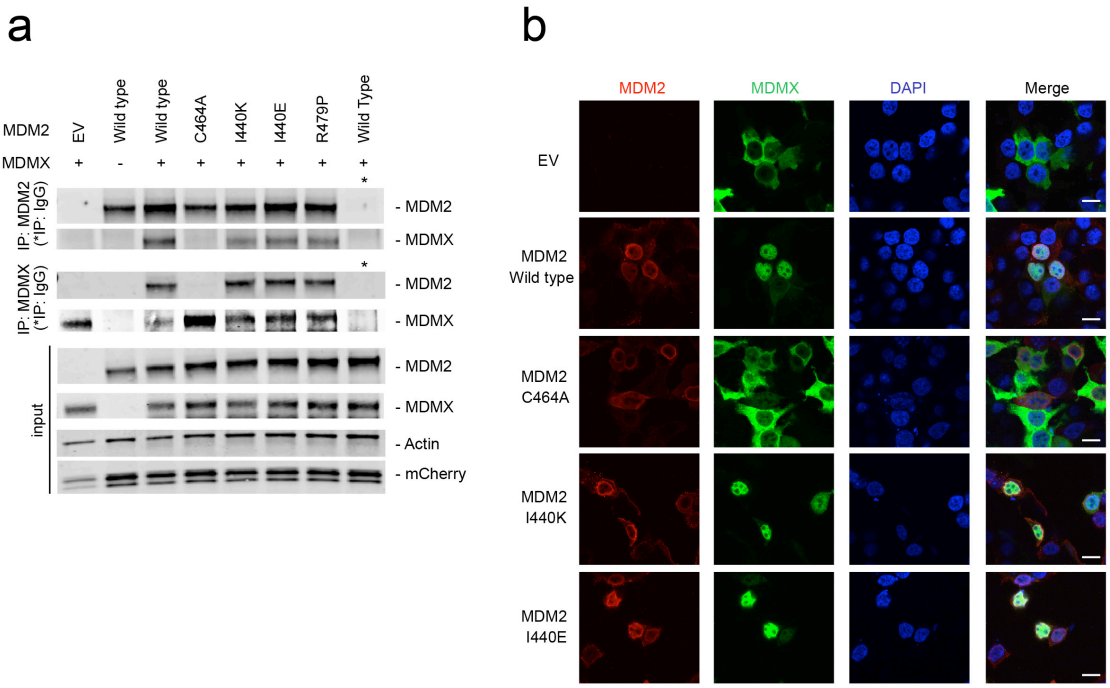

Figure 3-10: MDM2 I440 and R479 mutants can interact with MDMX

Interaction of MDM2 mutants with MDMX was tested by co-immunoprecipitation and immunofluorescence. U2OS cells were transiently transfected with combinations of plasmid vectors coding for myc-tagged MDMX (co-immunoprecipitation), GFP-tagged MDMX (immunofluorescence), mCherry (co-immunoprecipitation) and wild type MDM2 or the MDM2 I440 and/or R479 mutants for 24 hours. (a) Co-immunoprecipitation showing that MDM2 I440 and R479 mutants can interact with MDMX in solution. Cells were treated with proteasome inhibitor MG132 for 3 hours then lysates were immunoprecipitated using MDMX antibody (A300-287A) or MDM2 antibody (Ab-1) then analysed by western blot. (b) Subcellular localisation of over-expressed protein was detected by immunofluorescence using MDM2 antibody (Ab-1). MDMX primary localised in cytoplasm (because MDMX lacks NLS) but can localised in nucleus by dimerising with MDM2. Scale bars indicate 10 μm.

To confirm these results directly, I tested whether these MDM2 mutants are able to bind to p53 in a cell based Co-IP experiment. MDM2 mutant lacking p53-binding domain (Δp53BD) was used as a negative control. As expected, all mutants, including C464A, interacted with p53. These data suggest that interaction between MDM2 and E2-ubiquitin complex is not required for p53 to bind to the N-terminal of MDM2.

Taken together, although I440 and R479 mutants do not interact with E2-ubiquitin complex, they possess ability to dimerise with MDMX and p53, and their

loss of E3 ligase activity is due solely to the loss of interaction with E2-ubiquitin complex.

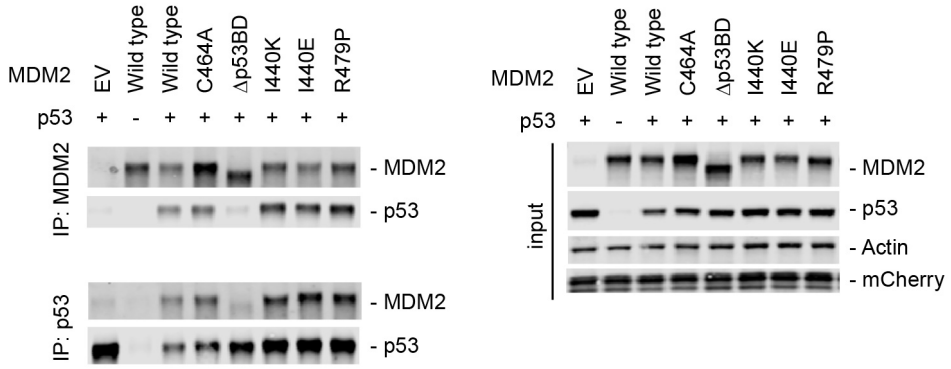

Figure 3-11: MDM2 I440 and R479 mutants can interact with p53

U2OS cells were transiently transfected with combinations of plasmid vectors coding for p53, mCherry and wild type MDM2, MDM2 Δp53BD (as a negative control) or the MDM2 I440 or R479 mutants for 24 hours. Cells were treated with proteasome inhibitor MG132 for 3 hours then lysates were immunoprecipitated using p53 antibody (FL393) or MDM2 antibody (Ab-1) then analysed by western blot.

3.2.1.4 MDMX can reactivate MDM2 C-terminal tail mutant but not I440 or R479 mutants

Previous studies have shown that E3 defective mutations in C-terminal tail of MDM2 can be reactivated by MDMX (Uldrijan et al., 2007, Poyurovsky et al., 2007). Structural analysis suggests that C-terminal tail of MDM2 is critical to interact with ubiquitin and this function could be provided by MDMX within the hetero-dimer (Figure 3-12).

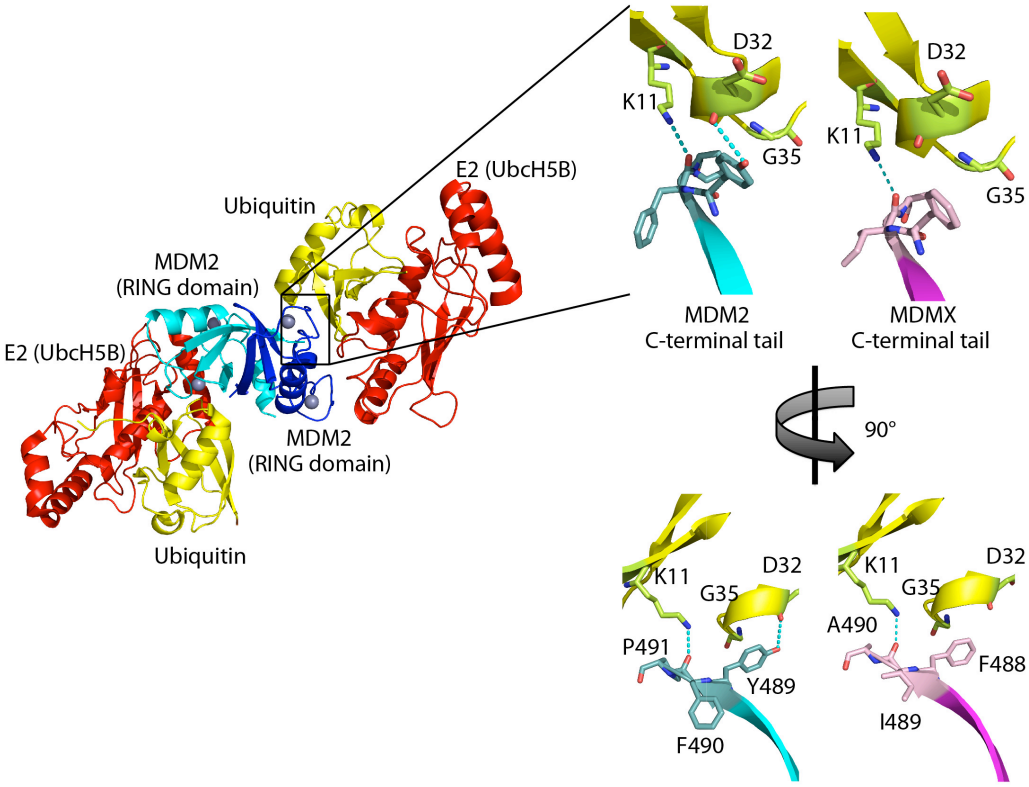

Figure 3-12: Model of the interaction between MDM2 C-terminal tail and E2–ubiquitin

Cartoon representation of the E2 (UbcH5B)–ubiquitin-MDM2^{RING}-MDM2^{RING} homo-dimer model: UbcH5B (red), ubiquitin (yellow), MDM2^{RING} (blue) and another MDM2^{RING} (cyan), and close-up view of C-terminal tail interactions of MDM2 (model) and MDMX. The last 3 C-terminal residues (MDM2: Y489, F490 and P491, and MDMX: F488, I489 and A490) are shown as sticks. Note that MDM2 homo-dimer can carry two E2–ubiquitin complexes. To obtain this model, UbcH5B–ubiquitin-MDM2^{RING} portion of the structure was superimposed onto MDMX^{RING} in the original structure. Cyan dots indicate hydrogen bonds.

To test whether I440 or R479 mutants can be reactivated by MDMX, p53 degradation assays and ubiquitination assays were carried out in the presence or absence of MDMX.

Although the C-terminal MDM2 mutant Y489D was reactivated by MDMX as previously described, MDM2 I440K, I440E, R479P and their double mutations were not reactivated by MDMX (Figure 3-13). This indicates that, as was suggested by the crystal structure, these mutants intrinsically cannot interact with E2-ubiquitin complex and therefore cannot be reactivated by MDMX.

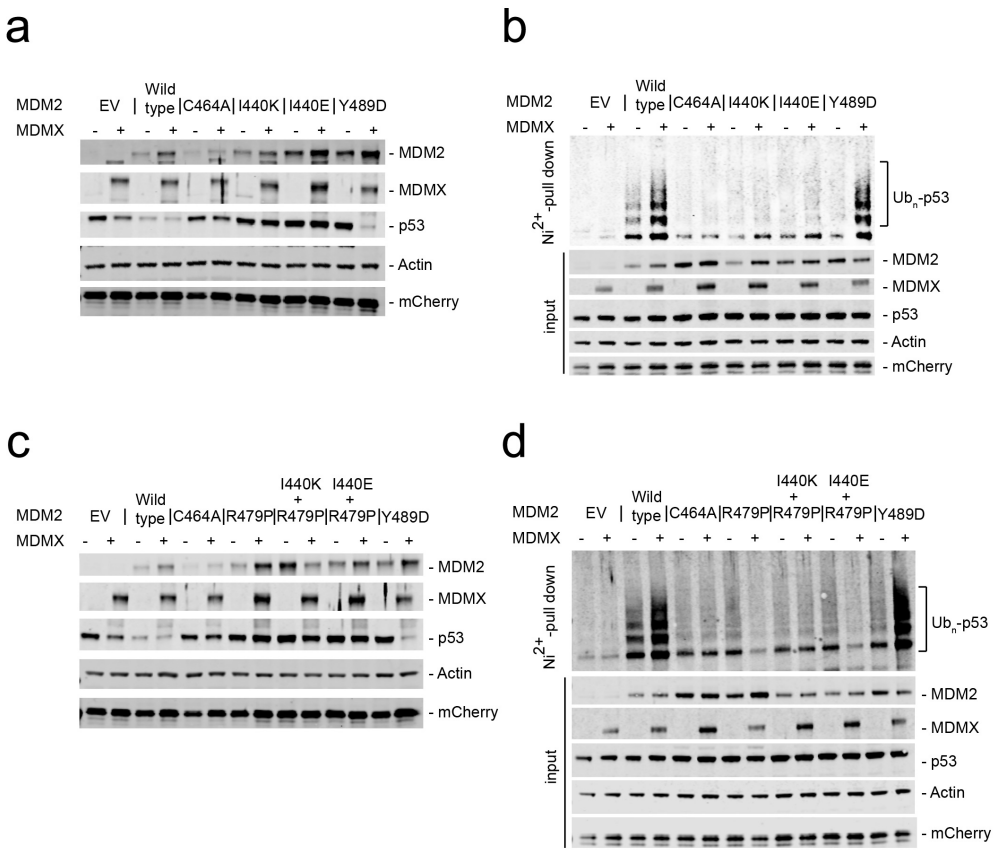

Figure 3-13: MDM2 I440 and R479 mutants do not be reactivated by MDMX

Activity of MDM2 I440 and R479 mutants in the presence or absence of MDMX was tested in cell-based p53 degradation assay and ubiquitination assay. U2OS cells were transiently transfected with combinations of plasmid vectors coding for p53, mCherry, myc-tagged MDMX (where indicated), His-Ubiquitin-GFP (ubiquitination assay) and wild type MDM2 or the MDM2 I440 or R479 mutants for 24 hours. MDM2 Y489D mutant was used as a positive control of reactivation. (a,c) p53 degradation assay showing that I440 and R479 mutants or the double mutants do not affect p53 degradation. (b,d) Cells were treated with proteasome inhibitor MG132 for 5 hours then lysates were pull-downed with the nickel beads (His-tag pull-down). Ubiquitin-conjugated p53 was detected by western blotting.

3.2.1.5 Other potential targets to separate E2–ubiquitin complex and MDM2

In addition to MDM2 I440 and R479, the structure shows other potential UbcH5B interaction sites including MDM2 V439, K473 and P476, which could form hydrogen bonds with the UbcH5B R5, F62 and S94 residues, respectively (Figure 3-14).

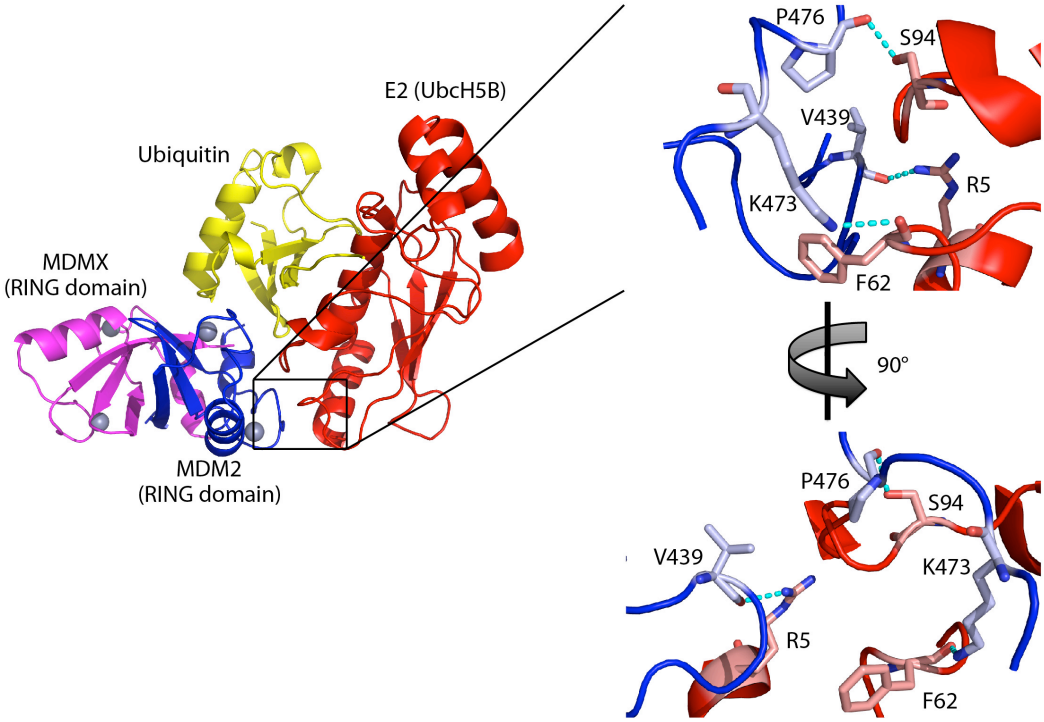

Figure 3-14: Other hydrogen bonds between E2 and MDM2 RING domain

Close-up view of other hydrogen bonds between UbcH5B and MDM2 RING domain. MDM2 V439, K473 and P476 could form hydrogen bonds between UbcH5B R5, F62 and S94, respectively. UbcH5B (red), ubiquitin (yellow), MDM2^{RING} (blue) and MDMX^{RING} (pink). Cyan dots indicate hydrogen bonds.

To test whether these possible interaction sites are important for the E3 ligase activity of MDM2, they were mutated into alanines.

The results suggest that mutation of V439A or P476A does not affect the ability of MDM2 to degrade p53 (Figure 3-15). However, the stability of MDM2 P476A mutant was quite high, with expression levels similar to the MDM2 C464A mutant, suggesting there may be some defect in auto-ubiquitination (Figure 3-15a). The MDM2 K473A mutant also retained some ability to degrade of p53, compared with no MDM2 expression or expression of C464A mutant, but its E3 activity was significantly less than that of wild type MDM2 (Figure 3-15).

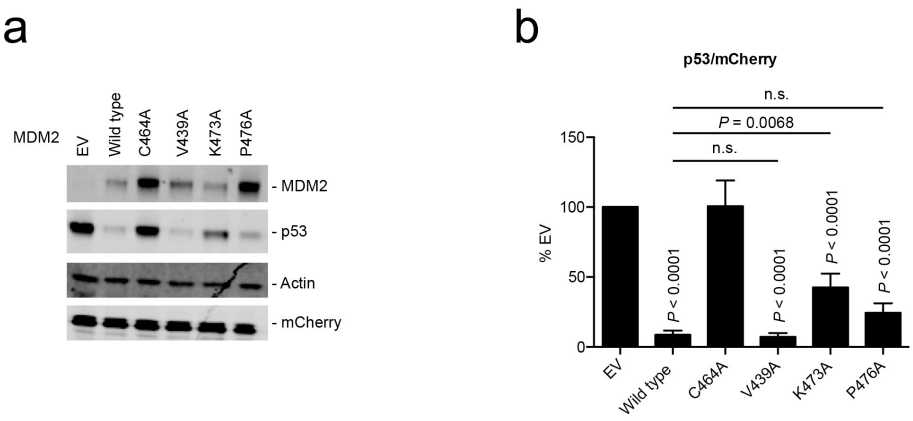

Figure 3-15: Effects of MDM2 V439, K473 and P476 mutants on p53 degradation

U2OS cells were transiently transfected with combinations of plasmid vectors coding for p53, mCherry, and wild type MDM2 or the indicated MDM2 mutants for 24 hours. (a,b) p53 degradation assay showing that, although MDM2 V439A and P476A mutants do not affect its E3 ligase activity, MDM2 K473A mutant has reduced ability to promote degradation of p53. *P* values (one-way ANOVA with Tukey's *post hoc* test): vs. EV (vertical), vs. wild type (horizontal). "n.s." indicates not significant vs. wild type. *F* (5, 12) = 66.57. Error bars indicate mean ± SD. *n* = 3 independent experiments.

In addition to the E2-MDM2 RING and interaction, the structure shows that ubiquitin-MDM2 interaction is also important for the formation of the active "closed" E2–ubiquitin conformation. While MDM2 R479 plays a critical role in stabilising the ubiquitin conformation, the structure shows that there are other potential interactions between ubiquitin and MDM2.

MDM2 serine 429 (S429) and asparagine 433 (N433) are located N-terminal to the RING domain and form a short helix that contacts the ubiquitin T9-K11 surface (Figure 3-16). In addition, MDM2 H457 (which co-ordinates Zn^{2+}) and V477 are also close proximity to the ubiquitin surface (Figure 3-16). Indeed, MDM2 H457 forms a hydrogen bond with the carbonyl oxygen of the ubiquitin E34 residue (Figure 3-16).

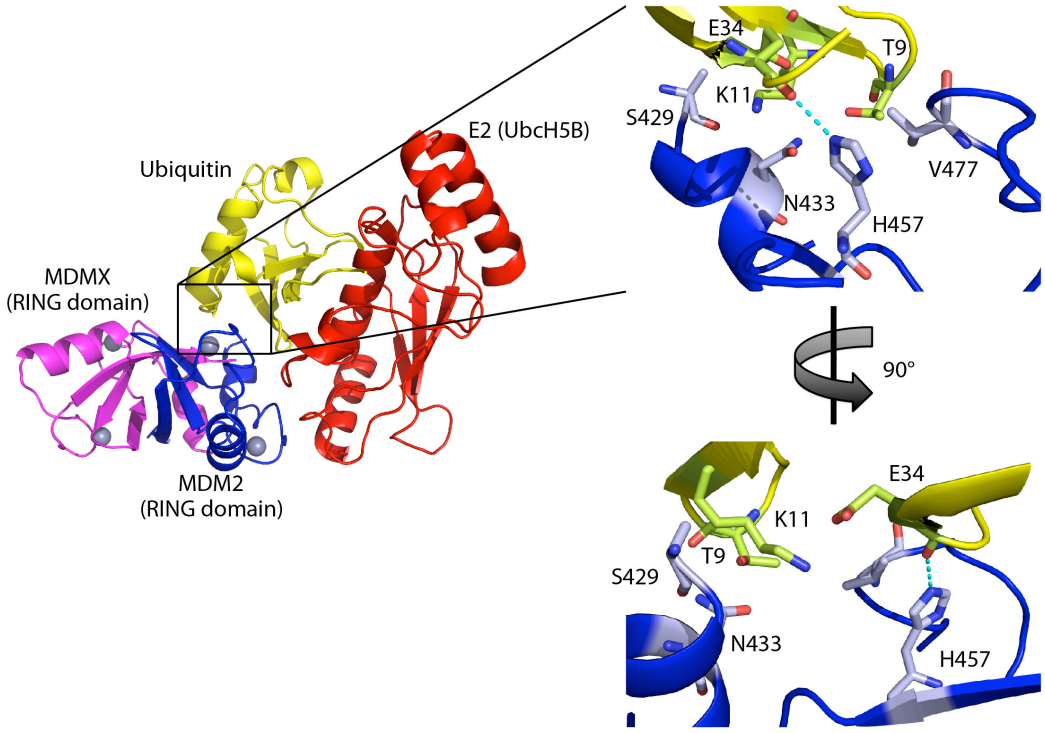

Figure 3-16: Other interaction sites between ubiquitin and MDM2 RING domain

Close-up view of interaction between ubiquitin and MDM2 RING domain. MDM2 H457 (which co-ordinates Zn^{2+}) forms a hydrogen bond with the carbonyl oxygen of the ubiquitin E34 residue. MDM2 S429, N433 and V477 are also important to interact with ubiquitin. UbcH5B (red), ubiquitin (yellow), $MDM2^{RING}$ (blue) and $MDMX^{RING}$ (pink). Cyan dots indicate hydrogen bonds.

Although my colleague has demonstrated that the E3 ligase activity has been compromised in MDM2 N433 and V477 mutants *in vitro* (Nomura et al., 2017), these mutants did not attenuate degradation of p53 in cells (Figure 3-17).

As expected, mutation of MDM2 H457 – a residue that is important to co-ordinate Zn^{2+} - into alanine completely abrogated E3 ligase activity, similar to C464A (Figure 3-17). Interestingly, mutation of MDM2 H457 into cysteine, which may retain co-ordination of Zn^{2+} but may have lost interaction with E34 on ubiquitin, did not affect its ability to degrade p53 (Figure 3-17).

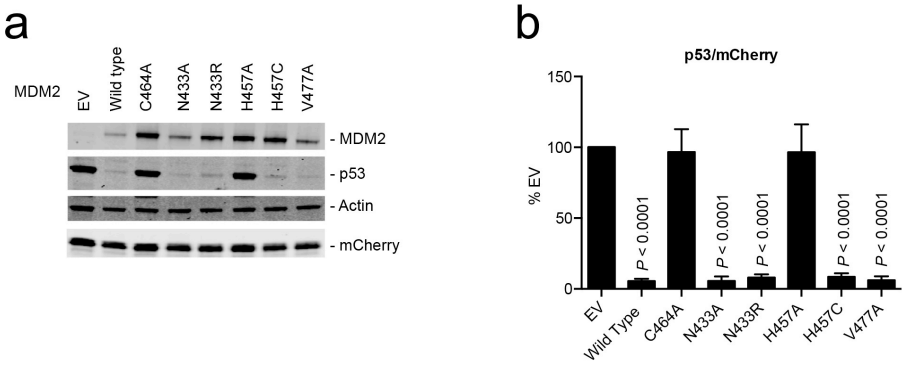

Figure 3-17: Effects of MDM2 N433, H453 and V477 mutants on p53 degradation

U2OS cells were transiently transfected with combinations of plasmid vectors coding for p53, mCherry, and wild type MDM2 or the indicated MDM2 mutants for 24 hours. (a,b) p53 degradation assay showing that, although MDM2 H457A mutant has no ability to promote degradation of p53, other indicated MDM2 mutants that could interact with ubiquitin do not affect its E3 ligase activity. *P* values (one-way ANOVA with Tukey's *post hoc* test): vs. EV. *F* (7, 16) = 78.47. Error bars indicate mean ± SD. *n* = 3 independent experiments.

Notably, it has been reported that phosphorylation of S429 alone, or with other MDM2 phosphorylation site upstream RING domain (S386, S395, S407, T419, S425 and S429) modulates the E3 ligase activity of MDM2 (Cheng et al., 2011). Therefore, these residues were mutated into aspartate (phosphorylation mimic as it is negatively charged) or alanine (non-phosphorylation mimic).

My results suggest that S429D or S429A do not affect the ability of MDM2 to promote p53 degradation compared to wild type MDM2 (Figure 3-18a, b). However, p53 degradation was attenuated by expressing MDM2 6D (S386D, S395D, S407D, T419D, S425D and S429D) mutant (Figure 3-18a, b). Therefore, I tested whether these MDM2 mutations affect its ability to hetero-dimerise or bind to p53. Based on Co-IP experiments, although MDM2 6D possesses the ability to dimerise with MDMX, it has lost its ability to bind to p53 (Figure 3-18c, d).

Taken together, these potential interaction sites in MDM2 with E2–ubiquitin complex are less critical than MDM2 I440 or R479. Although MDM2 6D attenuated degradation of p53, this may be due to the loss of interaction with p53 rather than the loss of interaction with E2–ubiquitin complex.

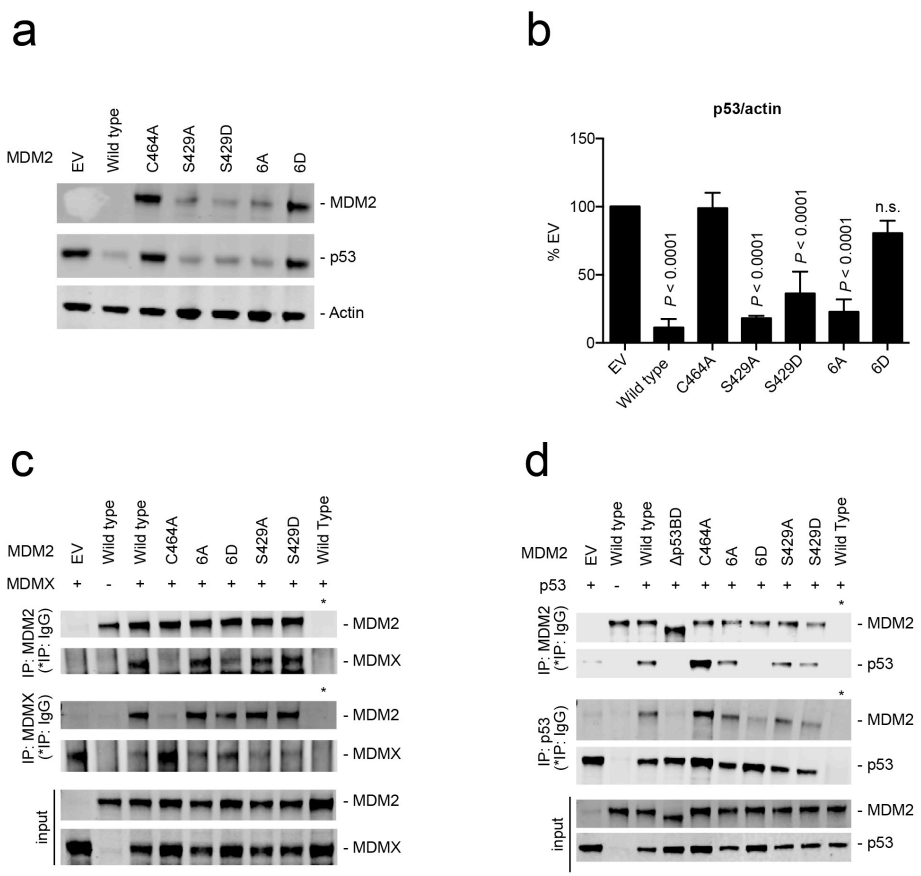

Figure 3-18: Phosphorylation of MDM2 upstream RING domain disrupts MDM2-p53 interaction

U2OS cells were transiently transfected with combinations of plasmid vectors coding for p53, MDMX (Co-IP) and wild type MDM2, MDM2 Δp53BD (Co-IP, as a negative control) or the indicated MDM2 mutants for 24 hours. (a,b) p53 degradation assay showing that, although MDM2 6D mutant does not affect its E3 ligase activity, MDM2 S429A, S429D and 6A mutant have reduced ability to promote degradation of p53. *P* values (one-way ANOVA with Tukey's *post hoc* test): vs. EV. "n.s." indicates not significant. *F* (6, 14) = 54.73. Error bars indicate mean ± SD. *n* = 3 independent experiments. (c,d) Cells were treated with proteasome inhibitor MG132 for 3 hours then lysates were immunoprecipitated using MDM2, MDMX or p53 antibody then analysed by western blot. Although MDM2 6D mutants can dimerise with MDMX, it has lost its ability to bind to p53.

3.2.2 Targeting MDM2-MDMX dimerisation

3.2.2.1 Dimerisation is critical for MDM2 E3 ligase activity

Dimerisation of MDM2, either with MDM2 itself (homo-dimerisation) or with MDMX (hetero-dimerisation) is important for E3 activity since the C-terminal tail of a partner of MDM2 is critical to interact with ubiquitin.

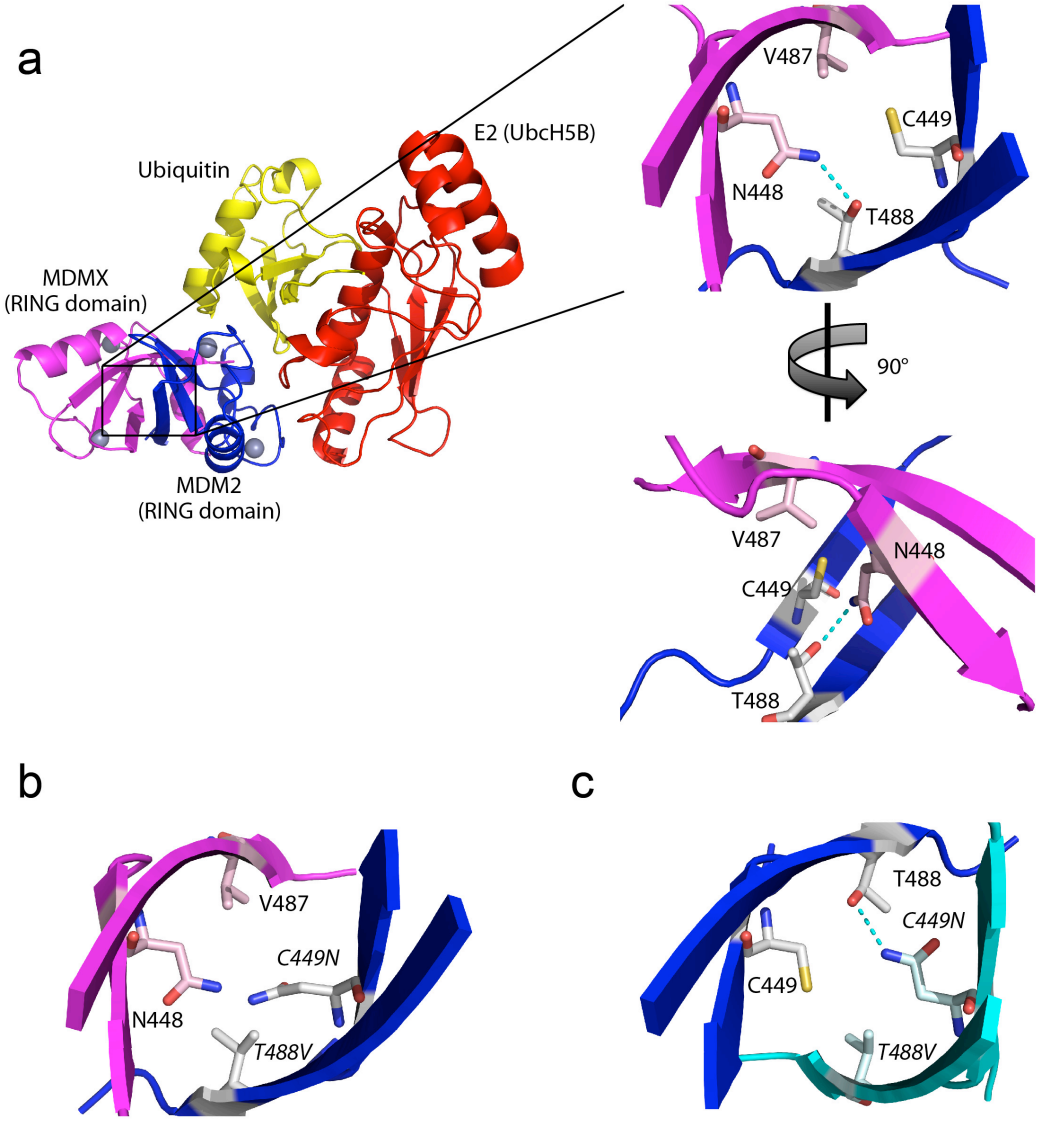

Figure 3-19: Dimerisation interface of MDM2 and MDMX

(a) Close-up view of dimerisation interface of MDM2 and MDMX RING domains. MDM2 and MDMX dimerise through hydrophobic interaction (between MDM2 C449 and MDMX V487) and hydrogen bond (between MDM2 T488 and MDMX N448). Cyan dots indicate hydrogen bonds. (b) Mutagenesis model showing that double mutation of C449N and T488V (as in MDMX) cannot dimerise with MDMX (and itself) since they lack hydrophobic interaction and hydrogen bond. Moreover the distance between the two asparagines at the dimer interface is too close and hydrophobic valine is not compatible with asparagine. These residues will likely create a steric hindrance thereby preventing dimerisation. To obtain this model, MDM2 residues were mutated *in silico*. (c) Mutagenesis model showing that double mutation of C449N and T488V (as in MDMX) (cyan) can dimerise with wild type MDM2 (blue). To obtain this model, MDM2 residues were mutated *in silico*. UbcH5B (red), ubiquitin (yellow), $MDM2^{RING}$ (blue), $MDMX^{RING}$ (pink) and $MDM2^{RING}$ DM (cyan).

Although cysteine 449 (C449) on MDM2 has been described as an important residue for dimerisation through hydrophobic interaction with MDMX V487, the structure suggests that threonine 488 (T488) may also be important for dimerisation by interacting with N448 on MDMX through hydrogen bounding (Figure 3-19a).

Therefore, I mutated MDM2 C449 to asparagine and T488 to valine as in MDMX, since MDMX cannot homo-dimerise likely due to the presence of these corresponding residues (N448 and V487). Indeed modelling of MDM2 C449N and T488V in the dimerisation interface suggests potential steric hindrances at the dimer interface and could explain why MDMX does not homodimerise (Figure 3-19b).

MDM2 C449N and T488V single point mutants did not affect in p53 degradation compared to wild type MDM2; significant reduction of p53 to 48.0 ± 19.2 % and, respectively (Figure 3-20a, b). Interestingly, T488V seems to potentiate p53 degradation but stabilise itself (Figure 3-20a, b). Double mutation of C449N and T488V in MDM2 (DM) significantly attenuated p53 and MDM2 degradation as well as p53 ubiquitination (Figure 3-20 a-c). As expected, C449N and DM did not interact with MDMX (Figure 3-20d, Figure 3-19b). Taken together, these results suggest that while individual mutation of C449N or T488V is not sufficient to disrupt MDM2 homo-dimerisation and subsequent degradation of p53, mutation of both sites results in a defect in degradation ability. This double mutation of MDM2 abrogates the E3 activity of MDM2 by disrupting their dimerisation. It is important to note that, although MDM2 C449N or DM mutants are not able to hetero-dimerise with MDMX or "homo"-dimerise (MDM2 C449N or DM mutants cannot dimerise with MDM2 C449N or DM mutants), they can dimerise with MDM2 (such as wild type MDM2 or other MDM2 variants that possess C449 and T488) (Figure 3-19c).

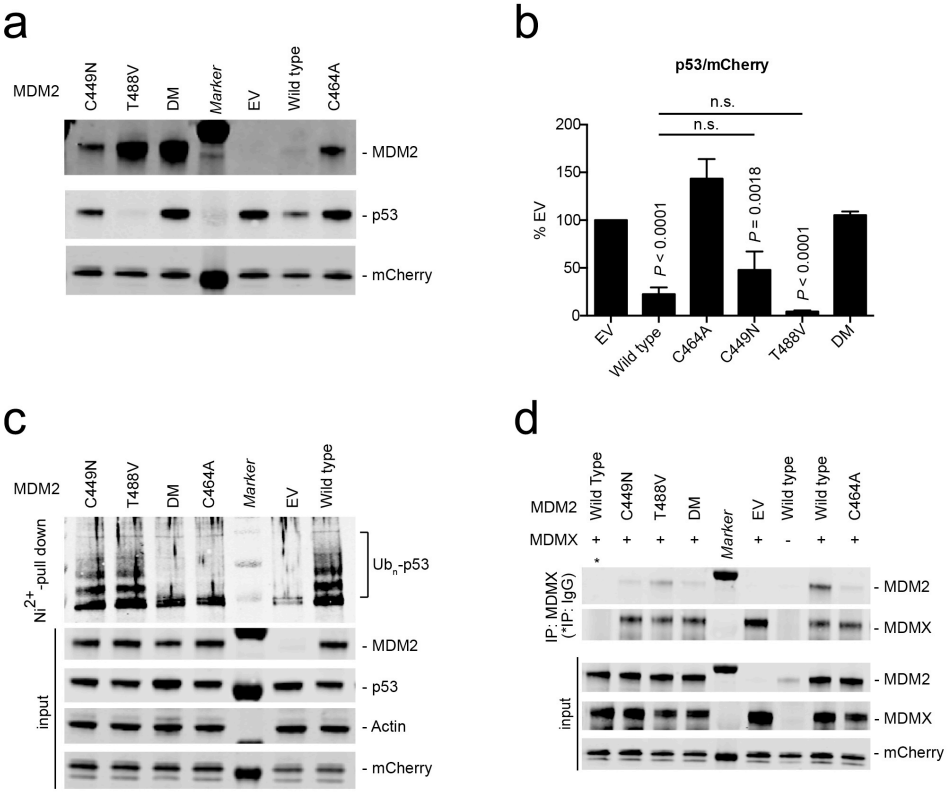

Figure 3-20: Effect of MDM2 dimerisation impairment on p53 degradation and ubiquitination

Activity of MDM2 C449N, T488V and C449N-T488V double mutant (DM) was tested in cell-based p53 degradation assay and ubiquitination assay. U2OS cells were transiently transfected with combinations of plasmid vectors coding for p53, mCherry, His-Ubiquitin-GFP (ubiquitination assay), myc-tagged MDMX (co-immunoprecipitation) and wild type MDM2 or the MDM2 C449N, T488V and its double mutants for 24 hours. (a,b) p53 degradation assay showing that MDM2 DM mutant has no ability to promote degradation of p53 whereas each single mutations were still able to promote p53 degradation. *P* values (one-way ANOVA with Tukey's *post hoc* test): vs. EV. "n.s." indicates not significant vs. wild type. *F* (5, 12) = 61.66. Error bars indicate mean ± SD. *n* = 3 independent experiments. (c) Cells were treated with proteasome inhibitor MG132 for 5 hours then lysates were pull-downed with the nickel beads (His-tag pull-down). Ubiquitin-conjugated p53 was detected by western blotting. (d) Interaction of MDM2 mutants with MDMX was tested by co-immunoprecipitation. Cells were treated with proteasome inhibitor MG132 for 3 hours then lysates were immunoprecipitated using MDMX antibody then analysed by western blot.

3.2.2.2 Complementation between MDM2 I440 and dimerisation mutants

Based on the model of active E3 dimers, MDM2 I440 mutants, which have lost the ability to bind to E2, may regain E3 activity by forming a dimer with a binding partner - like MDMX or other MDM2 proteins - that retains the ability to bind to the E2–ubiquitin complex. To test this hypothesis, the C449N-T488V double mutant (DM), which has lost the ability to homo-dimerise or bind MDMX (but can

dimerise with MDM2 and interact with E2–ubiquitin complex), was co-expressed with I440 mutants.

Unlike the MDM2 C464A mutant, MDM2 I440K and I440E mutants regained their ability to degrade and ubiquitinate p53 when they were co-expressed with C449N-T488V double mutation, from 97.3 ± 26.9 % to 34.8 ± 11.5 % and from 94.0 ± 19.6 % to 30.5 ± 3.6 %, respectively (Figure 3-21).

Therefore, this result suggests that I440 mutants were reactivated by acting as a binding partner of C449N-T488V double mutant.

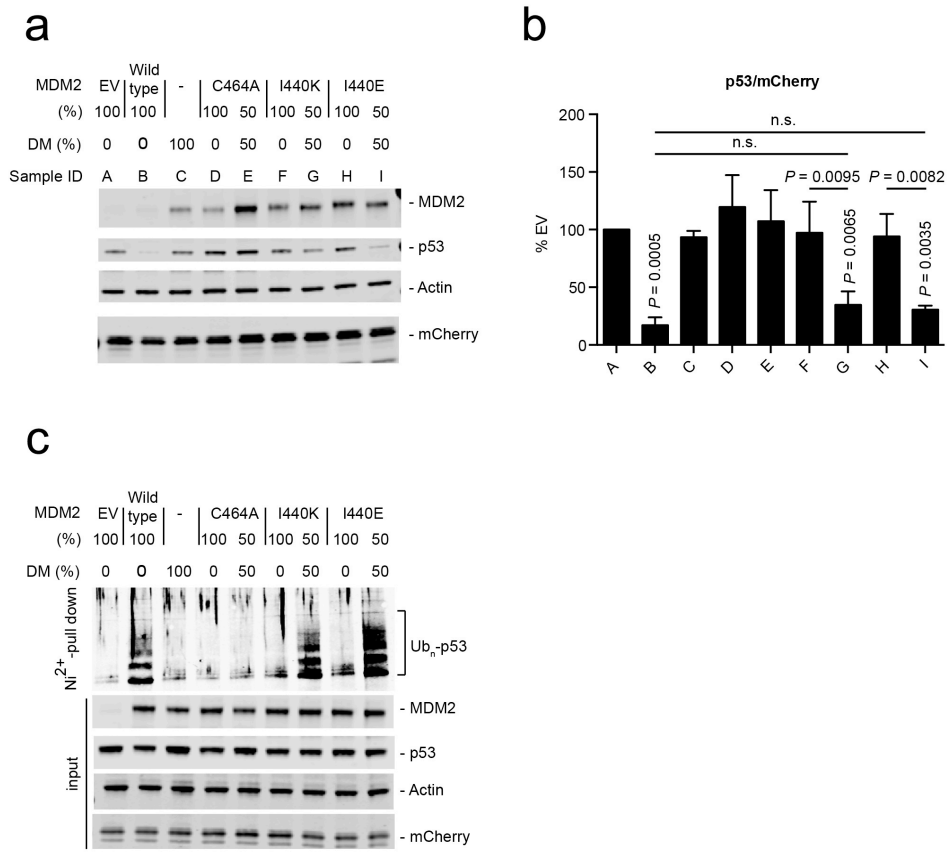

Figure 3-21: Complementation between I440 and dimerisation impairment mutant

Activity of MDM2 I440 mutants (no E2 interaction) in the presence or absence of C449N-T488V double mutant (DM) (no "homo"-dimerisation but can dimerise with other MDM2 variants) was tested in cell-based p53 degradation assay and ubiquitination assay. U2OS cells were transiently transfected with combinations of plasmid vectors coding for p53, mCherry, His-Ubiquitin-GFP (ubiquitination assay) and wild type MDM2 or the MDM2 mutants for 24 hours. (a,b) p53 degradation assay. *P* values (one-way ANOVA with Tukey's *post hoc* test): vs. EV (vertical), vs. each MDM2 I440 mutant without DM (F vs. G and H vs. I) (horizontal). "n.s." indicates not significant vs. wild type. *F* (8, 18) = 14.07. Error bars indicate mean ± SD. *n* = 3 independent experiments. (c) Cells were treated with proteasome inhibitor MG132 for 5 hours then lysates were pull-downed with the nickel beads (His-tag pull-down). Ubiquitin-conjugated p53 was detected by western blot.

3.3 E3 ligase activity of MDMX

3.3.1 Differences between MDM2 and MDMX

Although 52 % of amino acids (22 out of 42) between MDM2 RING domain (from C438 to R479) and MDMX RING domain (from C437 to K478) are identical (Figure 3-22), MDMX RING domain does not possess intrinsic E3 ligase activity. One main reason is probably that MDMX is not able to homo-dimerise. Although a recent study suggested that a single mutation in MDMX (N448C) is sufficient to activate the ability to catalyse p53 ubiquitination in vitro (Iyappan et al., 2010), we have been unable to reproduce this result.

Therefore, an *in silico* approach by superimposition of MDMX RING domain structure onto MDM2 RING domain portion in our structure of UbcH5B–ubiquitin-$MDM2^{RING}$-$MDMX^{RING}$ complex was used to investigate differences between MDM2 and MDMX RING domains. Based on the model created, MDMX may be able to interact with UbcH5B–ubiquitin complex through hydrophobic interaction (Figure 3-22b). However, model suggests that MDMX may not be able to align ubiquitin properly to the UbcH5B active site since K478 on MDMX cannot interact with Q92 in UbcH5B unlike R479 in MDM2 (Figure 3-22c).

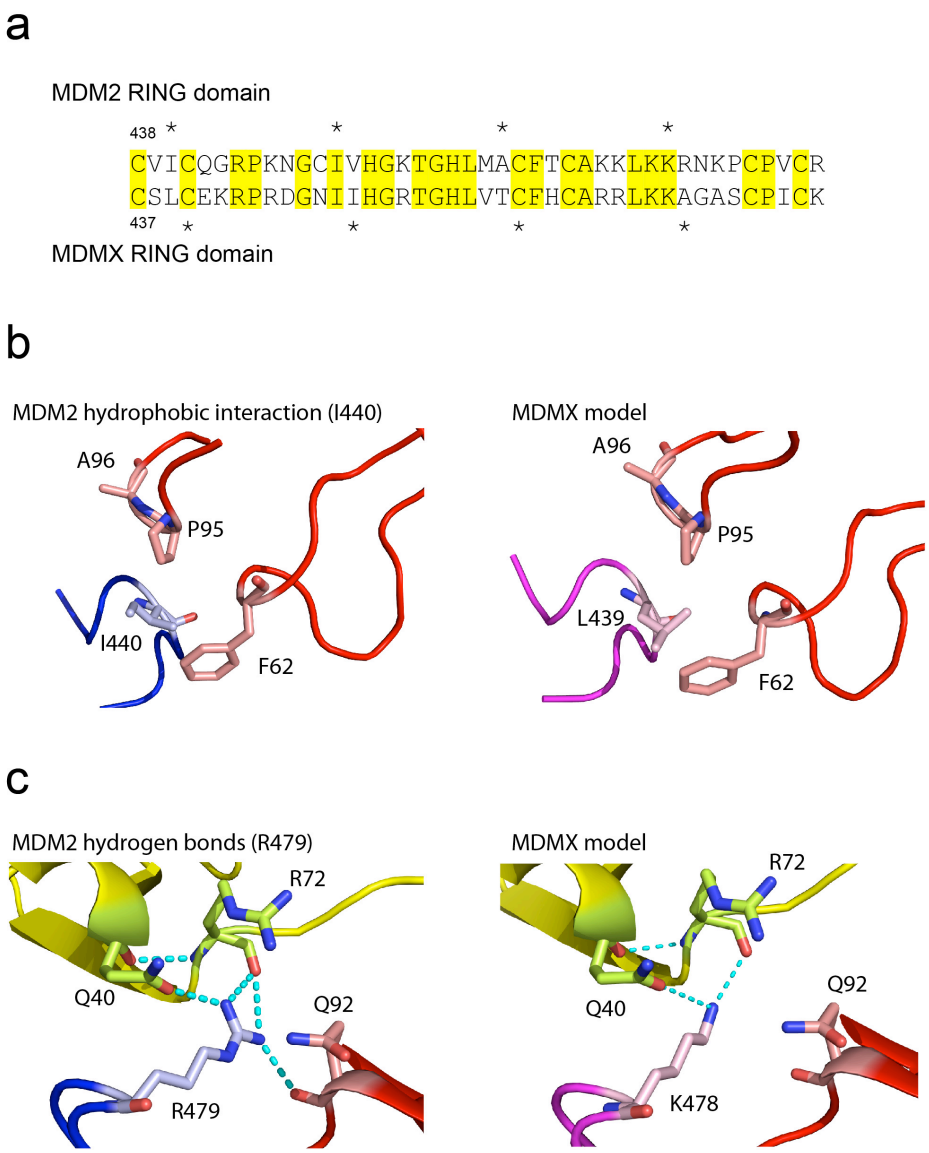

Figure 3-22: Differences between MDM2 and MDMX RING domains

(a) Differences of amino acid sequence between MDM2 and MDMX RING domains. Yellow boxes indicate the identical amino acids. (b) MDMX RING domain may interact with E2–ubiquitin complex through hydrophobic interaction. (e) MDMX may not be able to align ubiquitin to the E2 active site since K478 on MDMX cannot interact with Q92 in UbcH5B. To obtain these models, MDM2 was mutated into MDMX *in silico*. UbcH5B (red), ubiquitin (yellow), $MDM2^{RING}$ (blue) and $MDMX^{RING}$ (pink) (mutated *in silico*). Cyan dots indicate hydrogen bonds.

To assess why the MDMX RING fails to function as an E3, I used MDM2-MDMX chimera (1-421: MDM2, 422-490: MDMX) (Figure 3-23a). This chimeric protein retains the MDM2 NLS and NES, so removing the complication of differential subcellular localisation of MDMX compared to MDM2.

In addition to the N448C single mutation, the N448C-V487T double mutation, which mimics MDM2 dimer interface based on structural modeling, might allow homo-dimerisation, also failed to show any ubiquitination activity (Figure 3-23b). While MDMX-UbcH5B binding interface seems compatible (Figure 3-22b), it lacks key hydrophobic residues observed in MDM2 RING domain for example I440 is replaced with leucine in MDMX. However, additional mutation of L439I in N448C-V487T also failed to ubiquitinate p53 (Figure 3-23b). This may be because leucine and isoleucine have similar characteristics with high hydrophobicity and both can interact with the N-terminal α1 helix and L1 and L2 loops of UbcH5B.

Surprisingly, although mutations of R479K in MDM2 did not affect its E3 activity, double mutation of MDM2-MDMX chimera N448C with K478R allowed the MDM2-MDMX chimera to degrade and ubiquitinate p53 (Figure 3-23c, d). This indicates that K478R is necessary for MDMX E3 activity, possibly because lysine residue on MDMX cannot interact with Q92 in UbcH5B, while substitution of an arginine in this position allows for the interaction as seen with MDM2.

Introducing the same mutations in full length MDMX also led to E3 ligase activity, although to a lesser extent compared to the mutations in the MDM2/X chimera (Figure 3-23c, d). This suggests that domains of MDM2 other than RING (such as NLS, NES, or acidic domain) are also important to ubiquitinate p53.

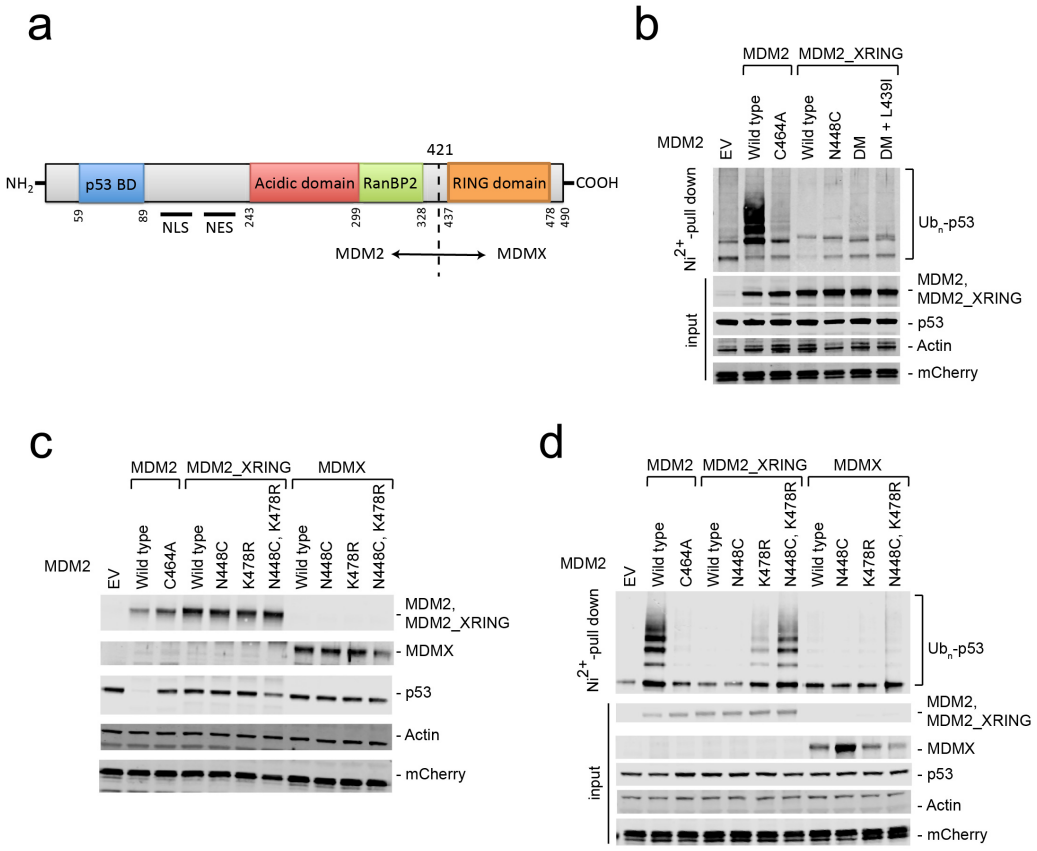

Figure 3-23: Mutation of MDMX K478R is necessary to give MDMX an E3 ligase activity

Activity of MDMX RING domain was tested in cell-based p53 degradation assay and ubiquitination assay using MDM2/MDMX chimera (1-421: MDM2, 422-490: MDMX) since MDMX lacks NLS and NES and has shorter acidic domain. U2OS cells were transiently transfected with combinations of plasmid vectors coding for p53, mCherry, His-Ubiquitin-GFP (ubiquitination assay) and MDM2 or its mutants, MDM2/MDMX chimera, myc-tagged MDMX or its mutants for 24 hours. (a) Schematic model of MDM2/MDMX chimera. (b) Cells were treated with proteasome inhibitor MG132 for 5 hours then lysates were pull-downed with the nickel beads (His-tag pull-down). Ubiquitin-conjugated p53 was detected by western blotting. DM: MDM2_XRING N448C-V487T double mutant. (c) Example western blot showing effect of MDM2/MDMX chimera mutants on p53 degradation. (d) Cells were treated with proteasome inhibitor MG132 for 5 hours then lysates were pull-downed with the nickel beads (His-tag pull-down). Ubiquitin-conjugated p53 was detected by western blotting.

SPR analyses, performed by Dr Gary Sibbet, have shown that while MDMX is unable to interact with UbcH5B-ubiquitin complex, a single mutation at K478R allows interaction with UbcH5B-ubiquitin complex (Figure 3-24).

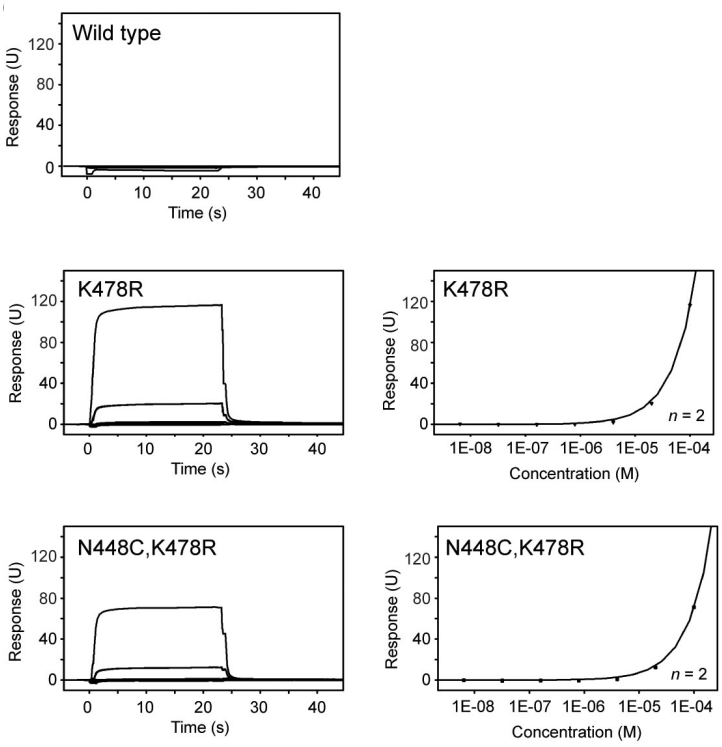

Figure 3-24: SPR analysis of MDMX variants binding affinities for UbcH5B–ubiquitin

Representative sensorgrams (left) and binding curves (right) for GST-MDMXR variants with UbcH5B–ubiquitin are shown. Wild type MDMX displayed no UbcH5B–ubiquitin binding up to 100 µM UbcH5B–ubiquitin whereas both K478R and N448C, K478R mutants exhibited UbcH5B–ubiquitin binding. However, K_d could not be estimated due to the weak binding affinity. All were performed in duplicates by Dr Gary Sibbet.

As I440 mutants can be reactivated by forming a dimer with a binding partner that retains the ability to bind to the E2–ubiquitin complex, MDMX K478R was co-expressed with MDM2 I440 mutants. MDM2 I440 mutants were reactivated by MDMX K478R but not by wild type MDMX, suggesting that MDMX K478R has acquired the ability to interact with E2–ubiquitin complex (and dimerise with MDM2 I440 mutants) and so ubiquitinate p53 (Figure 3-25).

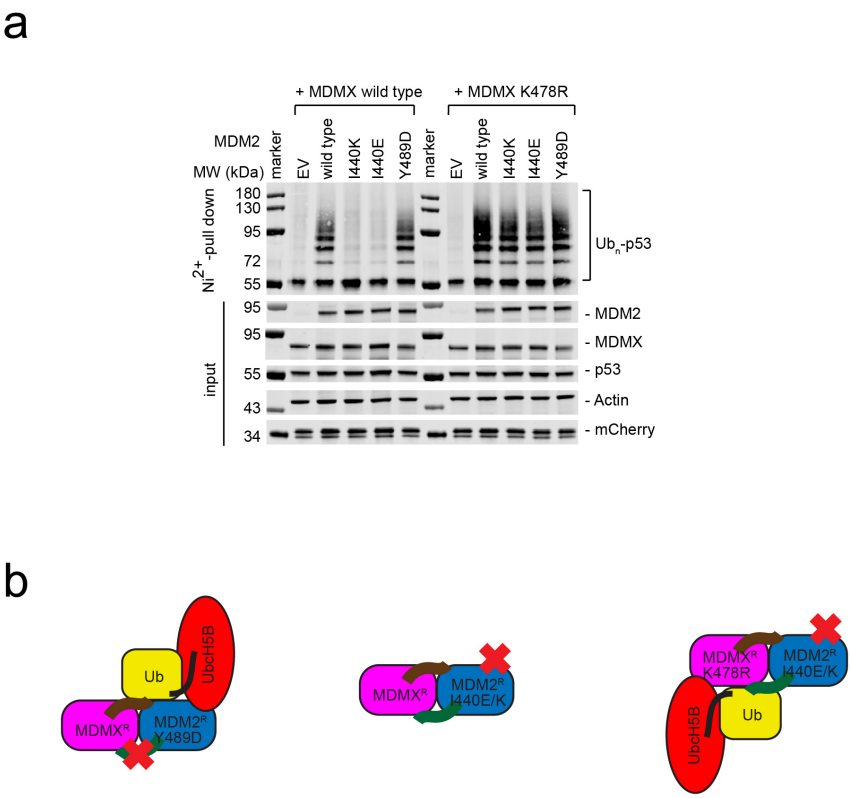

Figure 3-25: Complementation between MDM2 I440 mutants and MDMX K478R mutant

(a) Activity of MDM2 I440 mutants (no E2 interaction) in the presence or absence of MDMX K478R was tested in cell-based p53 ubiquitination assay. U2OS cells were transiently transfected with combinations of plasmid vectors coding for p53, mCherry, His-Ubiquitin-GFP, wild type MDMX or MDMX K478R and wild type MDM2 or the MDM2 mutants for 24 hours. Cells were treated with proteasome inhibitor MG132 for 5 hours then lysates were pull-downed with the nickel beads (His-tag pull-down). Ubiquitin-conjugated p53 was detected by western blot. (b) Models illustrating that, unlike MDM2 C-terminal tail mutant, MDM2 I440 mutants cannot be reactivated by wild type MDMX. This may be because neither MDM2 I440 mutants nor wild type MDMX can recruit E2–ubiquitin complex. MDM2 I440 mutants can be reactivated by MDMX K478R that can recruit E2–ubiquitin complex. Red cross indicates the point mutation.

3.4 Determination of the ubiquitination target of MDM2 by $p14^{ARF}$

As shown previously, $p14^{ARF}$ attenuates p53 degradation and MDM2 auto-degradation, but potentiates MDMX degradation and ubiquitination (Pan and Chen, 2003). This result could indicate that $p14^{ARF}$ does not completely inhibit the E3 ligase activity of MDM2 but rather switches the target of ubiquitination from p53 to MDMX. Interestingly, the MDM2 RING domain alone is sufficient to

degrade MDMX (de Graaf et al., 2003). However, it is still not clear whether this E3 ligase activity is derived from MDM2-MDMX hetero-dimer by changing the formation of this complex in the presence of $p14^{ARF}$.

To address whether $p14^{ARF}$ changes the composition of the MDM2-MDMX complex, I used MDM2 C-terminal tail mutants that only function as hetero-dimers. To test whether Y489D also degrades MDMX in the presence of $p14^{ARF}$, a protein half-life assay was performed using cycloheximide in the presence of MDMX. Wild type MDM2 and MDM2 Y489D mutant degrade p53 and MDM2 itself but not MDMX in the absence of $p14^{ARF}$ (Figure 3-26). However, in the presence of $p14^{ARF}$, wild type MDM2 and MDM2 Y489D mutant quickly degrade MDMX but stabilise p53 and MDM2 itself (Figure 3-26).

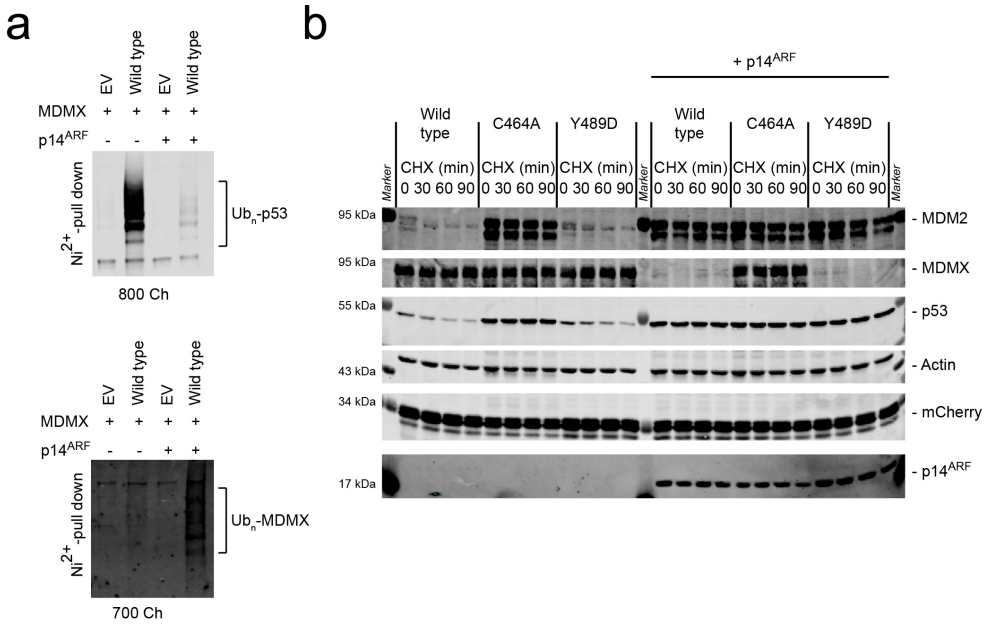

Figure 3-26: $p14^{ARF}$ switches substrate specificity of the MDM2-MDMX complex from p53 to MDMX

The effect of $p14^{ARF}$ was tested in cell-based ubiquitination assay and p53 half-life assay. U2OS cells were transiently transfected with combinations of plasmid vectors coding for p53, FLAG-tagged $p14^{ARF}$, mCherry, His-Ubiquitin-GFP (ubiquitination assay), myc-tagged MDMX and wild type MDM2 or the MDM2 mutants for 24 hours. (a) Cells were treated with proteasome inhibitor MG132 for 5 hours then lysates were pull-downed with the nickel beads (His-tag pull-down). Ubiquitin-conjugated p53 was detected by western blot. (b) Cells were treated with protein synthesis inhibitor cycloheximide for 0, 30 60 or 90 minutes then changes in p53/MDM2/MDMX levels were analysed by western blot.

As a second model, MDM2 I440 and R479 mutants with MDMX K478R were also tested to investigate whether p14^{ARF} interacts with the hetero-dimer to change E3 ligase activity from p53 and MDM2 to MDMX. The results suggest that, while these MDM2-MDMX complexes ubiquitinate and degrade p53 in the absent of p14^{ARF}, they switched their target to MDMX K478R in the presence of p14^{ARF} (Figure 3-27). Expression of wild type MDM2, MDM2 I440K, I440E and R479P mutants decreased MDMX K478R level in the presence of p14^{ARF} to 38 %, 56 %, 65 % and 69 % respectively compared with no MDM2 over-expression (Figure 3-27). Expression of MDM2 C464A did not affect this MDMX degradation, suggesting that dimerisation through their RING domain is required to degrade MDMX K478R (Figure 3-27).

Taken together, p53 degradation was attenuated and MDMX degradation was promoted in the presence of p14^{ARF} and this E3 ligase activity may be derived from MDM2-MDMX heterodimer. Although this could indicate that p14^{ARF} switches the ubiquitination target of MDM2 from p53 to MDMX, it is still possible that p14^{ARF} attenuates E3 ligase activity of MDM2 (MDMX) towards p53 and recruits other ubiquitin ligases to degrade p53. Therefore, further studies, such as siRNA screening, will be required to clarify this regulation.

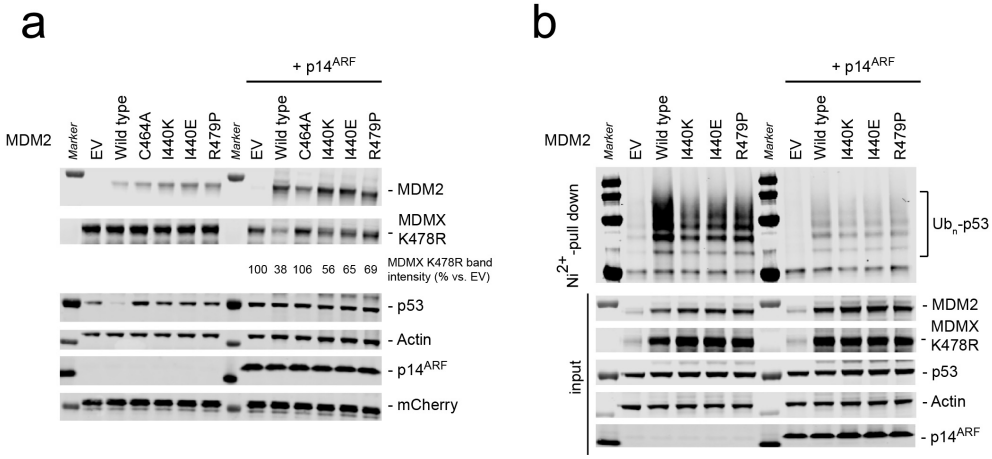

Figure 3-27: p14^{ARF} promotes MDMX K478R "auto-ubiquitination"

U2OS cells were transiently transfected with combinations of plasmid vectors coding for p53, FLAG-tagged p14^{ARF}, mCherry, His-Ubiquitin-GFP (ubiquitination assay), myc-tagged MDMX K478R and wild type MDM2 or the MDM2 mutants for 24 hours. (a) Example western blot showing the effect of p14^{ARF} on p53/MDM2/MDMX degradation. (b) Cells were treated with proteasome inhibitor MG132 for 5 hours then lysates were pull-downed with the nickel beads (His-tag pull-down). Ubiquitin-conjugated p53 was detected by western blot.

3.5 Summary and discussion

In this section, I have demonstrated that mutation of I440K, I440E in MDM2 (preventing E2 binding) and R479P (preventing E2 binding and ubiquitin aligning) are sufficient to abrogate MDM2 E3 activity, while they do not alter the ability to interact with p53 and MDMX. In addition, several biochemical assays, performed by colleagues in Professor Danny Huang's group, have confirmed these observations (Nomura et al., 2017). Single-turnover lysine discharge assays were performed to test whether UbcH5B charged with ubiquitin by E1 (UbcH5B thioester-bonded ubiquitin) discharges ubiquitin to the L-lysine in the presence of MDM2 variants *in vitro*. Their results showed that UbcH5B–ubiquitin discharges rapidly in the presence of wild type MDM2 (within 0.7 minutes), whereas it was delayed in the presence of MDM2 I440 and R479 mutants. This means that interaction between MDM2 RING domain and E2–ubiquitin complex is critical for MDM2-catalysed ubiquitin transfer. *In vitro* pull-down experiments have confirmed MDM2 I440 and R479 mutants can homo- and hetero-dimerise through their RING domain.

Other potential interaction sites in MDM2 between MDM2 RING domain and UbcH5B–ubiquitin complex were less critical than MDM2 I440 or R479 mutants. Interestingly, some phosphorylation sites near the RING domain can prevent p53-MDM2 interaction rather than interaction between E2–ubiquitin complex and MDM2 or its dimerisation. Although Cheng *et al*. (2011) suggests that MDM2 6D prevents its dimerisation (so that losses E3 ligase activity), results presented here suggest that it disrupts the ability to bind to p53. In addition, although these authors have shown that MDM2 6A enhances the E3 ligase activity, I was unable to reproduce this observation.

MDMX is an important binding partner of MDM2 by contributing to the E3 ligase activity of the hetero-dimeric complex, although previous studies have demonstrated that this dimerisation can either inhibit or enhance E3 ligase activity of MDM2 (Jackson and Berberich, 2000, Linares et al., 2003, Stad et al., 2000). Our structure shows that RING domain dimerisation is important for MDM2 E3 ligase activity since the C-terminal tail of an MDM2 binding partner is required to interact with ubiquitin to stabilise the active conformation of E2–ubiquitin complex for ubiquitin transfer. This supports the importance of the C-

terminal tail of MDM2 in E3 ligase activity and mutation of the MDM2 C-terminal can be compensated by MDMX (Uldrijan et al., 2007, Poyurovsky et al., 2007). Indeed, an *in vivo* model suggests that hetero-dimerisation is required to allow normal embryonic development (Tollini et al., 2014). As expected, a dimerisation-impaired MDM2 mutant (C449N-T488V double mutant) has lost its intrinsic E3 ligase activity. This also could be the reason why MDM2 C464A mutant has lost its E3 ligase activity as it cannot dimerise with MDMX. Indeed, in the presence of $p14^{ARF}$, MDM2 seems to switch its ubiquitination target from p53 to MDMX. Therefore, dimerisation may also be important for MDM2 to regulate MDMX activity towards p53.

Although MDM2 I440 and R479 mutants can dimerise with MDMX, they were not reactivated by MDMX, unlike the C-terminal mutants described previously (Uldrijan et al., 2007, Poyurovsky et al., 2007). Interestingly, I440K and I440E mutants can be reactivated by MDM2 variants that retain the ability to bind to E2–ubiquitin complex. Therefore, this complementation mechanism suggests that these mutants are only defective in interacting with E2–ubiquitin complex while all the other RING domain function is retained.

Unlike MDM2, wild type MDMX lacks ability to interact with E2–ubiquitin complex. It could also be shown that mutation of K478R on MDMX (as R479 in MDM2) is necessary to give MDMX an E3 activity by allowing MDMX to bind to E2–ubiquitin complex. MDM2/X chimera gained E3 ligase activity towards p53 by mutating N448C (to allow dimerisation) and K478R. Results of biochemical assays also support this observation: single-turnover lysine discharge assays showed a greatly improved activity in the presence of MDMX K478R compared with wild type MDMX. Further enhancement was observed in the presence of MDMX N448C-K478R double mutant.

Indeed, although I440 mutants cannot be reactivated by wild type MDMX, they were reactivated by MDMX K478R. In the presence of $p14^{ARF}$, this active dimer changed their ubiquitination target from p53 to MDMX K478R. Since the catalytic activity in these cases can only come from the MDM2-MDMX complexes, these results suggest that $p14^{ARF}$ interacts with the hetero-dimer to change E3 ligase activity from p53 and MDM2 to MDMX. It is also possible that other E3 ligases are involved in this MDMX ubiquitination in the presence of $p14^{ARF}$ since MDM2 I440

mutants are catalytically inactive. As the expression of C464A mutant did not affect the degradation of MDMX, we can conclude that dimerisation through the RING domains is essential to control MDMX level. In these experiments, however, U2OS contains certain amount of endogenous MDM2, therefore, there is a possibility that $p14^{ARF}$ increased endogenous MDM2, which could homo- or hetero-dimerise with over-expressed MDM2 mutants and degrade MDMX. Therefore, further experiments will be required to test this hypothesis using cells lacking endogenous MDM2. The mechanism by which $p14^{ARF}$ switches ubiquitination from p53 to MDMX would be an interesting topic for future study.

In conclusion, guided by a crystal structure, I was able to generate specific point mutations within the MDM2 RING domain that have lost its intrinsic E3 ligase activity without altering RING domain structure or their binding ability to p53. In particular, I could demonstrate that MDM2 I440 and R479 play an important role in interacting with E2–ubiquitin complex. In next chapter, I will show whether MDM2 I440 or R479 mutants can regulate p53 in an E3 ligase-independent manner.

Chapter 4 Regulation of the p53 activity by MDM2 and MDMX

4.1 MDM2 I440 and R479 mutants limit p53 activity

Although inhibition of MDM2 to elevate endogenous p53 level in cells is an attractive therapeutic strategy to treat cancer for patients retaining wild type p53, inhibition of MDM2 has not yet achieved clinically success due to on-target toxicity in normal unstressed cells caused by the uncontrolled p53 activity as discussed in Chapter 1 (Section 1.5.1.1). In order to control the p53 activity by MDM2, there are two important factors that are hypothesised by previously published papers; (1) MDM2 must bind to p53 and (2) MDM2 should retain integrity of RING domain structure (as MDM2 C464A mutant cannot limit p53 activity). As demonstrated in Chapter 3, MDM2 I440 or R479 mutants have lost their intrinsic E3 ligase activity without altering the RING domain structure or their ability to bind p53. Therefore, although these mutants contribute to elevate endogenous p53 level, it is possible that the mutants retain E3 ligase independent functions of MDM2, including attenuation of the p53 transcriptional activity in normal unstressed cells. To test this hypothesis, cell lines were generated to examine the regulation of the endogenous p53 activity by MDM2 mutants.

4.1.1 Generation and validation of tetracycline inducible p53 knockdown-*MDM2* knockout cells

The ability of MDM2 to degrade p53 was measured in cells following ectopic expression of both proteins in Chapter 3. However, I was interested in uncovering more subtle regulation of the activity of endogenous – rather than overexpressed – p53. Since the introduction of catalytically inactive MDM2 mutants into cells expressing p53 could cause the activation of a p53-dependent cell cycle arrest or apoptosis, I generated U2OS cells that were conditionally depleted of endogenous p53 through use of a doxycycline inducible shRNA targeting p53 (pLKO-tet-on shRNA). As expected, doxycycline treatment (2 μM, I always used this concentration) induced shRNA expression and p53 depletion within 48 hours and this effect was reversed within 5 days after discontinuing doxycycline treatment (Figure 4-1).

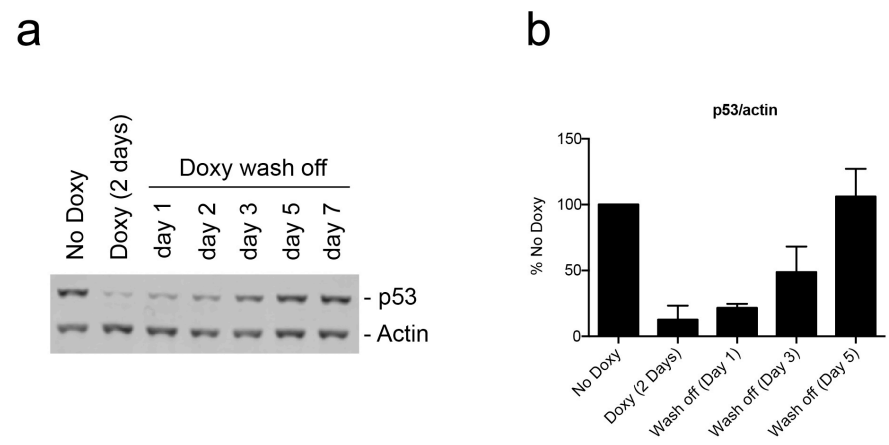

Figure 4-1: Generation of inducible and reversible knockdown of p53

(a,b) U2OS cells were infected with doxycycline-inducible pLKO-tet-on shRNA targeted for p53. After indicated time of treatment and wash-off, cells were treated with nutlin-3 (10 μM) for 3 hours and p53 expression level was analysed by western blot. Western blot showing that doxycycline treatment causes p53 knockdown in 2 days and this effect can be washed off in 5 days. Error bars indicate mean ± SD.

To examine the effects of the MDM2 mutants, I initially attempted to generate CRISPR/Cas9 knock-in clones of MDM2 I440 mutants (using CRISPR/Cas9 vectors targeting MDM2 RING domain near I440 and single strand DNA knock-in template or knock-in construct with silent mutations of the protospacer adjacent motif (PAM)) in the inducible p53 system. However, despite screening 288 clones, I was unable to generate these endogenous MDM2 mutants. Failures include the co-existence of CRISPR knock-in and knockout (Figure 4-2). This could be due to technical difficulties as I was unable to introduce silent mutation on PAM site in knock-in template, for example.

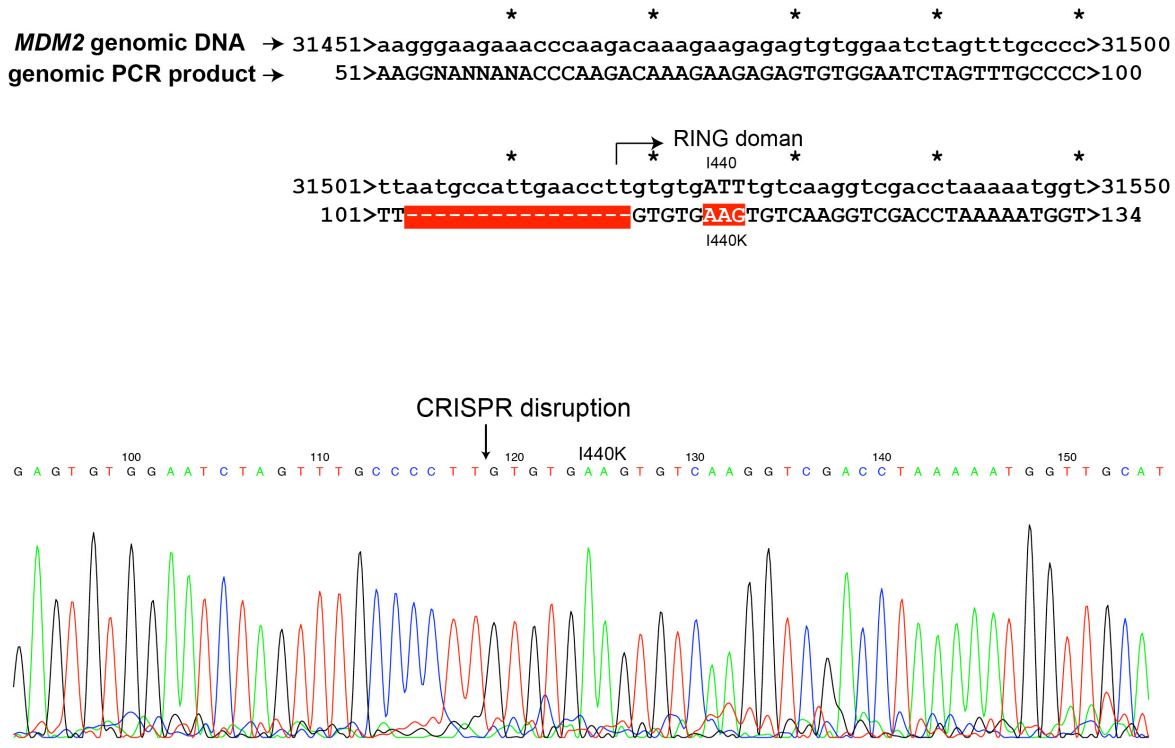

Figure 4-2: Attempt of the generation of CRISPR knock-in of *MDM2* I440K mutant

Genomic PCR followed by sequencing showing that although CRISPR knock-in of MDM2 I440K mutant was observed, CRISPR knockout was also introduced.

Therefore, I decided to introduce the MDM2 mutants by stable transfection. To make sure any observed phenotypes were due to the ectopically expressed mutant MDM2, I removed endogenous wild type *MDM2* from the p53 inducible cells using the CRISPR/Cas9 system. CRISPR/Cas9 vectors targeting the p53-binding domain of MDM2 were transfected into U2OS cells with doxycycline inducible p53 knockdown, clones isolated and CRISPR disruptions assessed by western blotting, then confirmed genomic PCR followed by DNA sequencing (Figure 4-3). Western blot with cells treated with 10 μM of nutlin-3 for 3 hours (5 days after doxycycline discontinuation) shows that no bands appeared when incubating with anti-MDM2 antibodies that recognise epitopes between p53-binding domain and acidic domain (MDM2 Ab-1 antibody) and between acidic domain and RING domain (MDM2 Ab-2 antibody), suggesting that endogenous *MDM2* was completely removed (Figure 4-3a). Genomic PCR sequencing

confirmed CRISPR disruption within the p53-binding domain of *MDM2* (Figure 4-3b); any translated product would be predicted to contain only the first 70 amino acids of MDM2 with a further 23 nonspecific amino acids (Figure 4-3c). Although it is possible that the C-terminal of MDM2 can be produced as a result of the internal initiation transcribed from internal methionine residues including M311, M459 or M484, all of them lack p53-binding domain and therefore they are not functional even if they are produced.

The *MDM2* null cells were then stably transfected with mutant MDM2 variants. Although this system lacks the p53-MDM2 feedback loop, it allows us to investigate regulation of endogenous p53 activity by mutant MDM2 variants upon discontinuation of doxycycline.

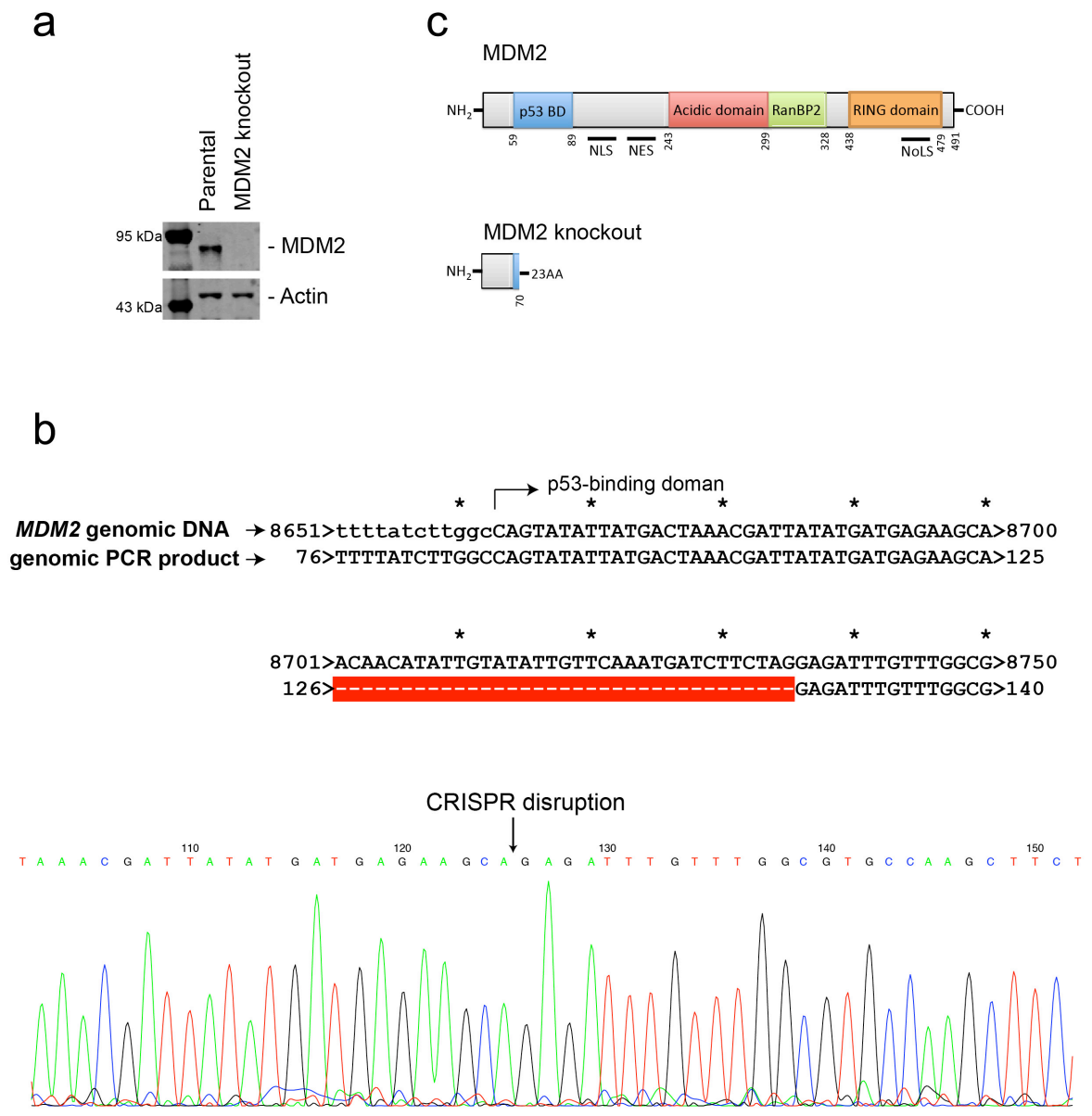

Figure 4-3: Generation and validation of *MDM2* knockout in the inducible p53 system

***MDM2* was disrupted by CRISPR in the inducible p53 system. (a) Immunoblotting showing CRISPR disruption (target p53-binding domain) resulted in *MDM2* knockout. (b,c) Genomic PCR followed by sequencing showing that CRISPR disruption (target-p53 binding domain) caused *MDM2* knockout.**

4.1.2 Effect of the MDM2 mutants on cell cycle

Using the system described above, I tested the ability of different MDM2 mutants to degrade endogenous p53. Stable transfection of wild type MDM2 into these cells, followed by re-expression of p53 (after removal of doxycycline), resulted in a clear degradation of p53 compared to EV transfected cells, while the MDM2 C464A, I440K, I440E and R479P mutants lost the ability to degrade p53 (Figure 4-

4a,b). These results were expected in light of the loss of E3 activity for each of these mutants, as discussed in Chapter 3.

Deletion of *MDM2* resulted in an increased expression the p53 target gene p21 mRNA level by 12.1 ± 0.5 fold following re-expression of p53 (without doxycycline), a response which is significantly attenuated by expressing wild type MDM2 (Figure 4-4c). Interestingly, p21 protein level was significantly lower in cells expressing C464A mutant compared with cells expressing no MDM2 (to 67.3 ± 5.8 %), suggesting that MDM2 C464A still has some activity to regulate p53 transcriptional activity, although the differences in the p21 mRNA induction level was difficult to observe (Figure 4-4). Nevertheless, this p21 protein level was significantly higher than cells expressing wild type MDM2 (Figure 4-4a, b). Interestingly however, despite failing to target p53 for degradation, the expression of the I440 or R479 mutants resulted in a significantly lower activation of p21 compared to that seen in cells expressing no MDM2 and the MDM2 C464A mutant, both at the mRNA level and protein level (Figure 4-4). Similarly, mRNA induction of other p53 target genes by MDM2 I440 mutants were significantly lower than no *MDM2* expressing cells, including *14.3.3σ* and *GADD45a* (Figure 4-4c). Indeed, induction of *GADD45a* by MDM2 I440 mutants was also significantly lower than cells expressing the MDM2 C464A mutant (Figure 4-4c). No expression of *MDM2* and expression of C464A mutant and I440 mutants, in the presence or absence of doxycycline, did not affect to the induction of *GADD45B*, which is not a target gene of p53 (Figure 4-4c). Taken together these results suggest that the I440 and R479 MDM2 mutants retain the ability to restrain p53 activity.

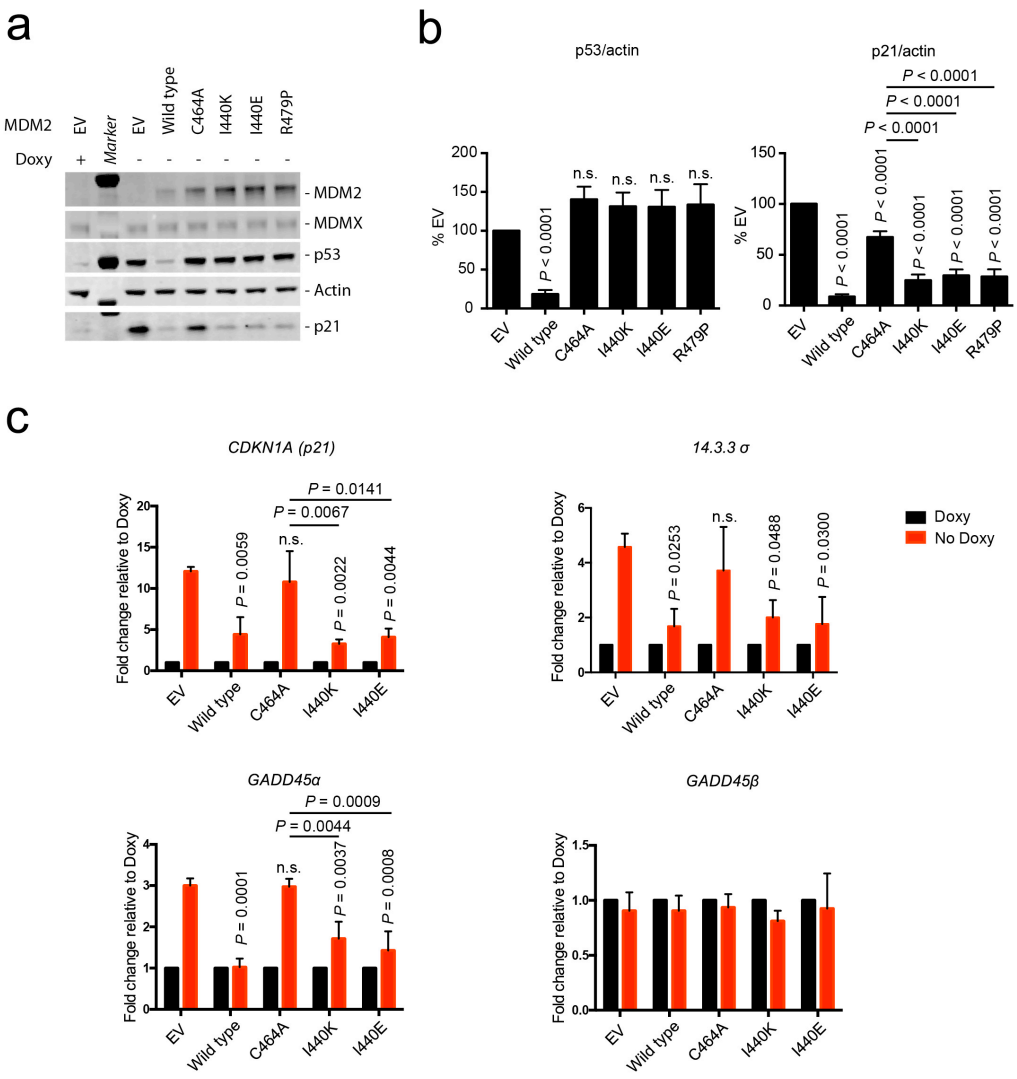

Figure 4-4: Effect of the expression of MDM2 mutants on p53 target genes involving in cell cycle regulation

(a,b) Western blot analysis showing that although MDM2 I440K, I440E and R479P do not degrade p53, induction of p21 is attenuated by these mutants. *P* values (one-way ANOVA with Tukey's *post hoc* test): vs. EV (vertical), vs. C464A (horizontal). "n.s." indicates not significant vs. EV. *F* (5, 12) = 21.96 (p53/actin) and *F* (5, 12) = 131.9 (p21/actin). Error bars indicate mean ± SD. *n* = 3 independent experiments each. (c) qPCR showing mRNA expression of p53 target genes (*GADD45β* is not a p53 target gene) is attenuated by MDM2 I440K, I440E but not by C464A. *P* values (one-way ANOVA with Tukey's *post hoc* test): vs. EV (No Doxy) (vertical), vs. C464A (No Doxy) (horizontal). "n.s." indicates not significant vs. EV (No Doxy). *F* (4, 10) = 13.01 (*CDKN1A (p21)*), *F* (4, 10) = 5.76 (*14.3.3σ*) and *F* (4, 10) = 25.14 (*GADD45α*). Error bars indicate mean ± SD. *n* = 3 independent experiments each.

In the absence of p53 (with doxycycline) all of the cell lines showed similar cell cycle profile (Figure 4-5). However, following re-introduction of endogenous p53, control cells (lacking MDM2 and so with no ability to control p53) underwent a G_1 cell cycle arrest (Figure 4-5). Expression of C464A mutant did not fully rescue this arrest while cells expressing wild type MDM2 continued to progress cell cycle (Figure 4-5). Unlike cells expressing MDM2 C464A mutant, cells expressing MDM2 I440 and R479 mutants did not show any deregulation of cell cycle, suggesting that these mutants are sufficient to control p53 activity under normal unstressed condition as efficiently as wild type MDM2 (Figure 4-5).

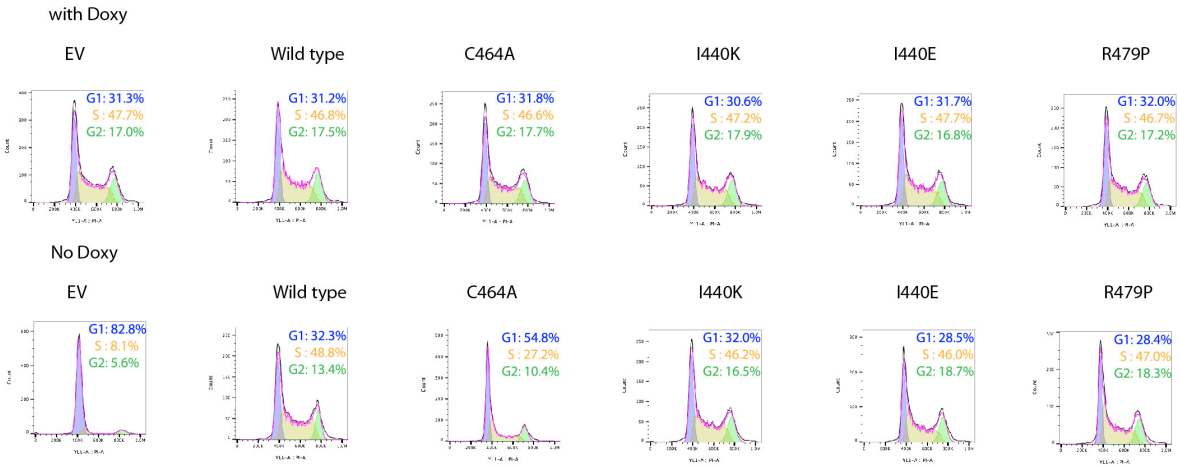

Figure 4-5: Effect of the expression of MDM2 mutants on cell cycle

Cells were stained with propidium iodine overnight and DNA content was analysed in channel FL2. Cell cycle analysis showing that deletion of *MDM2* causes cell cycle arrest at the G_1 phase, which can be rescued by expressing MDM2 wild type, I440 and R479 mutants. Deletion of *MDM2* or expression of MDM2 do not affect on cell cycle in absence of p53.

4.1.3 MDM2 I440 or R479 mutants localise on *p21* promoter

One mechanism to explain how the I440 and R479 mutants restrain p53 activity is that these MDM2 proteins may bind to p53 on actively transcribed sites to reduce p53 activity. To test if MDM2 I440 and R479 mutants directly bind to p53 on the chromatin, I carried out chromatin immunoprecipitation (ChIP) assays to look for MDM2 and p53 at the *p21* promoter.

As expected, wild type MDM2 expression reduced the overall amount of p53 protein, although an assessment of the ratio of p53 to MDM2 at the *p21* promoter suggested that low levels of both proteins were present (Figure 4-6a). By contrast, although MDM2 C464A retained the ability to interact with p53 when co-immunoprecipitated with cell lysate as shown in Chapter 3, this interaction was not maintained at the *p21* promoter; the level of p53 on the *p21* promoter was not significantly reduced by expressing MDM2 C464A mutants and the level of MDM2 on the *p21* promoter (via p53) was significantly low compared with wild type MDM2 (Figure 4-6a, b). These data suggest that this MDM2 mutant has reduced ability to inhibit chromatin bound p53 and could explain why MDM2 C464A fails to limit p53 activity. Interestingly, the I440 and R479 mutants were all found at the *p21* promoter with p53 at significantly higher levels than the MDM2 C464A mutant, suggesting that their ability to limit the p53 transcriptional activity reflects a direct perturbation of the formation of an active transcriptional complex at the promoter (Figure 4-6b). Furthermore, the amount of p53 on the *p21* promoter was also significantly lower in cells expressing MDM2 I440 mutants compared with cells expressing no MDM2 (Figure 4-6a). This could suggest that in addition to co-localising with p53 at the *p21* promoter, MDM2 I440 mutants may also prevent p53 efficient localisation and binding to the p21 promoter.

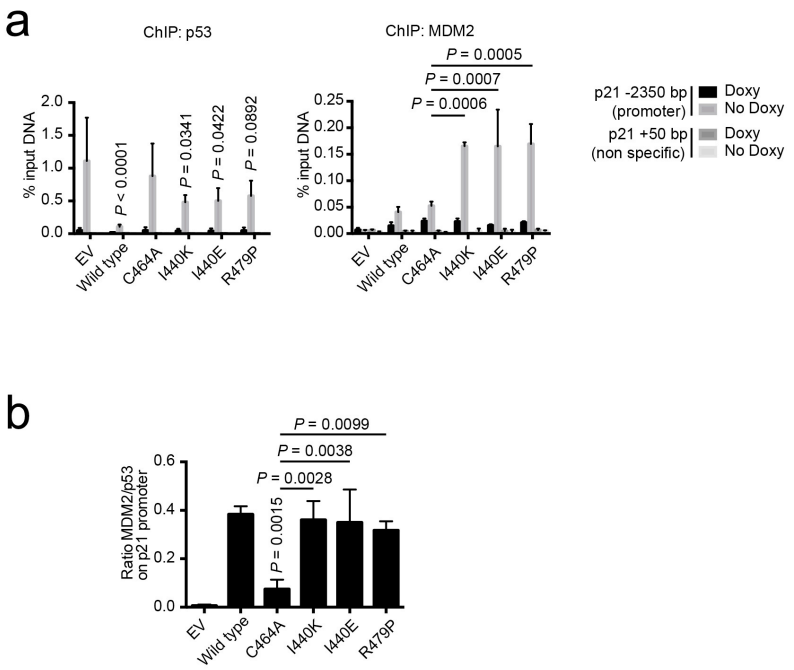

Figure 4-6: MDM2 I440 and R479 mutants localise on the *p21* promoter with p53

(a) ChIP for p53 and MDM2 with quantitative PCR for a p53 response element in the *p21* promoter (-2350 bp) and a non-specific binding region (+50 bp). *P* values (two-way ANOVA with Tukey's *post hoc* test): vs. EV (ChIP: p53), vs. C464A (ChIP: MDM2). *F* (5, 15) = 2.92 (ChIP:p53) and *F* (5, 15) = 8.69 (ChIP:MDM2) (b) Ratio of MDM2/p53 on the *p21* promoter based on the ChIP (Figure 4-6a, p21 -2350 No Doxy). MDM2 wild type, MDM2 I440 and R479 mutants were found at the *p21* promoter with p53. *P* values (one-way ANOVA with Tukey's *post hoc* test): vs. wild type (vertical), vs. C464A (horizontal). $F(5, 12) = 17.04$. Error bars indicate mean ± SD. *n* = 3 independent experiments (each with 2 technical replicates).

4.1.4 Effect of the MDM2 mutants on other p53 target genes

In addition to the induction of p53 target genes that involved in cell cycle regulation, the induction of other p53 target genes was also investigated. These included *TIGAR*, *PHLDA3*, *SESTRIN1*, *SESTRIN2*, *XPC* and *DRAM* - genes that are believed to be induced upon repairable stress - and *PIG3*, *PUMA*, *BAX* and *FAS* that are believed to be induced upon non-repairable stresses (discussed in Chapter 1 Sections 1.2.3 and 1.2.4). In addition to p53 target genes involved in cell cycle regulation, control of expression of these p53 target genes would also be necessary to allow normal cell growth and metabolism in normal unstressed cells.

Similar to the regulation of p21 induction, expression of the p53 target proteins TIGAR, PIG3 and BAX was attenuated by the expression of wild type MDM2 and MDM2 I440 and R479 mutants but not by the expression of MDM2 C464A mutant (Figure 4-7a). Similarly, expression of MDM2 I440 mutants (but not MDM2 C464A mutant) significantly attenuated mRNA induction of the expression of p53 target genes including *TIGAR*, *PHLDA3*, *SESTRIN2*, *PIG3*, *PUMA*, *BAX* and *FAS* (Figure 4-7b). Although similar patterns were observed in the induction of *SESTRIN1*, *XPC* and *DRAM*, no significance differences were observed between samples, even comparing *MDM2* knockout with MDM2 wild type (Figure 4-7b).

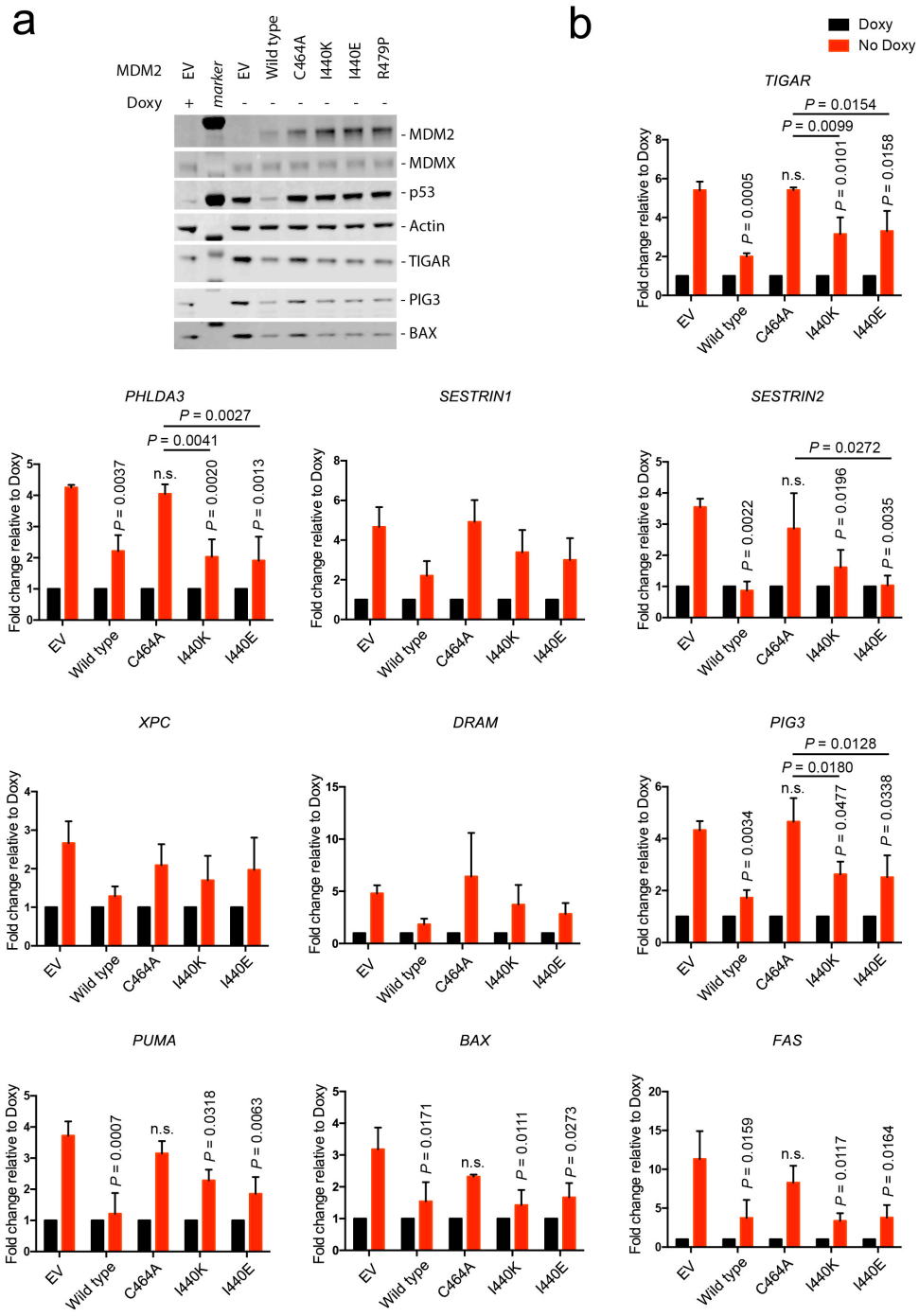

Figure 4-7: Effect of the expression of MDM2 mutants on other p53 target genes

(a) Western blot analysis showing that although MDM2 I440K, I440E and R479P do not degrade p53, induction of TIGAR, PIG3 and BAX is attenuated by these mutants. (b) qPCR showing mRNA expression of p53 target genes is attenuated by MDM2 I440K, I440E but not by C464A. *P* values (one-way ANOVA with Tukey's *post hoc* test): vs. EV (No Doxy) (vertical), vs. C464A (No Doxy) (horizontal). "n.s." indicates not significant vs. EV (No Doxy). *F* (4, 10) = 16.80 (*TIGAR*), *F* (4, 10) = 16.16 (*PHLDA3*), *F* (4, 10) = 5.76 (*14.3.3σ*), *F* (4, 10) = 11.16 (*SESTRIN2*), *F* (4, 10) = 12.11 (*PIG3*), *F* (4, 10) = 12.48 (*PUMA*), *F* (4, 10) = 6.35 (*BAX*) and *F* (4, 10) = 7.14 (*FAS*). Error bars indicate mean ± SD. *n* = 3 independent experiments each.

4.1.5 Effect of the MDM2 mutants on cell growth

As MDM2 the I440 and R479 mutants are able to limit p53 activity, I examined the effect of the expression of these MDM2 mutants on cell proliferation. In the absence of p53 (with doxycycline), all samples grow similarly (Figure 4-8). This reflects the fact that p53 target genes expression and cell cycle profile are similar between samples in the absent of p53 as shown above. In the presence of p53 (no doxycycline), cells expressing no MDM2 stopped growing quickly due to uncontrolled p53 (Figure 4-8). Re-expression of wild type MDM2 rescued this repression by controlling p53 target genes expression; similar levels to cells expressing no p53 (Figure 4-8). Expression of MDM2 C464A mutant significantly rescued cell growth compared with cells expressing no MDM2, indicating that MDM2 C464A mutant is not completely inactive (Figure 4-8). However, this growth rescue level was significantly lower than cells expressing wild type MDM2 (Figure 4-8). Despite not targeting p53 for degradation, the ability of the MDM2 I440 or R479 mutants to restrain p53 activity was sufficient to allow robust proliferation of these cells, demonstrating that repression of p53 dependent transcription by MDM2 is sufficient to allow cells to grow in unstressed conditions.

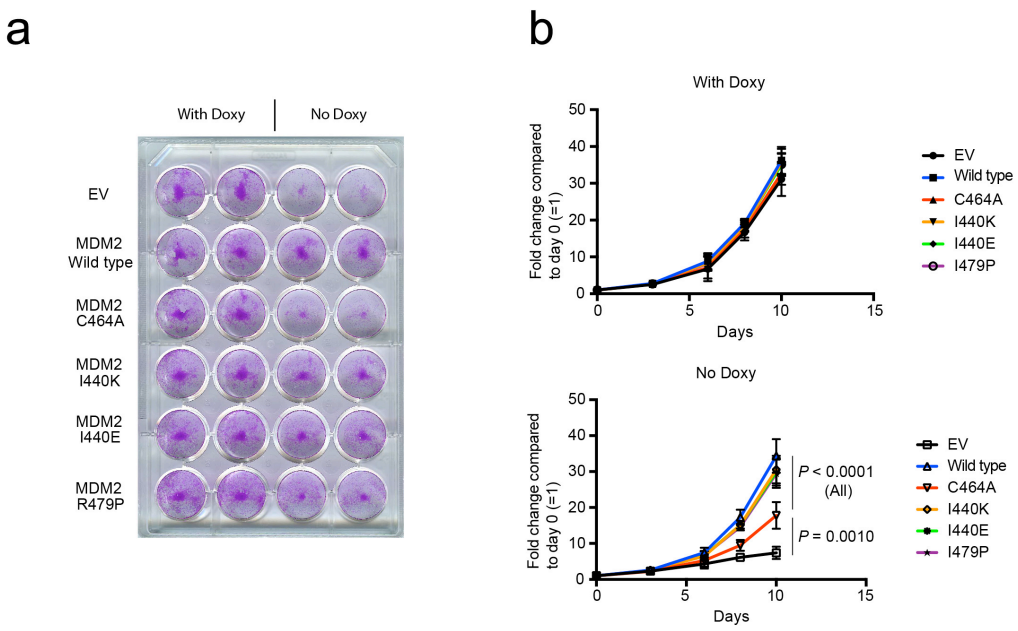

Figure 4-8: Effect of the expression of MDM2 mutants on cell growth

The inhibition of cell growth seen following restoration of p53 by removal of doxycycline (Doxy) in *MDM2* knockout cells was rescued by expressing MDM2 wild type, I440 and R479 mutants. P values (two-way ANOVA - main effect of mutants): vs. C464A. $F(5, 60) = 41.74$ (No Doxy, main effect of mutants). Error bars indicate mean ± SD. *n* = 3 independent experiments.

4.2 MDM2 I440 and R479 mutants render cells stress sensitive

So far, I have shown that MDM2 I440 and R479 mutants retain the ability to limit p53 transcriptional activity and allow cell proliferation, despite the high endogenous p53 level under normal unstressed condition.

Under stress condition, cells expressing wild type MDM2 accumulate p53 by inactivating MDM2, followed by the activation of target genes to induce cell cycle arrest or apoptosis. However, as cells expressing MDM2 I440 or R479 mutants have already elevated level of p53, they may be more stress sensitive and respond quicker than cells expressing wild type MDM2. In order to test this hypothesis, several chemicals that dissociate p53-MDM2 interaction were used to observe the stress responses in cells expressing different MDM2 mutants.

4.2.1 Dissociation of p53 and MDM2

Phosphorylation of N-terminal residues of p53 dissociates the interaction between p53 and MDM2. Although it had been reported that low dose (<5 nM) of actinomycin D (ActD) inactivates MDM2 through induction of ribosomal proteins, a higher dose of ActD induces phosphorylation of the N-terminal of p53 including serine 15 and serine 20, similar to the response to doxorubicin treatment (Figure 4-9, also shown in (Choong et al., 2009, Chen et al., 2014)). Nutlin-3, on the other hand, physically dissociates interactions between p53 and MDM2 by binding to the p53-binding domain of MDM2, without a requirement for phosphorylation of the N-terminal residues of p53.

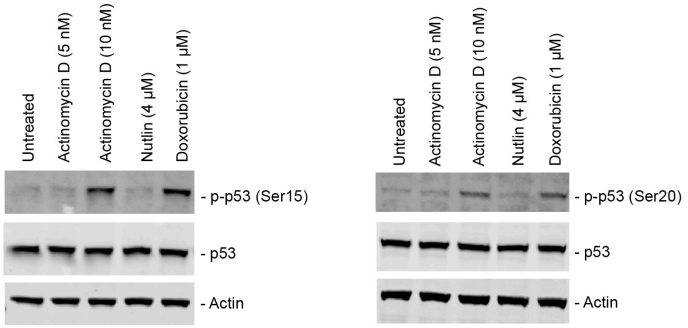

Figure 4-9: Phosphorylation of p53 by chemical treatments

***MDM2* knockout cells were treated with indicated drugs for 4 hours and phosphorylated p53 (serine 15 and serine 20) are analysed by western blot.**

4.2.2 Regulation of p53 target genes expression upon stress

To determine how the p53 stress response is influenced by E3 inactive MDM2 mutants I440 or R479, I treated cells described above with 10 nM ActD, which leads to the phosphorylation of N-terminal residues of p53, so resulting in loss of MDM2 binding.

An 18 hours treatment of ActD treatment did not further increase the expression of p53 target genes *p21*, *FAS* and *TIGAR* in cells lacking *MDM2* or cells expressing the MDM2 C464A mutant, suggesting that p53 activity is already maximally induced in these cells (Figure 4-10). This is consistent with the complete loss of p53 regulating activity, as shown above. Although cells expressing wild type MDM2 showed an induction of p53 target genes *p21*, *FAS* and *TIGAR* upon ActD treatment, at this time point the expression of these genes remained lower compared to cells lacking *MDM2* or expressing MDM2 C464A mutant (Figure 4-10). In contrast, cells expressing MDM2 I440K, I440E and R479P rapidly increased mRNA induction level of p53 target genes similar to cells lacking MDM2 or expressing MDM2 C464A mutant upon ActD treatment. This expression level was significantly higher than cells expressing wild type MDM2 (Figure 4-10).

Taken together, cells expressing MDM2 I440 or R479 mutants responded more robustly to a treatment of ActD compared to cells expressing wild type MDM2, leading to a higher expression of p53 target genes.

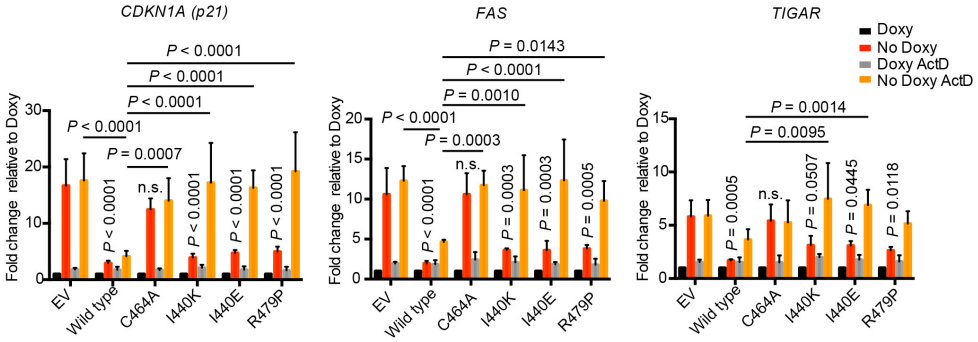

Figure 4-10: Cells expressing MDM2 I440 or R479 mutants can quickly induce p53 target genes upon stress

qPCR showing that expression of the indicated p53 target genes is attenuated by MDM2 I440K, I440E and R479P, and induced more strongly than in cells expressing wild type MDM2 following 18 hours treatment with actinomycin D (10 nM). *P* values (two-way ANOVA with Tukey's *post hoc* test): vs. EV (No Doxy) (vertical), vs. wild type (No Doxy ActD) (horizontal). "n.s." indicates not significant vs. EV (No Doxy). *F* (15, 36) = 5.72 (*CDKN1A (p21)*), *F* (15, 36) = 2.75 (*TIGAR*) and *F* (15, 36) = 4.23 (*FAS*). Error bars indicate mean ± SD. *n* = 3 independent experiments.

4.2.3 Time course study of the stress response

To investigate how quickly the cells expressing MDM2 mutants are able to respond to induce p53 target genes upon stress, I treated cells with ActD for 0, 6, 24, 48 or 72 hours.

As expected, ActD treatment leads to a stabilisation of p53 in cells expressing wild type MDM2, but did not affect the already stable and therefore higher p53 levels in cells expressing the E3 defective MDM2 I440K, I440E, R479P or C464A mutants (Figure 4-11). A time course of the p53 response showed cells expressing MDM2 I440 or R479 have a more rapid increase in expression of p53 target genes p21 and PIG3 in response to ActD treatment compared to a more gradual increased seen in cells expressing wild type MDM2 (Figure 4-11). This is likely to be due to the fact that p53 needs to accumulate in wild type MDM2 cells to induce a full p53 response. By contrast, p53 is already present at high levels in mutant MDM2 expressing cells and therefore only needs to be de-repressed. Interestingly, MDMX level was decreased upon ActD treatment in a time dependent manner, suggesting that ActD treatment could change

ubiquitination target of MDM2 from p53 to MDMX, as discussed in Chapter 3 (Figure 4-11a).

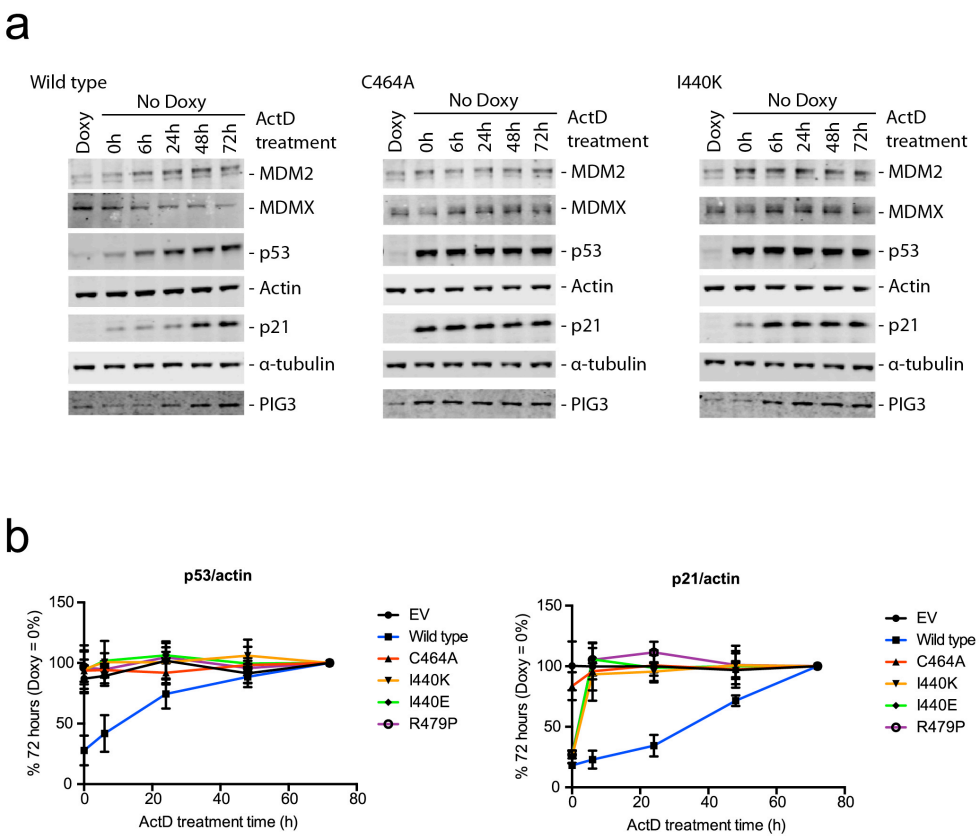

Figure 4-11: Time course study of ActD treatment in cells expressing MDM2 mutants

(a) Examples of immunoblots and (b) quantification of replicate blots showing that p21 and PIG3 are more rapidly induced in cells expressing MDM2 I440 and R479 mutants upon actinomycin D (10 nM) treatment compared to cells expressing wild type MDM2. Error bars indicate mean ± SD. *n* = 3 independent experiments.

Similarly, p21 level was quickly elevated in cells expressing MDM2 I440 or R479 mutants following the treatment with two other inhibitors of the p53-MDM2 interaction – nutlin-3 (Figure 4-12a) and doxorubicin (Figure 4-12b), indicating that cells expressing these mutants can rapidly respond to stress.

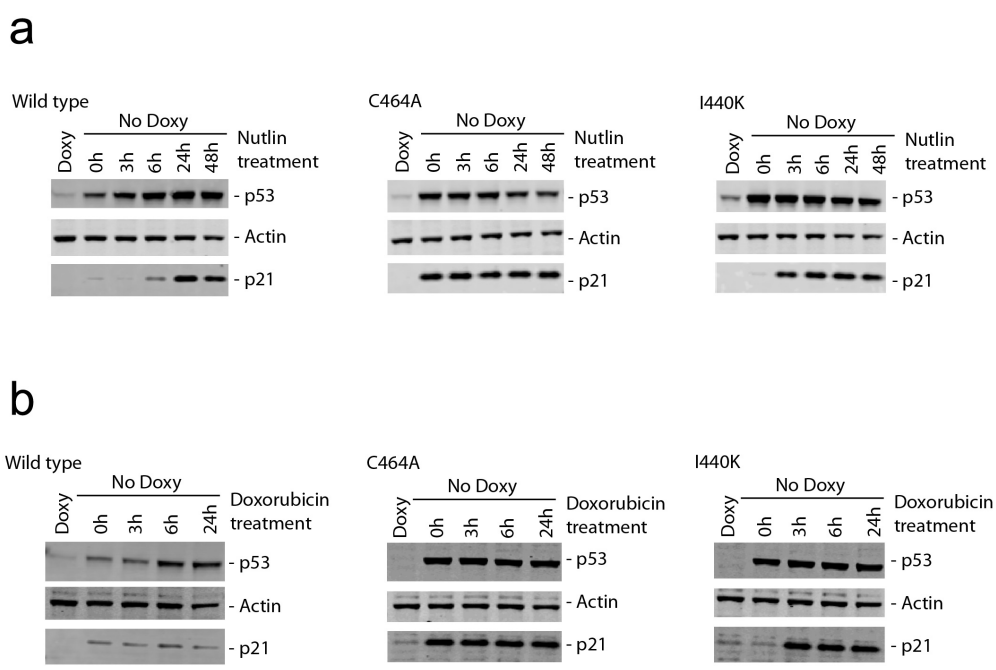

Figure 4-12: Time course study of nutlin-3 or doxorubicin treatment in cells expressing MDM2 mutants

Examples of immunoblots showing that p21 is more rapidly induced in cells expressing MDM2 I440K mutant upon (a) nutlin-3 (4 μM) and (b) doxorubicin (1 μM) treatments compared to cells expressing wild type MDM2.

4.2.4 Cell cycle and growth regulation upon stress

As cells expressing the MDM2 I440 or R479 mutants show a more rapid induction of p53 target gene expression, I monitored cell cycle and cell growth upon stress in cells expressing these MDM2 mutants.

Consistent with the induction of p53 target gene expression, cells expressing MDM2 I440 or R479 mutants showed a more rapid induction of cell cycle arrest in response to ActD, nutlin-3 or doxorubicin treatment than cells with wild type MDM2 (Figure 4-13).

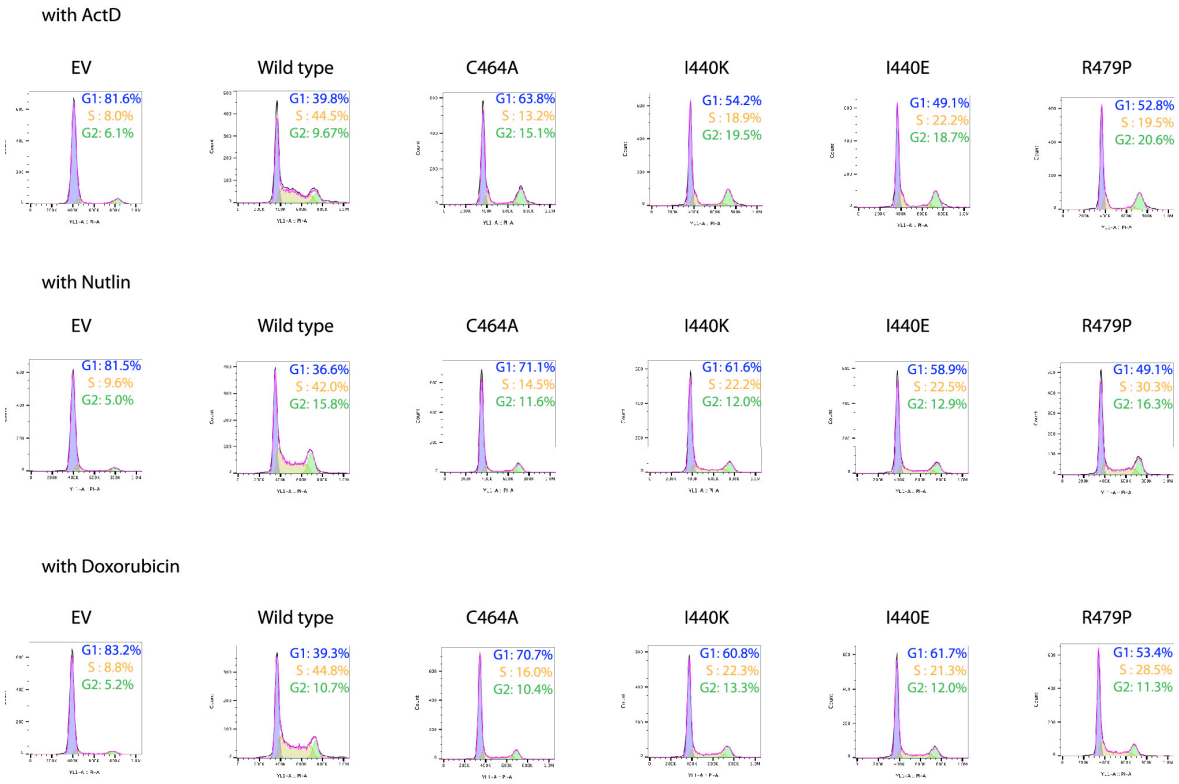

Figure 4-13: Cells expressing I440 or R479 mutants can quickly arrest cell cycle at the G_1 upon stress

Cells were treated with actinomycin D (10 nM) for 18 hours, nutlin-3 (4 μM) for 6 hours or doxorubicin (1 μM) for 6 hours. Cells were then stained with propidium iodine overnight and DNA content was analysed in channel FL2.

Reflecting the results shown above, cell growth was quickly arrested upon ActD treatment in cells expressing MDM2 I440 and R479 mutants (Figure 4-14). Without ActD treatment for 120 hours, cell growth was significantly attenuated following p53 expression in cells expressing no MDM2 or MDM2 C464A mutant compared to cells expressing wild type MDM2, whereas cells expressing I440 and R479 mutants did not affect in cell growth (Figure 4-14, also see Figure 4-8). Although 24 hours ActD treatment did not change this pattern of cell growth across samples (Figure 4-14), at 48-72 hours ActD treatment the cells expressing MDM2 I440 or R479 mutants showed a significantly greater attenuation of cell growth than those expressing wild type MDM2 (Figure 4-14).

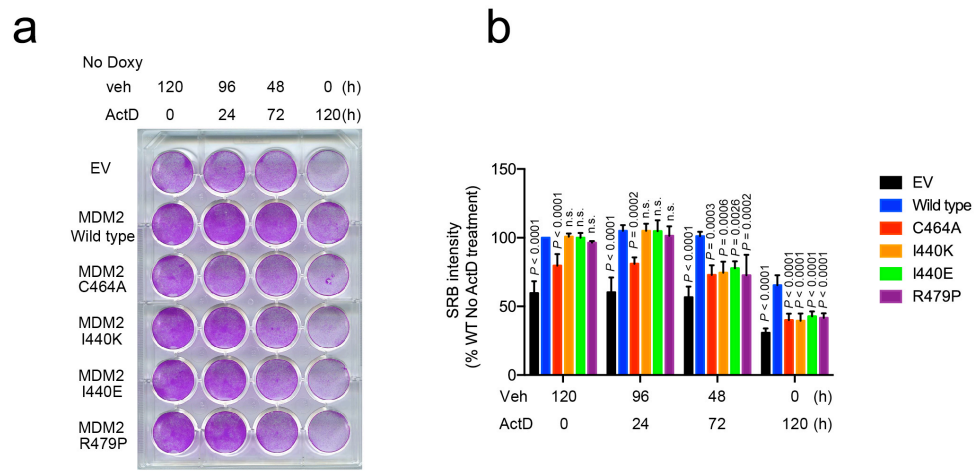

Figure 4-14: Effect of ActD treatment on cell growth in cells expressing MDM2 mutants

(a) The indicated cells were treated with vehicle or actinomycin D (10nM) for varying times, as shown, then were fixed and stained 120 hours after plating. Cells expressing MDM2 I440 or R479 mutants more rapidly attenuate cell growth in comparison to MDM2 wild type. (b) Quantification of cell growth experiments. SRB intensity was quantified using ImageJ software. P values (one-way ANOVA with Tukey's *post hoc* test): vs. each wild type. "n.s." indicates not significant. *F* (5, 24) = 50.50 (ActD 0h treatment), *F* (5, 24) = 35.76 (ActD 24h treatment), *F* (5, 24) = 14.39 (ActD 72h treatment) and *F* (5, 24) = 30.38 (ActD 120h treatment). Error bars indicate mean ± SD. *n* = 5 independent experiments.

In summary, although the MDM2 I440 or R479 mutants have lost their E3 ligase activity and do not promote p53 degradation, they are still able to limit p53 activity under normal unstressed condition. However, cells expressing these mutants accumulate high levels of p53 and are stress sensitive and can induce cell growth inhibition more rapidly than cells expressing wild type MDM2.

4.3 Regulation of p53 activity by MDM2 that do not dimerise

As discussed above, the MDM2 C464A mutant has disrupted RING domain and has reduced ability to limit p53 transcriptional activity. In order to test whether RING domain or ability to dimerise through RING domain is required to attenuate p53 activity, I generated cell line that express MDM2 lacking the RING domain (MDM2 ΔRING) or express MDM2 dimerisation-impaired mutant (MDM2 C449N-T488V double mutant).

4.3.1 MDM2 Δ RING cannot limit p53 activity

MDM2 ΔRING is unable to ubiquitinate p53 as RING domain is required for its catalytic activity. In order to test whether MDM2 ΔRING limits p53 activity, endogenous *MDM2* (in inducible p53 knockdown cells as described previously, Figure 4-1) was disrupted by CRISPR/Cas9 targeted the RING domain.

Targeted disruption of the MDM2 RING domain resulted in the expression of a truncated MDM2 protein (MDM2 1-430 with 4 additional amino acids) (Figure 4-15).

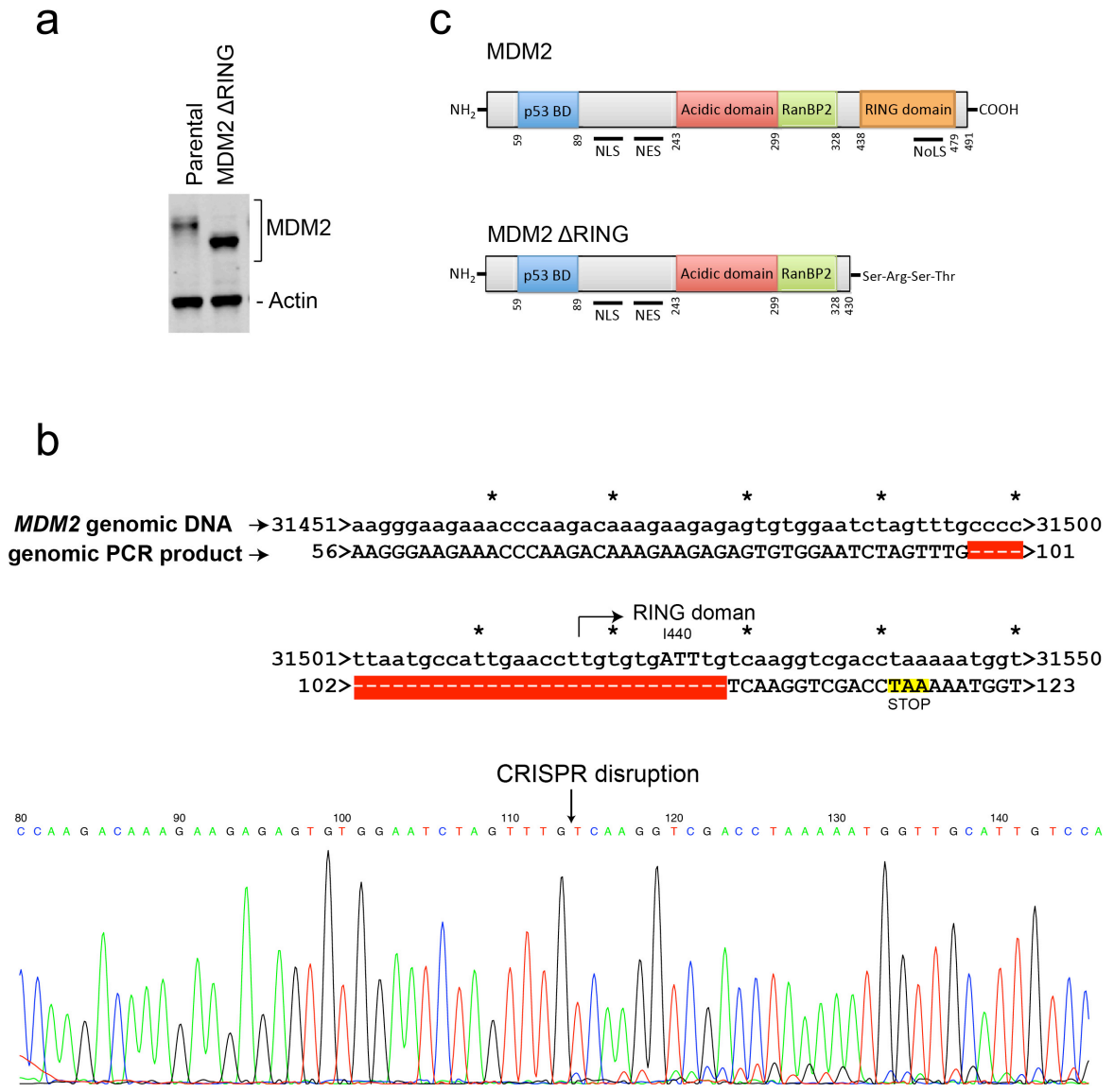

Figure 4-15: Generation and validation of *MDM2 Δ RING* mutant

***MDM2* was disrupted by CRISPR on inducible p53 knockdown cell line described previously. (a) Western blot showing CRISPR disruption (target RING domain) resulted in producing lighter molecular weight MDM2. (b,c) Genomic PCR followed by sequencing confirmed that CRISPR disruption (target RING domain) produced MDM2 ΔRING domain (1-430).**

Interestingly, MDM2 ΔRING is able to bind to p53 when co-immunoprecipitated with cell lysate similarly to MDM2 C464A (Figure 4-16a). Therefore, it is likely that MDM2 possessing the p53-binding domain can bind to p53 in solution, although this interaction was not maintained at the *p21* promoter for MDM2 C464A as shown above (Figure 4-6). As expected, although MDM2 ΔRING can bind to p53, this was unable to limit p21 induction (Figure 4-16b).

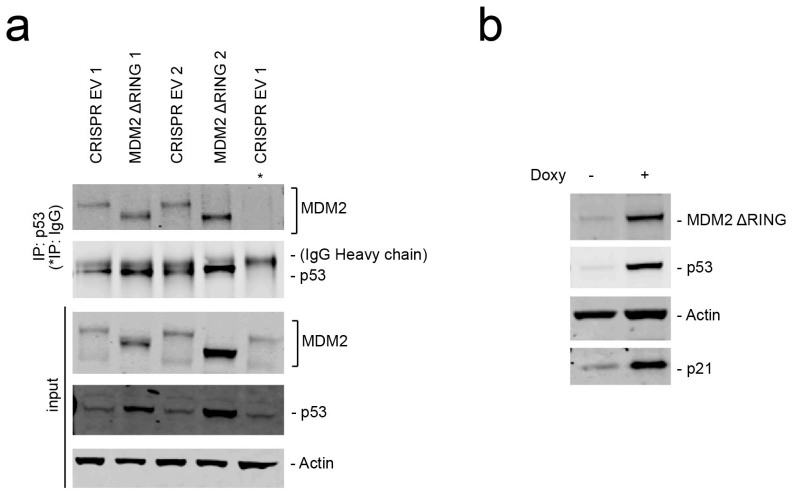

Figure 4-16: MDM2 ΔRING can bind to p53 but cannot limit p53 activity

(a) Co-immunoprecipitation result showing that MDM2 ΔRING can bind to p53. (b) Western blot analysis showing that MDM2 ΔRING does not degrade p53 and cannot limit p21 induction.

4.3.2 Dimerisation-impaired MDM2 mutants cannot limit p53 activity

MDM2 dimerises through its RING domain and MDM2 C449N-T488V double mutant (DM) is unable to homo- and hetero-dimerise (as shown in Chapter 3). To investigate whether dimerisation is required to regulate p53 activity, I transfected MDM2 DM into the inducible p53 knockdown-*MDM2* CRISPR knockout cells (Figure 4-1, 4-3).

Unlike MDM2 I440 or R479, and like MDM2 C464A, MDM2 DM was unable to limit the induction of p53 target genes such as *p21*, *TIGAR* and *FAS* (Figure 4-17). This indicates that the MDM2 monomer is not functional in the regulation of p53.

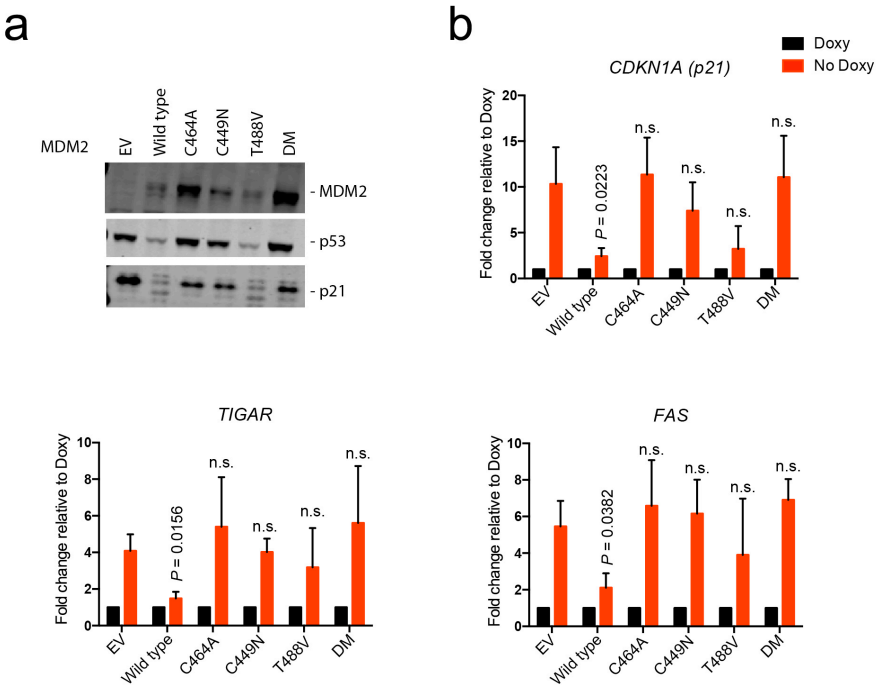

Figure 4-17: Dimerisation-impaired MDM2 mutants cannot limit p53 activity

(a) Western blot analysis showing that dimerisation-impaired MDM2 mutants cannot attenuate the induction of p21. (b) qPCR showing mRNA expression of p53 target genes cannot be attenuated by MDM2 mutants that do not dimerise. *P* values (one-way ANOVA with Tukey's *post hoc* test): vs. EV (No Doxy). *F* (5, 12) = 5.18 (*CDKN1A (p21)*), *F* (5, 12) = 3.80 (*TIGAR*) and *F* (5, 12) = 2.98 (*FAS*). Error bars indicate mean ± SD. *n* = 3 independent experiments each.

In summary, dimerisation-impaired MDM2 mutants, MDM2 ΔRING or C464A mutants are loss-of function mutants and unable to limit p53 transcriptional activity. This suggests that the integrity of MDM2 RING domain and the ability of MDM2 to dimerise through its RING domain are required to limit p53 transcriptional activity. Nonetheless they possess the p53-binding domain and are able to bind to p53 when co-immunoprecipitated with cell lysate. As shown before, MDM2 C464A mutant is unable to bind to p53 on the chromatin. Therefore, it is likely that MDM2 monomer is insufficient to localise on the chromatin with p53 to limit its transcriptional activity (discussed in Section 4.5).

4.4 Importance of MDMX to regulate p53 activity

As discussed above, MDM2 mutants that do not dimerise cannot limit p53 activity. Tollini *et al*. (2014) has also demonstrated that the ability of MDM2 to hetero-dimerise with MDMX is required during embryogenesis. These authors hypothesised that MDMX was an essential binding partner with MDM2 in the regulation of p53 activity. To test this hypothesis, MDM2-MDMX hetero-dimerisation was disrupted via concomitant deletion of MDMX by siRNA in cells expressing MDM2 I440K and R479 mutants.

Deletion of MDMX in cells expressing wild type MDM2 did not affect the regulation of p53 activity as active p53 can be degraded by MDM2 homo-dimer. Therefore, contribution of MDMX was unclear in the cells expressing wild type MDM2. Interestingly, although MDM2 I440K and R479P are able to limit p53 activity, this ability was significantly attenuated by knocking down of MDMX (Figure 4-18). The p21 mRNA expression was also significantly higher than that seen following MDMX depletion in cells expressing wild type MDM2 and similar to that seen in cells expressing MDM2 C464A (Figure 4-18).

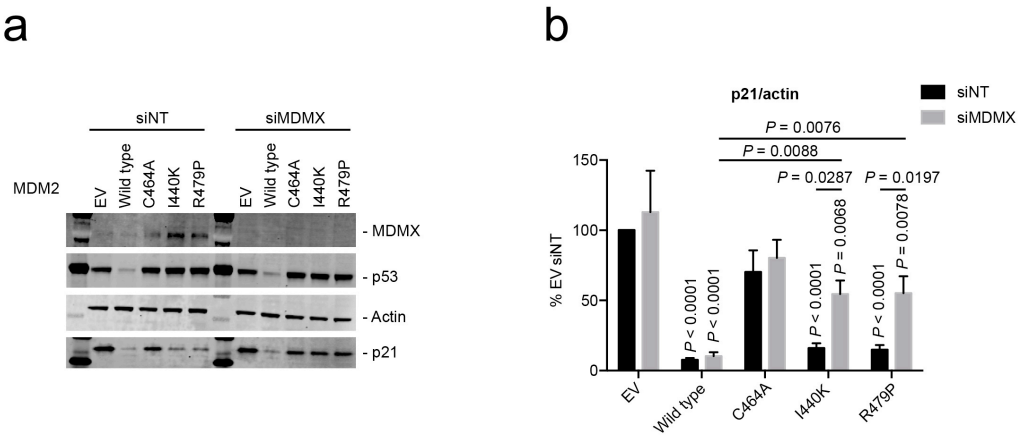

Figure 4-18: Effect of MDMX knockdown in cells expressing MDM2 I440K or R479P mutants

Cells were transfected with MDMX siRNA or control siRNA for 48 hours. (a,b) Western blot analysis showing that although MDM2 I440K and R479P mutants can limit p21 induction, they cannot limit this in the absence of MDMX. siNT = non-targeted siRNA, siMDMX = siRNA for MDMX. *P* values (one-way ANOVA with Tukey's *post hoc* test): vs. EV (siNT) (vertical), vs. C464A (siMDMX) or vs. corresponding siNT vs. siMDMX (horizontal). Error bars indicate mean ± SD. *F* (9, 20) = 29.32. Error bars indicate mean ± SD. *n* = 3 independent experiments each.

These results suggest that MDMX plays an important role in the regulation of p53 activity. It is possible that the importance of the dimerisation activity of MDM2 reflects a requirement to dimerise with MDMX, which is a cytoplasmic protein that requires dimerisation with MDM2 for nuclear translocation. Once in the nucleus, the MDMX-MDM2 hetero-dimer may be the key in attenuating the p53 transcriptional activity.

4.5 Summary and discussion

Previous studies examining the E3 activity of MDM2 were largely based on the analysis of MDM2 C464A (or C462A in mouse), a mutant that disrupts the Zn^{2+}-coordination and abolishes the RING domain fold (Itahana et al., 2007, Honda et al., 1997, Kubbutat et al., 1999, Geyer et al., 2000). It is therefore not clear whether failure of this mutant (or the mouse equivalent) to control p53 (Itahana et al., 2007) reflects a loss of E3 function, a loss of dimerisation or a failure to bind to p53 at promoters.

In order to answer this question and to investigate whether MDM2 I440 or R479 mutants can limit p53 activity in an E3 ligase independent manner, I developed a novel cell line to monitor the regulation of endogenous p53 by MDM2 mutants.

As shown above, MDM2 I440 and R479 mutants can repress the induction of a number of p53 target genes despite the high endogenous p53 level in cells. Although I showed that these mutants bind to p53 when co-immunoprecipitated in solution (as shown in Chapter 3), this could not fully explain why these mutants are able to limit p53 activity, because MDM2 C464A mutant can also bind to p53 in the same assays. Therefore, in order to understand the underlying mechanisms through which MDM2 I440 and R479 but not C464A can limit p53 activity, I performed chromatin immunoprecipitation and showed that MDM2 I440 or R479 but not C464A can be co-localised on *p21* promoter (via p53). This retention of binding to p53 at the promoter correlates with the ability of these MDM2 mutants to control the p53 transcriptional activity. An outstanding question is why MDM2 C464A retains the ability to bind p53 in solution but shows a weaker affinity to chromatin-bound p53. One possibility is that MDM2 C464A has a lower affinity for p53, which only become apparent under conditions where p53 is bound to chromatin. Alternatively, other proteins are required to

stabilise the MDM2-p53 interaction on chromatin, but are not recruited by MDM2 C464A. A recent study demonstrated that Mdm2 C462A (the mouse equivalent of human MDM2 C464A) enhances the acetylation of p53 and promotes p53 transcriptional activity, possibly through the augmentation of the interaction between p53 and acetyl-transferases (Tian et al., 2017). While not established, it is possible that this increase in acetylation weakens the p53-MDM2 interaction. Clearly, further experiments will be required to reveal the mechanisms underlying how MDM2 regulates p53 transcriptional activity in an E3 ligase activity independent manner.

Nevertheless, transcriptional repression by MDM2 I440 and R479 mutants is sufficient to keep p53 in check to allow proliferation, but renders cells hyper-sensitive to stressed conditions. Interestingly, MDM2 C464A also retains some effect on cell growth and modestly limits the induction of p53 target genes including *p21*, potentially reflecting the ability of this mutant to bind p53 when co-immunoprecipitated with cell lysate as shown in Chapter 3.

These findings confirm that MDM2 dependent transcriptional repression is sufficient to control p53 activity in unstressed cells, most likely reflecting a function of MDM2 as a transcriptional repressor when bound to p53. While MDM2 can repress transcription by ubiquitinating histones within promoters (Minsky and Oren, 2004), the activity I described here is independent of MDM2 E3 ligase activity.

The results also suggest that the ability of the RING domain of MDM2 to bind MDMX is required to limit p53 activity, as MDM2 I440 and R479 can no longer limit p53 activity in the absence of MDMX. Tollini *et al.* (2014) also demonstrated that the ability of an MDM2 C-terminal tail mutant to limit p53 activity is dependent on MDMX, although in this case the heterodimer of an MDM2 C-terminal mutant with MDMX should be catalytically active and degrade p53. Therefore, this study did not clarify whether the limitation of p53 activity is E3 ligase activity dependent or independent. In the work presented here, it is clear that heterodimers of MDM2 I440 or R479 with MDMX do not have E3 ligase activity (as shown in Chapter 3). Therefore, my results suggest that the ability of MDM2 to limit p53 activity is independent of its E3 ligase activity, but that this E3 independent activity can be dependent on MDMX. Again, further experiments

will be required to reveal the contribution of MDMX in the regulation of p53 activity.

A number of drugs targeting MDM2 E3 ligase activity - identified by screening for the inhibition of MDM2 auto-ubiquitination - have been developed (discussed in Chapter 1 Section 1.5.1.2) (Yang et al., 2005, Roxburgh et al., 2012, Sasiela et al., 2008). However, detailed mechanisms regarding how they function are yet to be revealed. As discussed above, only a small molecule that dissociates MDM2 and the E2–ubiquitin complex interaction will behave like MDM2 I440 and R479 mutants, whereas other strategies - such as disruption of the RING domain co-ordination or targeting dimerisation – are more likely to completely prevent regulation of p53 by MDM2 and so will behave like nutlin-3. For example, HLI98 was identified as an inhibitor of the E3 ligase activity of MDM2, but these compound results in the activation of p53 activity (Yang et al., 2005). *In silico* docking model (from Professor Peter Fischer, University of Nottingham) suggests that this compound is likely to bind to the MDM2 dimerisation core and disrupt subunit interaction. As I have shown above, dimerisation-impaired MDM2 mutants do not degrade p53 but also cannot limit its activity, resulting in uncontrolled p53 activity.

Taken together, although the p53 level was elevated in cells expressing MDM2 I440 and R479 mutants, p53 activity can be limited by these mutants under normal unstressed condition. Due to accumulated p53, cells expressing these mutants can respond to stress quickly. Since tumours have elevated levels of stress, targeting the interaction between MDM2 and E2–ubiquitin complex, to reactivate wild type p53 in tumours could open up a new therapeutic window to drive p53-dependent arrest of cancer cell growth while potentially avoiding the deleterious on-target side effects of completely disrupting the MDM2-p53 interaction. Finally, the strategy presented here may be applicable for investigating E3 ligase-independent function of other RING E3s.

Chapter 5 Murine MDM2

5.1 Human MDM2 and Murine MDM2

Human MDM2 and murine MDM2 have the same functional domains (Figure 5-1a) and a high degree of amino acid similarity (overall 81.7 % homology), particularly from the RING domain to the C-terminal (amino acid 433 to 491 in human MDM2 and amino acid 431 to 489 in murine MDM2) that displays 96.6 % homology (Figure 5-1b).

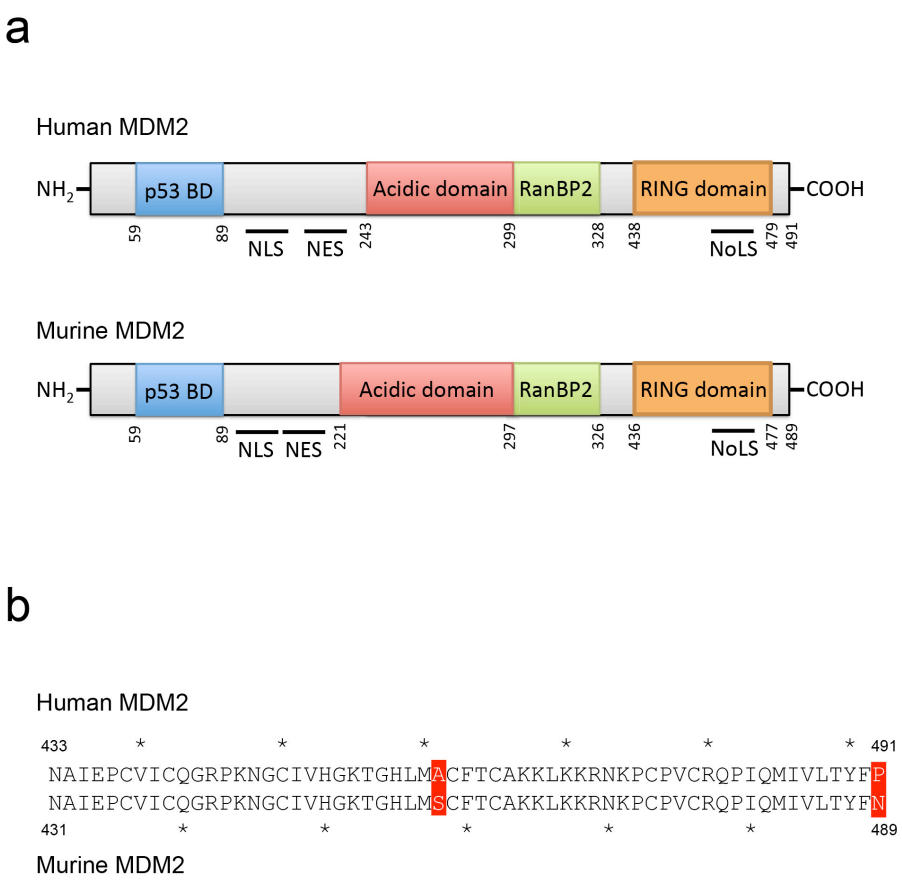

Figure 5-1: Human MDM2 and Murine MDM2

(a) Functional domains of human MDM2 and murine MDM2. Generated from UniProt Database (https://www.uniprot.org). (b) Amino acids of human MDM2 (amino acids 433-491) and murine MDM2 (amino acids 431-489) are shown. Red indicates the amino acids that are different between human and murine MDM2. p53 BD = p53-binding domain, RanBP2 = RAN binding protein 2 (RanBP2)-type zinc finger domain, NLS = nuclear localisation signal, NES = nuclear export signal and NoLS = nucleolar localisation signal.

In order to test whether the murine MDM2 RING domain shows the same function as human MDM2, I created equivalent mutations within the RING domain of murine MDM2 and then expressed these mutants along with murine p53 in primary mouse embryonic fibroblast cells (MEFs) to test the ability of the murine MDM2 mutants to degrade p53.

As expected, over-expression of wild type MDM2 led to significant degradation of murine p53, whereas over-expression of MDM2 I438K (I440K in human), I438E, R477P (R479P in human) and the C447N-T486V double mutant (C449N-T488V DM in human) did not promote degradation of murine p53 (Figure 5-2). Like these mutations in human MDM2 (Chapter 3), these murine mutant equivalents are also catalytically inactive.

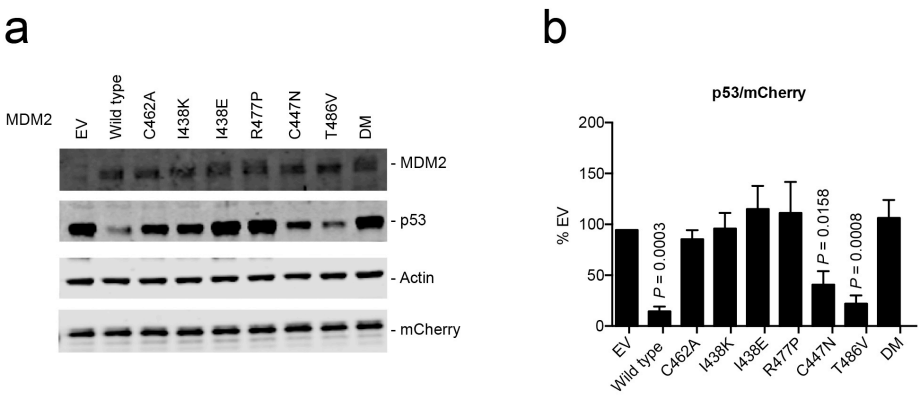

Figure 5-2: Effect of human-corresponding MDM2 mutation in murine cells

Primary MEFs were transiently transfected with combinations of plasmid vectors encoding murine p53, mCherry, and wild type MDM2 or the indicated MDM2 mutants for 24 hours. (a,b) p53 degradation assay showing that MDM2 mutants I438K, I438E, R477P and C447N-T486V double mutant (DM) do not promote degradation of p53. *P* values (one-way ANOVA with Tukey's *post hoc* test): vs. EV. *F* (8, 18) = 18.02. Error bars indicate mean ± SD. *n* = 3 independent experiments.

Based on the results shown in Chapter 4, we generated a mouse expressing MDM2 I438K (MDM2 I440K in human), a mutant that has lost E3 ligase activity but can still regulate p53 transcriptional activity in normal unstressed cells and allows for a more rapid response to stress. Although this mutant was able to regulate p53 function in cultured cells, we considered the possibility that this catalytically inactive MDM2 mutant may cause embryonic lethality. To

circumvent this possibility, we generated a mouse harbouring a conditional *Mdm2* I438K allele. Depending on which Cre system is used, this mouse allows us to investigate the effect of *Mdm2* I438K whole body knock-in, conditional knock-in at specific stages of development and tissue-type/cell-type specific knock-in.

5.2 Generating a murine *Mdm2* I438K conditional point mutant allele

In collaboration with Dr Douglas Strathdee at the Cancer Research UK Beatson Institute, we designed and generated an inducible point mutation in the endogenous *Mdm2* gene (Ensembl ID: ENSMUSG00000020184). This novel allele expresses wild type MDM2, but switches to express MDM2 I438K (I440K in human) following Cre recombination. To achieve this, we decided to duplicate the last 2 exons and place a wild type version of exon 11/12 (termed 11A/12A) bracketed by loxP sites, upstream of the endogenous sequences. Isoleucine 438 on the original exon 12 was replaced with lysine (I438K) (Figure 5-3). Therefore, our targeted allele is expected to express wild type MDM2 (transcribed from exon 11A/12A). Following Cre-mediated recombination, however, the wild type *Mdm2* 11A/12A exons are removed and allow for expression of MDM2 I438K (transcribed from mutated original exon 11/12) (Figure 5-3).

To expedite the cloning and targeting procedure, we removed a short (359bp) intron between exon 11 and 12 (leaving a single exon in place of 11 and 12). In addition, we opted to remove the large 3' UTR in exon 12A, replacing this UTR with a heterologous poly-adenylation signal sequence (SV40 poly-adenylation signal sequence) (Figure 5-3). Therefore, it is possible that the expression level of the wild type *Mdm2* from 11A/12A might be slightly different from that of wild type *Mdm2* from its endogenous locus. Following Cre recombination, however, the expression level of the mutant *Mdm2* (I438K) should be similar to the endogenous locus since the original 3' UTR is restored in our mutant allele (Figure 5-3).

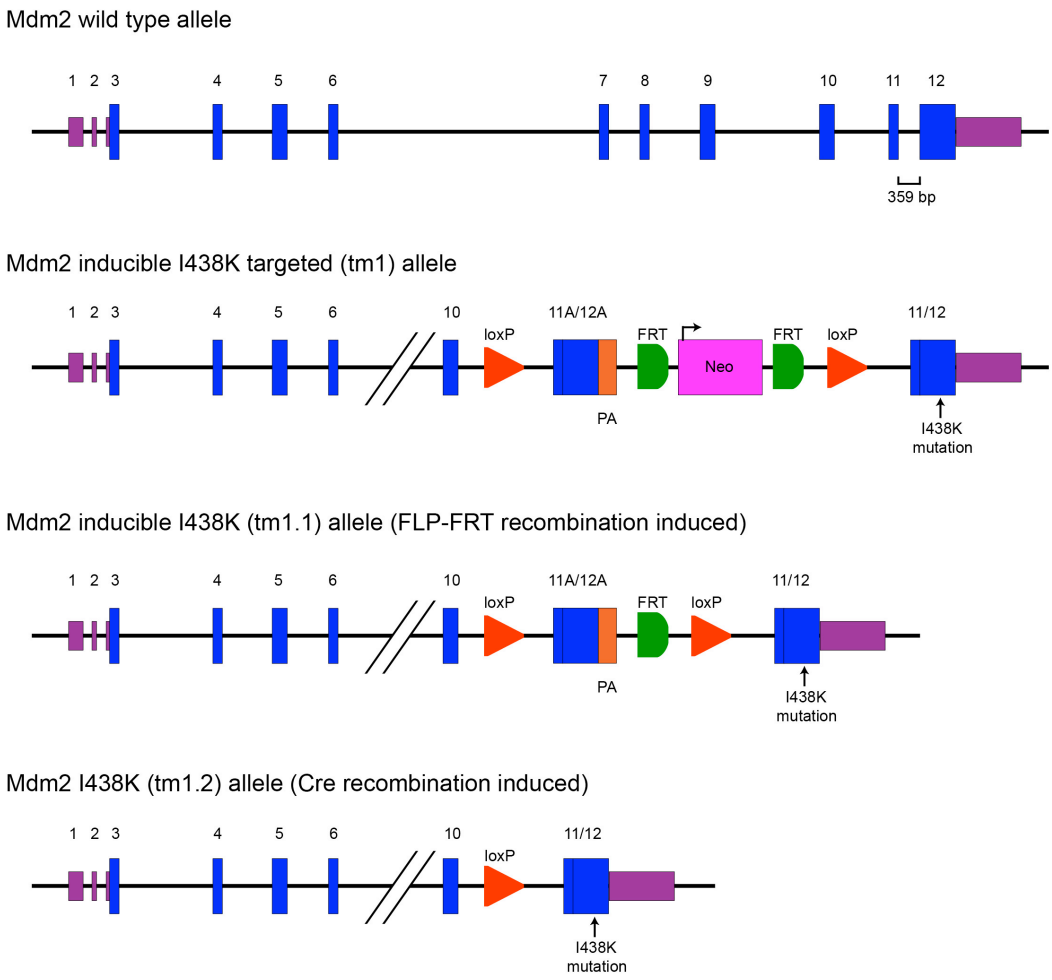

Figure 5-3: Generating a murine *Mdm2* I438K conditional point mutant allele

Numbers indicate exons. Blue boxes indicate the coding region and purple boxes indicate UTR. loxP = locus of X-over P1 site, PA = poly-adenylation signal sequence, FRT = flippase recognition target site and Neo = neomycin cassette.

Generation of the mouse strain carrying the *Mdm2* I438K targeted (tm1) allele (*Mdm2*$^{tm1a(exon12\ pt\ mut)Bea}$) was carried out by Dr Douglas Strathdee's group. Briefly, the targeting construct was transfected into HM1-embryonic stem (ES) cells (derived from 129P2/OlaHsd mice) where successful incorporation was confirmed by DNA screening to ensure that the vector was targeted correctly to the *Mdm2* locus. Cells from one of the successfully targeted clones were injected into the blastocoel cavity of mouse blastocysts (from C57BL/6J mice), which were then implanted into the uterus of a foster CD1-ICR albino mouse. A founder mouse born from this foster mother mouse carrying *Mdm2* inducible I438K targeted (tm1) allele (termed chimeric mouse) was crossed with a wild

type C57BL/6J mouse. Offspring from this mating that were genotyped as heterozygous for our *Mdm2* inducible I438K targeted allele (*Mdm2*$^{tm1/+}$) were subsequently used for *in vivo* experiments.

In order to prevent potential interference of the neomycin cassette on wild type *Mdm2* expression, we also generated mice carrying an *Mdm2* inducible I438K allele without the presence of a neomycin selection cassette (tm1.1) by excising the FRT (Flippase recognition target)-flanked neomycin using FLP (Flippase)-FRT site-directed recombination (Figure 5-3). Mice carrying the *Mdm2* I438K targeted allele (*Mdm2*$^{tm1/+}$) were crossed with mice carrying the *ACTB* (Actin beta) promoter-driven enhanced Flippase-expressing allele (*Tg*$^{(ACTFLPe)9205Dym}$, (Rodriguez et al., 2000)). Precise removal of the Neo cassette was verified by genotyping. Offspring mice carrying the FLP-FRT recombination-induced allele (*Mdm2*$^{tm1.1/+}$) were then crossed with wild type C57BL/6J mice to remove the Flippase-expressing allele. These mice are currently being used to produce mice carrying homozygous copies of the FLP-FRT recombination-induced *Mdm2* alleles (*Mdm2*$^{tm1.1/tm1.1}$).

These *in vivo* experiments are presently underway, but time constraints have not allowed me to complete all of the necessary crosses during the course of my PhD work. Anticipated future work with these mice is discussed in Section 5.3. In the meantime, I tested the effect of expression of our *Mdm2* I438K allele in murine cells *in vitro* by generating primary baby mouse kidney (BMK) and mouse embryonic fibroblast (MEF) cell lines from mice carrying the Mdm2 I438K alleles (tm1 in Figure 5-3).

5.2.1 Effect of *Mdm2* I438K mutant in BMK primary cells

Male and female mice, heterozygous for the *Mdm2* inducible I438K allele (*Mdm2*$^{tm1/+}$), were intercrossed to generate mice homozygous for the *Mdm2* inducible I438K alleles (*Mdm2*$^{tm1/tm1}$). 5-days-old baby mice from these matings were sacrificed to create primary BMK cell lines.

Genotyping identified BMK cells carrying wild type (*Mdm2*$^{+/+}$), heterozygous (*Mdm2*$^{tm1/+}$) or homozygous (*Mdm2*$^{tm1/tm1}$) copies of *Mdm2* inducible I438K

targeted alleles based on the difference (359 bp) of the intron between exons 11 and 12 (Figure 5-3) (Figure 5-4).

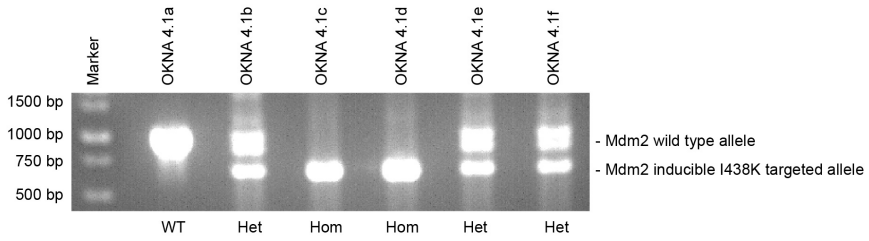

Figure 5-4: Genotyping of BMK primary cells

A piece of liver from baby mice was genotyped. DNA electrophoresis of PCR products; expected sizes are 1034 bp for *Mdm2* wild type allele and 675 bp for *Mdm2* inducible I438K targeted allele. WT = wild type, Het = heterozygous, Hom = homozygous.

BMK cells homozygous for the *Mdm2* inducible I438K targeted alleles (*Mdm2*$^{tm1/tm1}$) (OKNA 4.1c and 4.1d) and wild type alleles (*Mdm2*$^{+/+}$) (OKNA 4.1a) were then exposed to adeno-Cre for 24 hours and were used for experiments 5 days after adenovirus infection in order to minimise any effect of remaining wild type MDM2 protein in cells.

Western blotting results show that the expression level of p53 was the same between cells expressing wild type *Mdm2* (OKNA 4.1a, adeno-EV) and non-recombination-induced (*Mdm2*$^{tm1/tm1}$, expressing MDM2 wild type) cells (OKNA 4.1c and 4.1d, adeno-EV) (Figure 5-5a). Notably, the expression level of Mdm2 was also the same between these lines despite replacing the large 3' UTR in exon 12A with a poly-adenylation signal sequence. Even so, the p53 level was significantly increased in the recombination-induced (*Mdm2*$^{tm1.2/tm1.2}$, expressing MDM2 I438K mutant) cells (OKNA 4.1c and 4.1d, adeno-Cre), reflecting loss of MDM2 E3 ligase function in the *Mdm2* mutant cells (Figure 5-5a). Following 3 hours of nutlin-3 treatment in these cells, we observed increased p53 protein expression level in cells expressing wild type *Mdm2* but not in cells expressing *Mdm2* I438K mutant, suggesting that p53 was maximally induced. Although the

p53 level is very high in cells expressing *Mdm2* I438K mutant, the level of p21 protein was not elevated under normal condition in these cells. However, in response to nutlin-3, p21 levels rapidly increased (Figure 5-5a), suggesting that MDM2 I438K is sufficient to control p21 induction. In contrast to p21 levels, the MDM2 protein level (*Mdm2* is also a p53 target gene) was higher in cells expressing *Mdm2* I438K mutant compared to *Mdm2* wild type cells under normal condition (Figure 5-5a), although nutlin-3 treatment rapidly induced MDM2 protein expression in both cases (Figure 5-5a). This could indicate that auto-ubiquitination of MDM2 I438K was also attenuated, leading to the stabilisation (rather than increased expression) of this protein under normal conditions.

In order to confirm whether the MDM2 I438K mutant can control p53 target gene expression (both *p21* and *Mdm2*), I performed qPCR to observe changes in mRNA expression. As expected, mRNA levels of *p21* and *Mdm2* in cells expressing *Mdm2* I438K mutant were not significantly different to those seen in cells expressing wild type *Mdm2* (Figure 5-5b). In addition, treatment of the *Mdm2* I438K cells with nutlin-3 for one hour rapidly and significantly increased mRNA expression of *p21* and *Mdm2* relative to the levels expressed in treated *Mdm2* wild type cells (Figure 5-5b). Taken together, these results strongly suggest that although MDM2 I438K mutant has lost its E3 ligase activity, this mutant retains the ability to limit p53 transcriptional activity. Interestingly, mRNA expression of p53 target gene *Bax* was not induced upon nutlin-3 treatment in the *Mdm2* I438K-expressing cells (Figure 5-5b), suggesting that nutlin-3 primarily induces cell cycle arrest and that modifications of p53 such as phosphorylation may be required to induce the expression of p53 target genes involved in the induction of apoptosis.

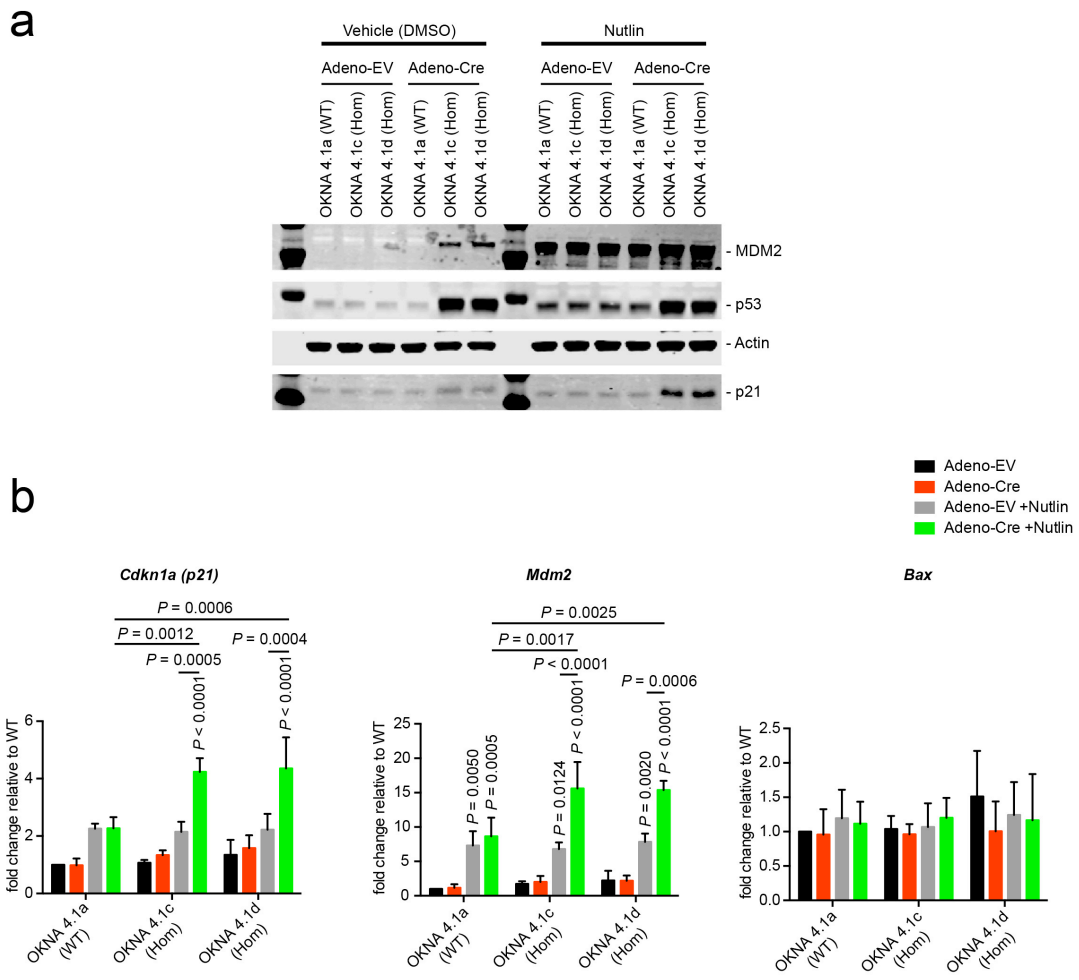

Figure 5-5: Effect of Cre recombination and nutlin-3 treatment in BMK primary cells

Recombination to induce mutant *Mdm2* expression was induced by exposing BMK primary cells to adeno-Cre (or an empty adenovirus for control) for 24 hours and treated with nutlin-3 (4 μM) for (a) 3 hours or (b) 1 hour, 5 days after adenovirus infection. (a) Western blot analysis showing expression of the indicated proteins. (b) qPCR showing mRNA expression of p53 target genes *p21*, *Mdm2* and *Bax*. *P* values (one-way ANOVA with Tukey's *post hoc* test): vs. wild type (vertical), vs. indicated samples (horizontal). *F* (11, 24) = 18.71 (*Cdkn1a (p21)*) and *F* (11, 24) = 29.37 (*Mdm2*). Error bars indicate mean ± SD. *n* = 3 independent experiments each.

BMK cells expressing either *Mdm2* wild type or *Mdm2* I438K were also treated with doxorubicin to observe their responses to induced DNA damage. In this system, we found that doxorubicin treatment for one hour rapidly and significantly induced *p21* and *Bax* in *Mdm2* I438K cells compared to cells expressing wild type *Mdm2* (Figure 5-6). Interestingly, although nutlin-3 treatment strongly induced *Mdm2* mRNA expression in the mutant cells, this was

not observed in cells treated with doxorubicin (Figure 5-6) suggesting a disruption of the p53-MDM2 negative feedback loop.

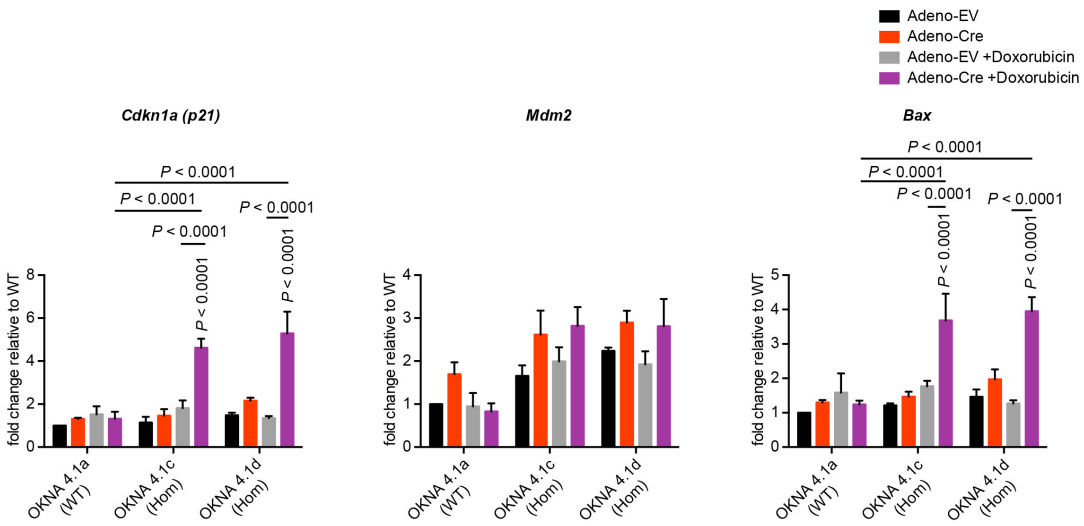

Figure 5-6: Effect of Cre recombination and doxorubicin treatment in BMK primary cells

Recombination to induce mutant MDM2 expression was induced by exposing BMK primary cells to adeno-Cre (or an empty adenovirus for control) for 24 hours and treated with doxorubicin (1 μM) for 1 hour, 5 days after adenovirus infection. qPCR showing mRNA expression of p53 target genes *p21*, *Mdm2* and *Bax*. *P* values (one-way ANOVA with Tukey's *post hoc* test): vs. wild type (OKNA 4.1a + adeno-EV) (vertical), vs. corresponding non-recombination-induced (expressing wild type MDM2) cells with doxorubicin treatment or vs. wild type (OKNA 4.1a + adeno-Cre) with doxorubicin treatment (horizontal). *F* (11, 24) = 40.14 (*Cdkn1a (p21)*), *F* (11, 24) = 14.08 (*Mdm2*) and *F* (11, 24) = 26.39 (*Bax*). Error bars indicate mean ± SD. *n* = 3 independent experiments each.

To assess the functional effect of mutant *Mdm2* expression, cell cycle analysis was carried out. As expected, cells expressing wild type *Mdm2* and *Mdm2* I438K showed similar cell cycle profiles under unstressed conditions, reflecting their ability to both control p53 activity (Figure 5-7). A short (8 hours) treatment of nutlin-3 or doxorubicin did not affect the cell cycle in cells expressing wild type *Mdm2* (Figure 5-7). In contrast, cells expressing the *Mdm2* I438K mutant quickly underwent a G_1 cell cycle arrest (Figure 5-7) consistent with more rapid induction of p53 target gene expression compared to *Mdm2* wild type cells (Figure 5-5, 5-6).

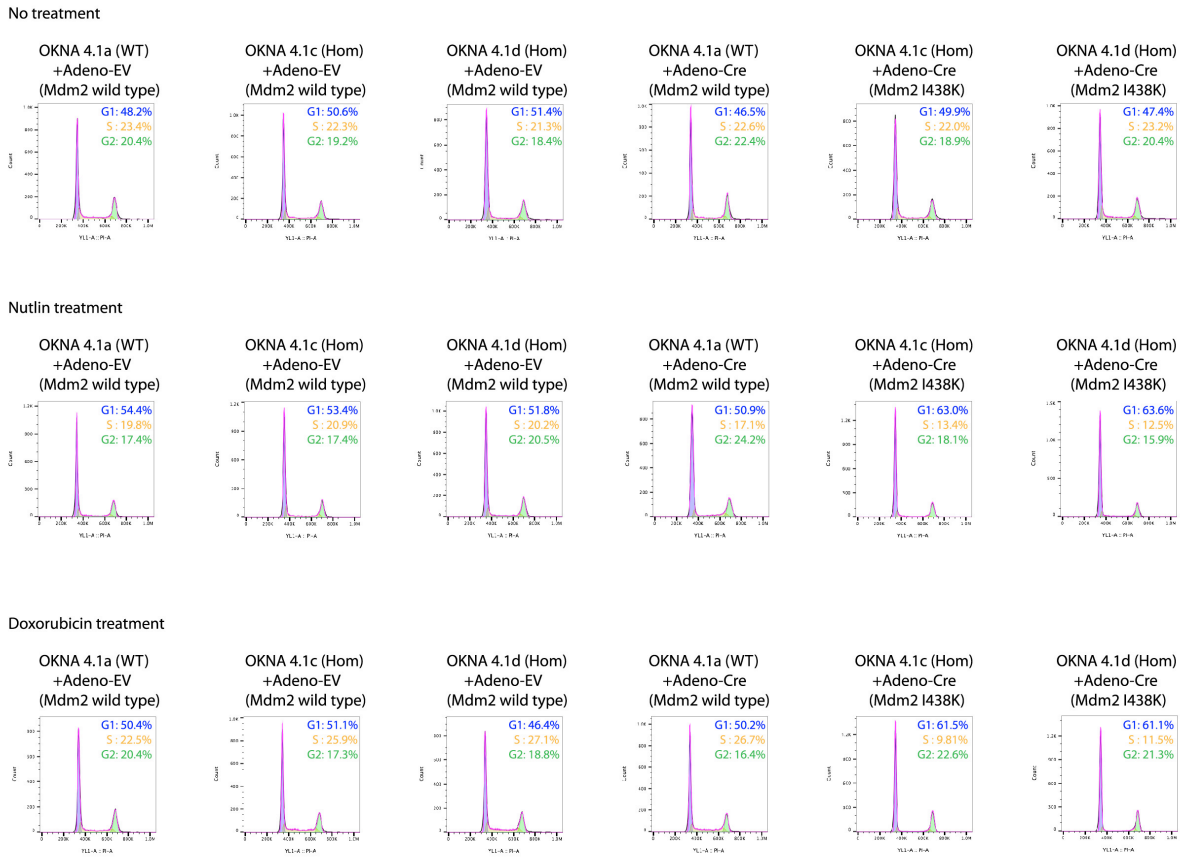

Figure 5-7: Cells expressing *Mdm2* I438K mutant can quickly arrest cell cycle at the G_1 upon stress

BMK primary cells were treated with nutlin-3 (4 μM) for 8 hours or doxorubicin (1 μM) for 8 hours, 5 days after adeno-Cre or adeno-EV infection. Cells were then stained with propidium iodine overnight and DNA content was analysed in channel FL2.

Taken together, these results show that MDM2 I438K behaves *ex vivo* as seen in cells, in that it does not promote degradation of p53 but can limit the induction of p53 target genes in normal unstressed condition and allows normal cell cycle progression. However, a more robust activation of p53 activity in response to nutlin-3 or doxorubicin was seen in the *Mdm2* 438K cells compared to cells expressing wild type *Mdm2*. These results are consistent with the model that E3 inhibition does not prevent MDM2 regulation of p53 under normal conditions, but allows for a stronger stress response.

5.2.2 Effect of inducible knock-in of *Mdm2* I438K mutant in MEFs

To examine the effect of *Mdm2* I438 expression *in vivo*, mice heterozygous for the *Mdm2* inducible I438K targeted allele (*Mdm2*$^{tm1/+}$) were crossed with mice carrying the *ROSA*-Cre-ER^{T2} (ubiquitous expression of the oestrogen receptor^{T2}-fusion Cre recombinase) (*Gt(ROSA)26Sor*$^{tm2(Cre/ERT2)Brn}$, (Hameyer et al., 2007)) allele. This will generate a 4-hydroxytamoxifen (4-OHT) inducible Cre recombination system in which the Cre-ER^{T2} fusion protein is sequestered by heat shock proteins (HSP) in the cytoplasm and translocated into the nucleus by binding to 4-OHT, where it exerts recombinase activity. As a breeding strategy offspring carrying a *ROSA*-Cre-ER^{T2} allele and heterozygous for the *Mdm2* inducible I438K targeted allele (*Mdm2*$^{tm1/+}$) were crossed with mice heterozygous for *Mdm2* inducible I438K targeted allele (*Mdm2*$^{tm1/+}$) without *ROSA*-Cre-ER^{T2} allele, as homozygous of *ROSA*-Cre-ER^{T2} alleles is toxic to the cell. 14 days after confirmed plugging (E14.5), female mice were sacrificed and MEFs were isolated from those embryos.

Genotyping targeted to detect the difference of the intron between exons 11 and 12, and the Cre recombinase, identified MEFs carrying wild type (*Mdm2*$^{+/+}$), heterozygous (*Mdm2*$^{tm1/+}$) and homozygous (*Mdm2*$^{tm1/tm1}$) copies of *Mdm2* inducible I438K targeted alleles with or without the *ROSA*-Cre-ER^{T2} allele (Figure 5-8).

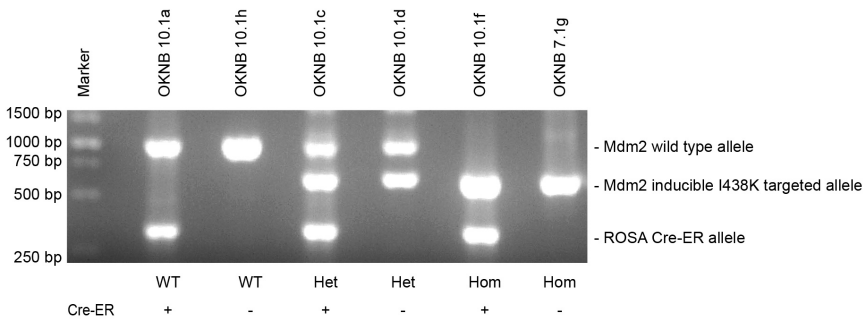

Figure 5-8: Genotyping of MEFs

A piece of E14.5 foetuses was genotyped. DNA electrophoresis of PCR products; expected sizes are 1034 bp for *Mdm2* wild type allele, 675 bp for *Mdm2* inducible I438K targeted allele and 353 bp for *ROSA*-Cre-ER^{T2} allele. WT = wild type, Het = heterozygous, Hom = homozygous.

MEFs homozygous for or wild type alleles with or without a copy of the *ROSA*-Cre-ER^{T2} allele were treated with 4-OHT to activate Cre recombinase (Figure 5-9). Western blotting showed that the level of p53 was rapidly increased upon 4-OHT treatment in *Mdm2*$^{tm1/tm1}$ MEFs carrying homozygous of *Mdm2* I438K targeted alleles (*Mdm2*$^{tm1/tm1}$) and the *ROSA*-Cre-ER^{T2} allele (OKNB 10.1f) (Figure 5-9b), whereas 4-OHT treatment itself (Figure 5-9a) or activation of Cre recombinase itself (OKNB 10.1a) (Figure 5-9b) did not affect p53 accumulation. MDM2 I438K protein was also accumulated upon 4-OHT treatment, reflecting the loss of auto-ubiquitination and increased stability of the MDM2 I438K protein, whereas p21 levels were not increased, showing that the MDM2 I438K mutant limits p53 transcriptional activity despite the high level of p53 in cells (Figure 5-9b).

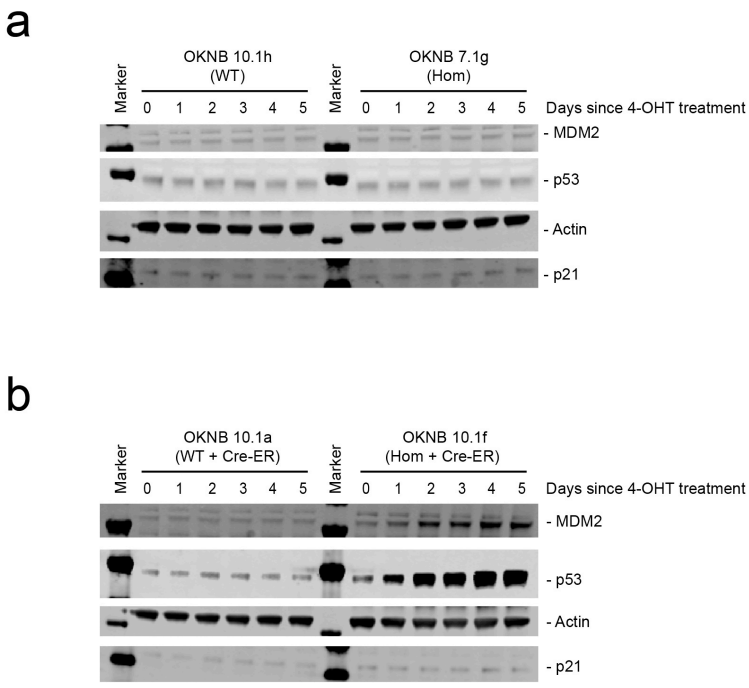

Figure 5-9: Effect of 4-OHT on inducible Mdm2 I438K knock-in system in MEFs

Cells were treated with 4-OHT (1 µM) for up to 48 hours (Day 0: no 4-OHT treatment, Day 1: 24 hours 4-OHT treatment, Day 2: 48 hours 4-OHT treatment, Day 3: 48 hours 4-OHT treatment followed by 24 hours discontinuation, Day 4: 48 hours 4-OHT treatment followed by 48 hours discontinuation and Day 5: 48 hours 4-OHT treatment followed by 72 hours discontinuation). Western blot analysis showing the expression of the indicated proteins. (a) MEFs carrying *Mdm2*$^{+/+}$ (WT) or *Mdm2*$^{tm1/tm1}$ (Hom) without *ROSA*-Cre-ER^{T2} allele (b) MEFs carrying *Mdm2*$^{+/+}$ (WT) or *Mdm2*$^{tm1/tm1}$ (Hom) with *ROSA*-Cre-ER^{T2} allele.

To test whether the expression of *Mdm2* I438K affects the growth of these cells, cells were induced to undergo recombination with 4-OHT and then were dosed with nutlin-3, doxorubicin or corresponding vehicle controls on Day 5 and left for 48 hours. In response to nutlin-3 treatment, cells expressing wild type *Mdm2* (OKNB 10.1h, OKNB 7.1g) grew at a similar rate and responded to nutlin-3 or doxorubicin similarly (Figure 5-10a and 5-10c). Activation of Cre recombinase by 4-OHT in *Mdm2* wild type cells (OKNB 10.1a) slightly reduced growth rate compared to cells carrying no *ROSA*-Cre-ER^{T2} allele, suggesting that expression of Cre recombinase is marginally toxic to the cells (Figure 5-10). Nevertheless, expression of *Mdm2* I438K (OKNB 10.1f) did not affect cell growth (Figure 5-10b, d), showing that this mutant can still limit p53 activity under basal conditions. Importantly, cells expressing this mutant arrested cell growth more rapidly than cells expressing wild type *Mdm2* in response to nutlin-3 or doxorubicin treatment (Figure 5-10b, d), although further experiments will be required to determine the physiological differences.

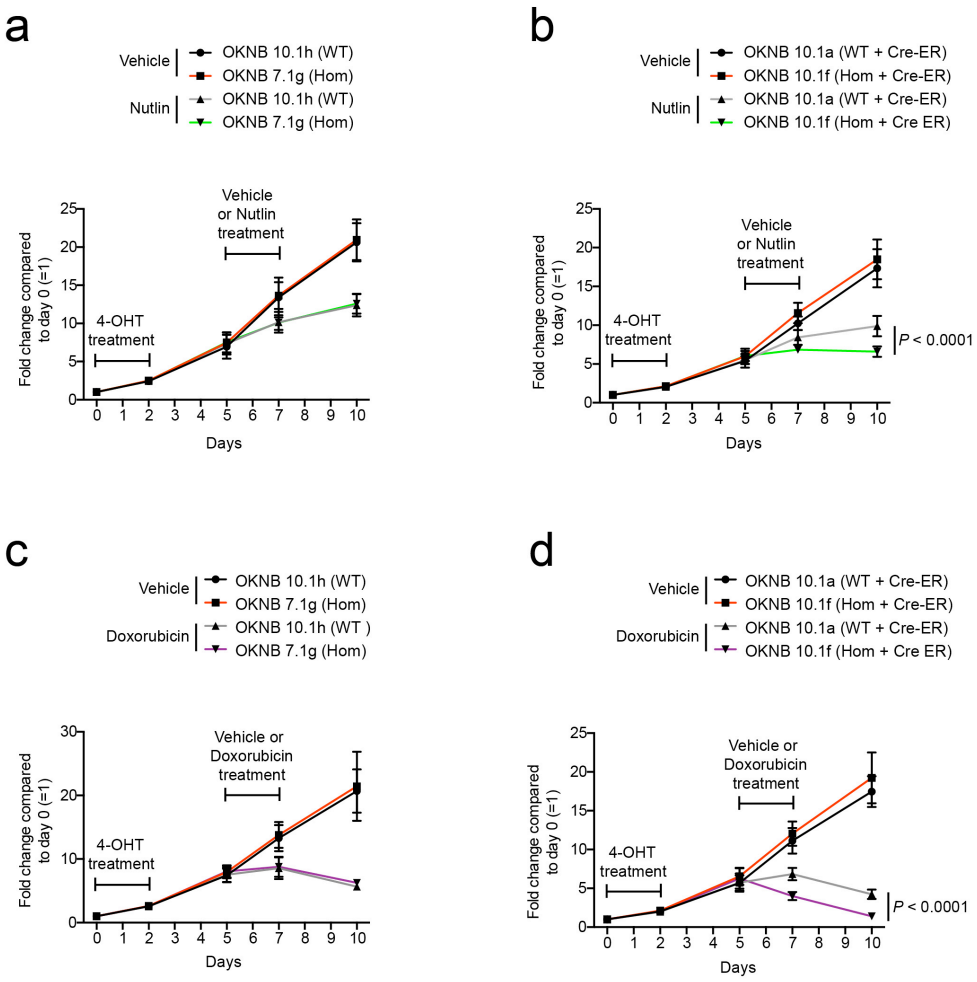

Figure 5-10: Effect of Cre recombination and nutlin-3 or doxorubicin treatment on cell growth

Cells were treated with 4-OHT (1 μM) for 48 hours 3 hours after seeding followed by 48 hours of treatment with vehicle, nutlin-3 (4 μM) or doxorubicin (1 μM) on Day 5. Cells were counted by the CASY cell counter. *P* values (two-way ANOVA - main effect of mutants): vs. wild type with Cre-ER^{T2} (OKNB 10.1a) with nutlin-3 or doxorubicin treatment. *F* (4, 16) = 16.28 (Figure 5-10b, main effect of mutants) and *F* (4, 16) = 13.34 (Figure 5-10d, main effect of mutants). Error bars indicate mean ± SD. *n* = 3 independent experiments.

5.3 Discussion

Human and murine MDM2 proteins are very similar and I have shown that human MDM2-equivalent mutations within the RING domain in murine MDM2 behave the same as their human MDM2 equivalents.

As discussed in Chapter 1 Section 1.3.2, a number of mouse models have been developed to assess the effect of *Mdm2* mutations *in vivo*. In general, mouse

models in which p53 transcriptional activity is not properly controlled by the MDM2/MDMX complex show an embryonic lethal phenotype. Indeed, Tollini *et al*. (2014) has recently shown that *Mdm2* C-terminal tail mutant mice, which can hetero-dimerise and therefore control p53 activity, are viable despite their elevated endogenous p53 level.

Although primary murine cells expressing *Mdm2* I438K accumulated high levels of p53, this mutant was sufficient to control p53 activity in terms of the induction of p53 target genes. While the protein expression level of MDM2 I438K was high, reflecting loss of its E3 ligase activity and subsequent loss of MDM2 auto-ubiquitination, nutlin-3 treatment further increased the protein level of this mutant. This response is likely to result from a p53-dependent increase in *Mdm2* mRNA expression - part of p53-MDM2 negative feedback loop. Interestingly, doxorubicin treatment did not further increase the expression level of the *Mdm2* I438K mutant, although this treatment did significantly induce *p21* and *Bax* expression.

Overall, in primary cells, MDM2 I438K mutant was able to control basal levels of p53 but allowed for a more rapid response to stress. This phenotype is also seen in the "Super-p53" and "Super-ARF/p53" mice that have enhanced p53 responsiveness and are resistant to tumour development as discussed in Chapter 1 Section 1.2. We now wish to understand the consequences of selective inhibition of the E3 ligase activity of MDM2 on normal and tumour development.

I am now conducting *in vivo* experiments with *Mdm2* I438K mutant mice to see if the suppression of p53 by the mutant is sufficient to allow for normal development. Analysing this mutant strain could allow us to mimic an inhibitor of MDM2 catalytic activity that could open up a novel therapeutic route to reactivate the tumour suppressor p53 *in vivo*.

5.3.1 Next steps for the *Mdm2* I438K mouse

Mice carrying a heterozygous copy of the *Mdm2* inducible I438K targeted allele (*Mdm2*$^{tm1/+}$), were crossed with mice carrying the X-linked Deletor-Cre (CMV promoter-driven ubiquitous expression of Cre recombinase) allele (*(Tg)*$^{(CMV\text{-}cre)1Cgn}$, (Schwenk et al., 1995)) to induce whole body/germline Cre recombination. Mice

carrying the recombination-induced allele (*Mdm2*$^{tm1.2/+}$) were then crossed with wild type C57BL/6J mice to remove the Deletor-Cre allele. At the time of writing, matings are ongoing to assess the viability (and functionality) of mice homozygous for the active *Mdm2*$^{I438K/I438K}$ allele.

As *Mdm2*$^{C462A/C462A}$ mice are embryonic lethal, it will be important to examine whether *Mdm2*$^{I438K/I438K}$ mice are viable. Tollini *et al*. (2014) previously showed that the E3 ligase activity of MDM2 is dispensable in embryogenesis. However, their model is expected to retain some E3 ligase activity towards p53 derived from MDM2/MDMX heterodimers (Uldrijan et al., 2007, Poyurovsky et al., 2007). As shown in Chapter 3, MDM2 I440K (MDM2 I438K in mouse) cannot be reactivated by MDMX. Consequently, our novel model will reveal whether E3 ligase activity of MDM2 is required for normal mouse development. Since MDM2 I438K is able to limit p53 activity in primary cells, *Mdm2*$^{I438K/I438K}$ mice are expected to be viable, although stresses during embryogenesis may result in lethality. If *Mdm2*$^{I438K/I438K}$ mice are embryonic lethal, we may investigate which embryonic stage they reach. If the mice are viable, irradiation sensitivity will be tested by irradiating mice with 5 Gy γ irradiation; sampling at 6 hours and 72 hours post-irradiation and analysing these mice using histological and molecular biological analysis to observe changes in protein expression such as p53, p21, Ki67 and BrdU in different organs. The survival of *Mdm2* I438K mice after irradiation will also be assessed, as Tollini *et al*. (2014) showed that E3 ligase activity of MDM2 is required to recover after irradiation. I will also investigate their long-term post-irradiation tumourigenesis.

In the future it would be interesting to cross *Mdm2*$^{I438K/I438K}$ mice into various genetically engineered mouse models (GEMMs) of cancer that retain wild type p53, including the *Apc*^{Min} (Multiple intestinal neoplasia mutation - encoding a nonsense mutation at codon 850) model of intestinal adenoma (Bilger et al., 1996), *Braf*^{V600E}-driven melanoma models (Dankort et al., 2009, Dhomen et al., 2009, Goel et al., 2009) and a mouse model of pancreatic ductal adenocarcinoma (PDAC) containing *Kras*$^{LSL-G12D}$; *Pdx1* (pancreatic and duodenal homeobox 1)-driven Cre (Hingorani et al., 2003), to assess the effect of *Mdm2* I438K mutant expression on tumour development.

5.3.2 Assessing post-developmental inducton of *Mdm2* I438K *in vivo*

If using the ubiquitous model (i.e. Deletor-Cre driven recombination) described above is incompatible with normal development, then the use of an inducible knock-in *Mdm2* I438K model will assess whether transcriptional repression of p53 by MDM2 binding alone is sufficient to keep p53 activity to a level that is compatible with adult life. To this end, mice heterozygous for *Mdm2* inducible I438K targeted allele ($Mdm2^{tm1/+}$) have been crossed with mice carrying the *ROSA*-Cre-ER^{T2} allele. Mice carrying both the *ROSA*-Cre-ER^{T2} allele and the *Mdm2* inducible I438K targeted allele were crossed with sibling mice carrying the *Mdm2* I438K mutant allele (without *ROSA*-Cre-ER^{T2}) to generate $Mdm2^{I438K/I438K}$; *ROSA*-Cre-ER^{T2} mice.

Deletion of *Mdm2* in adult mice is lethal (the mice become moribund within a few days) (Zhang et al., 2014b). Induction of the $Mdm2^{I438K/I438K}$ allele in adult mice by Tamoxifen will be carried out and mice monitor post-induction for phenotypic changes including weight change, irradiation sensitivity, long-term tumourigenesis and survival.

In addition, it would be interesting to induce *Mdm2* I438K in cancer bearing mice. This will model the effect of a small molecule inhibitor of MDM2 E3 activity as a cancer therapy.

5.3.3 Other options and future directions

As discussed, it is possible that mice with whole body expression of the mutant *Mdm2* will not be viable, as shown in $Mdm2^{-/-}$ or $Mdm2^{C464A/C464A}$ mice (Montes de Oca Luna et al., 1995, Jones et al., 1995, Itahana et al., 2007). Based on the preliminary data generated in primary cells, we think this is unlikely, but such a result would decrease enthusiasm for the development of an MDM2 E3 inhibitor. However, further studies would provide additional insight of *Mdm2* I438K mutant. If whole body expression of the *Mdm2* I438K mutant is incompatible with survival, tissue-type or cell-type specific Cre recombinase can be used to assess the sensitivity of different organs, tissues and cell types to complete loss of *Mdm2* compared to loss of E3 activity (tissue/cell type specific *Mdm2* deletion models are summarised in Chapter 1). It would also be interesting to determine whether

expression of the *Mdm2* I438K mutant affects the pattern of gene expression in response to p53 activation, which can be analysed by ChIP-seq or RNA-seq. Finally, we could use this system to examine p53-independent activities of this *Mdm2* mutant in p53 null mice.

Overall, these *in vivo* experiments will reveal the E3 ligase independent function of MDM2 *in vivo* and characterisation and development of these *Mdm2* mutant *in vivo* models. This will be the key to validate the utility of developing compounds with a differentiated mode of action than any MDM2 inhibitors presently in clinical development. So far my obtained data suggest that $Mdm2^{I438K/I438K}$ mice will be viable, may have enhanced p53 responsiveness, and could show increased resistance to tumour development. Such an outcome would increase enthusiasm for the development of an MDM2 E3 inhibitor in the future.

Chapter 6 Overall summary and conclusions

The p53 pathway, which is activated in response to various types of stress to induce cell cycle arrest to allow cells to adapt or eliminate the cell through cell death or senescence if the stress is persistent, is the most commonly dysregulated pathway in human cancer. Although approximately half of all human cancers have mutation in the *Tp53* locus resulting in the loss of p53 or expression of mutant p53, the other tumours show a variety of perturbations in the pathway that result in the retention of wild type p53 but defect in the response to stress. Indeed, mouse models have shown that reinstatement of p53 in cancer bearing mice led to tumour regression (Martins et al., 2006), suggesting that reactivation of wild type p53 activity could be a useful strategy for cancer treatment. Furthermore, mice carrying an extra copy of p53 are resistant to tumour development (Garcia-Cao et al., 2002, Matheu et al., 2007). On the other hand, while these activities of p53 are effective in preventing malignant progression, uncontrolled p53 activity is incompatible with cell or organismal viability.

Several drugs that target the N-terminal of MDM2 where p53 binds have been developed (Shangary et al., 2008, Vassilev et al., 2004, Ding et al., 2013) and show excellent on target specificity in stabilisation and activation of p53. Indeed, Idasanutlin (RG7388) is currently in Phase 3 clinical trials. However, on-target toxicities including thrombocytopaenia and neutropaenia appear to limit the efficacy and utility of these compounds (Andreeff et al., 2016, Ray-Coquard et al., 2012). Previous studies have also highlighted some p53 independent mechanisms through which these compounds can enhance toxicities to the cells, including disruption of the interactions between MDM2 and p73 (a protein related to p53), and MDM2 and E2F1 (Lau et al., 2008, Ray et al., 2011, Ambrosini et al., 2007). Although a number of other drugs that target MDM2 and MDMX to reactivate p53 through different mechanisms have been developed, the clinical application of these is not yet clear.

At the onset of this work, this project was aimed to explore in more detail the functional requirements for MDM2 E3 activity and to understand how important transcriptional repression of p53 by MDM2/MDMX independently of E3 ligase activity is to keep p53 in check. Prior studies of the MDM2 RING domain used MDM2 C464A to assess E3 ligase-independent functions in regulating p53, but

MDM2 C464A mutant abolishes the E3 ligase activity as well as the RING domain fold. Therefore, it remains unclear whether the RING domain fold is important for the E3 ligase-independent function of MDM2, since the RING domain is required to interact with proteins (including homo- and hetero-dimerisation with MDMX) in addition to recruit E2–ubiquitin complex. In fact, introduction of MDM2 C462A (MDM2 C464A in human) mutant in mice resulted in an uncontrolled p53 activity and embryonic lethal phenotype, like complete loss of *Mdm2* (Itahana et al., 2007). These results suggested that the integrity of RING domain fold, as well as their ability to bind to p53, is required to regulate p53 activity.

Therefore, by analysing the novel crystal structure of the E2–ubiquitin-MDM2^{RING}-MDMX^{RING} complex developed by Professor Danny Huang's group, I performed systematic and comprehensive mutational analysis of MDM2 RING domain to generate MDM2 mutants that do not interact with E2–ubiquitin complex but retain the RING domain fold. These mutants are therefore expected to (1) elevate endogenous p53 level but (2) be able to limit p53 activity in normal unstressed cells and (3) respond quickly to activate p53 pathway upon stress due to already accumulated p53 in cells.

First, I tested whether these mutants have lost their ligase activity (Chapter 3). Our crystal structure revealed several potential interaction sites between the MDM2-MDMX hetero-dimer and the E2–ubiquitin complex. Important residues on MDM2-MDMX heterodimer include (1) MDM2 I440 which interacts with E2 by hydrophobic interaction (2) MDM2 R479 which interacts with E2 and ubiquitin by hydrogen bonds and (3) The C-terminal tail of the dimerisation partner of MDM2 which interact with ubiquitin (therefore, dimerisation is required). Shown here, mutation of MDM2 I440 into hydrophilic amino acids or MDM2 R479 into hydrophobic amino acids abrogate its E3 ligase activity but retain the ability to hetero-dimerise with MDMX. As previously described, MDM2 C-terminal tail mutants lose E3 ligase activity, but these mutants can be reactivated when dimerised with MDMX (Uldrijan et al., 2007, Poyurovsky et al., 2007). Our structural analysis revealed that MDM2 residues C449 and T488 play an important role in dimerisation and a double mutation of MDM2 C449N-T488V has completely lost its E3 ligase activity, despite retaining the ability to bind to p53 when co-immunoprecipitated with cell lysate. This suggests that MDM2 is not able to

ubiquitinate p53 as a monomer, which also supports the observation that the C-terminal tail of the binding partner of MDM2 is required to ubiquitinate p53. This also fits the observation that MDM2 C464A mutant, which cannot dimerise, has lost its E3 ligase activity.

My findings also helped to reveal why MDMX possesses no intrinsic E3 ligase activity. As shown in Chapter 3, point mutation of MDMX K478R (as R479 in MDM2) was required to give MDMX an E3 ligase activity in addition to the ability to dimerise. In fact, SPR analysis has shown that although wild type MDMX was unable to interact with the E2–ubiquitin complex, MDMX K478R has acquired this ability. From the structure point of view, this "linchpin" arginine residue is required to interact with not only E2 but also ubiquitin, which may support the formation of the active "closed" conformation of E2–ubiquitin-E3 complex as shown in Chapter 3. Indeed, this MDMX K478R mutant was sufficient to reactivate MDM2 I440 mutants (that cannot interact with E2–ubiquitin complex), suggesting their complementation.

Secondly, I tested whether MDM2 mutant that has lost their E3 ligase activity can regulate p53 activity, despite the elevated p53 level in cells as shown in Chapter 4. Unlike MDM2 C464A mutant, MDM2 I440 or R479 mutants can be co-localised with p53 on the promoter of p53 target genes (at last on the *p21* promoter) and attenuate the p53 transcriptional activity. Importantly, although MDM2 C464A mutant is able to bind to p53 when co-immunoprecipitated with cell lysate, this binding was not maintained on the promoter of p53 target genes. Therefore the transcriptional repression by MDM2 I440 or R479 mutants is sufficient to keep p53 in check to allow proliferation, but renders cells hyper-sensitive to stressed conditions due to the elevated p53 in cells. The dimerisation-impaired Mdm2 C449N-T488V double mutant, on the other hand, was not able to limit the transcriptional activity of p53. In fact, Tollini *et al*. (2014) demonstrated, using Mdm2 C-terminal tail mutant in mice, that hetero-dimerisation is critical to regulate p53 transcriptional activity. Moreover, MDM2 I440 and R479 mutant can no longer limit p53 transcriptional activity in the absence of MDMX (Chapter 4). Therefore, it is possible that MDMX plays a critical role in regulating the p53 transcriptional activity and impairment of MDM2-MDMX hetero-dimerisation, which is necessary for MDMX to enter nucleus, results in uncontrolled p53

activity. In fact, mouse models where MDM2 cannot form a hetero-dimer with MDMX (including *Mdm2*$^{C462A/C462A}$, *Mdmx*$^{C462A/C462A}$ and *Mdmx*$^{\Delta RING/\Delta RING}$) show an embryonic lethal phenotype similar to the whole knockout of *Mdm2* or *Mdmx*.

Several inhibitors of the E3 ligase activity of MDM2 have been identified by screening for inhibitors of the auto-ubiquitination activity of MDM2. As discussed above, impairment of MDM2 dimerisation results in a loss of the E3 ligase activity of MDM2 (including auto-ubiquitination). Therefore, further characterisation of those compounds may be required in order to minimise on-target toxicity. For example, *in silico* docking result suggests that HLI98, which was identified through an MDM2 auto-ubiquitination screen, seems to bind to the MDM2 dimerisation core and disrupt their dimerisation. As introduction of MDM2 dimerisation-impaired mutant in cells results in an uncontrolled p53 activity (Chapter 4), clinical application of this kind of compounds may have no advantages over the compounds that inhibit the MDM2 p53-binding domain like nutlin-3 in terms of on-target toxicity. In contrast to this, inhibition of MDM2's E3 ligase activity without disrupting MDM2 dimerisation, including the strategy to disrupt the interaction between MDM2 and E2–ubiquitin complex (shown in MDM2 I440 or R479 mutants) would lead to different outcomes than inhibition of the MDM2-p53 interaction, RING domain co-ordination or MDM2 dimerisation.

Finally, we have designed and generated a conditional knock-in allele of *Mdm2* I438K (I440K in human) to investigate how *Mdm2*^{I438K} knock-in mice develop and their susceptibility to cancer development in comparison with wild type *Mdm2* mice. Preliminary and validation experiments using primary murine cells carrying the conditional *Mdm2* I438K knock-in allele revealed the regulation of murine p53 by MDM2 I438K mutant. As shown in Chapter 5, MDM2 I438K mutant has lost its E3 ligase activity but possessed an ability to limit p53 transcriptional activity consistent with the result shown in Chapter 4. Interestingly, MDM2 I438K also possessed the ability to limit the ability of p53 induced *Mdm2* - part of the negative feedback loop. From a clinical point of view, retaining this ability could also be beneficial as MDM2 has several p53- (and E3 ligase-) independent functions that may cause cytotoxic effects. Overall, the MDM2 I438K mutant is able to control p53 transcriptional activity and allows normal cell cycle and cell growth in normal unstressed condition but renders cells more sensitive to stress.

Therefore, based on these preliminary data, although stresses during embryogenesis are not negligible, *Mdm2* I438K mutant mice are expected to be (1) viable, (2) developmentally normal and (3) resistant to tumour development. Analysing our *in vivo* models will allow us to mimic an inhibitor of MDM2 catalytic activity and therefore validate the effect of the inhibition of MDM2 E3 ligase activity that will help the development of novel MDM2 inhibitors for anti-cancer therapy.

An important question is whether the interaction of MDM2 with E2–ubiquitin complex is druggable and how selective such a compound would be? This is a very difficult question as there are approximately 600 RING-type E3 ligases with similar RING domain structures. However, there are several good reasons to increase enthusiasm for the development of these MDM2 inhibitors. First, proteasome inhibitors such as Bortezomib, which in theory inhibit degradation of all ubiquitinated proteins (by not only RING-type E3 ligases but also other types of E3 ligases such as HECT-type E3 ligases), have already been approved for some applications. Therefore, even if the compounds inhibit many other RING E3 ligases, and as long as the compounds do not interfere the ability of MDM2/MDMX to limit p53 activity in normal unstressed cells, they would have clinical advantages over current MDM2 inhibitors or proteasome inhibitors. Second, MDM2 is a C_2H_2-C_4 type RING E3 ligase, which is unique from other RING E3 ligases (RING domains typically have C_3H-C_4 or C_4-C_4 zinc coordination as discussed in Chapter 1 Section 1.3.1.3). And third, we have a crystal structure of E2–ubiquitin-MDM2^{RING}-MDMX^{RING} that will help to design potential compounds *in silico*. Perhaps, inhibition of E2 ubiquitin-conjugating enzymes that interacts with MDM2 (such as UbcH5B) could be the other option. It is important to note that, like other chemotherapeutic agents, there may be several restrictions to use MDM2 E3 ligase inhibitors including that (1) confirmation of p53 status is required as this strategy will only work for tumours retaining wild type p53 and (2) subsequent testing for MDMX overexpression may also be required since MDMX overexpression could cause primary resistance to MDM2 E3 ligase inhibitors. In any case, targeting the catalytic activity of MDM2 to reactivate wild type p53 in tumours could open up a new therapeutic window to drive p53-dependent arrest of cancer cell growth while potentially avoiding the deleterious on-target side effects of completely disrupting the MDM2-p53 interaction.

In addition, the strategy presented here may be applicable for investigating E3 ligase-independent function of other RING type E3 ligases, which will broaden the scope of further anti-cancer therapy based on targeting RING type E3 ligases.

In summary, my main findings are following (also refer Table 6-1):

1. MDM2 I440 or R479 mutants do not interact with E2–ubiquitin complex

2. As a result, these mutants possess no E3 ligase activity

3. These mutants are able to bind to p53 and homo- and hetero-dimerise

4. Although p53 level is high in cells expressing these mutants, its transcriptional activity is controlled

5. Cells expressing these mutants respond to stress quickly due to already accumulated p53 in cells

6. Hetero-dimerisation with MDMX seems to be required to regulate p53 activity

These findings will help the development of promising new strategies to treat cancer patients carrying tumours expressing wild type p53 - estimated to be up to 50 % of all malignancies. Finally, our novel mouse models are expected to reveal the regulation of p53 by catalytically-inactive MDM2 mutants in cell, tissue, organ, organ system and organism level, which will provide deeper understanding of the regulation of p53-MDM2/MDMX network.

Table 6-1: Overall summary of selected MDM2 mutants in this study

MDM2	Wild type	C464A	I440K I440E	R479P	Y489D	C449N-T488V double mutant
Mutation (Structural estimation)	N/A	Disrupts RING domain co-ordination	Does not interact with E2–Ub complex (Disrupts hydrophobic interaction)	Does not interact with E2–Ub complex (Disrupts hydrogen bonds)	Prevents ubiquitin interaction	Prevents homo-dimerisation and MDMX dimerisation
Interaction with E2–ubiquitin complex	+++	*Not tested*	-	-	*Not tested*	*Not tested*
p53 binding (Co-IP)	+++	+++	+++	+++	+++	++
Dimerisation with MDMX	+++	-	+++	+++	+++	- (can dimerise with MDM2)
Ubiquitination of p53	+++	-	-	-	-	-
Inhibition of p53 activity	+++	+	+++	+++	*Not tested*	+
Localisation on *p21* promoter (via p53)	+++	+	+++	+++	*Not tested*	*Not tested*
Cell growth	+++	+	+++	+++	*Not tested*	*Not tested*
p53 activation after stress	Slow	N/A	Fast	Fast	*Not tested*	*Not tested*
Reactivation (Ubiquitination of p53)	N/A	-	When dimerised with appropriate binding partner (*1)	When dimerised with appropriate binding partner (*1)	When dimerised with MDMX	When dimerised with MDM2 (*2)

***1 Binding partner including MDM2 C449N-T488V double mutant and MDMX K478R**

***2 Including MDM2 I440K, I440E and R479P**

Bibliography

ABIDA, W. M. & GU, W. 2008. p53-Dependent and p53-independent activation of autophagy by ARF. *Cancer Res,* 68**,** 352-7.

ABIDA, W. M., NIKOLAEV, A., ZHAO, W., ZHANG, W. & GU, W. 2007. FBXO11 promotes the Neddylation of p53 and inhibits its transcriptional activity. *J Biol Chem,* 282**,** 1797-804.

ADHIKARY, S., MARINONI, F., HOCK, A., HULLEMAN, E., POPOV, N., BEIER, R., BERNARD, S., QUARTO, M., CAPRA, M., GOETTIG, S., KOGEL, U., SCHEFFNER, M., HELIN, K. & EILERS, M. 2005. The ubiquitin ligase HectH9 regulates transcriptional activation by Myc and is essential for tumor cell proliferation. *Cell,* 123**,** 409-21.

AGAH, R., FRENKEL, P. A., FRENCH, B. A., MICHAEL, L. H., OVERBEEK, P. A. & SCHNEIDER, M. D. 1997. Gene recombination in postmitotic cells. Targeted expression of Cre recombinase provokes cardiac-restricted, site-specific rearrangement in adult ventricular muscle in vivo. *J Clin Invest,* 100**,** 169-79.

AGARWAL, M. L., AGARWAL, A., TAYLOR, W. R. & STARK, G. R. 1995. p53 controls both the G2/M and the G1 cell cycle checkpoints and mediates reversible growth arrest in human fibroblasts. *Proc Natl Acad Sci U S A,* 92**,** 8493-7.

ALLIS, C. D., BERGER, S. L., COTE, J., DENT, S., JENUWIEN, T., KOUZARIDES, T., PILLUS, L., REINBERG, D., SHI, Y., SHIEKHATTAR, R., SHILATIFARD, A., WORKMAN, J. & ZHANG, Y. 2007. New nomenclature for chromatin-modifying enzymes. *Cell,* 131**,** 633-6.

ALLTON, K., JAIN, A. K., HERZ, H. M., TSAI, W. W., JUNG, S. Y., QIN, J., BERGMANN, A., JOHNSON, R. L. & BARTON, M. C. 2009. Trim24 targets endogenous p53 for degradation. *Proc Natl Acad Sci U S A,* 106**,** 11612-6.

ALMOND, J. B. & COHEN, G. M. 2002. The proteasome: a novel target for cancer chemotherapy. *Leukemia,* 16**,** 433-43.

AMARAVADI, R. K., YU, D., LUM, J. J., BUI, T., CHRISTOPHOROU, M. A., EVAN, G. I., THOMAS-TIKHONENKO, A. & THOMPSON, C. B. 2007. Autophagy inhibition enhances therapy-induced apoptosis in a Myc-induced model of lymphoma. *J Clin Invest,* 117**,** 326-36.

AMBROSINI, G., SAMBOL, E. B., CARVAJAL, D., VASSILEV, L. T., SINGER, S. & SCHWARTZ, G. K. 2007. Mouse double minute antagonist Nutlin-3a enhances chemotherapy-induced apoptosis in cancer cells with mutant p53 by activating E2F1. *Oncogene,* 26**,** 3473-81.

AMIR, R. E., IWAI, K. & CIECHANOVER, A. 2002. The NEDD8 pathway is essential for SCF(beta -TrCP)-mediated ubiquitination and processing of the NF-kappa B precursor p105. *J Biol Chem,* 277**,** 23253-9.

ANDREEFF, M., KELLY, K. R., YEE, K., ASSOULINE, S., STRAIR, R., POPPLEWELL, L., BOWEN, D., MARTINELLI, G., DRUMMOND, M. W., VYAS, P., KIRSCHBAUM, M., IYER, S. P., RUVOLO, V., GONZALEZ, G. M., HUANG, X., CHEN, G., GRAVES, B., BLOTNER, S., BRIDGE, P., JUKOFSKY, L., MIDDLETON, S., RECKNER, M., RUEGER, R., ZHI, J., NICHOLS, G. & KOJIMA, K. 2016. Results of the Phase I Trial of RG7112, a Small-Molecule MDM2 Antagonist in Leukemia. *Clin Cancer Res,* 22**,** 868-76.

ARAKI, S., EITEL, J. A., BATUELLO, C. N., BIJANGI-VISHEHSARAEI, K., XIE, X. J., DANIELPOUR, D., POLLOK, K. E., BOOTHMAN, D. A. & MAYO, L. D. 2010. TGF-beta1-induced expression of human Mdm2 correlates with late-stage metastatic breast cancer. *J Clin Invest,* 120**,** 290-302.

ARGENTINI, M., BARBOULE, N. & WASYLYK, B. 2001. The contribution of the acidic domain of MDM2 to p53 and MDM2 stability. *Oncogene,* 20**,** 1267-75.

ARMSTRONG, J. F., KAUFMAN, M. H., HARRISON, D. J. & CLARKE, A. R. 1995. High-frequency developmental abnormalities in p53-deficient mice. *Curr Biol,* 5**,** 931-6.

ASHERY-PADAN, R., MARQUARDT, T., ZHOU, X. & GRUSS, P. 2000. Pax6 activity in the lens primordium is required for lens formation and for correct placement of a single retina in the eye. *Genes Dev,* 14**,** 2701-11.

ASSAILY, W., RUBINGER, D. A., WHEATON, K., LIN, Y., MA, W., XUAN, W., BROWN-ENDRES, L., TSUCHIHARA, K., MAK, T. W. & BENCHIMOL, S. 2011. ROS-mediated p53 induction of Lpin1 regulates fatty acid oxidation in response to nutritional stress. *Mol Cell,* 44**,** 491-501.

BAATOUT, S., JACQUET, P., MICHAUX, A., BUSET, J., VANKERKOM, J., DERRADJI, H., YAN, J., VON SUCHODOLETZ, H., DE SAINT-GEORGES, L., DESAINTES, C. & MERGEAY, M. 2002. Developmental abnormalities induced by X-irradiation in p53 deficient mice. *In Vivo,* 16**,** 215-21.

BAEK, S., KUTCHUKIAN, P. S., VERDINE, G. L., HUBER, R., HOLAK, T. A., LEE, K. W. & POPOWICZ, G. M. 2012. Structure of the stapled p53 peptide bound to Mdm2. *J Am Chem Soc,* 134**,** 103-6.

BAKER, R. T. & BOARD, P. G. 1991. The human ubiquitin-52 amino acid fusion protein gene shares several structural features with mammalian ribosomal protein genes. *Nucleic Acids Res,* 19**,** 1035-40.

BARAK, Y., JUVEN, T., HAFFNER, R. & OREN, M. 1993. mdm2 expression is induced by wild type p53 activity. *Embo j,* 12**,** 461-8.

BARLEV, N. A., LIU, L., CHEHAB, N. H., MANSFIELD, K., HARRIS, K. G., HALAZONETIS, T. D. & BERGER, S. L. 2001. Acetylation of p53 activates transcription through recruitment of coactivators/histone acetyltransferases. *Mol Cell,* 8**,** 1243-54.

BATLLE, E., SANCHO, E., FRANCI, C., DOMINGUEZ, D., MONFAR, M., BAULIDA, J. & GARCIA DE HERREROS, A. 2000. The transcription factor snail is a repressor of E-cadherin gene expression in epithelial tumour cells. *Nat Cell Biol,* 2**,** 84-9.

BAYER, P., ARNDT, A., METZGER, S., MAHAJAN, R., MELCHIOR, F., JAENICKE, R. & BECKER, J. 1998. Structure determination of the small ubiquitin-related modifier SUMO-1. *J Mol Biol,* 280**,** 275-86.

BENSAAD, K., CHEUNG, E. C. & VOUSDEN, K. H. 2009. Modulation of intracellular ROS levels by TIGAR controls autophagy. *Embo j,* 28**,** 3015-26.

BENSAAD, K., TSURUTA, A., SELAK, M. A., VIDAL, M. N., NAKANO, K., BARTRONS, R., GOTTLIEB, E. & VOUSDEN, K. H. 2006. TIGAR, a p53-inducible regulator of glycolysis and apoptosis. *Cell,* 126**,** 107-20.

BERNAL, F., TYLER, A. F., KORSMEYER, S. J., WALENSKY, L. D. & VERDINE, G. L. 2007. Reactivation of the p53 tumor suppressor pathway by a stapled p53 peptide. *J Am Chem Soc,* 129**,** 2456-7.

BERNARDI, R., SCAGLIONI, P. P., BERGMANN, S., HORN, H. F., VOUSDEN, K. H. & PANDOLFI, P. P. 2004. PML regulates p53 stability by sequestering Mdm2 to the nucleolus. *Nat Cell Biol,* 6**,** 665-72.

BIEGING, K. T., MELLO, S. S. & ATTARDI, L. D. 2014. Unravelling mechanisms of p53-mediated tumour suppression. *Nat Rev Cancer,* 14**,** 359-70.

BILGER, A., SHOEMAKER, A. R., GOULD, K. A. & DOVE, W. F. 1996. Manipulation of the mouse germline in the study of Min-induced neoplasia. *Semin Cancer Biol,* 7**,** 249-60.

BINNE, U. K., CLASSON, M. K., DICK, F. A., WEI, W., RAPE, M., KAELIN, W. G., JR., NAAR, A. M. & DYSON, N. J. 2007. Retinoblastoma protein and anaphase-promoting complex physically interact and functionally cooperate during cell-cycle exit. *Nat Cell Biol,* 9**,** 225-32.

BLACK, R. A., RAUCH, C. T., KOZLOSKY, C. J., PESCHON, J. J., SLACK, J. L., WOLFSON, M. F., CASTNER, B. J., STOCKING, K. L., REDDY, P., SRINIVASAN, S., NELSON, N., BOIANI, N., SCHOOLEY, K. A., GERHART, M., DAVIS, R., FITZNER, J. N., JOHNSON, R. S., PAXTON, R. J., MARCH, C. J. & CERRETTI, D. P. 1997. A metalloproteinase disintegrin that releases tumour-necrosis factor-alpha from cells. *Nature,* 385**,** 729-33.

BLEES, J. S., BOKESCH, H. R., RUBSAMEN, D., SCHULZ, K., MILKE, L., BAJER, M. M., GUSTAFSON, K. R., HENRICH, C. J., MCMAHON, J. B., COLBURN, N. H., SCHMID, T. & BRUNE, B. 2012. Erioflorin stabilizes the tumor suppressor Pdcd4 by inhibiting its interaction with the E3-ligase beta-TrCP1. *PLoS One,* 7**,** e46567.

BOCCADORO, M., MORGAN, G. & CAVENAGH, J. 2005. Preclinical evaluation of the proteasome inhibitor bortezomib in cancer therapy. *Cancer Cell Int,* 5**,** 18.

BOESTEN, L. S., ZADELAAR, S. M., DE CLERCQ, S., FRANCOZ, S., VAN NIEUWKOOP, A., BIESSEN, E. A., HOFMANN, F., FEIL, S., FEIL, R., JOCHEMSEN, A. G., ZURCHER, C., HAVEKES, L. M., VAN VLIJMEN, B. J. & MARINE, J. C. 2006. Mdm2, but not Mdm4, protects terminally differentiated smooth muscle cells from p53-mediated caspase-3-independent cell death. *Cell Death Differ,* 13**,** 2089-98.

BOND, G. L., HU, W., BOND, E. E., ROBINS, H., LUTZKER, S. G., ARVA, N. C., BARGONETTI, J., BARTEL, F., TAUBERT, H., WUERL, P., ONEL, K., YIP, L., HWANG, S. J., STRONG, L. C., LOZANO, G. & LEVINE, A. J. 2004. A single nucleotide polymorphism in the MDM2 promoter attenuates the p53 tumor suppressor pathway and accelerates tumor formation in humans. *Cell,* 119**,** 591-602.

BONDESON, D. P., MARES, A., SMITH, I. E., KO, E., CAMPOS, S., MIAH, A. H., MULHOLLAND, K. E., ROUTLY, N., BUCKLEY, D. L., GUSTAFSON, J. L., ZINN, N., GRANDI, P., SHIMAMURA, S., BERGAMINI, G., FAELTH-SAVITSKI, M., BANTSCHEFF, M., COX, C., GORDON, D. A., WILLARD, R. R., FLANAGAN, J. J., CASILLAS, L. N., VOTTA, B. J., DEN BESTEN, W., FAMM, K., KRUIDENIER, L., CARTER, P. S., HARLING, J. D., CHURCHER, I. & CREWS, C. M. 2015. Catalytic in vivo protein knockdown by small-molecule PROTACs. *Nat Chem Biol,* 11**,** 611-7.

BORNSTEIN, G., BLOOM, J., SITRY-SHEVAH, D., NAKAYAMA, K., PAGANO, M. & HERSHKO, A. 2003. Role of the SCFSkp2 ubiquitin ligase in the degradation of p21Cip1 in S phase. *J Biol Chem,* 278**,** 25752-7.

BOUTET, S. C., DISATNIK, M. H., CHAN, L. S., IORI, K. & RANDO, T. A. 2007. Regulation of Pax3 by proteasomal degradation of monoubiquitinated protein in skeletal muscle progenitors. *Cell,* 130**,** 349-62.

BRADY, C. A., JIANG, D., MELLO, S. S., JOHNSON, T. M., JARVIS, L. A., KOZAK, M. M., KENZELMANN BROZ, D., BASAK, S., PARK, E. J., MCLAUGHLIN, M. E., KARNEZIS, A. N. & ATTARDI, L. D. 2011. Distinct p53 transcriptional programs dictate acute DNA-damage responses and tumor suppression. *Cell,* 145**,** 571-83.

BRANIGAN, E., PLECHANOVOVA, A., JAFFRAY, E. G., NAISMITH, J. H. & HAY, R. T. 2015. Structural basis for the RING-catalyzed synthesis of K63-linked ubiquitin chains. 22**,** 597-602.

BROWN, M. G., DRISCOLL, J. & MONACO, J. J. 1991. Structural and serological similarity of MHC-linked LMP and proteasome (multicatalytic proteinase) complexes. *Nature,* 353**,** 355-7.
BROWN, R. S. 2005. Zinc finger proteins: getting a grip on RNA. *Curr Opin Struct Biol,* 15**,** 94-8.
BRZOVIC, P. S., KEEFFE, J. R., NISHIKAWA, H., MIYAMOTO, K., FOX, D., 3RD, FUKUDA, M., OHTA, T. & KLEVIT, R. 2003. Binding and recognition in the assembly of an active BRCA1/BARD1 ubiquitin-ligase complex. *Proc Natl Acad Sci U S A,* 100**,** 5646-51.
BRZOVIC, P. S., LISSOUNOV, A., CHRISTENSEN, D. E., HOYT, D. W. & KLEVIT, R. E. 2006. A UbcH5/ubiquitin noncovalent complex is required for processive BRCA1-directed ubiquitination. *Mol Cell,* 21**,** 873-80.
BUDANOV, A. V. & KARIN, M. 2008. p53 target genes sestrin1 and sestrin2 connect genotoxic stress and mTOR signaling. *Cell,* 134**,** 451-60.
BUDANOV, A. V., SABLINA, A. A., FEINSTEIN, E., KOONIN, E. V. & CHUMAKOV, P. M. 2004. Regeneration of peroxiredoxins by p53-regulated sestrins, homologs of bacterial AhpD. *Science,* 304**,** 596-600.
BUDHIDARMO, R., NAKATANI, Y. & DAY, C. L. 2012. RINGs hold the key to ubiquitin transfer. *Trends Biochem Sci,* 37**,** 58-65.
BUETOW, L., GABRIELSEN, M., ANTHONY, N. G., DOU, H., PATEL, A., AITKENHEAD, H., SIBBET, G. J., SMITH, B. O. & HUANG, D. T. 2015. Activation of a primed RING E3-E2-ubiquitin complex by non-covalent ubiquitin. *Mol Cell,* 58**,** 297-310.
BUETOW, L. & HUANG, D. T. 2016. Structural insights into the catalysis and regulation of E3 ubiquitin ligases. *Nat Rev Mol Cell Biol,* 17**,** 626-42.
BULLOCK, A. N. & FERSHT, A. R. 2001. Rescuing the function of mutant p53. *Nat Rev Cancer,* 1**,** 68-76.
BUSUTTIL, V., DROIN, N., MCCORMICK, L., BERNASSOLA, F., CANDI, E., MELINO, G. & GREEN, D. R. 2010. NF-kappaB inhibits T-cell activation-induced, p73-dependent cell death by induction of MDM2. *Proc Natl Acad Sci U S A,* 107**,** 18061-6.
CANMAN, C. E., LIM, D. S., CIMPRICH, K. A., TAYA, Y., TAMAI, K., SAKAGUCHI, K., APPELLA, E., KASTAN, M. B. & SILICIANO, J. D. 1998. Activation of the ATM kinase by ionizing radiation and phosphorylation of p53. *Science,* 281**,** 1677-9.
CAPPADOCIA, L., PICHLER, A. & LIMA, C. D. 2015. Structural basis for catalytic activation by the human ZNF451 SUMO E3 ligase. *Nat Struct Mol Biol,* 22**,** 968-75.
CARRANO, A. C., EYTAN, E., HERSHKO, A. & PAGANO, M. 1999. SKP2 is required for ubiquitin-mediated degradation of the CDK inhibitor p27. *Nat Cell Biol,* 1**,** 193-9.
CARRANO, A. C. & PAGANO, M. 2001. Role of the F-box protein Skp2 in adhesion-dependent cell cycle progression. *J Cell Biol,* 153**,** 1381-90.
CARTER, S., BISCHOF, O., DEJEAN, A. & VOUSDEN, K. H. 2007. C-terminal modifications regulate MDM2 dissociation and nuclear export of p53. *Nat Cell Biol,* 9**,** 428-35.
CASSAVAUGH, J. M., HALE, S. A., WELLMAN, T. L., HOWE, A. K., WONG, C. & LOUNSBURY, K. M. 2011. Negative regulation of HIF-1alpha by an FBW7-mediated degradation pathway during hypoxia. *J Cell Biochem,* 112**,** 3882-90.
CAVENEE, W. K., DRYJA, T. P., PHILLIPS, R. A., BENEDICT, W. F., GODBOUT, R., GALLIE, B. L., MURPHREE, A. L., STRONG, L. C. & WHITE, R. L. 1983.

Expression of recessive alleles by chromosomal mechanisms in retinoblastoma. *Nature,* 305**,** 779-84.
CHAN, T. A., HERMEKING, H., LENGAUER, C., KINZLER, K. W. & VOGELSTEIN, B. 1999. 14-3-3Sigma is required to prevent mitotic catastrophe after DNA damage. *Nature,* 401**,** 616-20.
CHANG, C. J., FREEMAN, D. J. & WU, H. 2004. PTEN regulates Mdm2 expression through the P1 promoter. *J Biol Chem,* 279**,** 29841-8.
CHANG, L. & BARFORD, D. 2014. Insights into the anaphase-promoting complex: a molecular machine that regulates mitosis. *Curr Opin Struct Biol,* 29**,** 1-9.
CHEN, C. S., HO, D. R., CHEN, F. Y., CHEN, C. R., KE, Y. D. & SU, J. G. 2014. AKT mediates actinomycin D-induced p53 expression. *Oncotarget,* 5**,** 693-703.
CHEN, D., KON, N., LI, M., ZHANG, W., QIN, J. & GU, W. 2005a. ARF-BP1/Mule is a critical mediator of the ARF tumor suppressor. *Cell,* 121**,** 1071-83.
CHEN, J., LIN, J. & LEVINE, A. J. 1995. Regulation of transcription functions of the p53 tumor suppressor by the mdm-2 oncogene. *Mol Med,* 1**,** 142-52.
CHEN, J. J., TSU, C. A., GAVIN, J. M., MILHOLLEN, M. A., BRUZZESE, F. J., MALLENDER, W. D., SINTCHAK, M. D., BUMP, N. J., YANG, X., MA, J., LOKE, H. K., XU, Q., LI, P., BENCE, N. F., BROWNELL, J. E. & DICK, L. R. 2011. Mechanistic studies of substrate-assisted inhibition of ubiquitin-activating enzyme by adenosine sulfamate analogues. *J Biol Chem,* 286**,** 40867-77.
CHEN, L., GILKES, D. M., PAN, Y., LANE, W. S. & CHEN, J. 2005b. ATM and Chk2-dependent phosphorylation of MDMX contribute to p53 activation after DNA damage. *Embo j,* 24**,** 3411-22.
CHEN, L., LI, Z., ZWOLINSKA, A. K., SMITH, M. A., CROSS, B., KOOMEN, J., YUAN, Z. M., JENUWEIN, T., MARINE, J. C., WRIGHT, K. L. & CHEN, J. 2010. MDM2 recruitment of lysine methyltransferases regulates p53 transcriptional output. *Embo j,* 29**,** 2538-52.
CHEN, Z. J. 2005. Ubiquitin signalling in the NF-kappaB pathway. *Nat Cell Biol,* 7**,** 758-65.
CHENG, Q. & CHEN, J. 2011. The phenotype of MDM2 auto-degradation after DNA damage is due to epitope masking by phosphorylation. *Cell Cycle,* 10**,** 1162-6.
CHENG, Q., CROSS, B., LI, B., CHEN, L., LI, Z. & CHEN, J. 2011. Regulation of MDM2 E3 ligase activity by phosphorylation after DNA damage. *Mol Cell Biol,* 31**,** 4951-63.
CHI, S. W., LEE, S. H., KIM, D. H., AHN, M. J., KIM, J. S., WOO, J. Y., TORIZAWA, T., KAINOSHO, M. & HAN, K. H. 2005. Structural details on mdm2-p53 interaction. *J Biol Chem,* 280**,** 38795-802.
CHIPUK, J. E., BOUCHIER-HAYES, L., KUWANA, T., NEWMEYER, D. D. & GREEN, D. R. 2005. PUMA couples the nuclear and cytoplasmic proapoptotic function of p53. *Science,* 309**,** 1732-5.
CHIPUK, J. E., KUWANA, T., BOUCHIER-HAYES, L., DROIN, N. M., NEWMEYER, D. D., SCHULER, M. & GREEN, D. R. 2004. Direct activation of Bax by p53 mediates mitochondrial membrane permeabilization and apoptosis. *Science,* 303**,** 1010-4.
CHO, Y., GORINA, S., JEFFREY, P. D. & PAVLETICH, N. P. 1994. Crystal structure of a p53 tumor suppressor-DNA complex: understanding tumorigenic mutations. *Science,* 265**,** 346-55.

CHOI, J. & DONEHOWER, L. A. 1999. p53 in embryonic development: maintaining a fine balance. *Cell Mol Life Sci,* 55**,** 38-47.
CHOONG, M. L., YANG, H., LEE, M. A. & LANE, D. P. 2009. Specific activation of the p53 pathway by low dose actinomycin D: a new route to p53 based cyclotherapy. *Cell Cycle,* 8**,** 2810-8.
CHRISTENSEN, D. E., BRZOVIC, P. S. & KLEVIT, R. E. 2007. E2-BRCA1 RING interactions dictate synthesis of mono- or specific polyubiquitin chain linkages. *Nat Struct Mol Biol,* 14**,** 941-8.
CHU, Y. & YANG, X. 2011. SUMO E3 ligase activity of TRIM proteins. *Oncogene,* 30**,** 1108-16.
CIECHANOVER, A., ELIAS, S., HELLER, H. & HERSHKO, A. 1982. "Covalent affinity" purification of ubiquitin-activating enzyme. *J Biol Chem,* 257**,** 2537-42.
CIECHANOVER, A. & SCHWARTZ, A. L. 2004. The ubiquitin system: pathogenesis of human diseases and drug targeting. *Biochim Biophys Acta,* 1695**,** 3-17.
CIEHANOVER, A., HOD, Y. & HERSHKO, A. 1978. A heat-stable polypeptide component of an ATP-dependent proteolytic system from reticulocytes. *Biochem Biophys Res Commun,* 81**,** 1100-5.
CILLONI, D. & SAGLIO, G. 2012. Molecular pathways: BCR-ABL. *Clin Cancer Res,* 18**,** 930-7.
COLLINS, G. A. & GOLDBERG, A. L. 2017. The Logic of the 26S Proteasome. *Cell,* 169**,** 792-806.
CONG, L., RAN, F. A., COX, D., LIN, S., BARRETTO, R., HABIB, N., HSU, P. D., WU, X., JIANG, W., MARRAFFINI, L. A. & ZHANG, F. 2013. Multiplex genome engineering using CRISPR/Cas systems. *Science,* 339**,** 819-23.
CONTRACTOR, T. & HARRIS, C. R. 2012. p53 negatively regulates transcription of the pyruvate dehydrogenase kinase Pdk2. *Cancer Res,* 72**,** 560-7.
COPPE, J. P., PATIL, C. K., RODIER, F., SUN, Y., MUNOZ, D. P., GOLDSTEIN, J., NELSON, P. S., DESPREZ, P. Y. & CAMPISI, J. 2008. Senescence-associated secretory phenotypes reveal cell-nonautonomous functions of oncogenic RAS and the p53 tumor suppressor. *PLoS Biol,* 6**,** 2853-68.
CRIGHTON, D., WILKINSON, S., O'PREY, J., SYED, N., SMITH, P., HARRISON, P. R., GASCO, M., GARRONE, O., CROOK, T. & RYAN, K. M. 2006. DRAM, a p53-induced modulator of autophagy, is critical for apoptosis. *Cell,* 126**,** 121-34.
CROCE, C. M. 2008. Oncogenes and cancer. *N Engl J Med,* 358**,** 502-11.
CUMMINS, J. M., RAGO, C., KOHLI, M., KINZLER, K. W., LENGAUER, C. & VOGELSTEIN, B. 2004. Tumour suppression: disruption of HAUSP gene stabilizes p53. *Nature,* 428**,** 1 p following 486.
DAGOGO-JACK, I. & SHAW, A. T. 2018. Tumour heterogeneity and resistance to cancer therapies. *Nat Rev Clin Oncol,* 15**,** 81-94.
DAI, M. S., ZENG, S. X., JIN, Y., SUN, X. X., DAVID, L. & LU, H. 2004. Ribosomal protein L23 activates p53 by inhibiting MDM2 function in response to ribosomal perturbation but not to translation inhibition. *Mol Cell Biol,* 24**,** 7654-68.
DANKORT, D., CURLEY, D. P., CARTLIDGE, R. A., NELSON, B., KARNEZIS, A. N., DAMSKY, W. E., JR., YOU, M. J., DEPINHO, R. A., MCMAHON, M. & BOSENBERG, M. 2009. Braf(V600E) cooperates with Pten loss to induce metastatic melanoma. *Nat Genet,* 41**,** 544-52.
DE BIE, P., ZAAROOR-REGEV, D. & CIECHANOVER, A. 2010. Regulation of the Polycomb protein RING1B ubiquitination by USP7. *Biochem Biophys Res Commun,* 400**,** 389-95.

DE GRAAF, P., LITTLE, N. A., RAMOS, Y. F., MEULMEESTER, E., LETTEBOER, S. J. & JOCHEMSEN, A. G. 2003. Hdmx protein stability is regulated by the ubiquitin ligase activity of Mdm2. *J Biol Chem,* 278**,** 38315-24.

DE VRIES, W. N., BINNS, L. T., FANCHER, K. S., DEAN, J., MOORE, R., KEMLER, R. & KNOWLES, B. B. 2000. Expression of Cre recombinase in mouse oocytes: a means to study maternal effect genes. *Genesis,* 26**,** 110-2.

DERBYSHIRE, D. J., BASU, B. P., SERPELL, L. C., JOO, W. S., DATE, T., IWABUCHI, K. & DOHERTY, A. J. 2002. Crystal structure of human 53BP1 BRCT domains bound to p53 tumour suppressor. *Embo j,* 21**,** 3863-72.

DESHAIES, R. J. & JOAZEIRO, C. A. 2009. RING domain E3 ubiquitin ligases. *Annu Rev Biochem,* 78**,** 399-434.

DEVIN, A., COOK, A., LIN, Y., RODRIGUEZ, Y., KELLIHER, M. & LIU, Z. 2000. The distinct roles of TRAF2 and RIP in IKK activation by TNF-R1: TRAF2 recruits IKK to TNF-R1 while RIP mediates IKK activation. *Immunity,* 12**,** 419-29.

DHOMEN, N., REIS-FILHO, J. S., DA ROCHA DIAS, S., HAYWARD, R., SAVAGE, K., DELMAS, V., LARUE, L., PRITCHARD, C. & MARAIS, R. 2009. Oncogenic Braf induces melanocyte senescence and melanoma in mice. *Cancer Cell,* 15**,** 294-303.

DICATO, M., BOCCADORO, M., CAVENAGH, J., HAROUSSEAU, J. L., LUDWIG, H., SAN MIGUEL, J. & SONNEVELD, P. 2006. Management of multiple myeloma with bortezomib: experts review the data and debate the issues. *Oncology,* 70**,** 474-82.

DING, B., SUN, Y. & HUANG, J. 2012. Overexpression of SKI oncoprotein leads to p53 degradation through regulation of MDM2 protein sumoylation. *J Biol Chem,* 287**,** 14621-30.

DING, K., LU, Y., NIKOLOVSKA-COLESKA, Z., QIU, S., DING, Y., GAO, W., STUCKEY, J., KRAJEWSKI, K., ROLLER, P. P., TOMITA, Y., PARRISH, D. A., DESCHAMPS, J. R. & WANG, S. 2005. Structure-based design of potent non-peptide MDM2 inhibitors. *J Am Chem Soc,* 127**,** 10130-1.

DING, Q., ZHANG, Z., LIU, J. J., JIANG, N., ZHANG, J., ROSS, T. M., CHU, X. J., BARTKOVITZ, D., PODLASKI, F., JANSON, C., TOVAR, C., FILIPOVIC, Z. M., HIGGINS, B., GLENN, K., PACKMAN, K., VASSILEV, L. T. & GRAVES, B. 2013. Discovery of RG7388, a potent and selective p53-MDM2 inhibitor in clinical development. *J Med Chem,* 56**,** 5979-83.

DING, W. X., NI, H. M., CHEN, X., YU, J., ZHANG, L. & YIN, X. M. 2007. A coordinated action of Bax, PUMA, and p53 promotes MG132-induced mitochondria activation and apoptosis in colon cancer cells. *Mol Cancer Ther,* 6**,** 1062-9.

DIPPOLD, W. G., JAY, G., DELEO, A. B., KHOURY, G. & OLD, L. J. 1981. p53 transformation-related protein: detection by monoclonal antibody in mouse and human cells. *Proc Natl Acad Sci U S A,* 78**,** 1695-9.

DOMINGUEZ, C., BONVIN, A. M., WINKLER, G. S., VAN SCHAIK, F. M., TIMMERS, H. T. & BOELENS, R. 2004. Structural model of the UbcH5B/CNOT4 complex revealed by combining NMR, mutagenesis, and docking approaches. *Structure,* 12**,** 633-44.

DONEHOWER, L. A., HARVEY, M., SLAGLE, B. L., MCARTHUR, M. J., MONTGOMERY, C. A., JR., BUTEL, J. S. & BRADLEY, A. 1992. Mice deficient for p53 are developmentally normal but susceptible to spontaneous tumours. *Nature,* 356**,** 215-21.

DORNAN, D., BHEDDAH, S., NEWTON, K., INCE, W., FRANTZ, G. D., DOWD, P., KOEPPEN, H., DIXIT, V. M. & FRENCH, D. M. 2004a. COP1, the negative

regulator of p53, is overexpressed in breast and ovarian adenocarcinomas. *Cancer Res,* 64**,** 7226-30.
DORNAN, D., WERTZ, I., SHIMIZU, H., ARNOTT, D., FRANTZ, G. D., DOWD, P., O'ROURKE, K., KOEPPEN, H. & DIXIT, V. M. 2004b. The ubiquitin ligase COP1 is a critical negative regulator of p53. *Nature,* 429**,** 86-92.
DOU, H., BUETOW, L., SIBBET, G. J., CAMERON, K. & HUANG, D. T. 2012. BIRC7-E2 ubiquitin conjugate structure reveals the mechanism of ubiquitin transfer by a RING dimer. *Nat Struct Mol Biol,* 19**,** 876-83.
DOU, H., BUETOW, L., SIBBET, G. J., CAMERON, K. & HUANG, D. T. 2013. Essentiality of a non-RING element in priming donor ubiquitin for catalysis by a monomeric E3. *Nat Struct Mol Biol,* 20**,** 982-986.
DUAN, W., GAO, L., DRUHAN, L. J., ZHU, W. G., MORRISON, C., OTTERSON, G. A. & VILLALONA-CALERO, M. A. 2004. Expression of Pirh2, a newly identified ubiquitin protein ligase, in lung cancer. *J Natl Cancer Inst,* 96**,** 1718-21.
DUDA, D. M., BORG, L. A., SCOTT, D. C., HUNT, H. W., HAMMEL, M. & SCHULMAN, B. A. 2008. Structural insights into NEDD8 activation of cullin-RING ligases: conformational control of conjugation. *Cell,* 134**,** 995-1006.
EISCHEN, C. M. 2017. Role of Mdm2 and Mdmx in DNA repair. *J Mol Cell Biol,* 9**,** 69-73.
EISCHEN, C. M., WEBER, J. D., ROUSSEL, M. F., SHERR, C. J. & CLEVELAND, J. L. 1999. Disruption of the ARF-Mdm2-p53 tumor suppressor pathway in Myc-induced lymphomagenesis. *Genes Dev,* 13**,** 2658-69.
EL-DAHR, S., HILLIARD, S. & SAIFUDEEN, Z. 2017. Regulation of kidney development by the Mdm2/Mdm4-p53 axis. *J Mol Cell Biol,* 9**,** 26-33.
EL-GAMAL, M. I., ANBAR, H. S., YOO, K. H. & OH, C. H. 2013. FMS Kinase Inhibitors: Current Status and Future Prospects. *Med Res Rev,* 33**,** 599-636.
ELIYAHU, D., GOLDFINGER, N., PINHASI-KIMHI, O., SHAULSKY, G., SKURNIK, Y., ARAI, N., ROTTER, V. & OREN, M. 1988. Meth A fibrosarcoma cells express two transforming mutant p53 species. *Oncogene,* 3**,** 313-21.
ENCHEV, R. I., SCHULMAN, B. A. & PETER, M. 2015. Protein neddylation: beyond cullin-RING ligases. *Nat Rev Mol Cell Biol,* 16**,** 30-44.
ESPINOSA, J. M. & EMERSON, B. M. 2001. Transcriptional regulation by p53 through intrinsic DNA/chromatin binding and site-directed cofactor recruitment. *Mol Cell,* 8**,** 57-69.
ESPOSITO, I., KLEEFF, J., ABIATARI, I., SHI, X., GIESE, N., BERGMANN, F., ROTH, W., FRIESS, H. & SCHIRMACHER, P. 2007. Overexpression of cellular inhibitor of apoptosis protein 2 is an early event in the progression of pancreatic cancer. *J Clin Pathol,* 60**,** 885-95.
ETLINGER, J. D. & GOLDBERG, A. L. 1977. A soluble ATP-dependent proteolytic system responsible for the degradation of abnormal proteins in reticulocytes. *Proc Natl Acad Sci U S A,* 74**,** 54-8.
FAKHARZADEH, S. S., TRUSKO, S. P. & GEORGE, D. L. 1991. Tumorigenic potential associated with enhanced expression of a gene that is amplified in a mouse tumor cell line. *Embo j,* 10**,** 1565-9.
FANG, S., JENSEN, J. P., LUDWIG, R. L., VOUSDEN, K. H. & WEISSMAN, A. M. 2000. Mdm2 is a RING finger-dependent ubiquitin protein ligase for itself and p53. *J Biol Chem,* 275**,** 8945-51.
FINCH, R. A., DONOVIEL, D. B., POTTER, D., SHI, M., FAN, A., FREED, D. D., WANG, C. Y., ZAMBROWICZ, B. P., RAMIREZ-SOLIS, R., SANDS, A. T. &

ZHANG, N. 2002. mdmx is a negative regulator of p53 activity in vivo. *Cancer Res,* 62**,** 3221-5.
FINLAY, C. A., HINDS, P. W. & LEVINE, A. J. 1989. The p53 proto-oncogene can act as a suppressor of transformation. *Cell,* 57**,** 1083-93.
FINLAY, C. A., HINDS, P. W., TAN, T. H., ELIYAHU, D., OREN, M. & LEVINE, A. J. 1988. Activating mutations for transformation by p53 produce a gene product that forms an hsc70-p53 complex with an altered half-life. *Mol Cell Biol,* 8**,** 531-9.
FINLEY, D., BARTEL, B. & VARSHAVSKY, A. 1989. The tails of ubiquitin precursors are ribosomal proteins whose fusion to ubiquitin facilitates ribosome biogenesis. *Nature,* 338**,** 394-401.
FISCHER, M. 2017. Census and evaluation of p53 target genes. *Oncogene,* 36**,** 3943-3956.
FRANCOZ, S., FROMENT, P., BOGAERTS, S., DE CLERCQ, S., MAETENS, M., DOUMONT, G., BELLEFROID, E. & MARINE, J. C. 2006. Mdm4 and Mdm2 cooperate to inhibit p53 activity in proliferating and quiescent cells in vivo. *Proc Natl Acad Sci U S A,* 103**,** 3232-7.
FREEDMAN, D. A., EPSTEIN, C. B., ROTH, J. C. & LEVINE, A. J. 1997. A genetic approach to mapping the p53 binding site in the MDM2 protein. *Mol Med,* 3**,** 248-59.
FREEDMAN, D. A. & LEVINE, A. J. 1998. Nuclear export is required for degradation of endogenous p53 by MDM2 and human papillomavirus E6. *Mol Cell Biol,* 18**,** 7288-93.
FRIBLEY, A. M., EVENCHIK, B., ZENG, Q., PARK, B. K., GUAN, J. Y., ZHANG, H., HALE, T. J., SOENGAS, M. S., KAUFMAN, R. J. & WANG, C. Y. 2006. Proteasome inhibitor PS-341 induces apoptosis in cisplatin-resistant squamous cell carcinoma cells by induction of Noxa. *J Biol Chem,* 281**,** 31440-7.
FU, W., MA, Q., CHEN, L., LI, P., ZHANG, M., RAMAMOORTHY, S., NAWAZ, Z., SHIMOJIMA, T., WANG, H., YANG, Y., SHEN, Z., ZHANG, Y., ZHANG, X., NICOSIA, S. V., ZHANG, Y., PLEDGER, J. W., CHEN, J. & BAI, W. 2009. MDM2 acts downstream of p53 as an E3 ligase to promote FOXO ubiquitination and degradation. *J Biol Chem,* 284**,** 13987-4000.
FUCHS, S. Y., ADLER, V., BUSCHMANN, T., WU, X. & RONAI, Z. 1998. Mdm2 association with p53 targets its ubiquitination. *Oncogene,* 17**,** 2543-7.
FUJITA, T., LIU, W., DOIHARA, H., DATE, H. & WAN, Y. 2008. Dissection of the APCCdh1-Skp2 cascade in breast cancer. *Clin Cancer Res,* 14**,** 1966-75.
GAMSJAEGER, R., LIEW, C. K., LOUGHLIN, F. E., CROSSLEY, M. & MACKAY, J. P. 2007. Sticky fingers: zinc-fingers as protein-recognition motifs. *Trends Biochem Sci,* 32**,** 63-70.
GANGULI, G. & WASYLYK, B. 2003. p53-independent functions of MDM2. *Mol Cancer Res,* 1**,** 1027-35.
GANNON, H. S., WODA, B. A. & JONES, S. N. 2012. ATM phosphorylation of Mdm2 Ser394 regulates the amplitude and duration of the DNA damage response in mice. *Cancer Cell,* 21**,** 668-79.
GARCIA-CAO, I., GARCIA-CAO, M., MARTIN-CABALLERO, J., CRIADO, L. M., KLATT, P., FLORES, J. M., WEILL, J. C., BLASCO, M. A. & SERRANO, M. 2002. "Super p53" mice exhibit enhanced DNA damage response, are tumor resistant and age normally. *Embo j,* 21**,** 6225-35.
GAREAU, J. R. & LIMA, C. D. 2010. The SUMO pathway: emerging mechanisms that shape specificity, conjugation and recognition. *Nat Rev Mol Cell Biol,* 11**,** 861-71.

GEIER, E., PFEIFER, G., WILM, M., LUCCHIARI-HARTZ, M., BAUMEISTER, W., EICHMANN, K. & NIEDERMANN, G. 1999. A giant protease with potential to substitute for some functions of the proteasome. *Science,* 283**,** 978-81.

GEMBARSKA, A., LUCIANI, F., FEDELE, C., RUSSELL, E. A., DEWAELE, M., VILLAR, S., ZWOLINSKA, A., HAUPT, S., DE LANGE, J., YIP, D., GOYDOS, J., HAIGH, J. J., HAUPT, Y., LARUE, L., JOCHEMSEN, A., SHI, H., MORICEAU, G., LO, R. S., GHANEM, G., SHACKLETON, M., BERNAL, F. & MARINE, J. C. 2012. MDM4 is a key therapeutic target in cutaneous melanoma. *Nat Med,* 18**,** 1239-47.

GEYER, R. K., YU, Z. K. & MAKI, C. G. 2000. The MDM2 RING-finger domain is required to promote p53 nuclear export. *Nat Cell Biol,* 2**,** 569-73.

GILKES, D. M., PAN, Y., COPPOLA, D., YEATMAN, T., REUTHER, G. W. & CHEN, J. 2008. Regulation of MDMX expression by mitogenic signaling. *Mol Cell Biol,* 28**,** 1999-2010.

GLAS, R., BOGYO, M., MCMASTER, J. S., GACZYNSKA, M. & PLOEGH, H. L. 1998. A proteolytic system that compensates for loss of proteasome function. *Nature,* 392**,** 618-22.

GLYNNE, R., POWIS, S. H., BECK, S., KELLY, A., KERR, L. A. & TROWSDALE, J. 1991. A proteasome-related gene between the two ABC transporter loci in the class II region of the human MHC. *Nature,* 353**,** 357-60.

GOEL, V. K., IBRAHIM, N., JIANG, G., SINGHAL, M., FEE, S., FLOTTE, T., WESTMORELAND, S., HALUSKA, F. S., HINDS, P. W. & HALUSKA, F. G. 2009. Melanocytic nevus-like hyperplasia and melanoma in transgenic BRAFV600E mice. *Oncogene,* 28**,** 2289-98.

GOH, A. M. & LANE, D. P. 2012. How p53 wields the scales of fate: arrest or death? *Transcription,* 3**,** 240-4.

GORINA, S. & PAVLETICH, N. P. 1996. Structure of the p53 tumor suppressor bound to the ankyrin and SH3 domains of 53BP2. *Science,* 274**,** 1001-5.

GRAUS-PORTA, D., BLAESS, S., SENFTEN, M., LITTLEWOOD-EVANS, A., DAMSKY, C., HUANG, Z., ORBAN, P., KLEIN, R., SCHITTNY, J. C. & MULLER, U. 2001. Beta1-class integrins regulate the development of laminae and folia in the cerebral and cerebellar cortex. *Neuron,* 31**,** 367-79.

GRAY, T. A., WILSON, A., FORTIN, P. J. & NICHOLLS, R. D. 2006. The putatively functional Mkrn1-p1 pseudogene is neither expressed nor imprinted, nor does it regulate its source gene in trans. *Proc Natl Acad Sci U S A,* 103**,** 12039-44.

GRIER, J. D., XIONG, S., ELIZONDO-FRAIRE, A. C., PARANT, J. M. & LOZANO, G. 2006. Tissue-specific differences of p53 inhibition by Mdm2 and Mdm4. *Mol Cell Biol,* 26**,** 192-8.

GU, B. & ZHU, W. G. 2012. Surf the post-translational modification network of p53 regulation. *Int J Biol Sci,* 8**,** 672-84.

GUO, J., LIU, X. & WANG, M. 2015. miR-503 suppresses tumor cell proliferation and metastasis by directly targeting RNF31 in prostate cancer. *Biochem Biophys Res Commun,* 464**,** 1302-8.

GUPTA, S., RADHA, V., FURUKAWA, Y. & SWARUP, G. 2001. Direct transcriptional activation of human caspase-1 by tumor suppressor p53. *J Biol Chem,* 276**,** 10585-8.

GUTERMAN, A. & GLICKMAN, M. H. 2004. Complementary roles for Rpn11 and Ubp6 in deubiquitination and proteolysis by the proteasome. *J Biol Chem,* 279**,** 1729-38.

HALL, T. M. 2005. Multiple modes of RNA recognition by zinc finger proteins. *Curr Opin Struct Biol,* 15**,** 367-73.

HAMEYER, D., LOONSTRA, A., ESHKIND, L., SCHMITT, S., ANTUNES, C., GROEN, A., BINDELS, E., JONKERS, J., KRIMPENFORT, P., MEUWISSEN, R., RIJSWIJK, L., BEX, A., BERNS, A. & BOCKAMP, E. 2007. Toxicity of ligand-dependent Cre recombinases and generation of a conditional Cre deleter mouse allowing mosaic recombination in peripheral tissues. *Physiol Genomics,* 31**,** 32-41.

HANAHAN, D. & WEINBERG, R. A. 2011. Hallmarks of cancer: the next generation. *Cell,* 144**,** 646-74.

HARTL, F. U. 2017. Protein Misfolding Diseases. *Annu Rev Biochem,* 86**,** 21-26.

HAYDEN, M. S. & GHOSH, S. 2004. Signaling to NF-kappaB. *Genes Dev,* 18**,** 2195-224.

HERMEKING, H. 2012. MicroRNAs in the p53 network: micromanagement of tumour suppression. *Nat Rev Cancer,* 12**,** 613-26.

HERSHKO, A. & CIECHANOVER, A. 1992. The ubiquitin system for protein degradation. *Annu Rev Biochem,* 61**,** 761-807.

HERSHKO, A. & CIECHANOVER, A. 1998. The ubiquitin system. *Annu Rev Biochem,* 67**,** 425-79.

HERSHKO, A., CIECHANOVER, A., HELLER, H., HAAS, A. L. & ROSE, I. A. 1980. Proposed role of ATP in protein breakdown: conjugation of protein with multiple chains of the polypeptide of ATP-dependent proteolysis. *Proc Natl Acad Sci U S A,* 77**,** 1783-6.

HERSHKO, A., HELLER, H., ELIAS, S. & CIECHANOVER, A. 1983. Components of ubiquitin-protein ligase system. Resolution, affinity purification, and role in protein breakdown. *J Biol Chem,* 258**,** 8206-14.

HIGASHITSUJI, H., HIGASHITSUJI, H., ITOH, K., SAKURAI, T., NAGAO, T., SUMITOMO, Y., MASUDA, T., DAWSON, S., SHIMADA, Y., MAYER, R. J. & FUJITA, J. 2005. The oncoprotein gankyrin binds to MDM2/HDM2, enhancing ubiquitylation and degradation of p53. *Cancer Cell,* 8**,** 75-87.

HILLIARD, S., ABOUDEHEN, K., YAO, X. & EL-DAHR, S. S. 2011. Tight regulation of p53 activity by Mdm2 is required for ureteric bud growth and branching. *Dev Biol,* 353**,** 354-66.

HINGORANI, S. R., PETRICOIN, E. F., MAITRA, A., RAJAPAKSE, V., KING, C., JACOBETZ, M. A., ROSS, S., CONRADS, T. P., VEENSTRA, T. D., HITT, B. A., KAWAGUCHI, Y., JOHANN, D., LIOTTA, L. A., CRAWFORD, H. C., PUTT, M. E., JACKS, T., WRIGHT, C. V., HRUBAN, R. H., LOWY, A. M. & TUVESON, D. A. 2003. Preinvasive and invasive ductal pancreatic cancer and its early detection in the mouse. *Cancer Cell,* 4**,** 437-50.

HIRAO, A., KONG, Y. Y., MATSUOKA, S., WAKEHAM, A., RULAND, J., YOSHIDA, H., LIU, D., ELLEDGE, S. J. & MAK, T. W. 2000. DNA damage-induced activation of p53 by the checkpoint kinase Chk2. *Science,* 287**,** 1824-7.

HJERPE, R., THOMAS, Y., CHEN, J., ZEMLA, A., CURRAN, S., SHPIRO, N., DICK, L. R. & KURZ, T. 2012. Changes in the ratio of free NEDD8 to ubiquitin triggers NEDDylation by ubiquitin enzymes. *Biochem J,* 441**,** 927-36.

HOCHSTRASSER, M. 2009. Origin and function of ubiquitin-like proteins. *Nature,* 458**,** 422-9.

HOCK, A. K., VIGNERON, A. M., CARTER, S., LUDWIG, R. L. & VOUSDEN, K. H. 2011. Regulation of p53 stability and function by the deubiquitinating enzyme USP42. *Embo j,* 30**,** 4921-30.

HOCK, A. K. & VOUSDEN, K. H. 2014. The role of ubiquitin modification in the regulation of p53. *Biochim Biophys Acta,* 1843**,** 137-49.

HOFMANN, R. M. & PICKART, C. M. 1999. Noncanonical MMS2-encoded ubiquitin-conjugating enzyme functions in assembly of novel polyubiquitin chains for DNA repair. *Cell,* 96**,** 645-53.
HONDA, R., TANAKA, H. & YASUDA, H. 1997. Oncoprotein MDM2 is a ubiquitin ligase E3 for tumor suppressor p53. *FEBS Lett,* 420**,** 25-7.
HU, M., GU, L., LI, M., JEFFREY, P. D., GU, W. & SHI, Y. 2006. Structural basis of competitive recognition of p53 and MDM2 by HAUSP/USP7: implications for the regulation of the p53-MDM2 pathway. *PLoS Biol,* 4**,** e27.
HU, W., CHAN, C. S., WU, R., ZHANG, C., SUN, Y., SONG, J. S., TANG, L. H., LEVINE, A. J. & FENG, Z. 2010. Negative regulation of tumor suppressor p53 by microRNA miR-504. *Mol Cell,* 38**,** 689-99.
HUANG, D. T., AYRAULT, O., HUNT, H. W., TAHERBHOY, A. M., DUDA, D. M., SCOTT, D. C., BORG, L. A., NEALE, G., MURRAY, P. J., ROUSSEL, M. F. & SCHULMAN, B. A. 2009. E2-RING expansion of the NEDD8 cascade confers specificity to cullin modification. *Mol Cell,* 33**,** 483-95.
HUANG, H. C., LIN, C. L. & LIN, J. K. 2011a. 1,2,3,4,6-penta-O-galloyl-beta-D-glucose, quercetin, curcumin and lycopene induce cell-cycle arrest in MDA-MB-231 and BT474 cells through downregulation of Skp2 protein. *J Agric Food Chem,* 59**,** 6765-75.
HUANG, H. L., WENG, H. Y., WANG, L. Q., YU, C. H., HUANG, Q. J., ZHAO, P. P., WEN, J. Z., ZHOU, H. & QU, L. H. 2012. Triggering Fbw7-mediated proteasomal degradation of c-Myc by oridonin induces cell growth inhibition and apoptosis. *Mol Cancer Ther,* 11**,** 1155-65.
HUANG, J., PEREZ-BURGOS, L., PLACEK, B. J., SENGUPTA, R., RICHTER, M., DORSEY, J. A., KUBICEK, S., OPRAVIL, S., JENUWEIN, T. & BERGER, S. L. 2006. Repression of p53 activity by Smyd2-mediated methylation. *Nature,* 444**,** 629-32.
HUANG, J., SENGUPTA, R., ESPEJO, A. B., LEE, M. G., DORSEY, J. A., RICHTER, M., OPRAVIL, S., SHIEKHATTAR, R., BEDFORD, M. T., JENUWEIN, T. & BERGER, S. L. 2007. p53 is regulated by the lysine demethylase LSD1. *Nature,* 449**,** 105-8.
HUANG, L., YAN, Z., LIAO, X., LI, Y., YANG, J., WANG, Z. G., ZUO, Y., KAWAI, H., SHADFAN, M., GANAPATHY, S. & YUAN, Z. M. 2011b. The p53 inhibitors MDM2/MDMX complex is required for control of p53 activity in vivo. *Proc Natl Acad Sci U S A,* 108**,** 12001-6.
HUANG, X., LUAN, B., WU, J. & SHI, Y. 2016. An atomic structure of the human 26S proteasome. *Nat Struct Mol Biol,* 23**,** 778-85.
HYER, M. L., MILHOLLEN, M. A., CIAVARRI, J., FLEMING, P., TRAORE, T., SAPPAL, D., HUCK, J., SHI, J., GAVIN, J., BROWNELL, J., YANG, Y., STRINGER, B., GRIFFIN, R., BRUZZESE, F., SOUCY, T., DUFFY, J., RABINO, C., RICEBERG, J., HOAR, K., LUBLINSKY, A., MENON, S., SINTCHAK, M., BUMP, N., PULUKURI, S. M., LANGSTON, S., TIRRELL, S., KURANDA, M., VEIBY, P., NEWCOMB, J., LI, P., WU, J. T., POWE, J. & DICK, L. R. 2018. A small-molecule inhibitor of the ubiquitin activating enzyme for cancer treatment. 24**,** 186-193.
IACOBUZIO-DONAHUE, C. A. 2009. Epigenetic changes in cancer. *Annu Rev Pathol,* 4**,** 229-49.
INOBE, T. & MATOUSCHEK, A. 2014. Paradigms of protein degradation by the proteasome. *Curr Opin Struct Biol,* 24**,** 156-64.
ISSAEVA, N., BOZKO, P., ENGE, M., PROTOPOPOVA, M., VERHOEF, L. G., MASUCCI, M., PRAMANIK, A. & SELIVANOVA, G. 2004. Small molecule RITA

binds to p53, blocks p53-HDM-2 interaction and activates p53 function in tumors. *Nat Med,* 10**,** 1321-8.
ITAHANA, K., MAO, H., JIN, A., ITAHANA, Y., CLEGG, H. V., LINDSTROM, M. S., BHAT, K. P., GODFREY, V. L., EVAN, G. I. & ZHANG, Y. 2007. Targeted inactivation of Mdm2 RING finger E3 ubiquitin ligase activity in the mouse reveals mechanistic insights into p53 regulation. *Cancer Cell,* 12**,** 355-66.
ITO, A., LAI, C. H., ZHAO, X., SAITO, S., HAMILTON, M. H., APPELLA, E. & YAO, T. P. 2001. p300/CBP-mediated p53 acetylation is commonly induced by p53-activating agents and inhibited by MDM2. *Embo j,* 20**,** 1331-40.
ITOH, Y., ISHIKAWA, M., NAITO, M. & HASHIMOTO, Y. 2010. Protein knockdown using methyl bestatin-ligand hybrid molecules: design and synthesis of inducers of ubiquitination-mediated degradation of cellular retinoic acid-binding proteins. *J Am Chem Soc,* 132**,** 5820-6.
IWAI, K. & TOKUNAGA, F. 2009. Linear polyubiquitination: a new regulator of NF-kappaB activation. *EMBO Rep,* 10**,** 706-13.
IYAPPAN, S., WOLLSCHEID, H. P., ROJAS-FERNANDEZ, A., MARQUARDT, A., TANG, H. C., SINGH, R. K. & SCHEFFNER, M. 2010. Turning the RING domain protein MdmX into an active ubiquitin-protein ligase. *J Biol Chem,* 285**,** 33065-72.
JACKS, T., REMINGTON, L., WILLIAMS, B. O., SCHMITT, E. M., HALACHMI, S., BRONSON, R. T. & WEINBERG, R. A. 1994. Tumor spectrum analysis in p53-mutant mice. *Curr Biol,* 4**,** 1-7.
JACKSON, M. W. & BERBERICH, S. J. 2000. MdmX protects p53 from Mdm2-mediated degradation. *Mol Cell Biol,* 20**,** 1001-7.
JAGELSKA, E. B., BRAZDA, V., PECINKA, P., PALECEK, E. & FOJTA, M. 2008. DNA topology influences p53 sequence-specific DNA binding through structural transitions within the target sites. *Biochem J,* 412**,** 57-63.
JAGELSKA, E. B., PIVONKOVA, H., FOJTA, M. & BRAZDA, V. 2010. The potential of the cruciform structure formation as an important factor influencing p53 sequence-specific binding to natural DNA targets. *Biochem Biophys Res Commun,* 391**,** 1409-14.
JAIN, A. K., ALLTON, K., DUNCAN, A. D. & BARTON, M. C. 2014. TRIM24 is a p53-induced E3-ubiquitin ligase that undergoes ATM-mediated phosphorylation and autodegradation during DNA damage. *Mol Cell Biol,* 34**,** 2695-709.
JANSSENS, S. & BEYAERT, R. 2003. Functional diversity and regulation of different interleukin-1 receptor-associated kinase (IRAK) family members. *Mol Cell,* 11**,** 293-302.
JEFFREY, P. D., GORINA, S. & PAVLETICH, N. P. 1995. Crystal structure of the tetramerization domain of the p53 tumor suppressor at 1.7 angstroms. *Science,* 267**,** 1498-502.
JEWELL, U. R., KVIETIKOVA, I., SCHEID, A., BAUER, C., WENGER, R. H. & GASSMANN, M. 2001. Induction of HIF-1alpha in response to hypoxia is instantaneous. *Faseb j,* 15**,** 1312-4.
JIANG, D., BRADY, C. A., JOHNSON, T. M., LEE, E. Y., PARK, E. J., SCOTT, M. P. & ATTARDI, L. D. 2011a. Full p53 transcriptional activation potential is dispensable for tumor suppression in diverse lineages. *Proc Natl Acad Sci U S A,* 108**,** 17123-8.
JIANG, J., JEDINAK, A. & SLIVA, D. 2011b. Ganodermanontriol (GDNT) exerts its effect on growth and invasiveness of breast cancer cells through the down-regulation of CDC20 and uPA. *Biochem Biophys Res Commun,* 415**,** 325-9.

JIANG, J. & SLIVA, D. 2010. Novel medicinal mushroom blend suppresses growth and invasiveness of human breast cancer cells. *Int J Oncol,* 37**,** 1529-36.
JIANG, L., KON, N., LI, T., WANG, S. J., SU, T., HIBSHOOSH, H., BAER, R. & GU, W. 2015a. Ferroptosis as a p53-mediated activity during tumour suppression. *Nature,* 520**,** 57-62.
JIANG, S., MINTER, L. C., STRATTON, S. A., YANG, P., ABBAS, H. A., AKDEMIR, Z. C., PANT, V., POST, S., GAGEA, M., LEE, R. G., LOZANO, G. & BARTON, M. C. 2015b. TRIM24 suppresses development of spontaneous hepatic lipid accumulation and hepatocellular carcinoma in mice. *J Hepatol,* 62**,** 371-9.
JIN, J., LI, X., GYGI, S. P. & HARPER, J. W. 2007. Dual E1 activation systems for ubiquitin differentially regulate E2 enzyme charging. *Nature,* 447**,** 1135-8.
JOAZEIRO, C. A. & WEISSMAN, A. M. 2000. RING finger proteins: mediators of ubiquitin ligase activity. *Cell,* 102**,** 549-52.
JOHNSON, D. G. & SCHNEIDER-BROUSSARD, R. 1998. Role of E2F in cell cycle control and cancer. *Front Biosci,* 3**,** d447-8.
JOHNSON, E. S. & BLOBEL, G. 1997. Ubc9p is the conjugating enzyme for the ubiquitin-like protein Smt3p. *J Biol Chem,* 272**,** 26799-802.
JONES, R. G., PLAS, D. R., KUBEK, S., BUZZAI, M., MU, J., XU, Y., BIRNBAUM, M. J. & THOMPSON, C. B. 2005. AMP-activated protein kinase induces a p53-dependent metabolic checkpoint. *Mol Cell,* 18**,** 283-93.
JONES, S. N., HANCOCK, A. R., VOGEL, H., DONEHOWER, L. A. & BRADLEY, A. 1998. Overexpression of Mdm2 in mice reveals a p53-independent role for Mdm2 in tumorigenesis. *Proc Natl Acad Sci U S A,* 95**,** 15608-12.
JONES, S. N., ROE, A. E., DONEHOWER, L. A. & BRADLEY, A. 1995. Rescue of embryonic lethality in Mdm2-deficient mice by absence of p53. *Nature,* 378**,** 206-8.
JOO, W. S., JEFFREY, P. D., CANTOR, S. B., FINNIN, M. S., LIVINGSTON, D. M. & PAVLETICH, N. P. 2002. Structure of the 53BP1 BRCT region bound to p53 and its comparison to the Brca1 BRCT structure. *Genes Dev,* 16**,** 583-93.
JUNG, C. H., RO, S. H., CAO, J., OTTO, N. M. & KIM, D. H. 2010. mTOR regulation of autophagy. *FEBS Lett,* 584**,** 1287-95.
JUNG, Y. S., HAKEM, A., HAKEM, R. & CHEN, X. 2011. Pirh2 E3 ubiquitin ligase monoubiquitinates DNA polymerase eta to suppress translesion DNA synthesis. *Mol Cell Biol,* 31**,** 3997-4006.
KADAKIA, M., BROWN, T. L., MCGORRY, M. M. & BERBERICH, S. J. 2002. MdmX inhibits Smad transactivation. *Oncogene,* 21**,** 8776-85.
KALES, S. C., RYAN, P. E., NAU, M. M. & LIPKOWITZ, S. 2010. Cbl and human myeloid neoplasms: the Cbl oncogene comes of age. *Cancer Res,* 70**,** 4789-94.
KAMIJO, T., VAN DE KAMP, E., CHONG, M. J., ZINDY, F., DIEHL, J. A., SHERR, C. J. & MCKINNON, P. J. 1999. Loss of the ARF tumor suppressor reverses premature replicative arrest but not radiation hypersensitivity arising from disabled atm function. *Cancer Res,* 59**,** 2464-9.
KARRA, H., REPO, H., AHONEN, I., LOYTTYNIEMI, E., PITKANEN, R., LINTUNEN, M., KUOPIO, T., SODERSTROM, M. & KRONQVIST, P. 2014. Cdc20 and securin overexpression predict short-term breast cancer survival. *Br J Cancer,* 110**,** 2905-13.
KASS, E. M., POYUROVSKY, M. V., ZHU, Y. & PRIVES, C. 2009. Mdm2 and PCAF increase Chk2 ubiquitination and degradation independently of their intrinsic E3 ligase activities. *Cell Cycle,* 8**,** 430-7.
KASTAN, M. B. 2007. Wild-type p53: tumors can't stand it. *Cell,* 128**,** 837-40.

KASTAN, M. B. & KUERBITZ, S. J. 1993. Control of G1 arrest after DNA damage. *Environ Health Perspect,* 101 Suppl 5**,** 55-8.

KASTAN, M. B., ONYEKWERE, O., SIDRANSKY, D., VOGELSTEIN, B. & CRAIG, R. W. 1991. Participation of p53 protein in the cellular response to DNA damage. *Cancer Res,* 51**,** 6304-11.

KATEGAYA, L., DI LELLO, P., ROUGE, L., PASTOR, R., CLARK, K. R., DRUMMOND, J., KLEINHEINZ, T., LIN, E., UPTON, J. P., PRAKASH, S., HEIDEKER, J., MCCLELAND, M., RITORTO, M. S., ALESSI, D. R., TROST, M., BAINBRIDGE, T. W., KWOK, M. C. M., MA, T. P., STIFFLER, Z., BRASHER, B., TANG, Y., JAISHANKAR, P., HEARN, B. R., RENSLO, A. R., ARKIN, M. R., COHEN, F., YU, K., PEALE, F., GNAD, F., CHANG, M. T., KLIJN, C., BLACKWOOD, E., MARTIN, S. E., FORREST, W. F., ERNST, J. A., NDUBAKU, C., WANG, X., BERESINI, M. H., TSUI, V., SCHWERDTFEGER, C., BLAKE, R. A., MURRAY, J., MAURER, T. & WERTZ, I. E. 2017. USP7 small-molecule inhibitors interfere with ubiquitin binding. *Nature,* 550**,** 534-538.

KAWAI, H., WIEDERSCHAIN, D., KITAO, H., STUART, J., TSAI, K. K. & YUAN, Z. M. 2003a. DNA damage-induced MDMX degradation is mediated by MDM2. *J Biol Chem,* 278**,** 45946-53.

KAWAI, H., WIEDERSCHAIN, D. & YUAN, Z. M. 2003b. Critical contribution of the MDM2 acidic domain to p53 ubiquitination. *Mol Cell Biol,* 23**,** 4939-47.

KAWAKAMI, T., CHIBA, T., SUZUKI, T., IWAI, K., YAMANAKA, K., MINATO, N., SUZUKI, H., SHIMBARA, N., HIDAKA, Y., OSAKA, F., OMATA, M. & TANAKA, K. 2001. NEDD8 recruits E2-ubiquitin to SCF E3 ligase. *Embo j,* 20**,** 4003-12.

KAWASE, T., OHKI, R., SHIBATA, T., TSUTSUMI, S., KAMIMURA, N., INAZAWA, J., OHTA, T., ICHIKAWA, H., ABURATANI, H., TASHIRO, F. & TAYA, Y. 2009. PH domain-only protein PHLDA3 is a p53-regulated repressor of Akt. *Cell,* 136**,** 535-50.

KAWAUCHI, K., ARAKI, K., TOBIUME, K. & TANAKA, N. 2008. p53 regulates glucose metabolism through an IKK-NF-kappaB pathway and inhibits cell transformation. *Nat Cell Biol,* 10**,** 611-8.

KELLY, A., POWIS, S. H., GLYNNE, R., RADLEY, E., BECK, S. & TROWSDALE, J. 1991. Second proteasome-related gene in the human MHC class II region. *Nature,* 353**,** 667-8.

KERN, S. E., KINZLER, K. W., BRUSKIN, A., JAROSZ, D., FRIEDMAN, P., PRIVES, C. & VOGELSTEIN, B. 1991. Identification of p53 as a sequence-specific DNA-binding protein. *Science,* 252**,** 1708-11.

KHELLA, H. W., BAKHET, M., ALLO, G., JEWETT, M. A., GIRGIS, A. H., LATIF, A., GIRGIS, H., VON BOTH, I., BJARNASON, G. A. & YOUSEF, G. M. 2013. miR-192, miR-194 and miR-215: a convergent microRNA network suppressing tumor progression in renal cell carcinoma. *Carcinogenesis,* 34**,** 2231-9.

KHOO, K. H., VERMA, C. S. & LANE, D. P. 2014. Drugging the p53 pathway: understanding the route to clinical efficacy. *Nat Rev Drug Discov,* 13**,** 217-36.

KIM, E. J., KIM, S. H., JIN, X., JIN, X. & KIM, H. 2017. KCTD2, an adaptor of Cullin3 E3 ubiquitin ligase, suppresses gliomagenesis by destabilizing c-Myc. *Cell Death Differ,* 24**,** 649-659.

KIM, H. R., ROE, J. S., LEE, J. E., CHO, E. J. & YOUN, H. D. 2013. p53 regulates glucose metabolism by miR-34a. *Biochem Biophys Res Commun,* 437**,** 225-31.

KIM, J., KUNDU, M., VIOLLET, B. & GUAN, K. L. 2011a. AMPK and mTOR regulate autophagy through direct phosphorylation of Ulk1. *Nat Cell Biol,* 13**,** 132-41.

KIM, W., BENNETT, E. J., HUTTLIN, E. L., GUO, A., LI, J., POSSEMATO, A., SOWA, M. E., RAD, R., RUSH, J., COMB, M. J., HARPER, J. W. & GYGI, S. P. 2011b. Systematic and quantitative assessment of the ubiquitin-modified proteome. *Mol Cell,* 44**,** 325-40.

KINCAID, E. Z. & MURATA, S. 2016. Specialized proteasome subunits have an essential role in the thymic selection of CD8(+) T cells. 17**,** 938-45.

KIRISAKO, T., KAMEI, K., MURATA, S., KATO, M., FUKUMOTO, H., KANIE, M., SANO, S., TOKUNAGA, F., TANAKA, K. & IWAI, K. 2006. A ubiquitin ligase complex assembles linear polyubiquitin chains. *Embo j,* 25**,** 4877-87.

KIRKPATRICK, D. S., HATHAWAY, N. A., HANNA, J., ELSASSER, S., RUSH, J., FINLEY, D., KING, R. W. & GYGI, S. P. 2006. Quantitative analysis of in vitro ubiquitinated cyclin B1 reveals complex chain topology. *Nat Cell Biol,* 8**,** 700-10.

KISANUKI, Y. Y., HAMMER, R. E., MIYAZAKI, J., WILLIAMS, S. C., RICHARDSON, J. A. & YANAGISAWA, M. 2001. Tie2-Cre transgenic mice: a new model for endothelial cell-lineage analysis in vivo. *Dev Biol,* 230**,** 230-42.

KITAYNER, M., ROZENBERG, H., KESSLER, N., RABINOVICH, D., SHAULOV, L., HARAN, T. E. & SHAKKED, Z. 2006. Structural basis of DNA recognition by p53 tetramers. *Mol Cell,* 22**,** 741-53.

KLUG, A. 1999. Zinc finger peptides for the regulation of gene expression. *J Mol Biol,* 293**,** 215-8.

KNIPPSCHILD, U., MILNE, D. M., CAMPBELL, L. E., DEMAGGIO, A. J., CHRISTENSON, E., HOEKSTRA, M. F. & MEEK, D. W. 1997. p53 is phosphorylated in vitro and in vivo by the delta and epsilon isoforms of casein kinase 1 and enhances the level of casein kinase 1 delta in response to topoisomerase-directed drugs. *Oncogene,* 15**,** 1727-36.

KODAMA, T., TAKEHARA, T., HIKITA, H., SHIMIZU, S., SHIGEKAWA, M., TSUNEMATSU, H., LI, W., MIYAGI, T., HOSUI, A., TATSUMI, T., ISHIDA, H., KANTO, T., HIRAMATSU, N., KUBOTA, S., TAKIGAWA, M., TOMIMARU, Y., TOMOKUNI, A., NAGANO, H., DOKI, Y., MORI, M. & HAYASHI, N. 2011. Increases in p53 expression induce CTGF synthesis by mouse and human hepatocytes and result in liver fibrosis in mice. *J Clin Invest,* 121**,** 3343-56.

KOEGL, M., HOPPE, T., SCHLENKER, S., ULRICH, H. D., MAYER, T. U. & JENTSCH, S. 1999. A novel ubiquitination factor, E4, is involved in multiubiquitin chain assembly. *Cell,* 96**,** 635-44.

KOLIOPOULOS, M. G., ESPOSITO, D., CHRISTODOULOU, E., TAYLOR, I. A. & RITTINGER, K. 2016. Functional role of TRIM E3 ligase oligomerization and regulation of catalytic activity. 35**,** 1204-18.

KOMANDER, D., CLAGUE, M. J. & URBE, S. 2009. Breaking the chains: structure and function of the deubiquitinases. *Nat Rev Mol Cell Biol,* 10**,** 550-63.

KOMANDER, D. & RAPE, M. 2012. The ubiquitin code. *Annu Rev Biochem,* 81**,** 203-29.

KOMAROVA, E. A., DIATCHENKO, L., ROKHLIN, O. W., HILL, J. E., WANG, Z. J., KRIVOKRYSENKO, V. I., FEINSTEIN, E. & GUDKOV, A. V. 1998. Stress-induced secretion of growth inhibitors: a novel tumor suppressor function of p53. *Oncogene,* 17**,** 1089-96.

KON, N., ZHONG, J., QIANG, L., ACCILI, D. & GU, W. 2012. Inactivation of arf-bp1 induces p53 activation and diabetic phenotypes in mice. *J Biol Chem,* 287**,** 5102-11.

KONDOH, H., LLEONART, M. E., GIL, J., WANG, J., DEGAN, P., PETERS, G., MARTINEZ, D., CARNERO, A. & BEACH, D. 2005. Glycolytic enzymes can modulate cellular life span. *Cancer Res,* 65**,** 177-85.

KORTLEVER, R. M., HIGGINS, P. J. & BERNARDS, R. 2006. Plasminogen activator inhibitor-1 is a critical downstream target of p53 in the induction of replicative senescence. *Nat Cell Biol,* 8**,** 877-84.

KRAJEWSKA, M., KRAJEWSKI, S., BANARES, S., HUANG, X., TURNER, B., BUBENDORF, L., KALLIONIEMI, O. P., SHABAIK, A., VITIELLO, A., PEEHL, D., GAO, G. J. & REED, J. C. 2003. Elevated expression of inhibitor of apoptosis proteins in prostate cancer. *Clin Cancer Res,* 9**,** 4914-25.

KRAJEWSKI, M., OZDOWY, P., D'SILVA, L., ROTHWEILER, U. & HOLAK, T. A. 2005. NMR indicates that the small molecule RITA does not block p53-MDM2 binding in vitro. *Nat Med,* 11**,** 1135-6; author reply 1136-7.

KRAMER, E. R., SCHEURINGER, N., PODTELEJNIKOV, A. V., MANN, M. & PETERS, J. M. 2000. Mitotic regulation of the APC activator proteins CDC20 and CDH1. *Mol Biol Cell,* 11**,** 1555-69.

KRUISWIJK, F., LABUSCHAGNE, C. F. & VOUSDEN, K. H. 2015. p53 in survival, death and metabolic health: a lifeguard with a licence to kill. *Nat Rev Mol Cell Biol,* 16**,** 393-405.

KRUSE, J. P. & GU, W. 2009. MSL2 promotes Mdm2-independent cytoplasmic localization of p53. *J Biol Chem,* 284**,** 3250-63.

KUBBUTAT, M. H., JONES, S. N. & VOUSDEN, K. H. 1997. Regulation of p53 stability by Mdm2. *Nature,* 387**,** 299-303.

KUBBUTAT, M. H. G., LUDWIG, R. L., LEVINE, A. J. & VOUSDEN, K. H. 1999. Analysis of the degradation function of Mdm2. *Cell Growth & Differentiation,* 10**,** 87-92.

KUHBANDNER, S., BRUMMER, S., METZGER, D., CHAMBON, P., HOFMANN, F. & FEIL, R. 2000. Temporally controlled somatic mutagenesis in smooth muscle. *Genesis,* 28**,** 15-22.

KUHN, D. J., CHEN, Q., VOORHEES, P. M., STRADER, J. S., SHENK, K. D., SUN, C. M., DEMO, S. D., BENNETT, M. K., VAN LEEUWEN, F. W., CHANAN-KHAN, A. A. & ORLOWSKI, R. Z. 2007. Potent activity of carfilzomib, a novel, irreversible inhibitor of the ubiquitin-proteasome pathway, against preclinical models of multiple myeloma. *Blood,* 110**,** 3281-90.

KULATHU, Y. & KOMANDER, D. 2012. Atypical ubiquitylation - the unexplored world of polyubiquitin beyond Lys48 and Lys63 linkages. *Nat Rev Mol Cell Biol,* 13**,** 508-23.

KULIKOV, R., LETIENNE, J., KAUR, M., GROSSMAN, S. R., ARTS, J. & BLATTNER, C. 2010. Mdm2 facilitates the association of p53 with the proteasome. *Proc Natl Acad Sci U S A,* 107**,** 10038-43.

KUSSIE, P. H., GORINA, S., MARECHAL, V., ELENBAAS, B., MOREAU, J., LEVINE, A. J. & PAVLETICH, N. P. 1996. Structure of the MDM2 oncoprotein bound to the p53 tumor suppressor transactivation domain. *Science,* 274**,** 948-53.

LABAER, J., GARRETT, M. D., STEVENSON, L. F., SLINGERLAND, J. M., SANDHU, C., CHOU, H. S., FATTAEY, A. & HARLOW, E. 1997. New functional activities for the p21 family of CDK inhibitors. *Genes Dev,* 11**,** 847-62.

LAM, S., LODDER, K., TEUNISSE, A. F., RABELINK, M. J., SCHUTTE, M. & JOCHEMSEN, A. G. 2010. Role of Mdm4 in drug sensitivity of breast cancer cells. *Oncogene,* 29**,** 2415-26.

LAM, Y. A., DEMARTINO, G. N., PICKART, C. M. & COHEN, R. E. 1997. Specificity of the ubiquitin isopeptidase in the PA700 regulatory complex of 26 S proteasomes. *J Biol Chem,* 272**,** 28438-46.
LANE, D. P. 1992. Cancer. p53, guardian of the genome. *Nature,* 358**,** 15-6.
LANE, D. P. & CRAWFORD, L. V. 1979. T antigen is bound to a host protein in SV40-transformed cells. *Nature,* 278**,** 261-3.
LANG, G. A., IWAKUMA, T., SUH, Y. A., LIU, G., RAO, V. A., PARANT, J. M., VALENTIN-VEGA, Y. A., TERZIAN, T., CALDWELL, L. C., STRONG, L. C., EL-NAGGAR, A. K. & LOZANO, G. 2004. Gain of function of a p53 hot spot mutation in a mouse model of Li-Fraumeni syndrome. *Cell,* 119**,** 861-72.
LARONGA, C., YANG, H. Y., NEAL, C. & LEE, M. H. 2000. Association of the cyclin-dependent kinases and 14-3-3 sigma negatively regulates cell cycle progression. *J Biol Chem,* 275**,** 23106-12.
LATRES, E., CHIARLE, R., SCHULMAN, B. A., PAVLETICH, N. P., PELLICER, A., INGHIRAMI, G. & PAGANO, M. 2001. Role of the F-box protein Skp2 in lymphomagenesis. *Proc Natl Acad Sci U S A,* 98**,** 2515-20.
LAU, L. M., NUGENT, J. K., ZHAO, X. & IRWIN, M. S. 2008. HDM2 antagonist Nutlin-3 disrupts p73-HDM2 binding and enhances p73 function. *Oncogene,* 27**,** 997-1003.
LAZEBNIK, Y. 2010. What are the hallmarks of cancer? *Nat Rev Cancer,* 10**,** 232-3.
LE CAM, L., LINARES, L. K., PAUL, C., JULIEN, E., LACROIX, M., HATCHI, E., TRIBOULET, R., BOSSIS, G., SHMUELI, A., RODRIGUEZ, M. S., COUX, O. & SARDET, C. 2006. E4F1 is an atypical ubiquitin ligase that modulates p53 effector functions independently of degradation. *Cell,* 127**,** 775-88.
LE, M. T., TEH, C., SHYH-CHANG, N., XIE, H., ZHOU, B., KORZH, V., LODISH, H. F. & LIM, B. 2009. MicroRNA-125b is a novel negative regulator of p53. *Genes Dev,* 23**,** 862-76.
LEBRON, C., CHEN, L., GILKES, D. M. & CHEN, J. 2006. Regulation of MDMX nuclear import and degradation by Chk2 and 14-3-3. *Embo j,* 25**,** 1196-206.
LEE, E. W., KIM, J. H., AHN, Y. H., SEO, J., KO, A., JEONG, M., KIM, S. J., RO, J. Y., PARK, K. M., LEE, H. W., PARK, E. J., CHUN, K. H. & SONG, J. 2012a. Ubiquitination and degradation of the FADD adaptor protein regulate death receptor-mediated apoptosis and necroptosis. *Nat Commun,* 3**,** 978.
LEE, E. W., LEE, M. S., CAMUS, S., GHIM, J., YANG, M. R., OH, W., HA, N. C., LANE, D. P. & SONG, J. 2009. Differential regulation of p53 and p21 by MKRN1 E3 ligase controls cell cycle arrest and apoptosis. *Embo j,* 28**,** 2100-13.
LEE, I. H., KAWAI, Y., FERGUSSON, M. M., ROVIRA, II, BISHOP, A. J., MOTOYAMA, N., CAO, L. & FINKEL, T. 2012b. Atg7 modulates p53 activity to regulate cell cycle and survival during metabolic stress. *Science,* 336**,** 225-8.
LEE, J. W., BAE, S. H., JEONG, J. W., KIM, S. H. & KIM, K. W. 2004. Hypoxia-inducible factor (HIF-1)alpha: its protein stability and biological functions. *Exp Mol Med,* 36**,** 1-12.
LEE, S. B., KIM, J. J., NAM, H. J., GAO, B., YIN, P., QIN, B., YI, S. Y., HAM, H., EVANS, D., KIM, S. H., ZHANG, J., DENG, M., LIU, T., ZHANG, H., BILLADEAU, D. D., WANG, L., GIAIME, E., SHEN, J., PANG, Y. P., JEN, J., VAN DEURSEN, J. M. & LOU, Z. 2015. Parkin Regulates Mitosis and Genomic Stability through Cdc20/Cdh1. *Mol Cell,* 60**,** 21-34.
LEE, S. B., KIM, S. H., BELL, D. W., WAHRER, D. C., SCHIRIPO, T. A., JORCZAK, M. M., SGROI, D. C., GARBER, J. E., LI, F. P., NICHOLS, K. E., VARLEY, J.

M., GODWIN, A. K., SHANNON, K. M., HARLOW, E. & HABER, D. A. 2001. Destabilization of CHK2 by a missense mutation associated with Li-Fraumeni Syndrome. *Cancer Res,* 61**,** 8062-7.

LENG, R. P., LIN, Y., MA, W., WU, H., LEMMERS, B., CHUNG, S., PARANT, J. M., LOZANO, G., HAKEM, R. & BENCHIMOL, S. 2003. Pirh2, a p53-induced ubiquitin-protein ligase, promotes p53 degradation. *Cell*, 112**,** 779-91.

LI, C., CHEN, L. & CHEN, J. 2002. DNA damage induces MDMX nuclear translocation by p53-dependent and -independent mechanisms. *Mol Cell Biol*, 22**,** 7562-71.

LI, F. P. & FRAUMENI, J. F., JR. 1969. Soft-tissue sarcomas, breast cancer, and other neoplasms. A familial syndrome? *Ann Intern Med,* 71**,** 747-52.

LI, M., BROOKS, C. L., KON, N. & GU, W. 2004. A dynamic role of HAUSP in the p53-Mdm2 pathway. *Mol Cell,* 13**,** 879-86.

LI, M., BROOKS, C. L., WU-BAER, F., CHEN, D., BAER, R. & GU, W. 2003. Mono- versus polyubiquitination: differential control of p53 fate by Mdm2. *Science,* 302**,** 1972-5.

LI, T., KON, N., JIANG, L., TAN, M., LUDWIG, T., ZHAO, Y., BAER, R. & GU, W. 2012. Tumor suppression in the absence of p53-mediated cell-cycle arrest, apoptosis, and senescence. *Cell,* 149**,** 1269-83.

LI, W., BENGTSON, M. H., ULBRICH, A., MATSUDA, A., REDDY, V. A., ORTH, A., CHANDA, S. K., BATALOV, S. & JOAZEIRO, C. A. 2008. Genome-wide and functional annotation of human E3 ubiquitin ligases identifies MULAN, a mitochondrial E3 that regulates the organelle's dynamics and signaling. *PLoS One,* 3**,** e1487.

LIAKOPOULOS, D., DOENGES, G., MATUSCHEWSKI, K. & JENTSCH, S. 1998. A novel protein modification pathway related to the ubiquitin system. *Embo j,* 17**,** 2208-14.

LINARES, L. K., HENGSTERMANN, A., CIECHANOVER, A., MULLER, S. & SCHEFFNER, M. 2003. HdmX stimulates Hdm2-mediated ubiquitination and degradation of p53. *Proc Natl Acad Sci U S A,* 100**,** 12009-14.

LINDSTROM, M. S., JIN, A., DEISENROTH, C., WHITE WOLF, G. & ZHANG, Y. 2007. Cancer-associated mutations in the MDM2 zinc finger domain disrupt ribosomal protein interaction and attenuate MDM2-induced p53 degradation. *Mol Cell Biol,* 27**,** 1056-68.

LINZER, D. I. & LEVINE, A. J. 1979. Characterization of a 54K dalton cellular SV40 tumor antigen present in SV40-transformed cells and uninfected embryonal carcinoma cells. *Cell,* 17**,** 43-52.

LIU, J., CHUNG, H. J., VOGT, M., JIN, Y., MALIDE, D., HE, L., DUNDR, M. & LEVENS, D. 2011. JTV1 co-activates FBP to induce USP29 transcription and stabilize p53 in response to oxidative stress. *Embo j,* 30**,** 846-58.

LIU, Y., HE, Y., JIN, A., TIKUNOV, A. P., ZHOU, L., TOLLINI, L. A., LESLIE, P., KIM, T. H., LI, L. O., COLEMAN, R. A., GU, Z., CHEN, Y. Q., MACDONALD, J. M., GRAVES, L. M. & ZHANG, Y. 2014. Ribosomal protein-Mdm2-p53 pathway coordinates nutrient stress with lipid metabolism by regulating MCD and promoting fatty acid oxidation. *Proc Natl Acad Sci U S A,* 111**,** E2414-22.

LIVERA, G., UZBEKOV, R., JARRIER, P., FOUCHECOURT, S., DUQUENNE, C., PARENT, A. S., MARINE, J. C. & MONGET, P. 2016. Loss of oocytes due to conditional ablation of Murine double minute 2 (Mdm2) gene is p53-dependent and results in female sterility. *FEBS Lett,* 590**,** 2566-74.

LOGAN, I. R., GAUGHAN, L., MCCRACKEN, S. R., SAPOUNTZI, V., LEUNG, H. Y. & ROBSON, C. N. 2006. Human PIRH2 enhances androgen receptor signaling

through inhibition of histone deacetylase 1 and is overexpressed in prostate cancer. *Mol Cell Biol,* 26**,** 6502-10.
LOHRUM, M. A., ASHCROFT, M., KUBBUTAT, M. H. & VOUSDEN, K. H. 2000a. Contribution of two independent MDM2-binding domains in p14(ARF) to p53 stabilization. *Curr Biol,* 10**,** 539-42.
LOHRUM, M. A., ASHCROFT, M., KUBBUTAT, M. H. & VOUSDEN, K. H. 2000b. Identification of a cryptic nucleolar-localization signal in MDM2. *Nat Cell Biol,* 2**,** 179-81.
LOPES, U. G., ERHARDT, P., YAO, R. & COOPER, G. M. 1997. p53-dependent induction of apoptosis by proteasome inhibitors. *J Biol Chem,* 272**,** 12893-6.
LOPEZ-PAJARES, V., KIM, M. M. & YUAN, Z. M. 2008. Phosphorylation of MDMX mediated by Akt leads to stabilization and induces 14-3-3 binding. *J Biol Chem,* 283**,** 13707-13.
LOWE, S. W., SCHMITT, E. M., SMITH, S. W., OSBORNE, B. A. & JACKS, T. 1993. p53 is required for radiation-induced apoptosis in mouse thymocytes. *Nature,* 362**,** 847-9.
LU, H. & LEVINE, A. J. 1995. Human TAFII31 protein is a transcriptional coactivator of the p53 protein. *Proc Natl Acad Sci U S A,* 92**,** 5154-8.
LU, X., YAN, C., HUANG, Y., SHI, D., FU, Z., QIU, J. & YIN, Y. 2016. Mouse double minute 2 (MDM2) upregulates Snail expression and induces epithelial-to-mesenchymal transition in breast cancer cells in vitro and in vivo. *Oncotarget,* 7**,** 37177-37191.
LU, Y., LEE, B. H., KING, R. W., FINLEY, D. & KIRSCHNER, M. W. 2015a. Substrate degradation by the proteasome: a single-molecule kinetic analysis. *Science,* 348**,** 1250834.
LU, Y., WANG, W. & KIRSCHNER, M. W. 2015b. Specificity of the anaphase-promoting complex: a single-molecule study. *Science,* 348**,** 1248737.
LUKASHCHUK, N. & VOUSDEN, K. H. 2007. Ubiquitination and degradation of mutant p53. *Mol Cell Biol,* 27**,** 8284-95.
LUNDGREN, K., MONTES DE OCA LUNA, R., MCNEILL, Y. B., EMERICK, E. P., SPENCER, B., BARFIELD, C. R., LOZANO, G., ROSENBERG, M. P. & FINLAY, C. A. 1997. Targeted expression of MDM2 uncouples S phase from mitosis and inhibits mammary gland development independent of p53. *Genes Dev,* 11**,** 714-25.
LYDEARD, J. R., SCHULMAN, B. A. & HARPER, J. W. 2013. Building and remodelling Cullin-RING E3 ubiquitin ligases. *EMBO Rep,* 14**,** 1050-61.
MA, J., CHENG, L., LIU, H., ZHANG, J., SHI, Y., ZENG, F., MIELE, L., SARKAR, F. H., XIA, J. & WANG, Z. 2013. Genistein down-regulates miR-223 expression in pancreatic cancer cells. *Curr Drug Targets,* 14**,** 1150-6.
MA, J., MARTIN, J. D., ZHANG, H., AUGER, K. R., HO, T. F., KIRKPATRICK, R. B., GROOMS, M. H., JOHANSON, K. O., TUMMINO, P. J., COPELAND, R. A. & LAI, Z. 2006. A second p53 binding site in the central domain of Mdm2 is essential for p53 ubiquitination. *Biochemistry,* 45**,** 9238-45.
MA, W., ZHAO, P., ZANG, L., ZHANG, K., LIAO, H. & HU, Z. 2016. Tumour suppressive function of HUWE1 in thyroid cancer. *J Biosci,* 41**,** 395-405.
MACIAS, E., JIN, A., DEISENROTH, C., BHAT, K., MAO, H., LINDSTROM, M. S. & ZHANG, Y. 2010. An ARF-independent c-MYC-activated tumor suppression pathway mediated by ribosomal protein-Mdm2 Interaction. *Cancer Cell,* 18**,** 231-43.
MADISON, B. B., DUNBAR, L., QIAO, X. T., BRAUNSTEIN, K., BRAUNSTEIN, E. & GUMUCIO, D. L. 2002. Cis elements of the villin gene control expression in

restricted domains of the vertical (crypt) and horizontal (duodenum, cecum) axes of the intestine. *J Biol Chem,* 277**,** 33275-83.

MAEDA, T., HANNA, A. N., SIM, A. B., CHUA, P. P., CHONG, M. T. & TRON, V. A. 2002. GADD45 regulates G2/M arrest, DNA repair, and cell death in keratinocytes following ultraviolet exposure. *J Invest Dermatol,* 119**,** 22-6.

MALKIN, D. 1993. p53 and the Li-Fraumeni syndrome. *Cancer Genet Cytogenet,* 66**,** 83-92.

MALKIN, D., LI, F. P., STRONG, L. C., FRAUMENI, J. F., JR., NELSON, C. E., KIM, D. H., KASSEL, J., GRYKA, M. A., BISCHOFF, F. Z., TAINSKY, M. A. & ET AL. 1990. Germ line p53 mutations in a familial syndrome of breast cancer, sarcomas, and other neoplasms. *Science,* 250**,** 1233-8.

MANDKE, P., WYATT, N., FRASER, J., BATES, B., BERBERICH, S. J. & MARKEY, M. P. 2012. MicroRNA-34a modulates MDM4 expression via a target site in the open reading frame. *PLoS One,* 7**,** e42034.

MAO, J. H., PEREZ-LOSADA, J., WU, D., DELROSARIO, R., TSUNEMATSU, R., NAKAYAMA, K. I., BROWN, K., BRYSON, S. & BALMAIN, A. 2004. Fbxw7/Cdc4 is a p53-dependent, haploinsufficient tumour suppressor gene. *Nature,* 432**,** 775-9.

MAO, Y., LI, K., LU, L., SI-TU, J., LU, M. & GAO, X. 2016. Overexpression of Cdc20 in clinically localized prostate cancer: Relation to high Gleason score and biochemical recurrence after laparoscopic radical prostatectomy. *Cancer Biomark,* 16**,** 351-8.

MARCHENKO, N. D., WOLFF, S., ERSTER, S., BECKER, K. & MOLL, U. M. 2007. Monoubiquitylation promotes mitochondrial p53 translocation. *Embo j,* 26**,** 923-34.

MARCHENKO, N. D., ZAIKA, A. & MOLL, U. M. 2000. Death signal-induced localization of p53 protein to mitochondria. A potential role in apoptotic signaling. *J Biol Chem,* 275**,** 16202-12.

MARIN, I., LUCAS, J. I., GRADILLA, A. C. & FERRUS, A. 2004. Parkin and relatives: the RBR family of ubiquitin ligases. *Physiol Genomics,* 17**,** 253-63.

MARTI, A., WIRBELAUER, C., SCHEFFNER, M. & KREK, W. 1999. Interaction between ubiquitin-protein ligase SCFSKP2 and E2F-1 underlies the regulation of E2F-1 degradation. *Nat Cell Biol,* 1**,** 14-9.

MARTIN, K., TROUCHE, D., HAGEMEIER, C., SORENSEN, T. S., LA THANGUE, N. B. & KOUZARIDES, T. 1995. Stimulation of E2F1/DP1 transcriptional activity by MDM2 oncoprotein. *Nature,* 375**,** 691-4.

MARTINS, C. P., BROWN-SWIGART, L. & EVAN, G. I. 2006. Modeling the therapeutic efficacy of p53 restoration in tumors. *Cell,* 127**,** 1323-34.

MATHEU, A., MARAVER, A., KLATT, P., FLORES, I., GARCIA-CAO, I., BORRAS, C., FLORES, J. M., VINA, J., BLASCO, M. A. & SERRANO, M. 2007. Delayed ageing through damage protection by the Arf/p53 pathway. *Nature,* 448**,** 375-9.

MATSUOKA, S., ROTMAN, G., OGAWA, A., SHILOH, Y., TAMAI, K. & ELLEDGE, S. J. 2000. Ataxia telangiectasia-mutated phosphorylates Chk2 in vivo and in vitro. *Proc Natl Acad Sci U S A,* 97**,** 10389-94.

MATTHEWS, J. M. & SUNDE, M. 2002. Zinc fingers--folds for many occasions. *IUBMB Life,* 54**,** 351-5.

MAYA, R., BALASS, M., KIM, S. T., SHKEDY, D., LEAL, J. F., SHIFMAN, O., MOAS, M., BUSCHMANN, T., RONAI, Z., SHILOH, Y., KASTAN, M. B., KATZIR, E. & OREN, M. 2001. ATM-dependent phosphorylation of Mdm2 on serine 395: role in p53 activation by DNA damage. *Genes Dev,* 15**,** 1067-77.

MAYO, L. D. & DONNER, D. B. 2001. A phosphatidylinositol 3-kinase/Akt pathway promotes translocation of Mdm2 from the cytoplasm to the nucleus. *Proc Natl Acad Sci U S A,* 98**,** 11598-603.

MCEVOY, J., ULYANOV, A., BRENNAN, R., WU, G., POUNDS, S., ZHANG, J. & DYER, M. A. 2012. Analysis of MDM2 and MDM4 single nucleotide polymorphisms, mRNA splicing and protein expression in retinoblastoma. *PLoS One,* 7**,** e42739.

MELCHIOR, F. & HENGST, L. 2002. SUMO-1 and p53. *Cell Cycle,* 1**,** 245-9.

MELLON, I., RAJPAL, D. K., KOI, M., BOLAND, C. R. & CHAMPE, G. N. 1996. Transcription-coupled repair deficiency and mutations in human mismatch repair genes. *Science,* 272**,** 557-60.

MENDRYSA, S. M., MCELWEE, M. K., MICHALOWSKI, J., O'LEARY, K. A., YOUNG, K. M. & PERRY, M. E. 2003. mdm2 Is critical for inhibition of p53 during lymphopoiesis and the response to ionizing irradiation. *Mol Cell Biol,* 23**,** 462-72.

MENG, P. & GHOSH, R. 2014. Transcription addiction: can we garner the Yin and Yang functions of E2F1 for cancer therapy? *Cell Death Dis,* 5**,** e1360.

MERIIN, A. B., GABAI, V. L., YAGLOM, J., SHIFRIN, V. I. & SHERMAN, M. Y. 1998. Proteasome inhibitors activate stress kinases and induce Hsp72. Diverse effects on apoptosis. *J Biol Chem,* 273**,** 6373-9.

METZGER, M. B., HRISTOVA, V. A. & WEISSMAN, A. M. 2012. HECT and RING finger families of E3 ubiquitin ligases at a glance. *J Cell Sci,* 125**,** 531-7.

MEULMEESTER, E., FRENK, R., STAD, R., DE GRAAF, P., MARINE, J. C., VOUSDEN, K. H. & JOCHEMSEN, A. G. 2003. Critical role for a central part of Mdm2 in the ubiquitylation of p53. *Mol Cell Biol,* 23**,** 4929-38.

MEULMEESTER, E., MAURICE, M. M., BOUTELL, C., TEUNISSE, A. F., OVAA, H., ABRAHAM, T. E., DIRKS, R. W. & JOCHEMSEN, A. G. 2005. Loss of HAUSP-mediated deubiquitination contributes to DNA damage-induced destabilization of Hdmx and Hdm2. *Mol Cell,* 18**,** 565-76.

MEYER, H. J. & RAPE, M. 2014. Enhanced protein degradation by branched ubiquitin chains. *Cell,* 157**,** 910-21.

MIGLIORINI, D., BOGAERTS, S., DEFEVER, D., VYAS, R., DENECKER, G., RADAELLI, E., ZWOLINSKA, A., DEPAEPE, V., HOCHEPIED, T., SKARNES, W. C. & MARINE, J. C. 2011. Cop1 constitutively regulates c-Jun protein stability and functions as a tumor suppressor in mice. *J Clin Invest,* 121**,** 1329-43.

MIGLIORINI, D., DANOVI, D., COLOMBO, E., CARBONE, R., PELICCI, P. G. & MARINE, J. C. 2002a. Hdmx recruitment into the nucleus by Hdm2 is essential for its ability to regulate p53 stability and transactivation. *J Biol Chem,* 277**,** 7318-23.

MIGLIORINI, D., LAZZERINI DENCHI, E., DANOVI, D., JOCHEMSEN, A., CAPILLO, M., GOBBI, A., HELIN, K., PELICCI, P. G. & MARINE, J. C. 2002b. Mdm4 (Mdmx) regulates p53-induced growth arrest and neuronal cell death during early embryonic mouse development. *Mol Cell Biol,* 22**,** 5527-38.

MILNE, A. N., LEGUIT, R., CORVER, W. E., MORSINK, F. H., POLAK, M., DE LENG, W. W., CARVALHO, R. & OFFERHAUS, G. J. 2010. Loss of CDC4/FBXW7 in gastric carcinoma. *Cell Oncol,* 32**,** 347-59.

MINSKY, N. & OREN, M. 2004. The RING domain of Mdm2 mediates histone ubiquitylation and transcriptional repression. *Mol Cell,* 16**,** 631-9.

MIURA, K., KARASAWA, H. & SASAKI, I. 2009. cIAP2 as a therapeutic target in colorectal cancer and other malignancies. *Expert Opin Ther Targets,* 13**,** 1333-45.

MOLL, U. M. & PETRENKO, O. 2003. The MDM2-p53 interaction. *Mol Cancer Res,* 1**,** 1001-8.
MOMAND, J., JUNG, D., WILCZYNSKI, S. & NILAND, J. 1998. The MDM2 gene amplification database. *Nucleic Acids Res,* 26**,** 3453-9.
MOMAND, J., ZAMBETTI, G. P., OLSON, D. C., GEORGE, D. & LEVINE, A. J. 1992. The mdm-2 oncogene product forms a complex with the p53 protein and inhibits p53-mediated transactivation. *Cell,* 69**,** 1237-45.
MONTES DE OCA LUNA, R., WAGNER, D. S. & LOZANO, G. 1995. Rescue of early embryonic lethality in mdm2-deficient mice by deletion of p53. *Nature,* 378**,** 203-6.
MORIMOTO, M., NISHIDA, T., HONDA, R. & YASUDA, H. 2000. Modification of cullin-1 by ubiquitin-like protein Nedd8 enhances the activity of SCF(skp2) toward p27(kip1). *Biochem Biophys Res Commun,* 270**,** 1093-6.
MUNSCH, D., WATANABE-FUKUNAGA, R., BOURDON, J. C., NAGATA, S., MAY, E., YONISH-ROUACH, E. & REISDORF, P. 2000. Human and mouse Fas (APO-1/CD95) death receptor genes each contain a p53-responsive element that is activated by p53 mutants unable to induce apoptosis. *J Biol Chem,* 275**,** 3867-72.
MURATA, S., SASAKI, K., KISHIMOTO, T., NIWA, S., HAYASHI, H., TAKAHAMA, Y. & TANAKA, K. 2007. Regulation of CD8+ T cell development by thymus-specific proteasomes. *Science,* 316**,** 1349-53.
MURPHREE, A. L. & BENEDICT, W. F. 1984. Retinoblastoma: clues to human oncogenesis. *Science,* 223**,** 1028-33.
NAKANO, K. & VOUSDEN, K. H. 2001. PUMA, a novel proapoptotic gene, is induced by p53. *Mol Cell,* 7**,** 683-94.
NEMETH, Z. H., WONG, H. R., ODOMS, K., DEITCH, E. A., SZABO, C., VIZI, E. S. & HASKO, G. 2004. Proteasome inhibitors induce inhibitory kappa B (I kappa B) kinase activation, I kappa B alpha degradation, and nuclear factor kappa B activation in HT-29 cells. *Mol Pharmacol,* 65**,** 342-9.
NIEHRS, C. & SCHAFER, A. 2012. Active DNA demethylation by Gadd45 and DNA repair. *Trends Cell Biol,* 22**,** 220-7.
NIGG, E. A. 1995. Cyclin-dependent protein kinases: key regulators of the eukaryotic cell cycle. *Bioessays,* 17**,** 471-80.
NISHISHO, I., NAKAMURA, Y., MIYOSHI, Y., MIKI, Y., ANDO, H., HORII, A., KOYAMA, K., UTSUNOMIYA, J., BABA, S. & HEDGE, P. 1991. Mutations of chromosome 5q21 genes in FAP and colorectal cancer patients. *Science,* 253**,** 665-9.
NISHIYAMA, M., OSHIKAWA, K., TSUKADA, Y., NAKAGAWA, T., IEMURA, S., NATSUME, T., FAN, Y., KIKUCHI, A., SKOULTCHI, A. I. & NAKAYAMA, K. I. 2009. CHD8 suppresses p53-mediated apoptosis through histone H1 recruitment during early embryogenesis. *Nat Cell Biol,* 11**,** 172-82.
NOMURA, K., KLEJNOT, M., KOWALCZYK, D., HOCK, A. K., SIBBET, G. J., VOUSDEN, K. H. & HUANG, D. T. 2017. Structural analysis of MDM2 RING separates degradation from regulation of p53 transcription activity. *Nat Struct Mol Biol,* 24**,** 578-587.
NORIMURA, T., NOMOTO, S., KATSUKI, M., GONDO, Y. & KONDO, S. 1996. p53-dependent apoptosis suppresses radiation-induced teratogenesis. *Nat Med,* 2**,** 577-80.
ODA, E., OHKI, R., MURASAWA, H., NEMOTO, J., SHIBUE, T., YAMASHITA, T., TOKINO, T., TANIGUCHI, T. & TANAKA, N. 2000. Noxa, a BH3-only member of the Bcl-2 family and candidate mediator of p53-induced apoptosis. *Science,* 288**,** 1053-8.

OFIR-ROSENFELD, Y., BOGGS, K., MICHAEL, D., KASTAN, M. B. & OREN, M. 2008. Mdm2 regulates p53 mRNA translation through inhibitory interactions with ribosomal protein L26. *Mol Cell,* 32**,** 180-9.

OH, W., LEE, E. W., LEE, D., YANG, M. R., KO, A., YOON, C. H., LEE, H. W., BAE, Y. S., CHOI, C. Y. & SONG, J. 2010. Hdm2 negatively regulates telomerase activity by functioning as an E3 ligase of hTERT. *Oncogene,* 29**,** 4101-12.

OHKI, Y., FUNATSU, N., KONISHI, N. & CHIBA, T. 2009. The mechanism of poly-NEDD8 chain formation in vitro. *Biochem Biophys Res Commun,* 381**,** 443-7.

OHLSSON, C., KLEY, N., WERNER, H. & LEROITH, D. 1998. p53 regulates insulin-like growth factor-I (IGF-I) receptor expression and IGF-I-induced tyrosine phosphorylation in an osteosarcoma cell line: interaction between p53 and Sp1. *Endocrinology,* 139**,** 1101-7.

OHTANI, K., DEGREGORI, J. & NEVINS, J. R. 1995. Regulation of the cyclin E gene by transcription factor E2F1. *Proc Natl Acad Sci U S A,* 92**,** 12146-50.

OJESINA, A. I., LICHTENSTEIN, L., FREEMAN, S. S., PEDAMALLU, C. S., IMAZ-ROSSHANDLER, I., PUGH, T. J., CHERNIACK, A. D., AMBROGIO, L., CIBULSKIS, K., BERTELSEN, B., ROMERO-CORDOBA, S., TREVINO, V., VAZQUEZ-SANTILLAN, K., GUADARRAMA, A. S., WRIGHT, A. A., ROSENBERG, M. W., DUKE, F., KAPLAN, B., WANG, R., NICKERSON, E., WALLINE, H. M., LAWRENCE, M. S., STEWART, C., CARTER, S. L., MCKENNA, A., RODRIGUEZ-SANCHEZ, I. P., ESPINOSA-CASTILLA, M., WOIE, K., BJORGE, L., WIK, E., HALLE, M. K., HOIVIK, E. A., KRAKSTAD, C., GABINO, N. B., GOMEZ-MACIAS, G. S., VALDEZ-CHAPA, L. D., GARZA-RODRIGUEZ, M. L., MAYTORENA, G., VAZQUEZ, J., RODEA, C., CRAVIOTO, A., CORTES, M. L., GREULICH, H., CRUM, C. P., NEUBERG, D. S., HIDALGO-MIRANDA, A., ESCARENO, C. R., AKSLEN, L. A., CAREY, T. E., VINTERMYR, O. K., GABRIEL, S. B., BARRERA-SALDANA, H. A., MELENDEZ-ZAJGLA, J., GETZ, G., SALVESEN, H. B. & MEYERSON, M. 2014. Landscape of genomic alterations in cervical carcinomas. *Nature,* 506**,** 371-5.

OLINER, J. D., PIETENPOL, J. A., THIAGALINGAM, S., GYURIS, J., KINZLER, K. W. & VOGELSTEIN, B. 1993. Oncoprotein MDM2 conceals the activation domain of tumour suppressor p53. *Nature,* 362**,** 857-60.

OLIVE, K. P., TUVESON, D. A., RUHE, Z. C., YIN, B., WILLIS, N. A., BRONSON, R. T., CROWLEY, D. & JACKS, T. 2004. Mutant p53 gain of function in two mouse models of Li-Fraumeni syndrome. *Cell,* 119**,** 847-60.

OLSEN, S. K. & LIMA, C. D. 2013. Structure of a ubiquitin E1-E2 complex: insights to E1-E2 thioester transfer. *Mol Cell,* 49**,** 884-96.

ONDER, T. T., KARA, N., CHERRY, A., SINHA, A. U., ZHU, N., BERNT, K. M., CAHAN, P., MARCARCI, B. O., UNTERNAEHRER, J., GUPTA, P. B., LANDER, E. S., ARMSTRONG, S. A. & DALEY, G. Q. 2012. Chromatin-modifying enzymes as modulators of reprogramming. *Nature,* 483**,** 598-602.

ONG, K. R., WOODWARD, E. R., KILLICK, P., LIM, C., MACDONALD, F. & MAHER, E. R. 2007. Genotype-phenotype correlations in von Hippel-Lindau disease. *Hum Mutat,* 28**,** 143-9.

ORLOWSKI, R. Z. & KUHN, D. J. 2008. Proteasome inhibitors in cancer therapy: lessons from the first decade. *Clin Cancer Res,* 14**,** 1649-57.

ORTIZ-NAVARRETE, V., SEELIG, A., GERNOLD, M., FRENTZEL, S., KLOETZEL, P. M. & HAMMERLING, G. J. 1991. Subunit of the '20S' proteasome (multicatalytic proteinase) encoded by the major histocompatibility complex. *Nature,* 353**,** 662-4.

PAN, Y. & CHEN, J. 2003. MDM2 promotes ubiquitination and degradation of MDMX. *Mol Cell Biol,* 23**,** 5113-21.
PAN, Y. & CHEN, J. 2005. Modification of MDMX by sumoylation. *Biochem Biophys Res Commun,* 332**,** 702-9.
PANT, V., XIONG, S., IWAKUMA, T., QUINTAS-CARDAMA, A. & LOZANO, G. 2011. Heterodimerization of Mdm2 and Mdm4 is critical for regulating p53 activity during embryogenesis but dispensable for p53 and Mdm2 stability. *Proc Natl Acad Sci U S A,* 108**,** 11995-2000.
PAO, K. C., WOOD, N. T., KNEBEL, A., RAFIE, K., STANLEY, M., MABBITT, P. D., SUNDARAMOORTHY, R., HOFMANN, K., VAN AALTEN, D. M. F. & VIRDEE, S. 2018. Activity-based E3 ligase profiling uncovers an E3 ligase with esterification activity. *Nature,* 556**,** 381-385.
PARANT, J., CHAVEZ-REYES, A., LITTLE, N. A., YAN, W., REINKE, V., JOCHEMSEN, A. G. & LOZANO, G. 2001a. Rescue of embryonic lethality in Mdm4-null mice by loss of Trp53 suggests a nonoverlapping pathway with MDM2 to regulate p53. *Nat Genet,* 29**,** 92-5.
PARANT, J. M., REINKE, V., MIMS, B. & LOZANO, G. 2001b. Organization, expression, and localization of the murine mdmx gene and pseudogene. *Gene,* 270**,** 277-83.
PARZYCH, K. R. & KLIONSKY, D. J. 2014. An overview of autophagy: morphology, mechanism, and regulation. *Antioxid Redox Signal,* 20**,** 460-73.
PAVLETICH, N. P., CHAMBERS, K. A. & PABO, C. O. 1993. The DNA-binding domain of p53 contains the four conserved regions and the major mutation hot spots. *Genes Dev,* 7**,** 2556-64.
PEARSON, P. L. & VAN DER LUIJT, R. B. 1998. The genetic analysis of cancer. *J Intern Med,* 243**,** 413-7.
PELZER, C., KASSNER, I., MATENTZOGLU, K., SINGH, R. K., WOLLSCHEID, H. P., SCHEFFNER, M., SCHMIDTKE, G. & GROETTRUP, M. 2007. UBE1L2, a novel E1 enzyme specific for ubiquitin. *J Biol Chem,* 282**,** 23010-4.
PENG, Y. & CROCE, C. M. 2016. The role of MicroRNAs in human cancer. *Signal Transduct Target Ther,* 1**,** 15004.
PERRY, M. E., MENDRYSA, S. M., SAUCEDO, L. J., TANNOUS, P. & HOLUBAR, M. 2000. p76(MDM2) inhibits the ability of p90(MDM2) to destabilize p53. *J Biol Chem,* 275**,** 5733-8.
PETERS, A. H., O'CARROLL, D., SCHERTHAN, H., MECHTLER, K., SAUER, S., SCHOFER, C., WEIPOLTSHAMMER, K., PAGANI, M., LACHNER, M., KOHLMAIER, A., OPRAVIL, S., DOYLE, M., SIBILIA, M. & JENUWEIN, T. 2001. Loss of the Suv39h histone methyltransferases impairs mammalian heterochromatin and genome stability. *Cell,* 107**,** 323-37.
PETERS, J. M., FRANKE, W. W. & KLEINSCHMIDT, J. A. 1994. Distinct 19 S and 20 S subcomplexes of the 26 S proteasome and their distribution in the nucleus and the cytoplasm. *J Biol Chem,* 269**,** 7709-18.
PETROSKI, M. D. & DESHAIES, R. J. 2005. Function and regulation of cullin-RING ubiquitin ligases. *Nat Rev Mol Cell Biol,* 6**,** 9-20.
PETROSKI, M. D., ZHOU, X., DONG, G., DANIEL-ISSAKANI, S., PAYAN, D. G. & HUANG, J. 2007. Substrate modification with lysine 63-linked ubiquitin chains through the UBC13-UEV1A ubiquitin-conjugating enzyme. *J Biol Chem,* 282**,** 29936-45.
PHILLIPS, A., TEUNISSE, A., LAM, S., LODDER, K., DARLEY, M., EMADUDDIN, M., WOLF, A., RICHTER, J., DE LANGE, J., VERLAAN-DE VRIES, M., LENOS, K., BOHNKE, A., BARTEL, F., BLAYDES, J. P. & JOCHEMSEN, A. G. 2010. HDMX-L is expressed from a functional p53-responsive promoter in the

first intron of the HDMX gene and participates in an autoregulatory feedback loop to control p53 activity. *J Biol Chem,* 285**,** 29111-27.
PICHLER, A. & MELCHIOR, F. 2002. Ubiquitin-related modifier SUMO1 and nucleocytoplasmic transport. *Traffic,* 3**,** 381-7.
PICKART, C. M. 2000. Ubiquitin in chains. *Trends Biochem Sci,* 25**,** 544-8.
PICKART, C. M. & EDDINS, M. J. 2004. Ubiquitin: structures, functions, mechanisms. *Biochim Biophys Acta,* 1695**,** 55-72.
PICKSLEY, S. M. & LANE, D. P. 1993. The p53-mdm2 autoregulatory feedback loop: a paradigm for the regulation of growth control by p53? *Bioessays,* 15**,** 689-90.
PINHASI-KIMHI, O., MICHALOVITZ, D., BEN-ZEEV, A. & OREN, M. 1986. Specific interaction between the p53 cellular tumour antigen and major heat shock proteins. *Nature,* 320**,** 182-4.
PISHAS, K. I., AL-EJEH, F., ZINONOS, I., KUMAR, R., EVDOKIOU, A., BROWN, M. P., CALLEN, D. F. & NEILSEN, P. M. 2011. Nutlin-3a is a potential therapeutic for ewing sarcoma. *Clin Cancer Res,* 17**,** 494-504.
PLECHANOVOVA, A., JAFFRAY, E. G., TATHAM, M. H., NAISMITH, J. H. & HAY, R. T. 2012. Structure of a RING E3 ligase and ubiquitin-loaded E2 primed for catalysis. *Nature,* 489**,** 115-20.
POPOWICZ, G. M., CZARNA, A., WOLF, S., WANG, K., WANG, W., DOMLING, A. & HOLAK, T. A. 2010. Structures of low molecular weight inhibitors bound to MDMX and MDM2 reveal new approaches for p53-MDMX/MDM2 antagonist drug discovery. *Cell Cycle,* 9**,** 1104-11.
POST, S. M., QUINTAS-CARDAMA, A., PANT, V., IWAKUMA, T., HAMIR, A., JACKSON, J. G., MACCIO, D. R., BOND, G. L., JOHNSON, D. G., LEVINE, A. J. & LOZANO, G. 2010. A high-frequency regulatory polymorphism in the p53 pathway accelerates tumor development. *Cancer Cell,* 18**,** 220-30.
POSTIC, C., SHIOTA, M., NISWENDER, K. D., JETTON, T. L., CHEN, Y., MOATES, J. M., SHELTON, K. D., LINDNER, J., CHERRINGTON, A. D. & MAGNUSON, M. A. 1999. Dual roles for glucokinase in glucose homeostasis as determined by liver and pancreatic beta cell-specific gene knock-outs using Cre recombinase. *J Biol Chem,* 274**,** 305-15.
POYUROVSKY, M. V., KATZ, C., LAPTENKO, O., BECKERMAN, R., LOKSHIN, M., AHN, J., BYEON, I. J., GABIZON, R., MATTIA, M., ZUPNICK, A., BROWN, L. M., FRIEDLER, A. & PRIVES, C. 2010. The C terminus of p53 binds the N-terminal domain of MDM2. *Nat Struct Mol Biol,* 17**,** 982-9.
POYUROVSKY, M. V., PRIEST, C., KENTSIS, A., BORDEN, K. L., PAN, Z. Q., PAVLETICH, N. & PRIVES, C. 2007. The Mdm2 RING domain C-terminus is required for supramolecular assembly and ubiquitin ligase activity. *Embo j,* 26**,** 90-101.
PRAKASH, S., TIAN, L., RATLIFF, K. S., LEHOTZKY, R. E. & MATOUSCHEK, A. 2004. An unstructured initiation site is required for efficient proteasome-mediated degradation. *Nat Struct Mol Biol,* 11**,** 830-7.
PRUNEDA, J. N., LITTLEFIELD, P. J., SOSS, S. E., NORDQUIST, K. A., CHAZIN, W. J., BRZOVIC, P. S. & KLEVIT, R. E. 2012. Structure of an E3:E2~Ub complex reveals an allosteric mechanism shared among RING/U-box ligases. *Mol Cell,* 47**,** 933-42.
QIN, J. Z., ZIFFRA, J., STENNETT, L., BODNER, B., BONISH, B. K., CHATURVEDI, V., BENNETT, F., POLLOCK, P. M., TRENT, J. M., HENDRIX, M. J., RIZZO, P., MIELE, L. & NICKOLOFF, B. J. 2005. Proteasome inhibitors trigger NOXA-mediated apoptosis in melanoma and myeloma cells. *Cancer Res,* 65**,** 6282-93.

RAUPACH, B., PEUSCHEL, S. K., MONACK, D. M. & ZYCHLINSKY, A. 2006. Caspase-1-mediated activation of interleukin-1beta (IL-1beta) and IL-18 contributes to innate immune defenses against Salmonella enterica serovar Typhimurium infection. *Infect Immun,* 74**,** 4922-6.

RAVI, R., MOOKERJEE, B., BHUJWALLA, Z. M., SUTTER, C. H., ARTEMOV, D., ZENG, Q., DILLEHAY, L. E., MADAN, A., SEMENZA, G. L. & BEDI, A. 2000. Regulation of tumor angiogenesis by p53-induced degradation of hypoxia-inducible factor 1alpha. *Genes Dev,* 14**,** 34-44.

RAVID, D., MAOR, S., WERNER, H. & LISCOVITCH, M. 2005. Caveolin-1 inhibits cell detachment-induced p53 activation and anoikis by upregulation of insulin-like growth factor-I receptors and signaling. *Oncogene,* 24**,** 1338-47.

RAY-COQUARD, I., BLAY, J. Y., ITALIANO, A., LE CESNE, A., PENEL, N., ZHI, J., HEIL, F., RUEGER, R., GRAVES, B., DING, M., GEHO, D., MIDDLETON, S. A., VASSILEV, L. T., NICHOLS, G. L. & BUI, B. N. 2012. Effect of the MDM2 antagonist RG7112 on the P53 pathway in patients with MDM2-amplified, well-differentiated or dedifferentiated liposarcoma: an exploratory proof-of-mechanism study. *Lancet Oncol,* 13**,** 1133-40.

RAY, R. M., BHATTACHARYA, S. & JOHNSON, L. R. 2011. Mdm2 inhibition induces apoptosis in p53 deficient human colon cancer cells by activating p73- and E2F1-mediated expression of PUMA and Siva-1. *Apoptosis,* 16**,** 35-44.

REISMAN, D., TAKAHASHI, P., POLSON, A. & BOGGS, K. 2012. Transcriptional Regulation of the p53 Tumor Suppressor Gene in S-Phase of the Cell-Cycle and the Cellular Response to DNA Damage. *Biochem Res Int,* 2012**,** 808934.

RESNITZKY, D. & REED, S. I. 1995. Different roles for cyclins D1 and E in regulation of the G1-to-S transition. *Mol Cell Biol,* 15**,** 3463-9.

REYES-TURCU, F. E., VENTII, K. H. & WILKINSON, K. D. 2009. Regulation and cellular roles of ubiquitin-specific deubiquitinating enzymes. *Annu Rev Biochem,* 78**,** 363-97.

RIES, S., BIEDERER, C., WOODS, D., SHIFMAN, O., SHIRASAWA, S., SASAZUKI, T., MCMAHON, M., OREN, M. & MCCORMICK, F. 2000. Opposing effects of Ras on p53: transcriptional activation of mdm2 and induction of p19ARF. *Cell,* 103**,** 321-30.

RILEY, T., SONTAG, E., CHEN, P. & LEVINE, A. 2008. Transcriptional control of human p53-regulated genes. *Nat Rev Mol Cell Biol,* 9**,** 402-12.

ROCK, K. L., YORK, I. A., SARIC, T. & GOLDBERG, A. L. 2002. Protein degradation and the generation of MHC class I-presented peptides. *Adv Immunol,* 80**,** 1-70.

RODRIGUEZ, C. I., BUCHHOLZ, F., GALLOWAY, J., SEQUERRA, R., KASPER, J., AYALA, R., STEWART, A. F. & DYMECKI, S. M. 2000. High-efficiency deleter mice show that FLPe is an alternative to Cre-loxP. *Nat Genet,* 25**,** 139-40.

ROSE, A. E., WANG, G., HANNIFORD, D., MONNI, S., TU, T., SHAPIRO, R. L., BERMAN, R. S., PAVLICK, A. C., PAGANO, M., DARVISHIAN, F., MAZUMDAR, M., HERNANDO, E. & OSMAN, I. 2011. Clinical relevance of SKP2 alterations in metastatic melanoma. *Pigment Cell Melanoma Res,* 24**,** 197-206.

ROTH, J., DOBBELSTEIN, M., FREEDMAN, D. A., SHENK, T. & LEVINE, A. J. 1998. Nucleo-cytoplasmic shuttling of the hdm2 oncoprotein regulates the levels of the p53 protein via a pathway used by the human immunodeficiency virus rev protein. *Embo j,* 17**,** 554-64.

ROXBURGH, P., HOCK, A. K., DICKENS, M. P., MEZNA, M., FISCHER, P. M. & VOUSDEN, K. H. 2012. Small molecules that bind the Mdm2 RING stabilize and activate p53. *Carcinogenesis,* 33**,** 791-8.

ROY, B., BEAMON, J., BALINT, E. & REISMAN, D. 1994. Transactivation of the human p53 tumor suppressor gene by c-Myc/Max contributes to elevated mutant p53 expression in some tumors. *Mol Cell Biol,* 14**,** 7805-15.

ROY, S. K., SRIVASTAVA, R. K. & SHANKAR, S. 2010. Inhibition of PI3K/AKT and MAPK/ERK pathways causes activation of FOXO transcription factor, leading to cell cycle arrest and apoptosis in pancreatic cancer. *J Mol Signal,* 5**,** 10.

RYU, K. S., CHOI, Y. S., KO, J., KIM, S. O., KIM, H. J., CHEONG, H. K., JEON, Y. H., CHOI, B. S. & CHEONG, C. 2008. Direct characterization of E2-dependent target specificity and processivity using an artificial p27-linker-E2 ubiquitination system. *BMB Rep,* 41**,** 852-7.

SABATINI, D. M. 2017. Twenty-five years of mTOR: Uncovering the link from nutrients to growth. *Proc Natl Acad Sci U S A,* 114**,** 11818-11825.

SABLINA, A. A., BUDANOV, A. V., ILYINSKAYA, G. V., AGAPOVA, L. S., KRAVCHENKO, J. E. & CHUMAKOV, P. M. 2005. The antioxidant function of the p53 tumor suppressor. *Nat Med,* 11**,** 1306-13.

SAEKI, Y., KUDO, T., SONE, T., KIKUCHI, Y., YOKOSAWA, H., TOH-E, A. & TANAKA, K. 2009. Lysine 63-linked polyubiquitin chain may serve as a targeting signal for the 26S proteasome. *Embo j,* 28**,** 359-71.

SAH, V. P., ATTARDI, L. D., MULLIGAN, G. J., WILLIAMS, B. O., BRONSON, R. T. & JACKS, T. 1995. A subset of p53-deficient embryos exhibit exencephaly. *Nat Genet,* 10**,** 175-80.

SAHA, V., CHAPLIN, T., GREGORINI, A., AYTON, P. & YOUNG, B. D. 1995. The leukemia-associated-protein (LAP) domain, a cysteine-rich motif, is present in a wide range of proteins, including MLL, AF10, and MLLT6 proteins. *Proc Natl Acad Sci U S A,* 92**,** 9737-41.

SAITO, S., GOODARZI, A. A., HIGASHIMOTO, Y., NODA, Y., LEES-MILLER, S. P., APPELLA, E. & ANDERSON, C. W. 2002. ATM mediates phosphorylation at multiple p53 sites, including Ser(46), in response to ionizing radiation. *J Biol Chem,* 277**,** 12491-4.

SAKAMURO, D., SABBATINI, P., WHITE, E. & PRENDERGAST, G. C. 1997. The polyproline region of p53 is required to activate apoptosis but not growth arrest. *Oncogene,* 15**,** 887-98.

SANCHEZ-MACEDO, N., FENG, J., FAUBERT, B., CHANG, N., ELIA, A., RUSHING, E. J., TSUCHIHARA, K., BUNGARD, D., BERGER, S. L., JONES, R. G., MAK, T. W. & ZAUGG, K. 2013. Depletion of the novel p53-target gene carnitine palmitoyltransferase 1C delays tumor growth in the neurofibromatosis type I tumor model. *Cell Death Differ,* 20**,** 659-68.

SANCHEZ, J. G., CHIANG, J. J., SPARRER, K. M. J., ALAM, S. L., CHI, M., ROGANOWICZ, M. D., SANKARAN, B., GACK, M. U. & PORNILLOS, O. 2016. Mechanism of TRIM25 Catalytic Activation in the Antiviral RIG-I Pathway. *Cell Rep,* 16**,** 1315-1325.

SANDRI, M. 2013. Protein breakdown in muscle wasting: role of autophagy-lysosome and ubiquitin-proteasome. *Int J Biochem Cell Biol,* 45**,** 2121-9.

SARNOW, P., HO, Y. S., WILLIAMS, J. & LEVINE, A. J. 1982. Adenovirus E1b-58kd tumor antigen and SV40 large tumor antigen are physically associated with the same 54 kd cellular protein in transformed cells. *Cell,* 28**,** 387-94.

SARTOR, H., EHLERT, F., GRZESCHIK, K. H., MULLER, R. & ADOLPH, S. 1992. Assignment of two human cell cycle genes, CDC25C and CCNB1, to 5q31 and 5q12, respectively. *Genomics,* 13**,** 911-2.

SASHIDA, G., LIU, Y., ELF, S., MIYATA, Y., OHYASHIKI, K., IZUMI, M., MENENDEZ, S. & NIMER, S. D. 2009. ELF4/MEF activates MDM2 expression and blocks oncogene-induced p16 activation to promote transformation. *Mol Cell Biol,* 29**,** 3687-99.

SASIELA, C. A., STEWART, D. H., KITAGAKI, J., SAFIRAN, Y. J., YANG, Y., WEISSMAN, A. M., OBEROI, P., DAVYDOV, I. V., GONCHAROVA, E., BEUTLER, J. A., MCMAHON, J. B. & O'KEEFE, B. R. 2008. Identification of inhibitors for MDM2 ubiquitin ligase activity from natural product extracts by a novel high-throughput electrochemiluminescent screen. *J Biomol Screen,* 13**,** 229-37.

SAVILLE, M. K., SPARKS, A., XIRODIMAS, D. P., WARDROP, J., STEVENSON, L. F., BOURDON, J. C., WOODS, Y. L. & LANE, D. P. 2004. Regulation of p53 by the ubiquitin-conjugating enzymes UbcH5B/C in vivo. *J Biol Chem,* 279**,** 42169-81.

SAWADA, G., UEO, H., MATSUMURA, T., UCHI, R., ISHIBASHI, M., MIMA, K., KURASHIGE, J., TAKAHASHI, Y., AKIYOSHI, S., SUDO, T., SUGIMACHI, K., DOKI, Y., MORI, M. & MIMORI, K. 2013. Loss of COP1 expression determines poor prognosisin patients with gastric cancer. *Oncol Rep,* 30**,** 1971-5.

SCHEFFNER, M. & KUMAR, S. 2014. Mammalian HECT ubiquitin-protein ligases: biological and pathophysiological aspects. *Biochim Biophys Acta,* 1843**,** 61-74.

SCHEFFNER, M., WERNESS, B. A., HUIBREGTSE, J. M., LEVINE, A. J. & HOWLEY, P. M. 1990. The E6 oncoprotein encoded by human papillomavirus types 16 and 18 promotes the degradation of p53. *Cell,* 63**,** 1129-36.

SCHINDLER, U., BECKMANN, H. & CASHMORE, A. R. 1993. HAT3.1, a novel Arabidopsis homeodomain protein containing a conserved cysteine-rich region. *Plant J,* 4**,** 137-50.

SCHLERETH, K., BEINORAVICIUTE-KELLNER, R., ZEITLINGER, M. K., BRETZ, A. C., SAUER, M., CHARLES, J. P., VOGIATZI, F., LEICH, E., SAMANS, B., EILERS, M., KISKER, C., ROSENWALD, A. & STIEWE, T. 2010. DNA binding cooperativity of p53 modulates the decision between cell-cycle arrest and apoptosis. *Mol Cell,* 38**,** 356-68.

SCHMIDT, D. & MULLER, S. 2002. Members of the PIAS family act as SUMO ligases for c-Jun and p53 and repress p53 activity. *Proc Natl Acad Sci U S A,* 99**,** 2872-7.

SCHNEEKLOTH, A. R., PUCHEAULT, M., TAE, H. S. & CREWS, C. M. 2008. Targeted intracellular protein degradation induced by a small molecule: En route to chemical proteomics. *Bioorg Med Chem Lett,* 18**,** 5904-8.

SCHREINER, P., CHEN, X., HUSNJAK, K., RANDLES, L., ZHANG, N., ELSASSER, S., FINLEY, D., DIKIC, I., WALTERS, K. J. & GROLL, M. 2008. Ubiquitin docking at the proteasome through a novel pleckstrin-homology domain interaction. *Nature,* 453**,** 548-52.

SCHULMAN, B. A. & HARPER, J. W. 2009. Ubiquitin-like protein activation by E1 enzymes: the apex for downstream signalling pathways. *Nat Rev Mol Cell Biol,* 10**,** 319-31.

SCHWENK, F., BARON, U. & RAJEWSKY, K. 1995. A cre-transgenic mouse strain for the ubiquitous deletion of loxP-flanked gene segments including deletion in germ cells. *Nucleic Acids Res,* 23**,** 5080-1.

SCOTT, D. C., SVIDERSKIY, V. O., MONDA, J. K., LYDEARD, J. R., CHO, S. E., HARPER, J. W. & SCHULMAN, B. A. 2014. Structure of a RING E3 trapped in action reveals ligation mechanism for the ubiquitin-like protein NEDD8. *Cell,* 157**,** 1671-84.

SHABEK, N., HERMAN-BACHINSKY, Y., BUCHSBAUM, S., LEWINSON, O., HAJ-YAHYA, M., HEJJAOUI, M., LASHUEL, H. A., SOMMER, T., BRIK, A. & CIECHANOVER, A. 2012. The size of the proteasomal substrate determines whether its degradation will be mediated by mono- or polyubiquitylation. *Mol Cell,* 48**,** 87-97.

SHANGARY, S., QIN, D., MCEACHERN, D., LIU, M., MILLER, R. S., QIU, S., NIKOLOVSKA-COLESKA, Z., DING, K., WANG, G., CHEN, J., BERNARD, D., ZHANG, J., LU, Y., GU, Q., SHAH, R. B., PIENTA, K. J., LING, X., KANG, S., GUO, M., SUN, Y., YANG, D. & WANG, S. 2008. Temporal activation of p53 by a specific MDM2 inhibitor is selectively toxic to tumors and leads to complete tumor growth inhibition. *Proc Natl Acad Sci U S A,* 105**,** 3933-8.

SHARP, D. A., KRATOWICZ, S. A., SANK, M. J. & GEORGE, D. L. 1999. Stabilization of the MDM2 oncoprotein by interaction with the structurally related MDMX protein. *J Biol Chem,* 274**,** 38189-96.

SHENG, Y., SARIDAKIS, V., SARKARI, F., DUAN, S., WU, T., ARROWSMITH, C. H. & FRAPPIER, L. 2006. Molecular recognition of p53 and MDM2 by USP7/HAUSP. *Nat Struct Mol Biol,* 13**,** 285-91.

SHI, D. & GU, W. 2012. Dual Roles of MDM2 in the Regulation of p53: Ubiquitination Dependent and Ubiquitination Independent Mechanisms of MDM2 Repression of p53 Activity. *Genes Cancer,* 3**,** 240-8.

SHI, D., POP, M. S., KULIKOV, R., LOVE, I. M., KUNG, A. L. & GROSSMAN, S. R. 2009. CBP and p300 are cytoplasmic E4 polyubiquitin ligases for p53. *Proc Natl Acad Sci U S A,* 106**,** 16275-80.

SHI, X., KACHIRSKAIA, I., YAMAGUCHI, H., WEST, L. E., WEN, H., WANG, E. W., DUTTA, S., APPELLA, E. & GOZANI, O. 2007. Modulation of p53 function by SET8-mediated methylation at lysine 382. *Mol Cell,* 27**,** 636-46.

SHIEH, S. Y., IKEDA, M., TAYA, Y. & PRIVES, C. 1997. DNA damage-induced phosphorylation of p53 alleviates inhibition by MDM2. *Cell,* 91**,** 325-34.

SHVARTS, A., STEEGENGA, W. T., RITECO, N., VAN LAAR, T., DEKKER, P., BAZUINE, M., VAN HAM, R. C., VAN DER HOUVEN VAN OORDT, W., HATEBOER, G., VAN DER EB, A. J. & JOCHEMSEN, A. G. 1996. MDMX: a novel p53-binding protein with some functional properties of MDM2. *Embo j,* 15**,** 5349-57.

SILICIANO, J. D., CANMAN, C. E., TAYA, Y., SAKAGUCHI, K., APPELLA, E. & KASTAN, M. B. 1997. DNA damage induces phosphorylation of the amino terminus of p53. *Genes Dev,* 11**,** 3471-81.

SIU, K. T., ROSNER, M. R. & MINELLA, A. C. 2012. An integrated view of cyclin E function and regulation. *Cell Cycle,* 11**,** 57-64.

SLACK, A., CHEN, Z., TONELLI, R., PULE, M., HUNT, L., PESSION, A. & SHOHET, J. M. 2005a. The p53 regulatory gene MDM2 is a direct transcriptional target of MYCN in neuroblastoma. *Proc Natl Acad Sci U S A,* 102**,** 731-6.

SLACK, A., LOZANO, G. & SHOHET, J. M. 2005b. MDM2 as MYCN transcriptional target: implications for neuroblastoma pathogenesis. *Cancer Lett,* 228**,** 21-7.

STAD, R., LITTLE, N. A., XIRODIMAS, D. P., FRENK, R., VAN DER EB, A. J., LANE, D. P., SAVILLE, M. K. & JOCHEMSEN, A. G. 2001. Mdmx stabilizes p53 and Mdm2 via two distinct mechanisms. *EMBO Rep,* 2**,** 1029-34.

STAD, R., RAMOS, Y. F., LITTLE, N., GRIVELL, S., ATTEMA, J., VAN DER EB, A. J. & JOCHEMSEN, A. G. 2000. Hdmx stabilizes Mdm2 and p53. *J Biol Chem,* 275**,** 28039-44.

STEIN, G. H., DRULLINGER, L. F., SOULARD, A. & DULIC, V. 1999. Differential roles for cyclin-dependent kinase inhibitors p21 and p16 in the mechanisms of senescence and differentiation in human fibroblasts. *Mol Cell Biol,* 19**,** 2109-17.

STEWART, M. D., RITTERHOFF, T., KLEVIT, R. E. & BRZOVIC, P. S. 2016. E2 enzymes: more than just middle men. *Cell Res,* 26**,** 423-40.

STOMMEL, J. M. & WAHL, G. M. 2004. Accelerated MDM2 auto-degradation induced by DNA-damage kinases is required for p53 activation. *Embo j,* 23**,** 1547-56.

STUART, E. T., HAFFNER, R., OREN, M. & GRUSS, P. 1995. Loss of p53 function through PAX-mediated transcriptional repression. *Embo j,* 14**,** 5638-45.

SULLIVAN, K. D., GALLANT-BEHM, C. L., HENRY, R. E., FRAIKIN, J. L. & ESPINOSA, J. M. 2012. The p53 circuit board. *Biochim Biophys Acta,* 1825**,** 229-44.

SUN, Y. 2006. E3 ubiquitin ligases as cancer targets and biomarkers. *Neoplasia,* 8**,** 645-54.

SURGET, S., KHOURY, M. P. & BOURDON, J. C. 2013. Uncovering the role of p53 splice variants in human malignancy: a clinical perspective. *Onco Targets Ther,* 7**,** 57-68.

SYKES, S. M., MELLERT, H. S., HOLBERT, M. A., LI, K., MARMORSTEIN, R., LANE, W. S. & MCMAHON, S. B. 2006. Acetylation of the p53 DNA-binding domain regulates apoptosis induction. *Mol Cell,* 24**,** 841-51.

TAKAGI, M., ABSALON, M. J., MCLURE, K. G. & KASTAN, M. B. 2005. Regulation of p53 translation and induction after DNA damage by ribosomal protein L26 and nucleolin. *Cell,* 123**,** 49-63.

TAN, B. X., LIEW, H. P., CHUA, J. S., GHADESSY, F. J., TAN, Y. S., LANE, D. P. & COFFILL, C. R. 2017. Anatomy of Mdm2 and Mdm4 in evolution. *J Mol Cell Biol,* 9**,** 3-15.

TANAKA, K. 2009. The proteasome: overview of structure and functions. *Proc Jpn Acad Ser B Phys Biol Sci,* 85**,** 12-36.

TANIMOTO, K., MAKINO, Y., PEREIRA, T. & POELLINGER, L. 2000. Mechanism of regulation of the hypoxia-inducible factor-1 alpha by the von Hippel-Lindau tumor suppressor protein. *Embo j,* 19**,** 4298-309.

TASDEMIR, E., MAIURI, M. C., GALLUZZI, L., VITALE, I., DJAVAHERI-MERGNY, M., D'AMELIO, M., CRIOLLO, A., MORSELLI, E., ZHU, C., HARPER, F., NANNMARK, U., SAMARA, C., PINTON, P., VICENCIO, J. M., CARNUCCIO, R., MOLL, U. M., MADEO, F., PATERLINI-BRECHOT, P., RIZZUTO, R., SZABADKAI, G., PIERRON, G., BLOMGREN, K., TAVERNARAKIS, N., CODOGNO, P., CECCONI, F. & KROEMER, G. 2008. Regulation of autophagy by cytoplasmic p53. *Nat Cell Biol,* 10**,** 676-87.

TATHAM, M. H., JAFFRAY, E., VAUGHAN, O. A., DESTERRO, J. M., BOTTING, C. H., NAISMITH, J. H. & HAY, R. T. 2001. Polymeric chains of SUMO-2 and SUMO-3 are conjugated to protein substrates by SAE1/SAE2 and Ubc9. *J Biol Chem,* 276**,** 35368-74.

TERZIAN, T., WANG, Y., VAN PELT, C. S., BOX, N. F., TRAVIS, E. L. & LOZANO, G. 2007. Haploinsufficiency of Mdm2 and Mdm4 in tumorigenesis and development. *Mol Cell Biol,* 27**,** 5479-85.

THROWER, J. S., HOFFMAN, L., RECHSTEINER, M. & PICKART, C. M. 2000. Recognition of the polyubiquitin proteolytic signal. *Embo j,* 19**,** 94-102.

TIAN, H., TACKMANN, N. R., JIN, A., ZHENG, J. & ZHANG, Y. 2017. Inactivation of the MDM2 RING domain enhances p53 transcriptional activity in mice. *J Biol Chem,* 292**,** 21614-21622.

TIAN, X., CHEN, Y., HU, W. & WU, M. 2011. E2F1 inhibits MDM2 expression in a p53-dependent manner. *Cell Signal,* 23**,** 193-200.

TIBBETTS, R. S., BRUMBAUGH, K. M., WILLIAMS, J. M., SARKARIA, J. N., CLIBY, W. A., SHIEH, S. Y., TAYA, Y., PRIVES, C. & ABRAHAM, R. T. 1999. A role for ATR in the DNA damage-induced phosphorylation of p53. *Genes Dev,* 13**,** 152-7.

TOKGOZ, Z., BOHNSACK, R. N. & HAAS, A. L. 2006. Pleiotropic effects of ATP.Mg2+ binding in the catalytic cycle of ubiquitin-activating enzyme. *J Biol Chem,* 281**,** 14729-37.

TOLLINI, L. A., JIN, A., PARK, J. & ZHANG, Y. 2014. Regulation of p53 by Mdm2 E3 ligase function is dispensable in embryogenesis and development, but essential in response to DNA damage. *Cancer Cell,* 26**,** 235-47.

TRUONG, A. H., CERVI, D., LEE, J. & BEN-DAVID, Y. 2005. Direct transcriptional regulation of MDM2 by Fli-1. *Oncogene,* 24**,** 962-9.

TSAI, W. W., WANG, Z., YIU, T. T., AKDEMIR, K. C., XIA, W., WINTER, S., TSAI, C. Y., SHI, X., SCHWARZER, D., PLUNKETT, W., ARONOW, B., GOZANI, O., FISCHLE, W., HUNG, M. C., PATEL, D. J. & BARTON, M. C. 2010. TRIM24 links a non-canonical histone signature to breast cancer. *Nature,* 468**,** 927-32.

TSIRIGOTIS, M., ZHANG, M., CHIU, R. K., WOUTERS, B. G. & GRAY, D. A. 2001. Sensitivity of mammalian cells expressing mutant ubiquitin to protein-damaging agents. *J Biol Chem,* 276**,** 46073-8.

TU, H. C., REN, D., WANG, G. X., CHEN, D. Y., WESTERGARD, T. D., KIM, H., SASAGAWA, S., HSIEH, J. J. & CHENG, E. H. 2009. The p53-cathepsin axis cooperates with ROS to activate programmed necrotic death upon DNA damage. *Proc Natl Acad Sci U S A,* 106**,** 1093-8.

TURNBULL, A. P., IOANNIDIS, S., KRAJEWSKI, W. W., PINTO-FERNANDEZ, A., HERIDE, C., MARTIN, A. C. L., TONKIN, L. M., TOWNSEND, E. C., BUKER, S. M., LANCIA, D. R., CARAVELLA, J. A., TOMS, A. V., CHARLTON, T. M., LAHDENRANTA, J., WILKER, E., FOLLOWS, B. C., EVANS, N. J., STEAD, L., ALLI, C., ZARAYSKIY, V. V., TALBOT, A. C., BUCKMELTER, A. J., WANG, M., MCKINNON, C. L., SAAB, F., MCGOURAN, J. F., CENTURY, H., GERSCH, M., PITTMAN, M. S., MARSHALL, C. G., RAYNHAM, T. M., SIMCOX, M., STEWART, L. M. D., MCLOUGHLIN, S. B., ESCOBEDO, J. A., BAIR, K. W., DINSMORE, C. J., HAMMONDS, T. R., KIM, S., URBE, S., CLAGUE, M. J., KESSLER, B. M. & KOMANDER, D. 2017. Molecular basis of USP7 inhibition by selective small-molecule inhibitors. *Nature,* 550**,** 481-486.

TYNER, S. D., VENKATACHALAM, S., CHOI, J., JONES, S., GHEBRANIOUS, N., IGELMANN, H., LU, X., SORON, G., COOPER, B., BRAYTON, C., PARK, S. H., THOMPSON, T., KARSENTY, G., BRADLEY, A. & DONEHOWER, L. A. 2002. p53 mutant mice that display early ageing-associated phenotypes. *Nature,* 415**,** 45-53.

ULDRIJAN, S., PANNEKOEK, W. J. & VOUSDEN, K. H. 2007. An essential function of the extreme C-terminus of MDM2 can be provided by MDMX. *Embo j,* 26**,** 102-12.

VAHTERISTO, P., TAMMINEN, A., KARVINEN, P., EEROLA, H., EKLUND, C., AALTONEN, L. A., BLOMQVIST, C., AITTOMAKI, K. & NEVANLINNA, H. 2001. p53, CHK2, and CHK1 genes in Finnish families with Li-Fraumeni

syndrome: further evidence of CHK2 in inherited cancer predisposition. *Cancer Res,* 61**,** 5718-22.

VALENTE, L. J., GRAY, D. H., MICHALAK, E. M., PINON-HOFBAUER, J., EGLE, A., SCOTT, C. L., JANIC, A. & STRASSER, A. 2013. p53 efficiently suppresses tumor development in the complete absence of its cell-cycle inhibitory and proapoptotic effectors p21, Puma, and Noxa. *Cell Rep,* 3**,** 1339-45.

VALENTIN-VEGA, Y. A., BOX, N., TERZIAN, T. & LOZANO, G. 2009. Mdm4 loss in the intestinal epithelium leads to compartmentalized cell death but no tissue abnormalities. *Differentiation,* 77**,** 442-9.

VALENTIN-VEGA, Y. A., OKANO, H. & LOZANO, G. 2008. The intestinal epithelium compensates for p53-mediated cell death and guarantees organismal survival. *Cell Death Differ,* 15**,** 1772-81.

VAN DE MARK, D., KONG, D., LONCAREK, J. & STEARNS, T. 2015. MDM1 is a microtubule-binding protein that negatively regulates centriole duplication. *Mol Biol Cell,* 26**,** 3788-802.

VAN NOSTRAND, J. L., BRADY, C. A., JUNG, H., FUENTES, D. R., KOZAK, M. M., JOHNSON, T. M., LIN, C. Y., LIN, C. J., SWIDERSKI, D. L., VOGEL, H., BERNSTEIN, J. A., ATTIE-BITACH, T., CHANG, C. P., WYSOCKA, J., MARTIN, D. M. & ATTARDI, L. D. 2014. Inappropriate p53 activation during development induces features of CHARGE syndrome. *Nature,* 514**,** 228-32.

VANDER KOOI, C. W., OHI, M. D., ROSENBERG, J. A., OLDHAM, M. L., NEWCOMER, M. E., GOULD, K. L. & CHAZIN, W. J. 2006. The Prp19 U-box crystal structure suggests a common dimeric architecture for a class of oligomeric E3 ubiquitin ligases. *Biochemistry,* 45**,** 121-30.

VARSHAVSKY, A. 2006. The early history of the ubiquitin field. *Protein Sci,* 15**,** 647-54.

VASEVA, A. V., MARCHENKO, N. D., JI, K., TSIRKA, S. E., HOLZMANN, S. & MOLL, U. M. 2012. p53 opens the mitochondrial permeability transition pore to trigger necrosis. *Cell,* 149**,** 1536-48.

VASSILEV, L. T., VU, B. T., GRAVES, B., CARVAJAL, D., PODLASKI, F., FILIPOVIC, Z., KONG, N., KAMMLOTT, U., LUKACS, C., KLEIN, C., FOTOUHI, N. & LIU, E. A. 2004. In vivo activation of the p53 pathway by small-molecule antagonists of MDM2. *Science,* 303**,** 844-8.

VEERIAH, S., TAYLOR, B. S., MENG, S., FANG, F., YILMAZ, E., VIVANCO, I., JANAKIRAMAN, M., SCHULTZ, N., HANRAHAN, A. J., PAO, W., LADANYI, M., SANDER, C., HEGUY, A., HOLLAND, E. C., PATY, P. B., MISCHEL, P. S., LIAU, L., CLOUGHESY, T. F., MELLINGHOFF, I. K., SOLIT, D. B. & CHAN, T. A. 2010. Somatic mutations of the Parkinson's disease-associated gene PARK2 in glioblastoma and other human malignancies. *Nat Genet,* 42**,** 77-82.

VERMA, R., ARAVIND, L., OANIA, R., MCDONALD, W. H., YATES, J. R., 3RD, KOONIN, E. V. & DESHAIES, R. J. 2002. Role of Rpn11 metalloprotease in deubiquitination and degradation by the 26S proteasome. *Science,* 298**,** 611-5.

VESUNA, F., VAN DIEST, P., CHEN, J. H. & RAMAN, V. 2008. Twist is a transcriptional repressor of E-cadherin gene expression in breast cancer. *Biochem Biophys Res Commun,* 367**,** 235-41.

VIJAY-KUMAR, S., BUGG, C. E. & COOK, W. J. 1987. Structure of ubiquitin refined at 1.8 A resolution. *J Mol Biol,* 194**,** 531-44.

VOUSDEN, K. H. & LANE, D. P. 2007. p53 in health and disease. *Nat Rev Mol Cell Biol,* 8**,** 275-83.

VOUSDEN, K. H. & RYAN, K. M. 2009. p53 and metabolism. *Nat Rev Cancer,* 9**,** 691-700.
WALLACE, M., WORRALL, E., PETTERSSON, S., HUPP, T. R. & BALL, K. L. 2006. Dual-site regulation of MDM2 E3-ubiquitin ligase activity. *Mol Cell,* 23**,** 251-63.
WANG, S. J., YU, G., JIANG, L., LI, T., LIN, Q., TANG, Y. & GU, W. 2013. p53-Dependent regulation of metabolic function through transcriptional activation of pantothenate kinase-1 gene. *Cell Cycle,* 12**,** 753-61.
WANG, S. P., WANG, W. L., CHANG, Y. L., WU, C. T., CHAO, Y. C., KAO, S. H., YUAN, A., LIN, C. W., YANG, S. C., CHAN, W. K., LI, K. C., HONG, T. M. & YANG, P. C. 2009. p53 controls cancer cell invasion by inducing the MDM2-mediated degradation of Slug. *Nat Cell Biol,* 11**,** 694-704.
WANG, X., TAPLICK, J., GEVA, N. & OREN, M. 2004. Inhibition of p53 degradation by Mdm2 acetylation. *FEBS Lett,* 561**,** 195-201.
WANG, Z., INUZUKA, H., ZHONG, J., FUKUSHIMA, H., WAN, L., LIU, P. & WEI, W. 2012. DNA damage-induced activation of ATM promotes beta-TRCP-mediated Mdm2 ubiquitination and destruction. *Oncotarget,* 3**,** 1026-35.
WATSON, J. V., CHAMBERS, S. H. & SMITH, P. J. 1987. A pragmatic approach to the analysis of DNA histograms with a definable G1 peak. *Cytometry,* 8**,** 1-8.
WEBER, H. O., LUDWIG, R. L., MORRISON, D., KOTLYAROV, A., GAESTEL, M. & VOUSDEN, K. H. 2005. HDM2 phosphorylation by MAPKAP kinase 2. *Oncogene,* 24**,** 1965-72.
WEGER, S., HAMMER, E. & HEILBRONN, R. 2005. Topors acts as a SUMO-1 E3 ligase for p53 in vitro and in vivo. *FEBS Lett,* 579**,** 5007-12.
WENZEL, D. M., LISSOUNOV, A., BRZOVIC, P. S. & KLEVIT, R. E. 2011. UBCH7 reactivity profile reveals parkin and HHARI to be RING/HECT hybrids. *Nature,* 474**,** 105-8.
WERNER, H., KARNIELI, E., RAUSCHER, F. J. & LEROITH, D. 1996. Wild-type and mutant p53 differentially regulate transcription of the insulin-like growth factor I receptor gene. *Proc Natl Acad Sci U S A,* 93**,** 8318-23.
WERNESS, B. A., LEVINE, A. J. & HOWLEY, P. M. 1990. Association of human papillomavirus types 16 and 18 E6 proteins with p53. *Science,* 248**,** 76-9.
WEST, L. E. & GOZANI, O. 2011. Regulation of p53 function by lysine methylation. *Epigenomics,* 3**,** 361-9.
WHITBY, F. G., XIA, G., PICKART, C. M. & HILL, C. P. 1998. Crystal structure of the human ubiquitin-like protein NEDD8 and interactions with ubiquitin pathway enzymes. *J Biol Chem,* 273**,** 34983-91.
WIBORG, O., PEDERSEN, M. S., WIND, A., BERGLUND, L. E., MARCKER, K. A. & VUUST, J. 1985. The human ubiquitin multigene family: some genes contain multiple directly repeated ubiquitin coding sequences. *Embo j,* 4**,** 755-9.
WIEDERSCHAIN, D., WEE, S., CHEN, L., LOO, A., YANG, G., HUANG, A., CHEN, Y., CAPONIGRO, G., YAO, Y. M., LENGAUER, C., SELLERS, W. R. & BENSON, J. D. 2009. Single-vector inducible lentiviral RNAi system for oncology target validation. *Cell Cycle,* 8**,** 498-504.
WILKINSON, K. D. 1997. Regulation of ubiquitin-dependent processes by deubiquitinating enzymes. *Faseb j,* 11**,** 1245-56.
WILLIS, A., JUNG, E. J., WAKEFIELD, T. & CHEN, X. 2004. Mutant p53 exerts a dominant negative effect by preventing wild-type p53 from binding to the promoter of its target genes. *Oncogene,* 23**,** 2330-8.

WINBORN, B. J., TRAVIS, S. M., TODI, S. V., SCAGLIONE, K. M., XU, P., WILLIAMS, A. J., COHEN, R. E., PENG, J. & PAULSON, H. L. 2008. The deubiquitinating enzyme ataxin-3, a polyglutamine disease protein, edits Lys63 linkages in mixed linkage ubiquitin chains. *J Biol Chem,* 283**,** 26436-43.

WINDHEIM, M., PEGGIE, M. & COHEN, P. 2008. Two different classes of E2 ubiquitin-conjugating enzymes are required for the mono-ubiquitination of proteins and elongation by polyubiquitin chains with a specific topology. *Biochem J,* 409**,** 723-9.

WINSTON, J. T., STRACK, P., BEER-ROMERO, P., CHU, C. Y., ELLEDGE, S. J. & HARPER, J. W. 1999. The SCFbeta-TRCP-ubiquitin ligase complex associates specifically with phosphorylated destruction motifs in IkappaBalpha and beta-catenin and stimulates IkappaBalpha ubiquitination in vitro. *Genes Dev,* 13**,** 270-83.

WU, C., MILOSLAVSKAYA, I., DEMONTIS, S., MAESTRO, R. & GALAKTIONOV, K. 2004. Regulation of cellular response to oncogenic and oxidative stress by Seladin-1. *Nature,* 432**,** 640-5.

WU, H., POMEROY, S. L., FERREIRA, M., TEIDER, N., MARIANI, J., NAKAYAMA, K. I., HATAKEYAMA, S., TRON, V. A., SALTIBUS, L. F., SPYRACOPOULOS, L. & LENG, R. P. 2011. UBE4B promotes Hdm2-mediated degradation of the tumor suppressor p53. *Nat Med,* 17**,** 347-55.

WUNDERLICH, M., GHOSH, M., WEGHORST, K. & BERBERICH, S. J. 2004. MdmX represses E2F1 transactivation. *Cell Cycle,* 3**,** 472-8.

XIE, Y., AVELLO, M., SCHIRLE, M., MCWHINNIE, E., FENG, Y., BRIC-FURLONG, E., WILSON, C., NATHANS, R., ZHANG, J., KIRSCHNER, M. W., HUANG, S. M. & CONG, F. 2013. Deubiquitinase FAM/USP9X interacts with the E3 ubiquitin ligase SMURF1 protein and protects it from ligase activity-dependent self-degradation. *J Biol Chem,* 288**,** 2976-85.

XIONG, S., PANT, V., SUH, Y. A., VAN PELT, C. S., WANG, Y., VALENTIN-VEGA, Y. A., POST, S. M. & LOZANO, G. 2010. Spontaneous tumorigenesis in mice overexpressing the p53-negative regulator Mdm4. *Cancer Res,* 70**,** 7148-54.

XIONG, S., VAN PELT, C. S., ELIZONDO-FRAIRE, A. C., FERNANDEZ-GARCIA, B. & LOZANO, G. 2007. Loss of Mdm4 results in p53-dependent dilated cardiomyopathy. *Circulation,* 115**,** 2925-30.

XIONG, S., VAN PELT, C. S., ELIZONDO-FRAIRE, A. C., LIU, G. & LOZANO, G. 2006. Synergistic roles of Mdm2 and Mdm4 for p53 inhibition in central nervous system development. *Proc Natl Acad Sci U S A,* 103**,** 3226-31.

XIONG, X., ZHAO, Y., HE, H. & SUN, Y. 2011. Ribosomal protein S27-like and S27 interplay with p53-MDM2 axis as a target, a substrate and a regulator. *Oncogene,* 30**,** 1798-811.

XIRODIMAS, D. P., CHISHOLM, J., DESTERRO, J. M., LANE, D. P. & HAY, R. T. 2002. P14ARF promotes accumulation of SUMO-1 conjugated (H)Mdm2. *FEBS Lett,* 528**,** 207-11.

XIRODIMAS, D. P., SAVILLE, M. K., BOURDON, J. C., HAY, R. T. & LANE, D. P. 2004. Mdm2-mediated NEDD8 conjugation of p53 inhibits its transcriptional activity. *Cell,* 118**,** 83-97.

XU, C., FAN, C. D. & WANG, X. 2015. Regulation of Mdm2 protein stability and the p53 response by NEDD4-1 E3 ligase. *Oncogene,* 34**,** 281-9.

YANG, E. S. & BURNSTEIN, K. L. 2003. Vitamin D inhibits G1 to S progression in LNCaP prostate cancer cells through p27Kip1 stabilization and Cdk2 mislocalization to the cytoplasm. *J Biol Chem,* 278**,** 46862-8.

YANG, F., LI, Q. J., GONG, Z. B., ZHOU, L., YOU, N., WANG, S., LI, X. L., LI, J. J., AN, J. Z., WANG, D. S., HE, Y. & DOU, K. F. 2014. MicroRNA-34a targets Bcl-2 and sensitizes human hepatocellular carcinoma cells to sorafenib treatment. *Technol Cancer Res Treat,* 13**,** 77-86.

YANG, G., AYALA, G., DE MARZO, A., TIAN, W., FROLOV, A., WHEELER, T. M., THOMPSON, T. C. & HARPER, J. W. 2002. Elevated Skp2 protein expression in human prostate cancer: association with loss of the cyclin-dependent kinase inhibitor p27 and PTEN and with reduced recurrence-free survival. *Clin Cancer Res,* 8**,** 3419-26.

YANG, J. Y., ZONG, C. S., XIA, W., WEI, Y., ALI-SEYED, M., LI, Z., BROGLIO, K., BERRY, D. A. & HUNG, M. C. 2006a. MDM2 promotes cell motility and invasiveness by regulating E-cadherin degradation. *Mol Cell Biol,* 26**,** 7269-82.

YANG, M., HSU, C. T., TING, C. Y., LIU, L. F. & HWANG, J. 2006b. Assembly of a polymeric chain of SUMO1 on human topoisomerase I in vitro. *J Biol Chem,* 281**,** 8264-74.

YANG, Y., KITAGAKI, J., DAI, R. M., TSAI, Y. C., LORICK, K. L., LUDWIG, R. L., PIERRE, S. A., JENSEN, J. P., DAVYDOV, I. V., OBEROI, P., LI, C. C., KENTEN, J. H., BEUTLER, J. A., VOUSDEN, K. H. & WEISSMAN, A. M. 2007. Inhibitors of ubiquitin-activating enzyme (E1), a new class of potential cancer therapeutics. *Cancer Res,* 67**,** 9472-81.

YANG, Y., LUDWIG, R. L., JENSEN, J. P., PIERRE, S. A., MEDAGLIA, M. V., DAVYDOV, I. V., SAFIRAN, Y. J., OBEROI, P., KENTEN, J. H., PHILLIPS, A. C., WEISSMAN, A. M. & VOUSDEN, K. H. 2005. Small molecule inhibitors of HDM2 ubiquitin ligase activity stabilize and activate p53 in cells. *Cancer Cell,* 7**,** 547-59.

YANG, Z. & KLIONSKY, D. J. 2010. Mammalian autophagy: core molecular machinery and signaling regulation. *Curr Opin Cell Biol,* 22**,** 124-31.

YU, J., ZHANG, L., HWANG, P. M., KINZLER, K. W. & VOGELSTEIN, B. 2001. PUMA induces the rapid apoptosis of colorectal cancer cells. *Mol Cell,* 7**,** 673-82.

YU, X., HARRIS, S. L. & LEVINE, A. J. 2006. The regulation of exosome secretion: a novel function of the p53 protein. *Cancer Res,* 66**,** 4795-801.

YUAN, J., LUO, K., ZHANG, L., CHEVILLE, J. C. & LOU, Z. 2010. USP10 regulates p53 localization and stability by deubiquitinating p53. *Cell,* 140**,** 384-96.

ZHAN, Q., ANTINORE, M. J., WANG, X. W., CARRIER, F., SMITH, M. L., HARRIS, C. C. & FORNACE, A. J., JR. 1999. Association with Cdc2 and inhibition of Cdc2/Cyclin B1 kinase activity by the p53-regulated protein Gadd45. *Oncogene,* 18**,** 2892-900.

ZHANG, C., LIN, M., WU, R., WANG, X., YANG, B., LEVINE, A. J., HU, W. & FENG, Z. 2011. Parkin, a p53 target gene, mediates the role of p53 in glucose metabolism and the Warburg effect. *Proc Natl Acad Sci U S A,* 108**,** 16259-64.

ZHANG, C., LIU, J., LIANG, Y., WU, R., ZHAO, Y., HONG, X., LIN, M., YU, H., LIU, L., LEVINE, A. J., HU, W. & FENG, Z. 2013. Tumour-associated mutant p53 drives the Warburg effect. *Nat Commun,* 4**,** 2935.

ZHANG, L. & WANG, C. 2006. F-box protein Skp2: a novel transcriptional target of E2F. *Oncogene,* 25**,** 2615-27.

ZHANG, Q., HE, X., CHEN, L., ZHANG, C., GAO, X., YANG, Z. & LIU, G. 2012a. Synergistic regulation of p53 by Mdm2 and Mdm4 is critical in cardiac endocardial cushion morphogenesis during heart development. *J Pathol,* 228**,** 416-28.

ZHANG, W., CAO, L., SUN, Z., XU, J., TANG, L., CHEN, W., LUO, J., YANG, F., WANG, Y. & GUAN, X. 2016. Skp2 is over-expressed in breast cancer and promotes breast cancer cell proliferation. *Cell Cycle,* 15**,** 1344-51.

ZHANG, X., ZHANG, Z., CHENG, J., LI, M., WANG, W., XU, W., WANG, H. & ZHANG, R. 2012b. Transcription factor NFAT1 activates the mdm2 oncogene independent of p53. *J Biol Chem,* 287**,** 30468-76.

ZHANG, Y., SCHIFF, D., PARK, D. & ABOUNADER, R. 2014a. MicroRNA-608 and microRNA-34a regulate chordoma malignancy by targeting EGFR, Bcl-xL and MET. *PLoS One,* 9**,** e91546.

ZHANG, Y., XIONG, S., LI, Q., HU, S., TASHAKORI, M., VAN PELT, C., YOU, M. J., PAGEON, L. & LOZANO, G. 2014b. Tissue-specific and age-dependent effects of global Mdm2 loss. *J Pathol,* 233**,** 380-91.

ZHAO, G., GUO, J., LI, D., JIA, C., YIN, W., SUN, R., LV, Z. & CONG, X. 2013. MicroRNA-34a suppresses cell proliferation by targeting LMTK3 in human breast cancer mcf-7 cell line. *DNA Cell Biol,* 32**,** 699-707.

ZHAO, H., KEGG, H., GRADY, S., TRUONG, H. T., ROBINSON, M. L., BAUM, M. & BATES, C. M. 2004. Role of fibroblast growth factor receptors 1 and 2 in the ureteric bud. *Dev Biol,* 276**,** 403-15.

ZHAO, X., D, D. A., LIM, W. K., BRAHMACHARY, M., CARRO, M. S., LUDWIG, T., CARDO, C. C., GUILLEMOT, F., ALDAPE, K., CALIFANO, A., IAVARONE, A. & LASORELLA, A. 2009. The N-Myc-DLL3 cascade is suppressed by the ubiquitin ligase Huwe1 to inhibit proliferation and promote neurogenesis in the developing brain. *Dev Cell,* 17**,** 210-21.

ZHENG, N., WANG, P., JEFFREY, P. D. & PAVLETICH, N. P. 2000. Structure of a c-Cbl-UbcH7 complex: RING domain function in ubiquitin-protein ligases. *Cell,* 102**,** 533-9.

ZHOU, J. X., LEE, C. H., QI, C. F., WANG, H., NAGHASHFAR, Z., ABBASI, S. & MORSE, H. C., 3RD 2009. IFN regulatory factor 8 regulates MDM2 in germinal center B cells. *J Immunol,* 183**,** 3188-94.

ZHU, Q., WANI, G., YAO, J., PATNAIK, S., WANG, Q. E., EL-MAHDY, M. A., PRAETORIUS-IBBA, M. & WANI, A. A. 2007. The ubiquitin-proteasome system regulates p53-mediated transcription at p21waf1 promoter. *Oncogene,* 26**,** 4199-208.

ZOU, Q., JIN, J., HU, H., LI, H. S., ROMANO, S., XIAO, Y., NAKAYA, M., ZHOU, X., CHENG, X., YANG, P., LOZANO, G., ZHU, C., WATOWICH, S. S., ULLRICH, S. E. & SUN, S. C. 2014. USP15 stabilizes MDM2 to mediate cancer-cell survival and inhibit antitumor T cell responses. *Nat Immunol,* 15**,** 562-70.

ZUCKERMAN, V., LENOS, K., POPOWICZ, G. M., SILBERMAN, I., GROSSMAN, T., MARINE, J. C., HOLAK, T. A., JOCHEMSEN, A. G. & HAUPT, Y. 2009. c-Abl phosphorylates Hdmx and regulates its interaction with p53. *J Biol Chem,* 284**,** 4031-9.

Databases / Tools

Ensembl genome browser
https://www.ensembl.org/index.html

Graphical Codon Usage Analyser
http://gcua.schoedl.de/

IARC Database
https://www.iarc.fr/

IARC TP53 Database
http://p53.iarc.fr/

Optimized CRISPR Design
http://crispr.mit.edu/

Primer BLAST (NCBI)
https://www.ncbi.nlm.nih.gov/tools/primer-blast/

Protein Data Bank
https://www.wwpdb.org/

PubChem Database (NCBI)
https://pubchem.ncbi.nlm.nih.gov/